

**Functionalized *nido*-C₄B₂, *closo*-C₂B₅ and -C₂B₁₀
Carboranes, and Reactivity Studies on Electron-Poor
2,3-Dihydro-1,3-diboroly Complexes of Ruthenium**

INAUGURAL - DISSERTATION

zur

Erlangung der Doktorwürde

der

Naturwissenschaftlich-Mathematischen

Gesamtfakultät

der

Ruprecht-Karls-Universität

Heidelberg

Vorgelegt von

Yong Nie (MSc.)

aus Shandong, P. R. China

2005

INAUGURAL - DISSERTATION

zur

Erlangung der Doktorwürde

der

Naturwissenschaftlich-Mathematischen

Gesamtfakultät

der

Ruprecht-Karls-Universität

Heidelberg

Vorgelegt von

Yong Nie (MSc.)

aus Shandong, P. R. China

Tag der mündlichen Prüfung: 11.3.2005

**Functionalized *nido*-C₄B₂, *closo*-C₂B₅ and -C₂B₁₀
Carboranes, and Reactivity Studies on Electron-Poor
2,3-Dihydro-1,3-diborolyyl Complexes of Ruthenium**

Gutachter: Prof. Dr. Walter Siebert

Prof. Dr. Lutz H. Gade

Many thanks to my supervisor, Prof. Dr. Walter Siebert, for his very helpful advice, stimulating ideas and fruitful discussions throughout my research in his group.

Dedicated to my parents

献给我的父母！

Part of the work described herein has been published:

1. Yong Nie, Stefan Schwiegk, Hans Pritzkow, Walter Siebert,*
One-Pot Synthesis of 1,6-Diiodo-2,3,4,5-tetracarba-*nido*-hexaboranes(6) and
Mechanistic Studies on the Reaction System Alkynes/ BI_3 / $\text{NaK}_{2,8}$.
Eur. J. Inorg. Chem., **2004**, 1630-1638.
2. Yong Nie, Hans Pritzkow, Walter Siebert,*
Reactivity Studies on 1,6-Diiodo-2,3,4,5-tetraethyl-2,3,4,5-tetracarba-*nido*-
hexaborane(6): Synthesis and Structures of New C_4B_2 -*nido*-carborane
Derivatives.
Eur. J. Inorg. Chem., **2004**, 2425-2433.
3. Yong Nie, Hans Pritzkow, Chunhua Hu, Thomas Oeser, Bettina Bach,
Thomas Müller, Walter Siebert,*
(η^7 -4-Borataborepine)(η^5 -pentamethylcyclopentadienyl)ruthenium
complexes: ruthenocene analogs with a novel C_5B_2 ligand.
Angew. Chem., **2005**, *117*, 638-640; *Angew. Chem. Int. Ed.*, **2005**, *44*,
632- 634.

Table of contents

Summary	
Zusammenfassung	
1 Introduction.....	1
1.1 Organoboranes and carboranes.....	1
1.2 Boron heterocycles as ligands to transition metals.....	9
2 Objectives	10
3 Results and discussion	11
3.1 Synthesis and reactivity of 2,3,4,5-tetracarba-<i>nido</i>-hexaboranes(6).....	11
3.1.1 One-pot synthesis and properties of 1,6-diiodo-2,3,4,5-tetracarba- <i>nido</i> -hexaboranes(6) (5a-5c)	12
3.1.2 Crystal structure of 1,6-diiodo-2,3,4,5-tetraethyl-2,3,4,5-tetracarba- <i>nido</i> -hexaborane(6) (5a)	14
3.1.3 Formation of <i>nido</i> -(EtC) ₄ (BI) ₄ (4) and crystal structure of 3,4-bis(diiodoboryl)-3-hexene (2)	16
3.1.4 Scope and limitations of the one-pot method.....	18
3.1.5 Mechanistic studies on the reaction system alkynes/BI ₃ /NaK _{2.8}	18
3.1.6 Reactivity of 1,6-diiodo-2,3,4,5-tetraethyl-2,3,4,5-tetracarba- <i>nido</i> -hexaborane(6) (5a)	22
3.1.6.1 Regiospecific substitution at the basal boron atom.....	22
3.1.6.2 Substitution reactions involving the apical boron atom.....	27
3.1.6.3 Cluster linkages involving 2,3,4,5-tetracarba- <i>nido</i> -hexaboranes(6)	33
3.1.7 Conclusion	37

3.2	Formation and properties of 2,3-dicarba-<i>closo</i>-heptaboranes(7).....	38
3.2.1	Facile synthesis of apically halogenated 2,3-dicarba- <i>closo</i> -heptaboranes(7) (19a,b) from 2,3-dicarba- <i>nido</i> -hexaborane(8)	38
3.2.2	Alkynyl-substituted 2,3-dicarba- <i>closo</i> -heptaboranes(7) (19c-f) via Pd-catalyzed cross-coupling reactions	39
3.2.3	Alkenyl-linked 2,3-dicarba- <i>closo</i> -heptaborane(7) clusters (20)	40
3.2.4	Reactions of 19c,d with cobalt complexes	40
3.2.4.1	Reactions of carboranylacetylenes 19c,d with Co ₂ (CO) ₈	40
3.2.4.2	Reactions of 19c with CpCo(C ₂ H ₄) ₂ : formation of CpCo(dicarboranylbutadiene) complex 23	41
3.2.5	Conclusion	42
3.3	C-Boryl-<i>o</i>-carborane compounds	42
3.3.1	C-Aminoboryl- <i>o</i> -carborane derivatives.....	43
3.3.2	Diborane(4)-yl- <i>o</i> -carboranes 28	45
3.3.3	<i>o</i> -Carboranes with <i>exo</i> -cluster boron heterocycles.....	47
3.3.4	Conclusion	48
3.4	Reactivity of (η⁵-pentamethylcyclopentadienyl)(η⁵-2,3-dihydro-1,3-diborolyl)-ruthenium complexes	49
3.4.1	Crystal and electronic structures of Ru and Fe complexes	50
3.4.1.1	Crystal structure of the B-trimethylsilylmethyl derivative 35b	50
3.4.1.2	Electronic structures of the model compounds of Ru (35) and Fe (36)	50
3.4.2	Insertion of alkynes into 1,3-diborolylruthenium complexes.....	58
3.4.2.1	Formation of novel 4-borataborepine complexes 38.....	58
3.4.2.2	Attempts to prepare 4-borataborepines from 1,3-diborole 37c	62
3.4.2.3	Formation of boratabenzene ruthenium complexes 39f,g.....	63
3.4.3	Formation of the triple-decker 46 with a bridging C ₅ B ₂ ligand.....	65

Table of contents

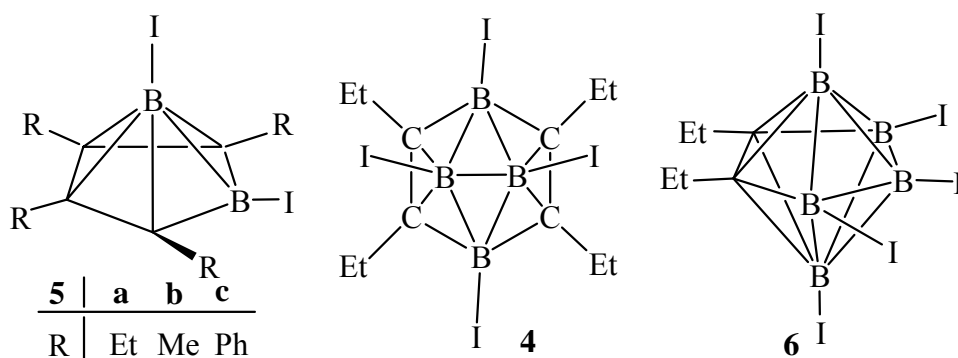
3.4.4	Interactions of η^5 -2,3-dihydro-1,3-diborole-(chloro)rhodium complexes with $\text{RCH}_2\text{C}_2\text{H}$ and $(\text{R}_2\text{P})_2\text{C}_2\text{H}_4$ ($\text{R} = \text{Ph}$).....	66
3.4.5	Crystal structure of the tetradecker complex 53a	68
3.4.6	Reaction of 35a with allylchloride: formation of “oligodecker” 58	69
3.4.7	Conclusion.....	73
3.5	Synthesis of the 1,3-diiodo-1,3-diborole 37d and formation of the 2,3,4,5,6-pentacarba-<i>nido</i>-hexaborane(6) cation (63⁺)	74
3.6	Synthesis and properties of some aminoborane derivatives	77
3.6.1	1,2-Dibromo-1,2-dipyrrolidinodiborane(4) (72b).....	79
3.6.2	Properties of $(\text{Me}_2\text{N})_2\text{B}_4[\text{B}(\text{NMe}_2)_2]_2$ (70)	84
3.6.2.1	Reactions with S_8 and Me_3NO	84
3.6.2.2	Rearrangement of 70 into the <i>cyclo</i> - B_6 isomer 67a	85
3.6.2.3	Reactions with isonitriles	86
3.6.3	Conclusion.....	87
4	Experimental section.....	88
5	References.....	125
6	Appendices	139
6.1	Abbreviations and Symbols	139
6.2	Selected NMR and MS spectra	140
6.3	Crystal data and refinement details.....	146

Acknowledgement

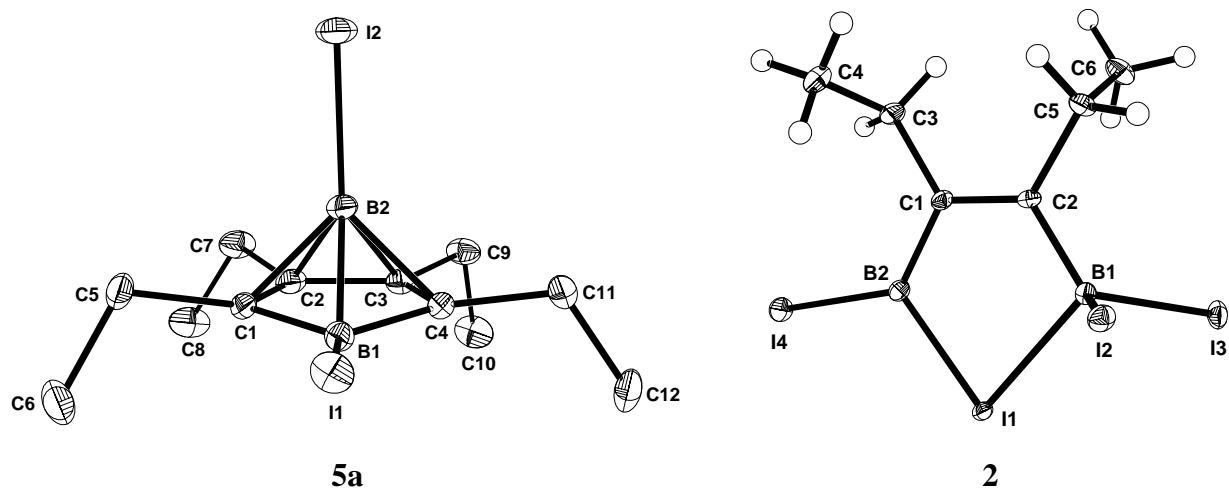
Summary

The results are described in six chapters on organoborane/carborane compounds (**3.1**, **3.2**, **3.3**, **3.5**), on the reactivity of 2,3-dihydro-1,3-diboroly complexes of ruthenium (**3.4**), and on aminoborane derivatives (**3.6**).

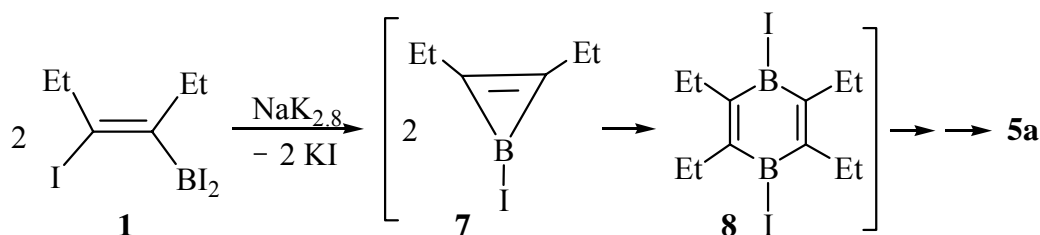
In Chapter **3.1**, a one-pot synthesis of 1,6-diiodo-2,3,4,5-tetracarba-*nido*-hexaborane(**6**) derivatives (**5a-c**) is reported, involving disubstituted alkynes and BI₃ (in 1:1 ratio) and NaK_{2,8} at low temperature. The reaction of 3-hexyne, BI₃ (2 equiv.) and NaK_{2,8} at r.t. affords a mixture of **5a**, *nido*-(EtC)₄(BI)₄ (**4**) and *closo*-(EtC)₂(BI)₅ (**6**).



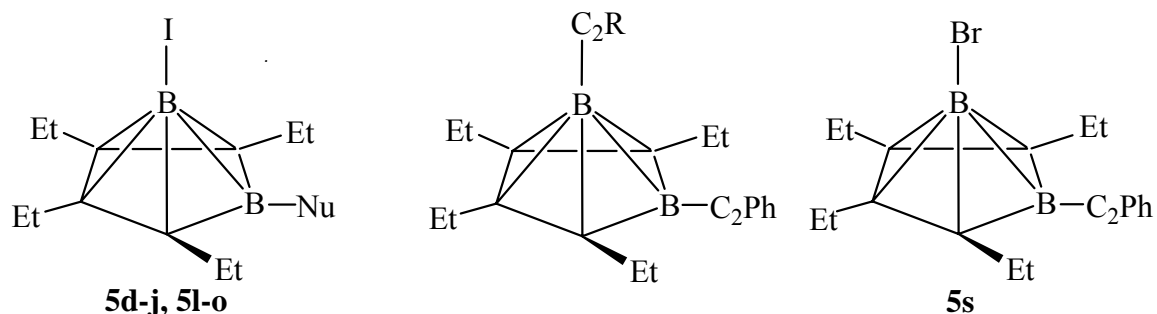
The alternative formation of **4** and **6** by dehalogenation of the known *cis*-I₂B(Et)C=C(Et)BI₂ (**2**) indicates that diborylalkenes are precursors for *nido*-C₄B₄ carboranes. In general, dehalogenation reactions proceed clean and give higher yields of carboranes at low temperature. The *nido*-C₄B₂ skeleton has been confirmed by an X-ray diffraction analysis of yellow **5a**. The structure of **2** exhibits a remarkable B-I-B bridge.



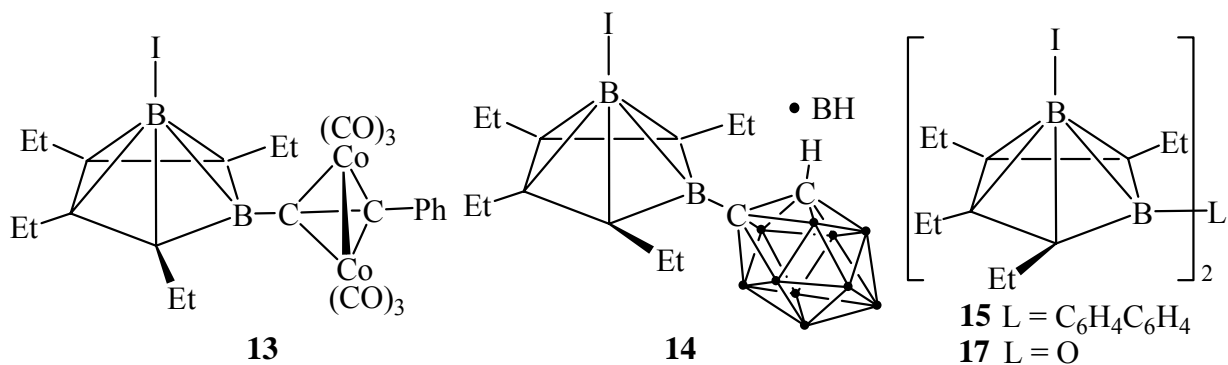
A possible mechanism of the formation of **5a** is proposed. The first step, the iodoboration of 3-hexyne with BI_3 has been clarified to give *cis*-**1** stereospecifically by an X-ray study of its pyridine adduct, and a *cis/trans* isomerization exists in **1** and some of its derivatives. Although evidence for the borirene **7** is only obtained in solution, the *in situ* formation of the dimerization product **8** has been achieved by the redox reaction of **2** and 3-hexyne, and its gradual rearrangement into carborane **5a** has been observed.



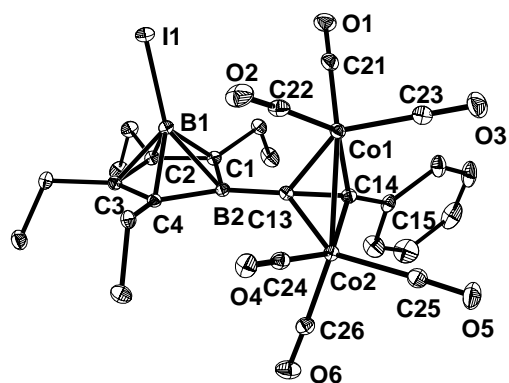
The reactivity of **5a** towards various nucleophiles has been investigated. In most cases, the substitution with hydride, alkynyl, diphenylphosphanyl, trimethylstannyl, fluoride, phenyl, $\text{CpFe}(\text{CO})_2$ anion, and even the bulky *o*-carboranyl group occurs regioselectively at the basal boron atom. Replacement of the “inert” apical iodine is realized by a $\text{Pd}(0)$ -catalyzed Negishi-type cross-coupling, as demonstrated by the synthesis of apically alkynyl-substituted **5q** and **5r**.



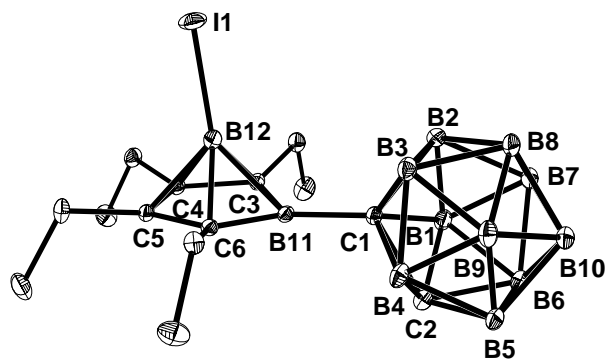
$\text{Nu} = \text{C}_2\text{R}$ ($\text{R} = \text{Ph}$, *t*Bu, SiMe_3 , *p*-tolyl), **5q** $\text{R} = \text{SiMe}_3$
 PPh_2 , $\text{CpFe}(\text{CO})_2$, H, F, Ph, SnMe_3 **5r** $\text{R} = \text{Ph}$



15 $\text{L} = \text{C}_6\text{H}_4\text{C}_6\text{H}_4$
17 $\text{L} = \text{O}$

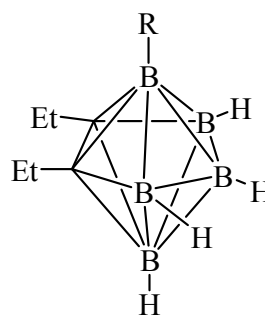
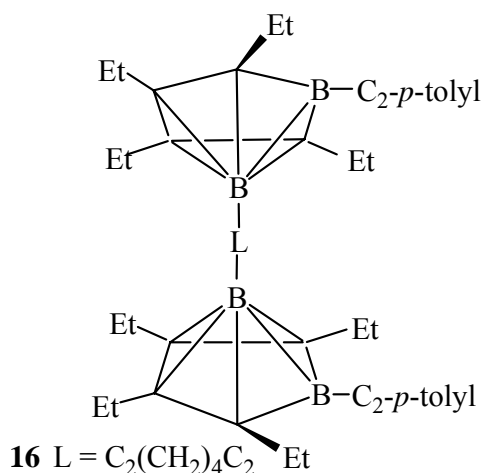


13



14

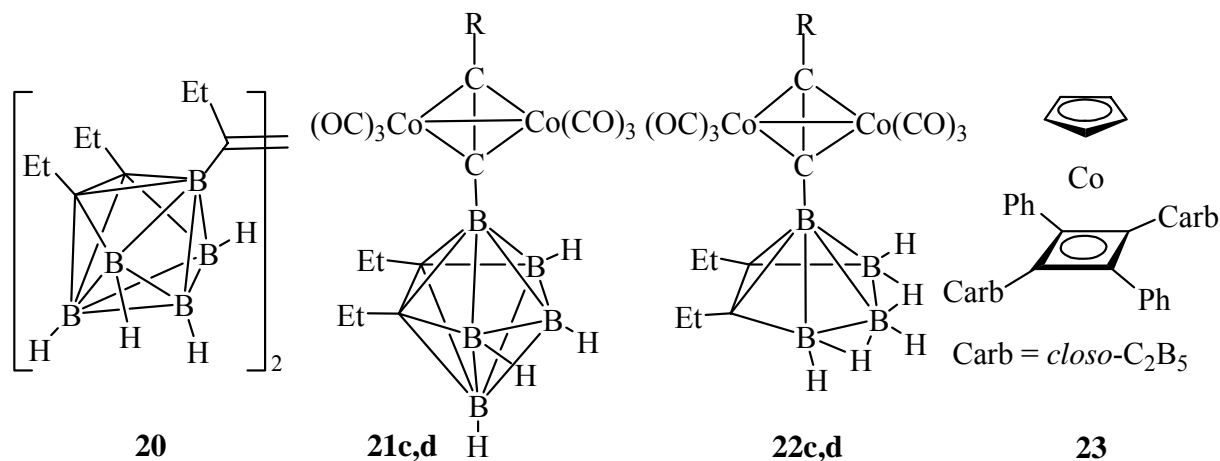
Attempts to prepare apically arylated/linked clusters by Pd(0)-catalyzed cross-coupling reactions of **5d** with 4,4'-(C₆H₄)₂(ZnCl)₂ and 1,3,5-C₆H₃(ZnCl)₃ (generated *in situ* from bromoarenes), respectively, lead only to apically brominated **5s**. A series of linked clusters with different types of linkages [via B–C bond in **13** and **14**, a C₆H₄C₆H₄ unit in **15**, a C₂(CH₂)₄C₂ unit in **16**, and an oxygen atom in **17**] are obtained by nucleophilic substitution (with bifunctional nucleophiles) or by transformations of the carboranyl acetylenes. The X-ray structure analyses of **5a,d,g,i,q,s**, **13** and **14** reveal that the substituent at the apical boron is bent away from the basal boron atom. The compounds **13** and **14** represent directly linked clusters, as shown by the X-ray diffraction analyses.



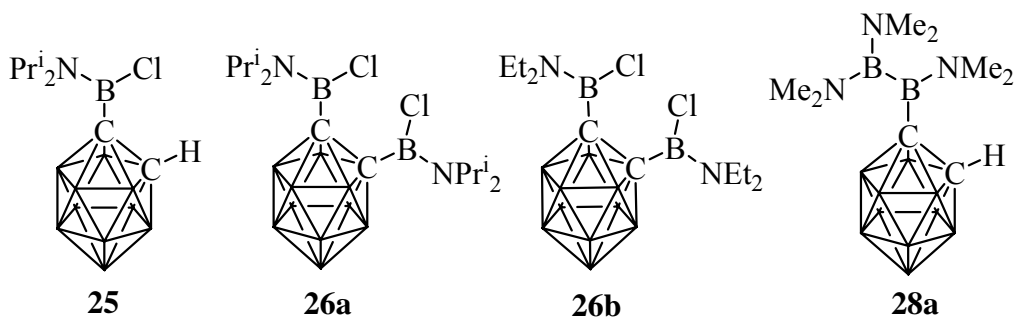
19	a	b	c	d	e	f
R	Br	I	C ₂ Ph	C ₂ SiMe ₃	C ₂ Me	C ₂ <i>t</i> Bu

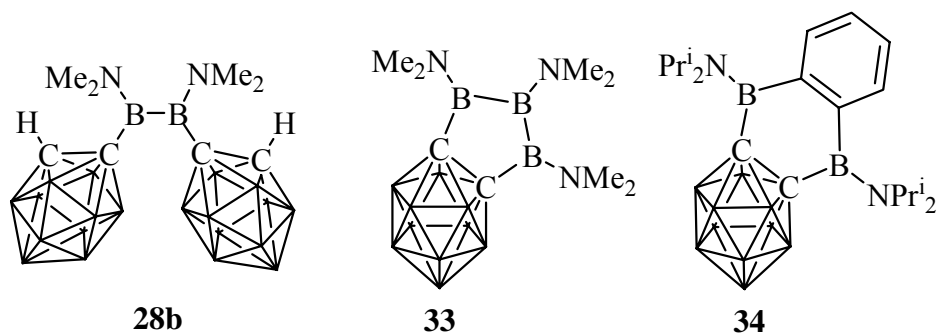
In Chapter **3.2**, treatment of the *nido*-2,3-Et₂C₂B₄H₄²⁻ dianion with the reagents BX₃ (X = Br, I) and PhC≡Ccat lead to apically functionalized *closo*-1-R-2,3-Et₂C₂B₅H₄ derivatives (**19a-c**). Similarly, **20** with two *closo*-C₂B₅ moieties linked via a C=C unit is obtained starting from *cis*-Cl₂B(Et)C=C(Et)BCl₂. A more efficient pathway is developed by the Pd-catalyzed

cross-coupling reactions of **19b** with $R'C\equiv CZnCl$ to give *closo*-1-C \equiv CR'-2,3-Et₂C₂B₅H₄ (**19d-f**). Like the synthesis of **13**, the reactions of **19c,d** and $Co_2(CO)_8$ afford diclusters **21c,d**, which lose the apical boron on silica gel to give the *nido*-C₂B₄-Co₂C₂ diclusters **22c,d**. The formation of carboranyl-substituted CpCo(cyclobutadiene) complex **23** is observed in the reaction of **19c** and $CpCo(C_2H_4)_2$.

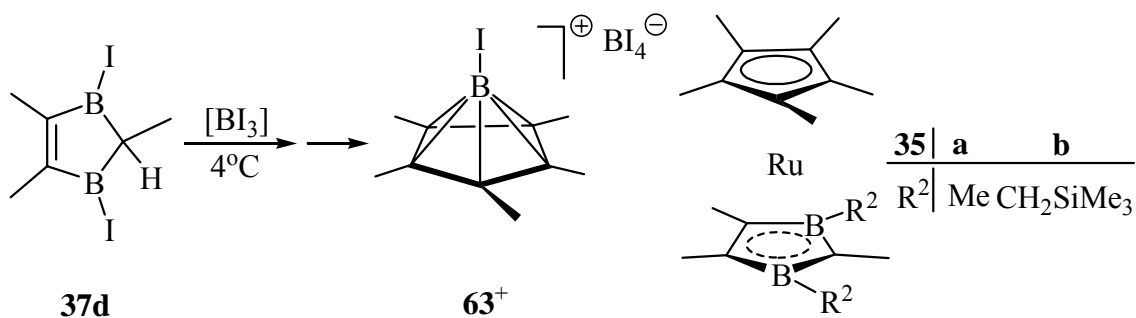


In Chapter 3.3, a series of C-boryl-*o*-carborane derivatives are reported by reacting dilithio-*o*-carborane and the corresponding chloroboranes, respectively. The monoborylation occurs as the main reaction with $Pr^i_2NBCl_2$ to give **25**, together with the diborylated species **26a** as a byproduct. In the same reaction with Et_2NBCl_2 the diborylated **26b** is obtained. The reaction with $Cl(NMe_2)B-B(NMe_2)Cl$ does not lead to a product with a four-membered *exo*-cycle, but to a mixture of *o*-carboranyl-substituted diborane(4) derivatives **28a** and **28b**. The reactions with $Cl(Me_2N)B-B(NMe_2)-B(NMe_2)Cl$ and $1,2-C_6H_4(Pr^i_2BCl)_2$, respectively, afford the *exo*-cyclic **33** with a five-membered ring and **34** with a six-membered heterocycle. X-ray structure analyses are carried out for the carboranes **25**, **26b**, **28a**, **33** and **34**.

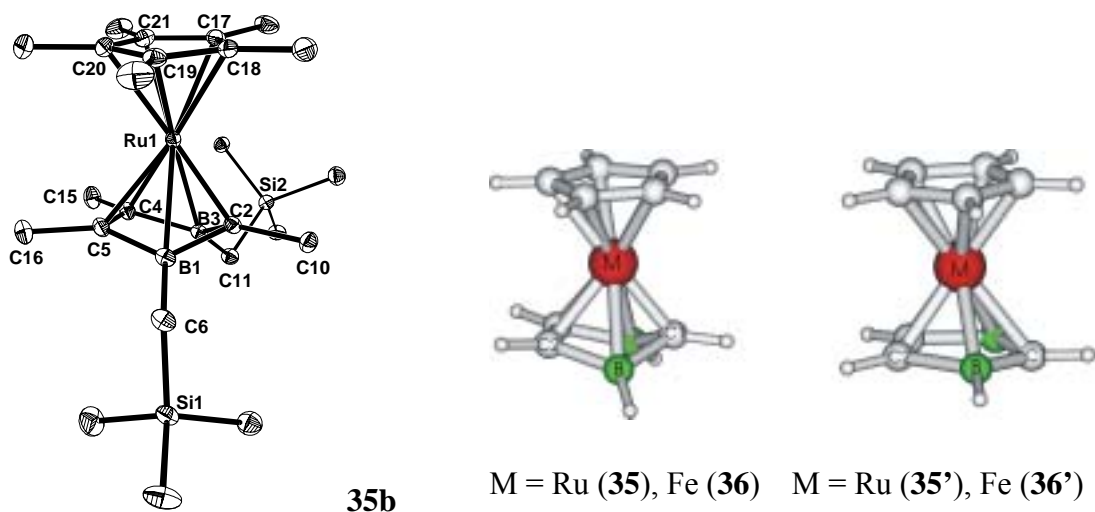




In Chapter 3.5, the formation of the 1,3-diboroles is outlined, in which the redox reaction between $(I_2B)_2CHMe$ and 2-butyne leads to the 1,3-diiodo derivative **37d** with elimination of iodine. The unprecedented transformation of **37d** into the known 2,3,4,5,6-pentacarbano-*nido*-hexaborane(6) cation (**63**⁺) is observed. A possible mechanism for its formation is proposed.



In Chapter 3.4, the long-sought crystal structure of the (η^5 -pentamethylcyclopentadienyl)-(η^5 -2,3-dihydro-1,3-diborolyl)ruthenium derivative **35b** is described. It finally confirms the folding along the B...B vector (40.7°) which is similar to the iron analog (41.3°).

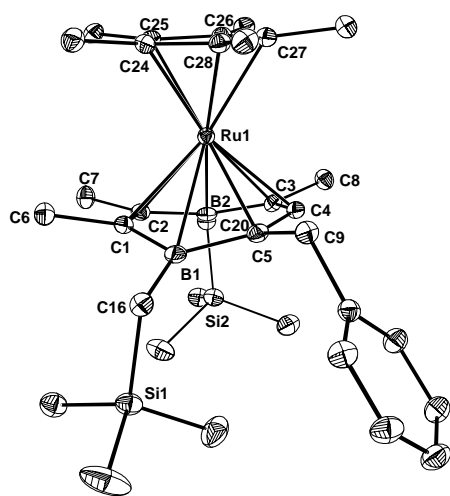


The electronic structures of the model sandwiches Ru (**35**) and Fe (**36**) have been studied (by Dr. I. Hyla-Kryspin, University of Münster). The DFT calculations indicate that the folding of the 1,3-diborolyl ligands is of electronic origin, and the parent compounds **35** and **36** with a folded 1,3-diborolyl ligand are more stable in energy (24.5 and 24.9 kcal/mol for Ru and Fe structures, respectively) than **35'** and **36'** with a planar ligand.

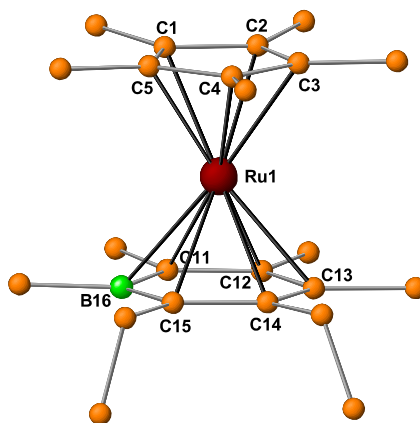


38	a	b	c	d	e	39	a	b	c	d	e	f	g
R ²	Me	CH ₂ SiMe ₃	Me	Me	Me	R ²	Me	CH ₂ SiMe ₃	Me	Me	Me	Me	Me
R ⁴	CH ₂ Ph	CH ₂ Ph	Ph	SiMe ₃	H	R ⁴	CH ₂ Ph	CH ₂ Ph	Ph	SiMe ₃	H	Et	<i>p</i> -Tolyl
						R ⁵	H	H	H	H	H	Et	<i>p</i> -Tolyl

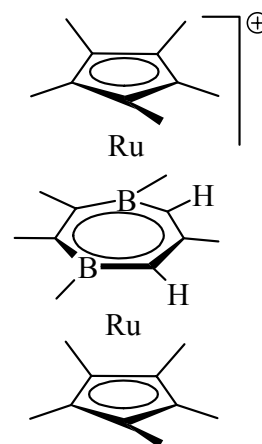
The reactivity of **35** is studied with respect to insertion of terminal alkynes into its C₃B₂ heterocycle which results in novel 18 VE ruthenocene analogs **38** with seven-membered 4-borataborepines as ligands. Additionally, boratabenzene complexes **39** and triarylbenzene species (in some cases) are identified as byproducts, the formation of **39** is a result of elimina-



38b



39f

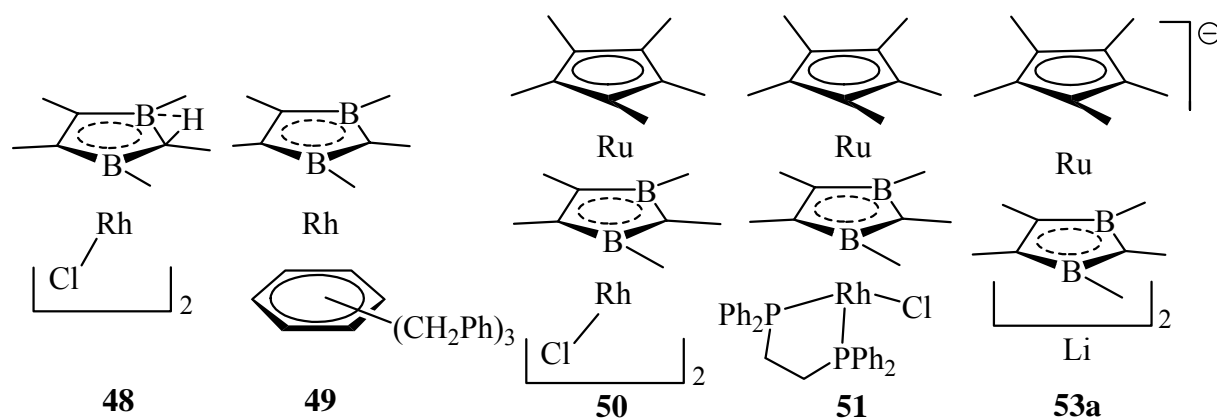


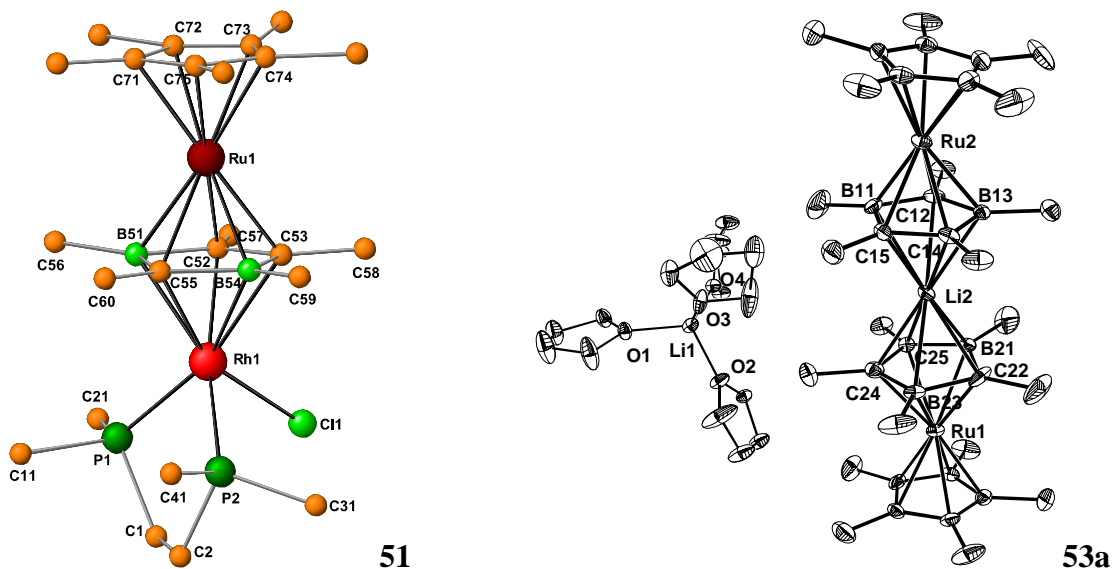
46

tion of the boranediyl $[:BR^2]$ moieties from the intermediate 4-borataborepine complexes. The 4-borataborepine functions as 6e ligand and exhibits a reduced folding along the B...B vector ($\alpha = 12.5^\circ$ in **38a**, 26° in **38b**, and 15.2° in **38c**) compared with 40.7° in **35b**.

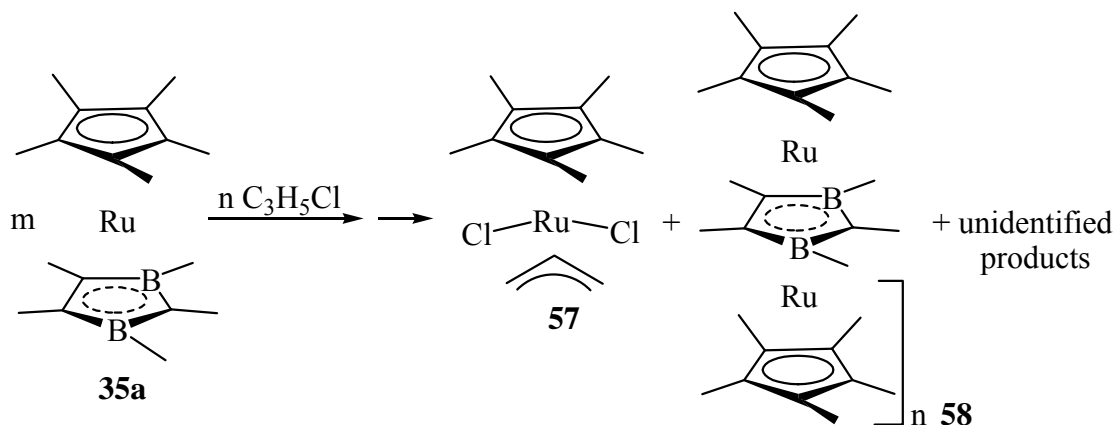
The boratabenzene complexes **39f,g** are formed as the main products in the reactions of **35a** and disubstituted alkynes (3-hexyne and di-*p*-tolylacetylene, respectively). The reaction with di-*p*-tolylacetylene gave a mixture of **39g**, (*Z,Z*)-1,2,3,4-tetratolyl-1,3-butadiene and the cationic triple-decker species **46**. The latter two byproducts are studied by crystal structure analyses, which reveal that **46** has a seven-membered C_3B_2 ring as the bridging ligand with two CH groups being separated by a CMe moiety. However, its formation is not yet clear.

The comparative study on the reactivity of the $[(1,3\text{-diborole})RhCl]_2$ dimer **48** with $PhCH_2C_2H$ is carried out, in which the cyclotrimerization occurs to give (1,3-diboroly)-Rh(arene) **49**. The reaction of **50** with phenylacetylene resulted in a yellow brown product, most likely a cyclobutadiene analog of **51**. The dimeric RuRh complex **50** reacts with dppe to afford the 30 VE triple-decker **51**. The anionic tetradecker **53a** obtained from the reaction mixture of **35a** and lithium is structurally characterized, in which one Li cation bridges two sandwich anions of $35a^-$, while the second solvated Li cation is separated from the tetradecker moiety.

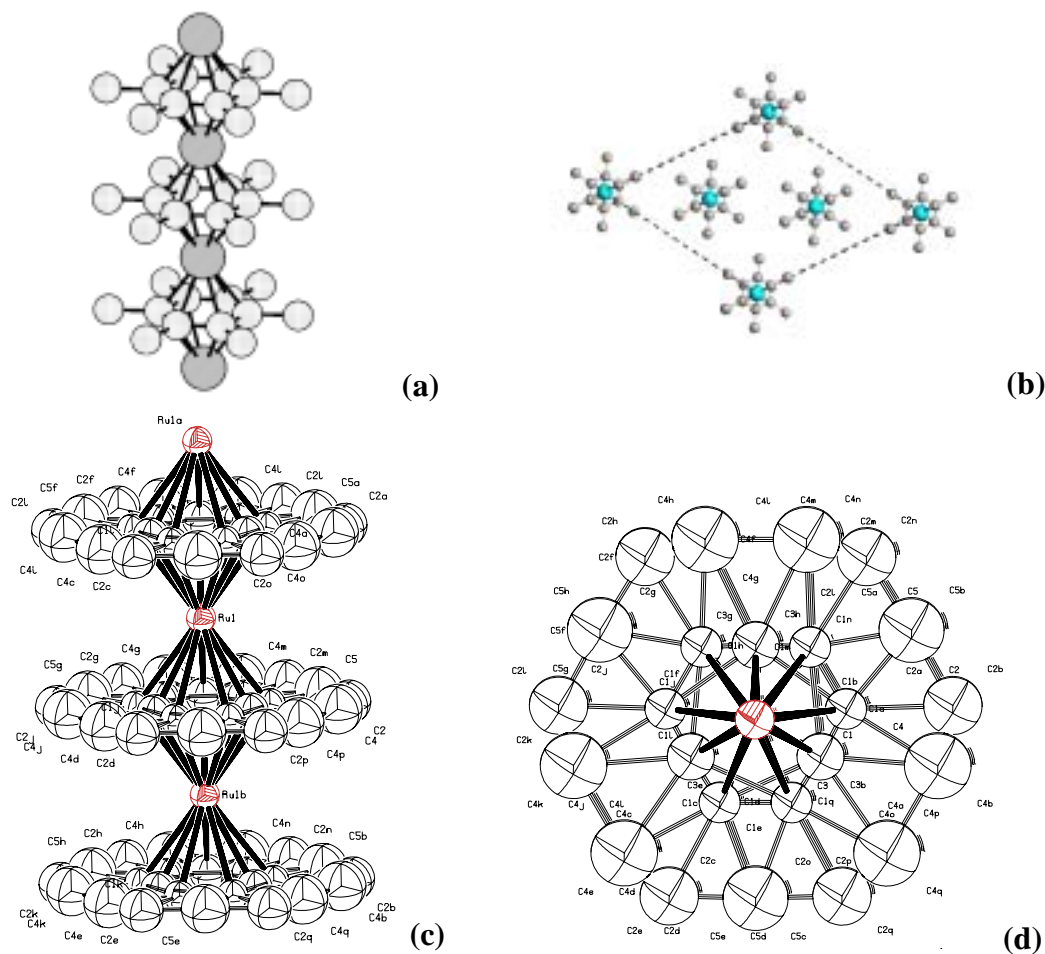




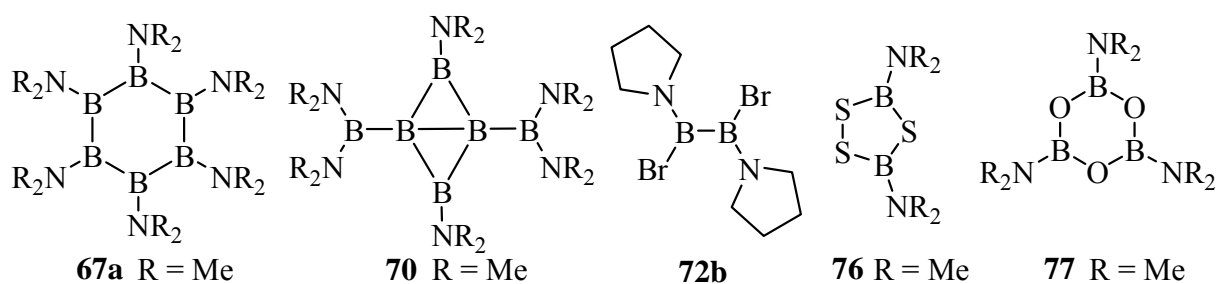
The complex reaction of **35a** with allylchloride in hexane affords a mixture of products, one is the novel complex **58**. Its identity and formation mechanism are not yet clear, however, the results from MS studies and two independent but only partially solved X-ray diffraction analyses indicate that it has a stack of ruthenium atoms with bridging Cp* and 1,3-diborolyl ligands.



Preliminary results of the X-ray structure of **58** are shown in Figs. (a) and (b) (Dr. C. Hu, Aachen); (c) and (d) (Prof. H. Wadepl). Figs. (a) and (c) side-view of the stacking, (b) and (d) top-view. The stacks are along a threefold axis which would be consistent with either extensive disorder or a tripling of the crystals.



In Chapter 3.6, the reactivity of $(\text{Me}_2\text{N})_2\text{B}_4[\text{B}(\text{NMe}_2)_2]_2$ (**70**) is studied, and some pyrrolidinoborane derivatives are prepared for new cyclo- or polyboranes. The reaction of tetrapyrrolidinodiborane(4) and BBr_3 (1 equiv.) gives a mixture, with two equiv. of BBr_3 , the crystalline **72b** as the main product is isolated, which shows dimorphism.

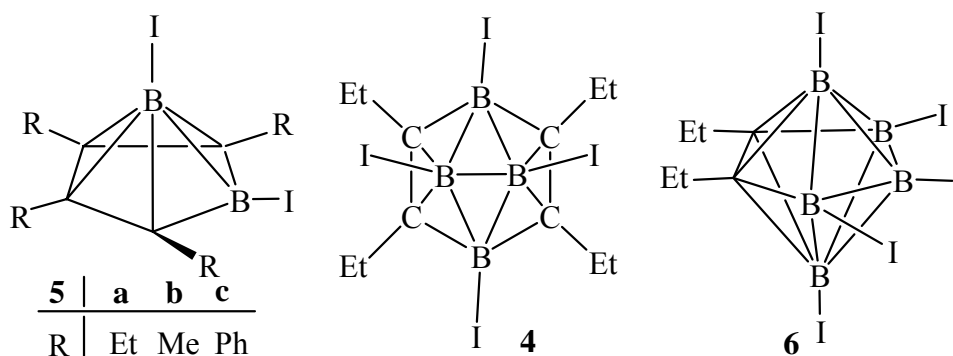


The reactions of **70** with S_8 and Me_3NO , respectively, lead to the known heterocyclic 1,2,4,3,5-trithiadiborolane **76** and boroxine **77**, with cleavage of the rhombohedral B_4 unit. On heating **70** rearranges into its classic isomer **67a**.

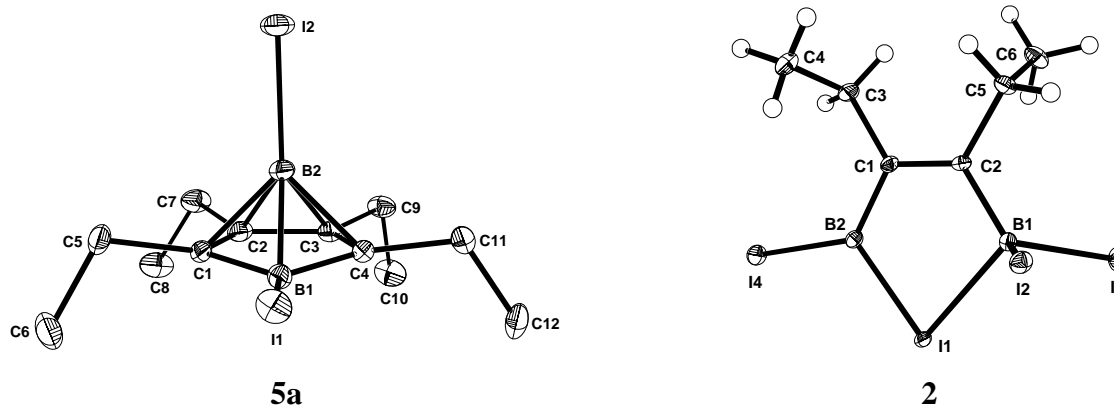
Zusammenfassung

Die Ergebnisse werden in sechs Kapiteln über Organoboran/Carboran-Verbindungen (**3.1**, **3.2**, **3.3**, **3.5**), über die Reaktivität von 2,3-Dihydro-1,3-diboroly-Komplexen von Ruthenium (**3.4**) und über Aminoboran-Derivate (**3.6**) beschrieben.

Im Kapitel **3.1** wird über eine Eintopf-Synthese von 1,6-Diiodo-2,3,4,5-tetracarba-*nido*-hexaboran(6)-Derivaten (**5a-c**) berichtet, in der disubstituierte Alkine und BI_3 (im 1:1-Verhältnis) mit $\text{NaK}_{2,8}$ bei tiefer Temperatur umgesetzt werden. Die Reaktion von 3-Hexin, BI_3 (2 Äquiv.) und $\text{NaK}_{2,8}$ bei Raumtemperatur ergibt ein Gemisch von **5a**, *nido*-(EtC) $_4$ (BI) $_4$ (**4**) und *closo*-(EtC) $_2$ (BI) $_5$ (**6**).

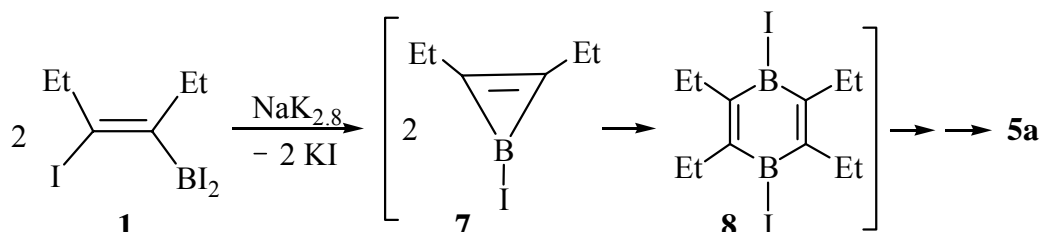


Die alternative Bildung von **4** und **6** durch Dehalogenierung von dem bekannten *cis*- $\text{I}_2\text{B}(\text{Et})\text{C}=\text{C}(\text{Et})\text{BI}_2$ (**2**) zeigt, dass Diborylalkene Vorstufen für *nido*- C_4B_4 -Carborane darstellen. Im allgemeinen verlaufen Dehalogenierungsreaktionen bei tiefen Temperaturen sauber und geben höhere Ausbeuten von Carboranen. Das *nido*- C_4B_2 -Gerüst ist durch eine Strukturanalyse des gelben **5a** bestätigt. Die Struktur von **2** zeigt eine bemerkenswerte B-I-B-Brücke.

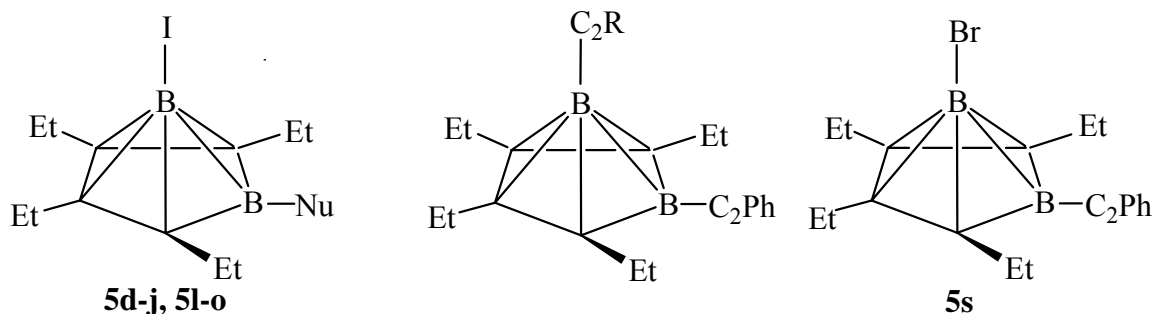


Ein möglicher Mechanismus wird für die Bildung von **5a** vorgeschlagen. Der erste Schritt der

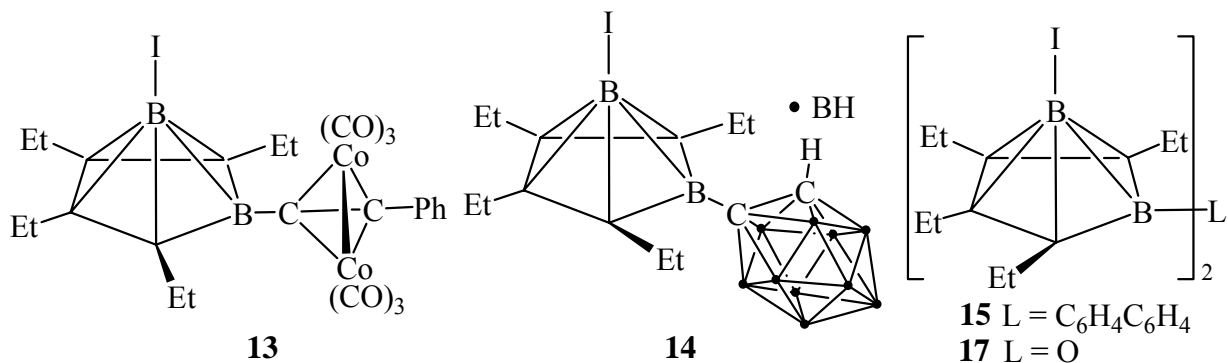
Iodoborierung von 3-Hexin mit BI_3 unter stereospezifischer Bildung von *cis*-**1** ist durch die Strukturanalyse des Pyridin-Addukts aufgeklärt. Eine *cis/trans* Isomerisierung tritt bei **1** und einigen Derivaten auf. Hinweise auf das Boriren **7** wurden nur in Lösung erhalten. Die *in situ*-Bildung des Dimeren **8** erfolgt auch durch die Redox-Reaktion von **2** mit 3-Hexin; es wird langsame Umlagerung von **8** in das Carboran **5a** beobachtet.

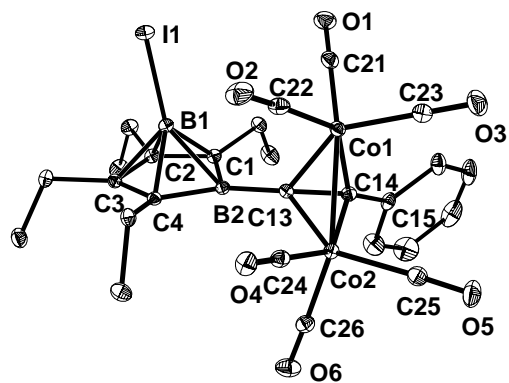


Die Reaktivität von **5a** wurde mit verschiedenen Nucleophilen getestet. In den meisten Fällen erfolgt die Substitution regiospezifisch mit Hydrid, Alkinid, Diphenylphosphanid, Trimethylstannat, Fluorid, Phenyl, $\text{CpFe}(\text{CO})_2$ -Anion und sogar mit der voluminösen *o*-Carboranyl-Gruppe am basalen Boratom. Der Austausch des 'inerten' apikalen Iods gelingt durch eine Pd(0)-katalysierte Negishi-Kreuz-Kupplung, was zur Synthese der apikalen Alkynyl-Derivate **5q** und **5r** führt.

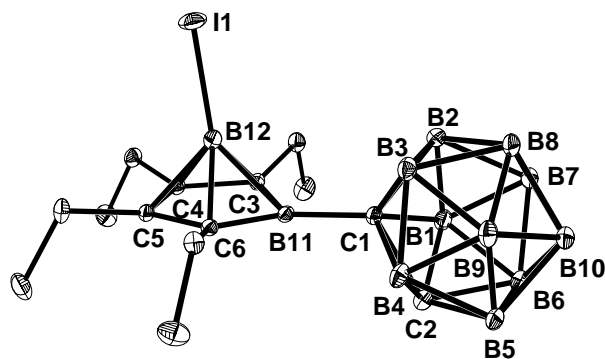


Nu = C_2R (R = Ph, *t*Bu, SiMe_3 , *p*-Tolyl), PPh_2 , $\text{CpFe}(\text{CO})_2$, H, F, Ph, SnMe_3
5q R = SiMe_3
5r R = Ph



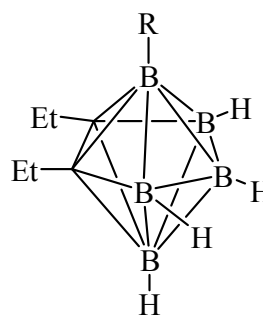
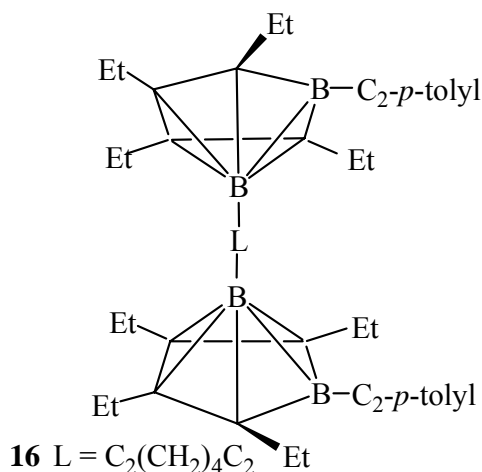


13



14

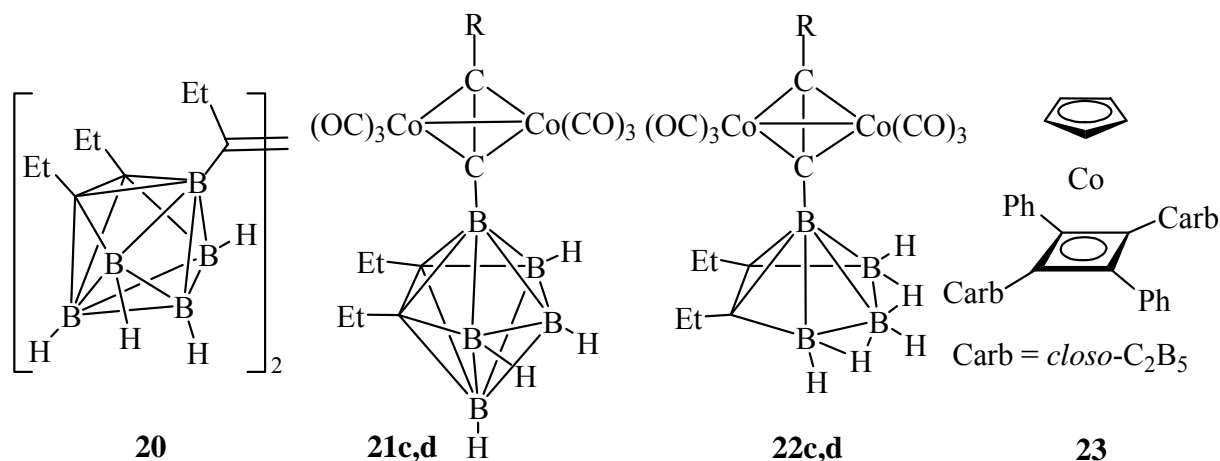
Versuche zur Herstellung von apikal arylierten/verknüpften Cluster durch Pd(0)-katalysierte Kreuz-Kupplung-Reaktionen von **5d** mit 4,4'-(C₆H₄)₂(ZnCl)₂ und 1,3,5-C₆H₃(ZnCl)₃ (*in situ* aus Bromarenen hergestellt) führen nur zum apikal bromierten **5s**. Ein Reihe von Cluster-Verknüpfungen [via B–C-Bindung in **13** und **14**, durch eine C₆H₄C₆H₄-Einheit in **15**, eine C₂(CH₂)₄C₂-Einheit in **16**, und durch ein Sauerstoffatom in **17**] werden durch nukleophile Substitutionen (mit bifunktionalen Nucleophilen) oder durch Umwandlung von Carboranyl-acetylen erhalten. Die Strukturanalysen von **5a,d,g,i,q,s**, **13** und **14** ergeben, dass der Substituent am apikalen Boratom von dem basalen Boratom wegzeigt. Die Verbindungen **13** und **14** stellen direkt verknüpfte Cluster dar, was durch die Strukturanalysen belegt wird.



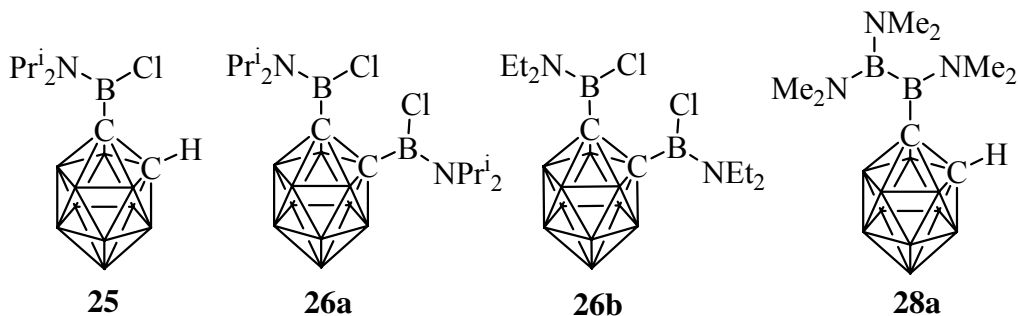
19	a	b	c	d	e	f
R	Br	I	C ₂ Ph	C ₂ SiMe ₃	C ₂ Me	C ₂ <i>t</i> Bu

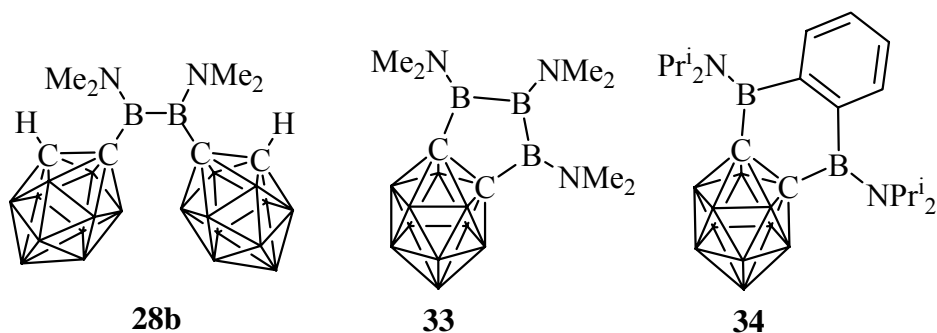
Im Kapitel **3.2** werden die Umsetzungen des *nido*-2,3-Et₂C₂B₄H₄²⁻ Dianions mit BX₃ (X = Br, I) und PhC≡Cbat zu apikal funktionalisierten *closo*-1-R-2,3-Et₂C₂B₅H₄-Derivaten (**19a-c**) vorgestellt. Analog sind in **20** zwei *closo*-C₂B₅-Gruppierungen durch eine C=C-Einheit verknüpft, wenn man die Umsetzung mit *cis*-Cl₂B(Et)C=C(Et)BCl₂ durchführt. Ein effizienter

Weg wurde mit der Pd-katalysierten Kreuz-Kupplungsreaktion von **19b** mit $R'C\equiv CZnCl$ gefunden, die *closo*-1- $C\equiv CR'$ -2,3- $Et_2C_2B_5H_4$ (**19d-f**) liefert. Analog der Synthese von **13** ergibt die Reaktion von **19c,d** mit $Co_2(CO)_8$ die Dicluster **21c,d**, die auf Silikagel die apikale Borgruppe unter Bildung der *nido*- $C_2B_4-CO_2C_2$ Dicluster **22c,d** verlieren. Die Bildung des Carboranyl- substituierten CpCo(cyclobutadien)-Komplexes **23** erfolgt durch Umsetzung von **19c** mit $CpCo(C_2H_4)_2$.

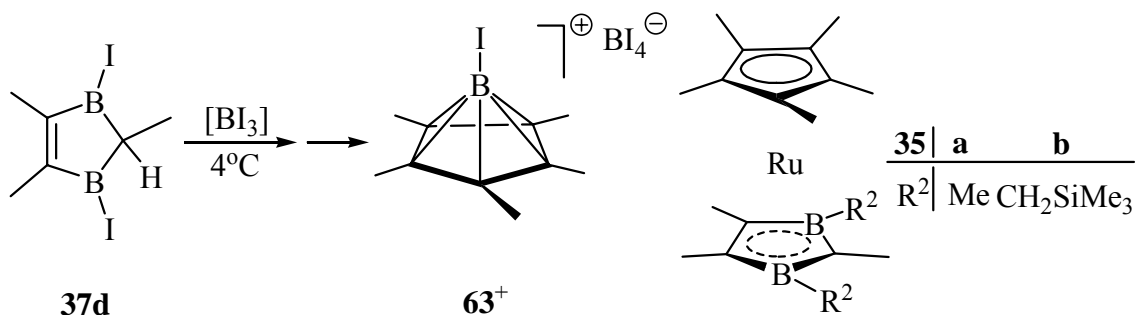


Im Kapitel 3.3 wird die Synthese einer Reihe von C-Boryl-*o*-carboran-Derivaten durch Umsetzung von Dilithio-*o*-carboranen mit den entsprechenden Chloroboranen beschrieben. Die Borylierung mit $Pr^i_2NBCl_2$ führt zu **25** und zur diborylierten Spezies **26a** als Nebenprodukt. In der gleichen Reaktion wird mit Et_2NBCl_2 das diborylierte **26b** erhalten. Durch Umsetzung mit $Cl(NMe_2)B-B(NMe_2)Cl$ bildet sich kein ankondensierter Vierring, sondern eine Mischung der *o*-Carboranyl-substituierten Diboran(4)-Derivate **28a** und **28b**. Die Reaktionen mit $Cl(Me_2N)B-B(NMe_2)-B(NMe_2)Cl$ und $1,2-C_6H_4(Pr^i_2BCl)_2$ ergeben das *exo*-cyclische **33** mit einem fünfgliedrigen Ring und **34** mit einem Sechsring. Strukturanalysen sind von den Carboranen **25**, **26b**, **28a**, **33** und **34** durchgeführt worden.

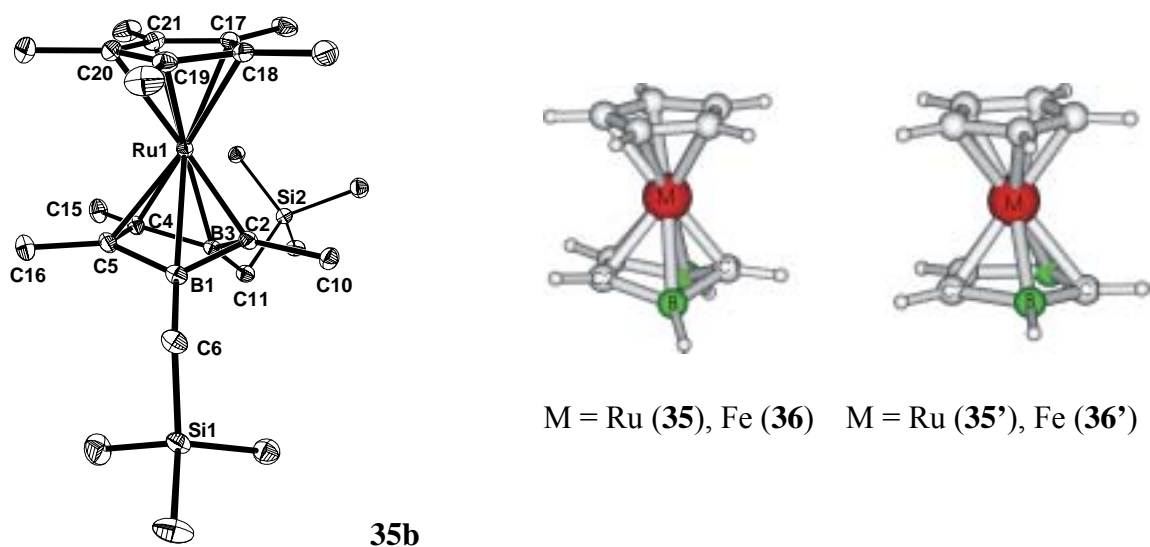




Im Kapitel 3.5 wird die Bildung von 1,3-Diborolen erläutert, die durch Redox-Reaktion zwischen $(I_2B)_2CHMe$ und 2-Butin zu dem 1,3-Diiodo-Derivat **37d** unter Eliminierung von Iod erfolgt. Die überraschende Umwandlung von **37d** zu dem bekannten 2,3,4,5,6-Pentacarbano-hexaboran(6)-Kation (**63⁺**) wird beobachtet und ein möglicher Mechanismus für die Bildung von **63⁺** vorgeschlagen.

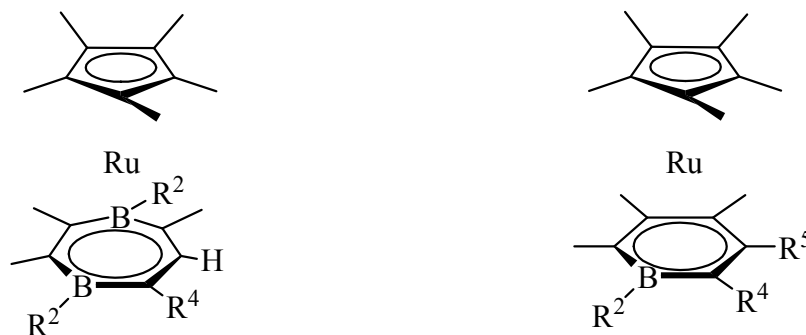


Im Kapitel 3.4 wird die langgesuchte Struktur des $(\eta^5\text{-Pentamethylcyclopentadienyl})(\eta^5\text{-2,3-dihydro-1,3-diboroly})$ ruthenium Derivates **35b** vorgestellt, dessen Faltung entlang des B...B Vektors (40.7°) sehr ähnlich wie im analogen Eisen-Komplex (41.3°) ist. Die Elektronenstruktur der Modell-Sandwichkomplexe Ru (**35**) und Fe (**36**) wurde untersucht (von Dr. I. Hyla-



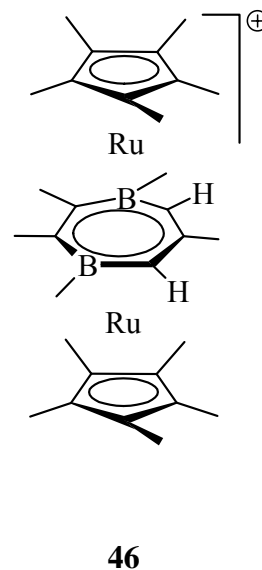
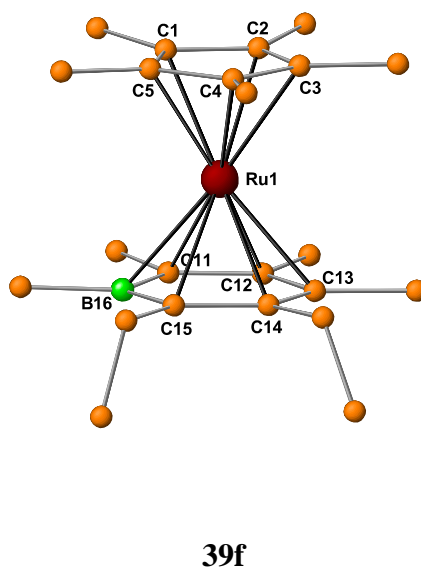
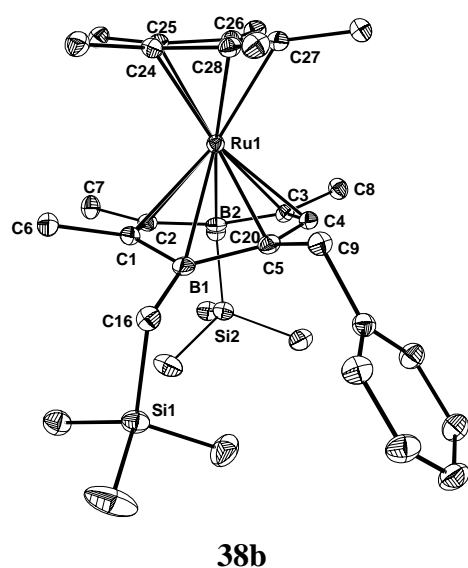
Kryspin, Universität Münster). Die DFT Rechnungen zeigen, dass die Faltung des 1,3-Diborolyl-Liganden elektronischen Ursprungs ist, und die Grundkörper **35** and **36** mit einem gefalteten 1,3-Diborolyl-Liganden energetisch stabiler sind (24.5 und 24.9 kcal/mol für die Ru- und Fe-Komplexe im Vergleich zu **35'** und **36'**) als mit planaren Liganden.

Die Reaktivität von **35** wird hinsichtlich einer Insertion von terminalen Alkinen in den C₃B₂-Heterocyclus untersucht, was zu den neuen 18 VE Ruthenocen-analogen Komplexen **38** mit siebengliedrigen 4-Borataborepin-Liganden führt. Zusätzlich werden die Boratabenzol-Komplexe **39** und Triarylbenzol-Derivate (in einigen Fällen) als Nebenprodukte identifiziert. Die Bildung von **39** ist das Ergebnis einer Eliminierung von Borandiyl [:BR²] aus den intermediären 4-Borataborepin-Komplexen. Die 4-Borataborepine fungieren in **38** als 6e Liganden und zeigen eine reduzierte Faltung entlang des B...B Vectors ($\alpha = 12.5^\circ$ in **38a**, 26° in **38b** und 15.2° in **38c**) im Vergleich zu 40.7° in **35b**.

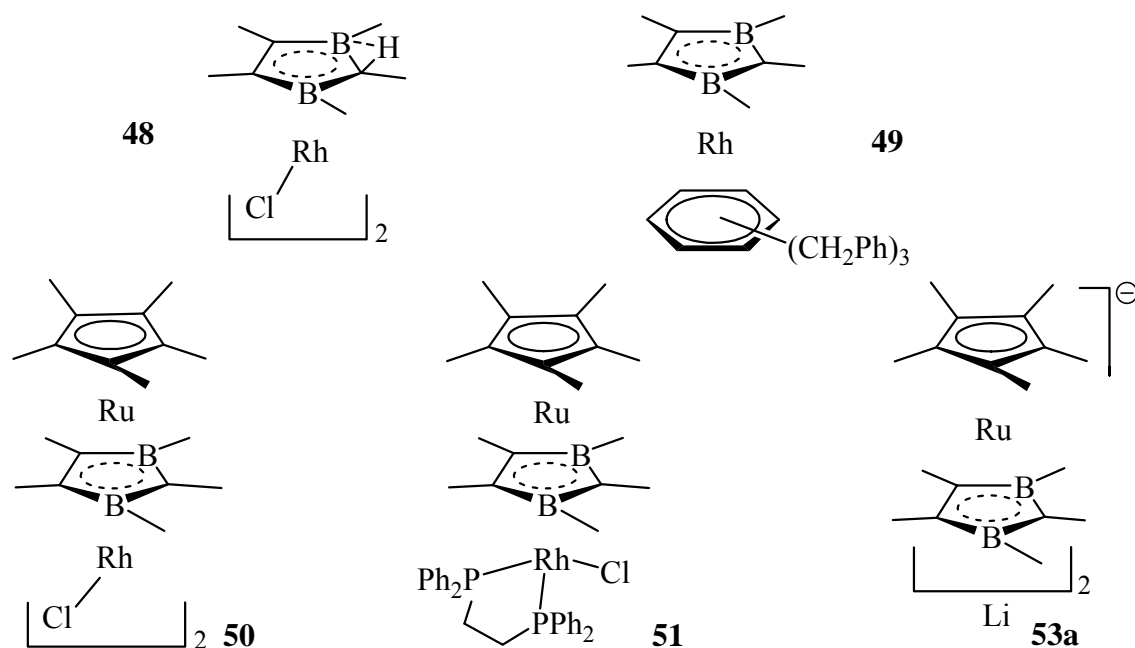


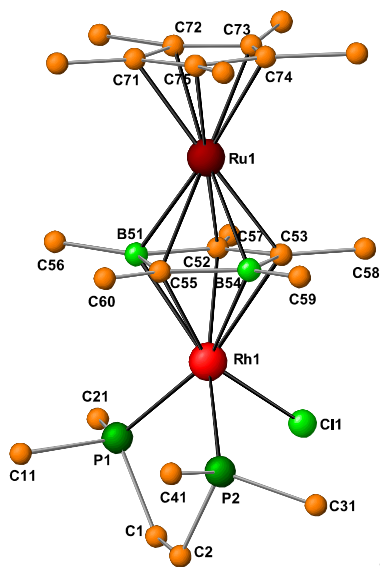
38	a	b	c	d	e	39	a	b	c	d	e	f	g
R ²	Me	CH ₂ SiMe ₃	Me	Me	Me	R ²	Me	CH ₂ SiMe ₃	Me	Me	Me	Me	Me
R ⁴	CH ₂ Ph	CH ₂ Ph	Ph	SiMe ₃	H	R ⁴	CH ₂ Ph	CH ₂ Ph	Ph	SiMe ₃	H	Et	<i>p</i> -Tolyl
						R ⁵	H	H	H	H	H	Et	<i>p</i> -Tolyl

Die Boratabenzol-Komplexe **39f,g** werden als Hauptprodukt in der Umsetzung von **35a** mit disubstituierten Acetylen (3-Hexin und Di-*p*-tolylacetylen) erhalten. Die letztere Reaktion ergibt eine Mischung von **39g**, (*Z,Z*)-1,2,3,4-Tetratolyl-1,3-butadien und den kationischen Tripeldecker-Komplex **46**, der strukturanalytisch untersucht ist. In **46** liegt ein siebengliedriger C₅B₂-Ring als Brückenligand mit zwei CH-Gruppen vor, die durch eine CMe-Gruppe getrennt sind.

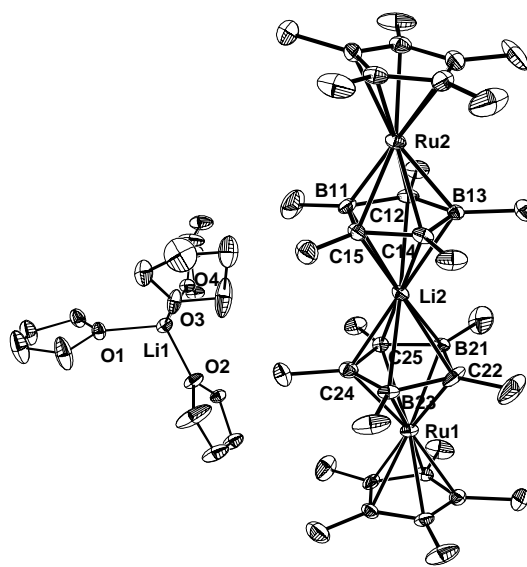


Eine vergleichende Untersuchung über die Reaktivität des [(1,3-diborol)RhCl]₂-Dimers **48** zeigt, dass die Umsetzung mit PhCH₂C₂H unter Cyclotrimerisierung zum (1,3-Diboroly)-Rh(arene) **49** führt. Die Reaktion von **50** mit Phenylacetylen ergab ein gelb-braunes Produkt, das vermutlich ein Cyclobutadien-Analogen von **51** ist. Der dimere RuRh-Komplex **50** reagiert mit dppe zu dem strukturell untersuchten 30 VE Tripeldecker **51**. Der anionische Tetradecker **53a** wurde durch Umsetzung von **35a** mit Lithium erhalten und strukturell charakterisiert. In **53a** verbrückt ein Li-Kation zwei Sandwich-Anionen **35a**⁻, während das zweite mit THF solvatisiert ist und separiert vorliegt.



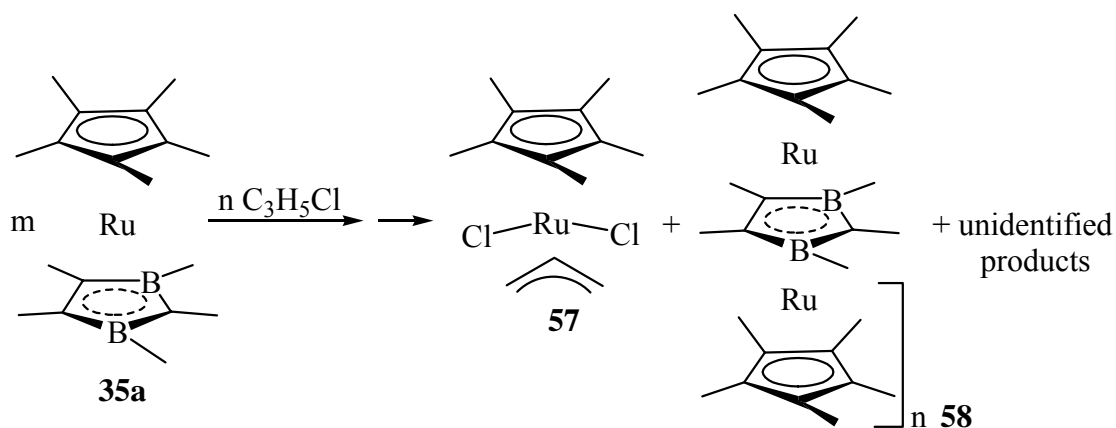


51

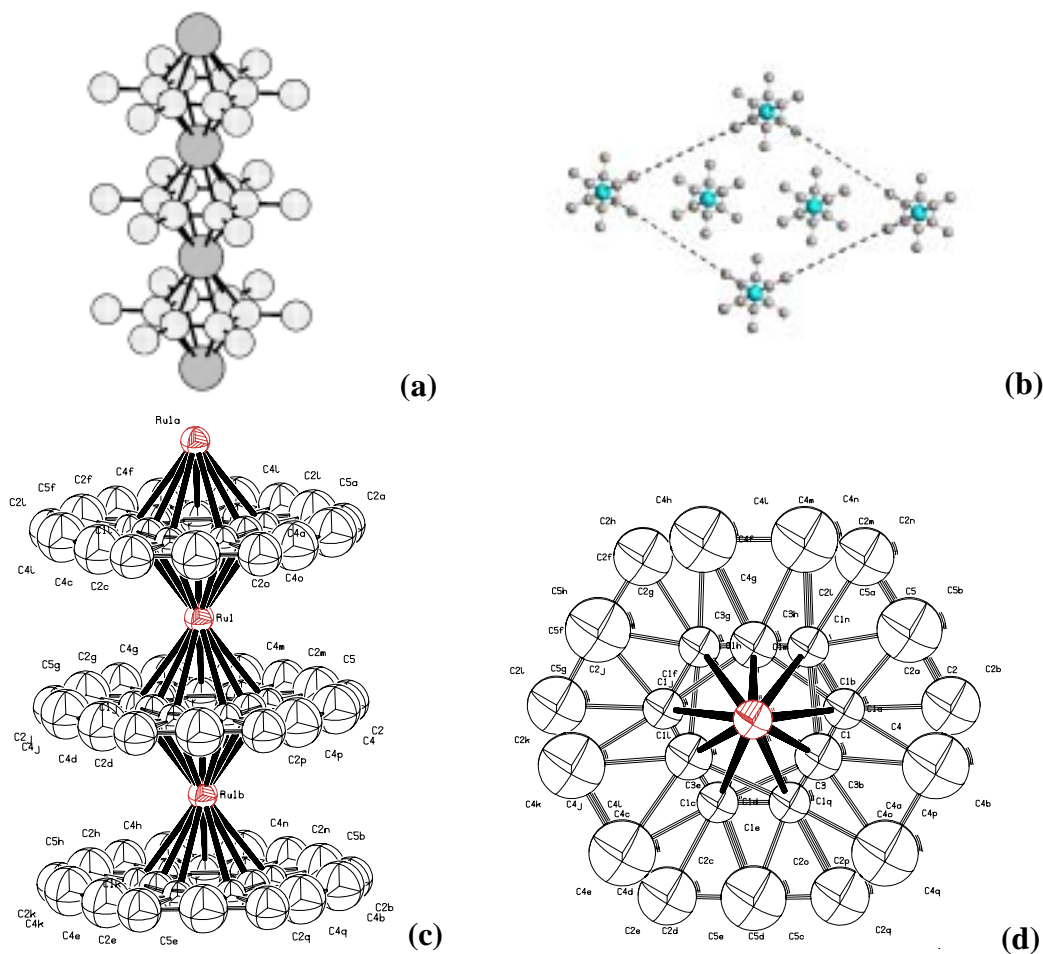


53a

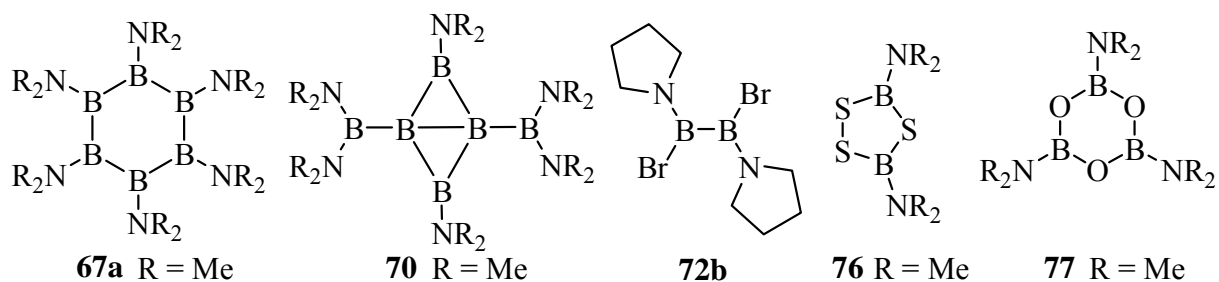
Die komplexe Reaktion von **35a** mit Allylchlorid führt zu **57** und einem Gemisch, aus dem der neue Komplex **58** isoliert wurde. Seine Identität und der Mechanismus der Bildung sind noch nicht geklärt. Jedoch zeigen die Ergebnisse von MS-Studien und zwei unabhängige, aber nur partiell gelöste Strukturanalysen, dass **58** eine Stapel-Anordnung von Rutheniumatomen mit verbrückenden Cp*- und 1,3-Diborolyl-Liganden aufweist. Die Umsetzung von **35a** und **57** ergibt den Tripeldecker **58** mit $n = 1$. Durch Stapelung des Tripeldeckers **58** mit Cp*Ru-Komplexfragmenten entsteht vermutlich der kristalline Oligodecker **58** ($n \geq 2$).



Vorläufige Ergebnisse der Strukturanalyse von **58** sind in Abb. (a) und (b) (Dr. C. Hu, Aachen) sowie in (c) und (d) (Prof. H. Wadepohl) dargestellt. (a) und (c) zeigen Seitensichten der Stapel, (b) und (d) Aufsichten. Die Stapel sind entlang einer dreizähligen Achse angeordnet, was entweder mit intensiven Fehlerrordnungen oder mit einer Drillingsbildung der Kristalle vereinbar sein würde. Im Massen-Spektrum werden als grösste Molekülionen die Tetradecker $(\text{Cp}^*\text{Ru})_3\text{Cp}^*$ und $(\text{Cp}^*\text{Ru})_3(\text{C}_3\text{B}_2\text{Me}_5)$ gefunden.



Im Kapitel 3.6 wird die Reaktivität von $(\text{Me}_2\text{N})_2\text{B}_4[\text{B}(\text{NMe}_2)_2]_2$ (**70**) untersucht, und es werden einige Pyrrolidinboran-Derivate hergestellt, um neue cyclische Borane aufzubauen. Die Umsetzung von Tetrapyrrolidinodiboran(4) mit BBr_3 (1 Äquiv.) gibt eine Gemisch, mit zwei Äquiv. BBr_3 wird kristallines **72b** als Hauptprodukt erhalten, das Dimorphismus zeigt.



Die Umsetzung vom **70** mit S_8 und Me_3NO führt zu den bekannten Heterocyclen 1,2,4,3,5-Trithiadiborolan **76** und Boroxin **77** unter Spaltung der rhombischen B_4 -Einheit. Durch Erhitzen des nichtklassischen **70** erfolgt eine Umlagerung in das klassische **67a**.

1. Introduction

1.1 Organoboranes and carboranes

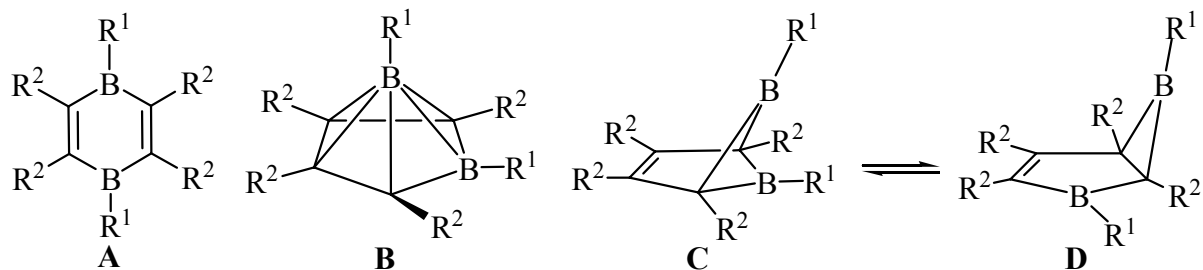
Since the pioneering work of Stock et al.^[1] on boron hydrides almost a century ago, boron chemistry has developed into a fascinating area including organoboranes, polyhedral borane and carborane clusters.^[2] Research in these fields has led to much progress on both theoretical aspects and practical applications.^[3,4]

The bonding of the electron-deficient boron atoms (3 valence electrons, 4 valence orbitals) involves classic two-center, two-electron (2c-2e) bonds, and nonclassic multi-center bonds (BBB and BHB three-center, two-electron, 3c-2e), first proposed by H. Longuet-Higgins^[5] and developed by W. N. Lipscomb.^[3a] The geometries of the polyhedral borane and carborane clusters can be predicted, with some exceptions, by the Wade-Mingos^[6] electron counting rules: a *closo* structure contains $2n + 2$ SE (n = number of vertices of a polyhedron, SE = skeletal electrons), a *nido* structure $2n + 4$ SE, and an *arachno* structure needs $2n + 6$ SE.

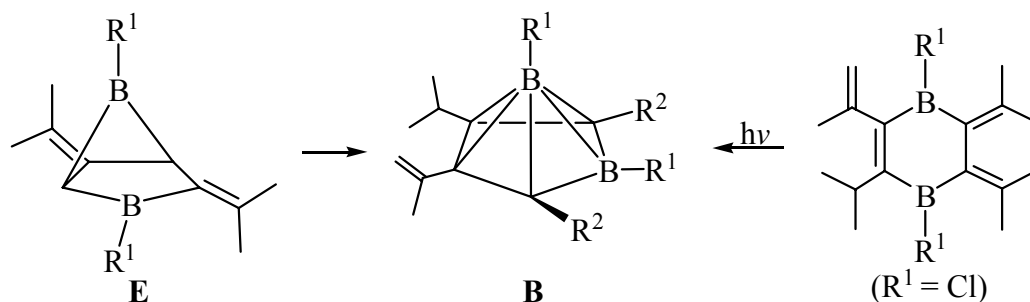
The synthetic strategies for carboranes include cage or polyhedron growth via carbon or boron insertion, cage fusion, selective cage degradation, and cage coupling.^[7] The first carboranes, i.e., the *closo*-carboranes, 1,5-C₂B₃H₅, 1,2-C₂B₄H₆, 1,6-C₂B₄H₆, and 2,4-C₂B₅H₇, were discovered by Williams et al. in the early 1960s, from the reaction of pentaborane(9) and C₂H₂ in low yield.^[8] Although many carborane derivatives have been prepared and characterized, there is a limited number of carborane clusters prepared via organoboranes. By selecting appropriate substituents with various electronic and/or steric properties on boron atoms, small organoboranes can serve as starting materials for carborane clusters, which has been demonstrated as a practical pathway.^[9] The methods commonly used are (i) hydroboration of unsaturated boraheterocycles or species containing (exocyclic) double or triple bonds, (ii) reduction of (unsaturated) organo(halo)boranes or boraheterocycles, (iii) thermal or photochemical isomerization and/or partial decomposition, or a combination of these methods.

The carbon-rich organoborane/carborane systems have attracted considerable interest because the structures lie on the border between the classic and nonclassic structures, depending to a large extent on the substituents at the boron atoms. In this context the C₄B₂H₆ is

a typical example. With $R^1 = \text{F}$, OMe or ferrocenyl groups, the structure observed is a 1,4-dibora-2,5-cyclohexadiene **A**.^[10]

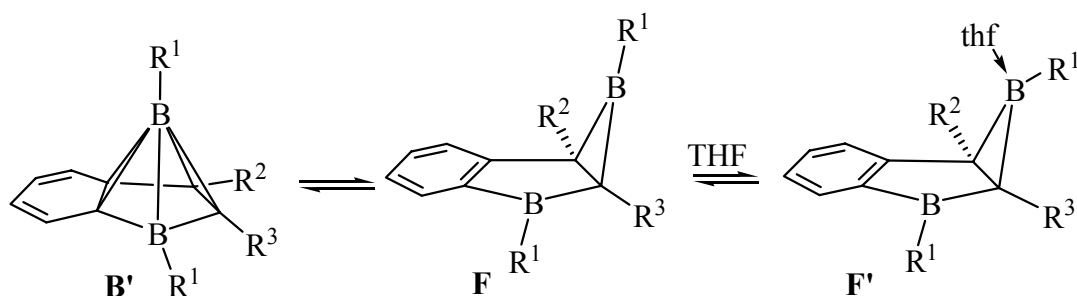


When $R^1 = \text{alkyl}$, aryl, H or Cl, Br and I substituents, the carborane structure 2,3,4,5-tetracarba-1,6-*nido*-hexaborane(6) **B** dominates.^[11] With one amino substituent **B** is still favored, but with two amino groups it rearranges into a bicyclic structure, where an equilibrium exists between **C** and **D**.^[12]



Scheme 1

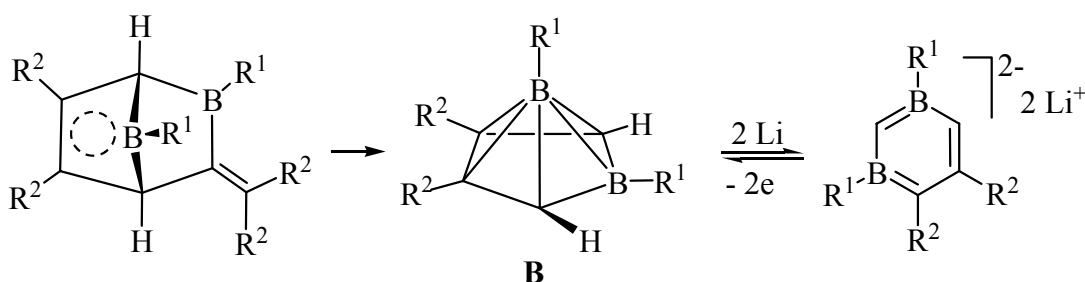
The intermediate compound of **E** ($R^1 = t\text{Bu}$) rearranges into a carborane at ambient temperature (Scheme 1). The photochemical transformation of a diboraheterocycle leads to the same carborane framework **B**.^[13]



Scheme 2

An equilibrium exists between the benzocarborane **B'** ($R^1 = t\text{Bu}$) and the benzobicyclic species **F** (Scheme 2), in which the carborane structure dominates, whereas with $R^1 = \text{mesityl}$, **B'** and **F** are of similar amount in solution. In the presence of Lewis bases such as

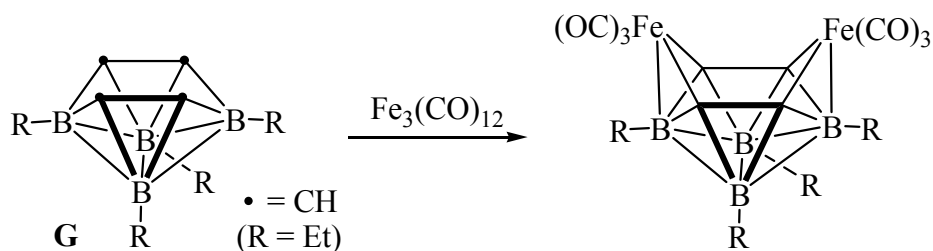
tetrahydrofuran the adduct **F'** is formed, which on heating gives back the benzoring **F**.^[14]



Scheme 3

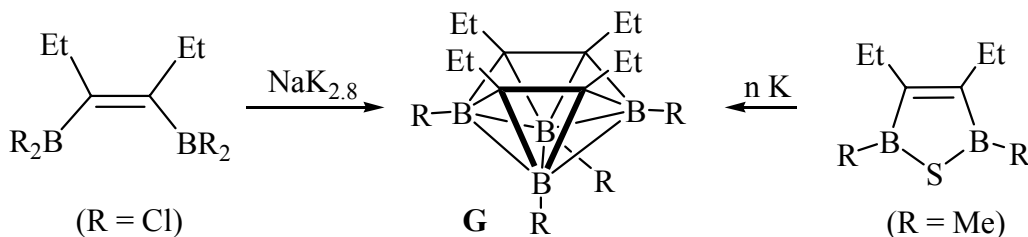
On heating, the bridged bishomoborirene ($R^1 = t\text{Bu}$, $R^2 = \text{SiMe}_3$, Scheme 3) eliminates bis(trimethylsilyl)ethyne and forms the carborane derivative **B**. Its reductive opening with Li produces a 1,3-diboratabenzene, which on oxidation gives back the carborane **B**.^[15]

Derivatives of the *nido*-C₄B₄H₈ **G** have been obtained by transition metal-promoted reactions of polyboron clusters.^[16] By hydroboration of bis(diethylboryl)acetylene with an excess of (Et₂BH)₂ (“hydride bath”), the intermediates are proposed to be cyclic species, which, by Et₂BH-catalyzed elimination of BEt₃ afford the *nido*-C₄B₄ carborane **G** (Scheme 4).



Scheme 4

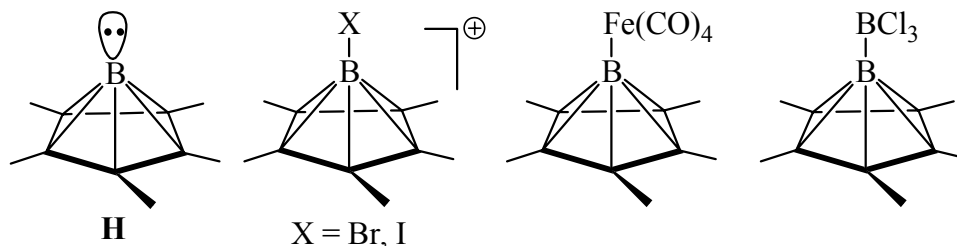
The products have been studied by NMR, *ab initio* calculations, and X-ray structure analyses. **G** reacts with Fe₃(CO)₁₂ to give the crystalline hexacarbonyldiferracarborane derivative, which is isostructural with *nido*-decaborane(14).^[17]



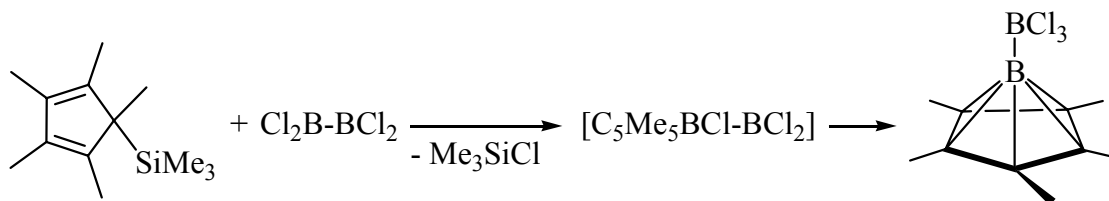
Scheme 5

Different pathways were found to generate other derivatives^[18] (Scheme 5). Both the reduction of organo-substituted 1-thia-2,5-diborole with potassium, and the dehalogenation of (*Z*)-3,4-bis(dichloroboryl)-3-hexene with copper vapor or NaK_{2.8} alloy led to new *nido*-C₄B₄

carborane derivatives **G** (R = Me, Cl) in low yields, the *nido*-structure has been confirmed by an X-ray diffraction analysis of the tetrachloro compound.^[18d]



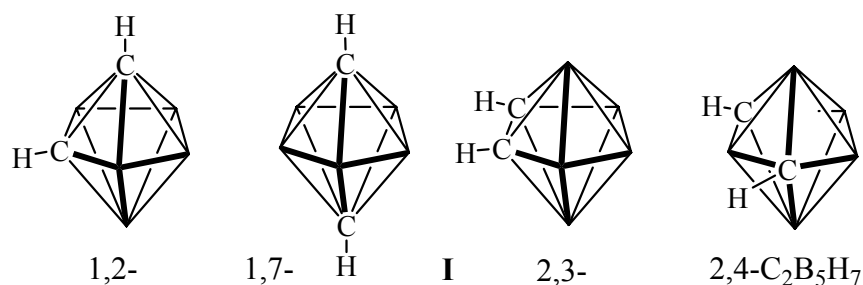
While the free 1-boranediy1-2,3,4,5,6-pentacarbora-*nido*-hexaborane(6) **H** is not known, its stabilization has been realized by Lewis acidic groups, such as Br^+ , I^+ , $\text{Fe}(\text{CO})_4$ and BCl_3 . The first derivatives $[\text{H-X}]^+\text{BX}_4^-$ (X = Br, I) were prepared by Jutzi et al.^[19] by the reaction of $\text{Me}_5\text{C}_5\text{-GeMe}_3$ with an excess of BX_3 (X = Br, I). The analogous reaction of $[(\text{Me}_5\text{C}_5)\text{Al}]_4$ with BBr_3 afforded $[\text{H-Br}]^+\text{AlBr}_4^-$, which was confirmed by an X-ray diffraction study.^[20]



Scheme 6

$\text{C}_5\text{Me}_5\text{-BCl}_2$ reacts with $\text{Na}_2[\text{Fe}(\text{CO})_4]$ to give $\text{H-Fe}(\text{CO})_4$, theoretical and structural studies indicate that the *nido*-skeleton acts as a 2e donor to the metal complex fragment $\text{Fe}(\text{CO})_4$.^[21] $(\eta^5\text{-Me}_5\text{C}_5)_2\text{Si}$ reacts with B_2Cl_4 to give a mixture, from which $\text{C}_5\text{Me}_5\text{B-BCl}_2\text{-SiCl}_2\text{C}_5\text{Me}_5$ and $\text{C}_5\text{Me}_5\text{B-BCl}_2\text{-Si}(\text{C}_5\text{Me}_5)_2\text{Cl}$ were identified. A direct synthesis was realized from $\text{C}_5\text{Me}_5\text{-SiMe}_3$ and B_2Cl_4 to produce the carboranediyl-trichloroborane adduct **H-BCl₃** (Scheme 6).^[22]

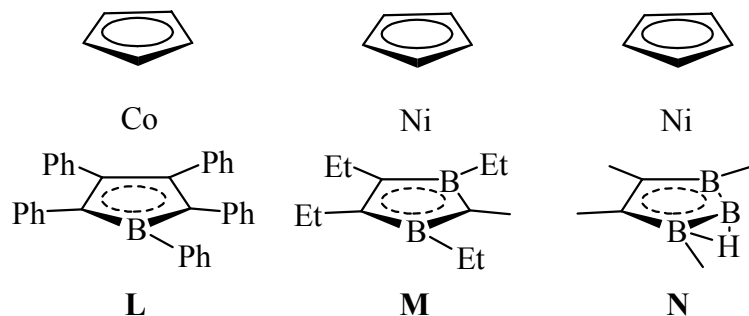
Of the four possible isomers of the *closo*- $\text{C}_2\text{B}_5\text{H}_7$ carborane (**I**) (1,2-, 1,7-, 2,3- and 2,4-), only the 2,3- and 2,4-isomers are known, and studies on its chemistry have been focused on the 2,4-isomers.^[23] The 2,3-isomer is predicted by calculations to be 15-25 kcal/mol less stable than the 2,4-isomer.^[24]



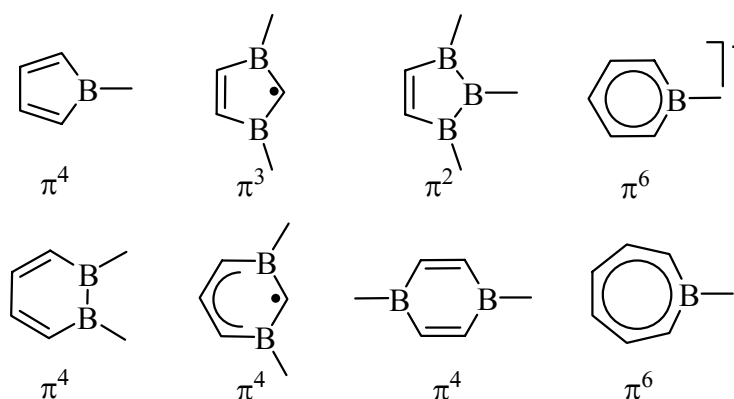
carborane 1,2-[C₆H₄(CH₂)₂]-3-Ph-1,2-C₂B₁₀H₁₀ (**K**); the shape of the cluster is that of a hencosahedron. Theoretical studies predict that it might be possible for other even larger skeletons to be discovered.

1.2 Boron heterocycles as ligands to transition metals

Since the serendipitous discovery of ferrocene [Cp₂Fe]^[32] in 1951 and the following studies,^[33] the carbocyclic π-complexes involving C₈H₈²⁻, C₇H₇⁺, C₆H₆, C₅H₅⁻, C₄H₄²⁻ have been extensively studied. Soon after the synthesis of carborane^[8] and boron heterocycle^[34] in the late 1950s, the first carborane-containing ferrocene analog [(C₂B₉H₁₁)₂Fe]²⁻ with a five-membered “C₂B₃” open face was reported by Hawthorne.^[35] The first metallocenes with boron-containing heterocycles were reported in the 1970s. **L-N**^[36] are representative examples:

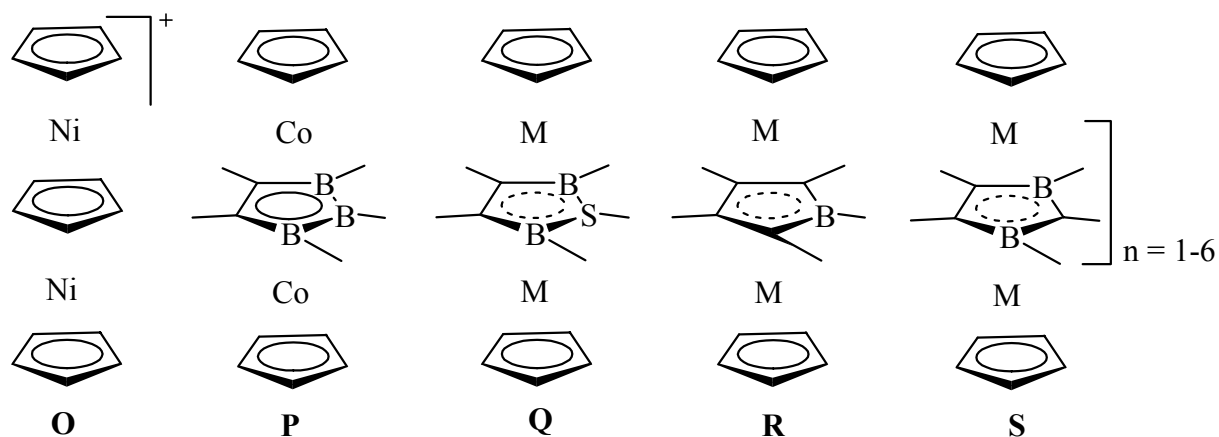


Organoboron heterocycles are important in organometallic chemistry, and link together the classic areas of π-complexes and polyhedral systems such as metallaboranes and metallacarboranes.^[37] Typical boron heterocyclic ligands (with the respective number of π electrons) are shown below.^[38]

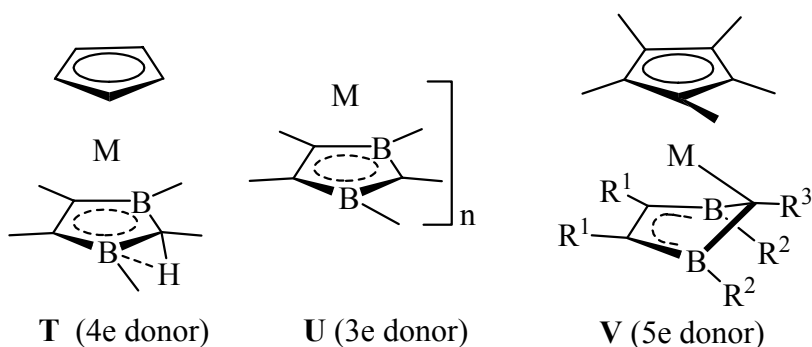


Many transition metal complexes have been synthesized and characterized with boron heterocycles as ligands, incorporating additional heteroatoms such as N, S, O, etc. as well. The

replacement of carbon atoms in carbocycles by electron-poor boron atoms gives rise to high acceptor capabilities, which allows the mono- and bifacial coordination with transition metals to form oligodecker and even stacked multidecker complexes (polydecker), while the carbocyclic π -systems benzene and cyclopentadienyl at present only allow the formation of triple-decker complexes.



The first triple-decker complex cation $[\text{Cp}_3\text{Ni}_2]^+$ (**O**) reported by Werner and Salzer has a bridging C_5H_5 ligand bifacially coordinated to two CpNi fragments.^[39] Shortly thereafter, Grimes et al. reported the first boron-containing analog $[\text{CpCo}(\mu\text{-C}_2\text{B}_3)\text{CoCp}]$ ^[40] (**P**) with a bridging boron heterocycle. Since Hoffmann's calculations^[41] on triple-decker complexes, new types of complexes were reported (**Q**,^[42] **R**^[43] and **S**^[44]).



The 2,3-dihydro-1,3-diborole(y) ligand (C_3B_2) is of particular interest. The neutral 1,3-diborole in **T** acts as a 4e ligand (via the $\text{C}=\text{C}$ double bond and a $\text{C}-\text{H} \rightarrow \text{M}$ 3c-2e interaction), while the 1,3-diborolyl in most of the cases functions as a 3e ligand, which allows the formation of sandwich complexes of type **M**, a series of oligodecker (triple-, tetra-, penta-, hexadecker) (**S**)^[44] and even polydecker complexes (**U**).^[45] In a few special cases, the 1,3-diborolyl ligand donates five electrons (**V**, see below) to metal centers, forming structures of

type **V** ($M = \text{Fe}^{[46]}$, $\text{Ru}^{[46d,47]}$).

The first complete family of triple-decker sandwich complexes of 1,3-diborolyl ligand $\text{CpM}(\mu\text{-C}_3\text{B}_2)\text{M}'\text{Cp}$ have a combination of metal pairs ranging from $\text{MM}' = \text{FeFe}^+$ cation (28 VE) to NiNi^- anion (34 VE). A series of mixed-ligand triple-decker complexes containing 1,3-diborolyl and carboranyl or heteroboranyl ligands have also been prepared.^[48]

The most exciting discovery in this direction is the synthesis and characterization of the first and currently only known polydecker complexes $[\text{M}(\mu\text{-C}_3\text{B}_2)]_n$, ($M = \text{Ni}, \text{Rh}$) (**U**).^[45] Conductivity investigations indicate that nickel-containing polydeckers are semiconductors whereas the rhodium complexes are insulators.

The green iron complex **V**^[46c,d] ($\text{R}^1 = i\text{Pr}$, $\text{R}^2 = \text{Et}$, $\text{R}^3 = \text{Me}$, Fig. 1) is a formally 16 VE species, having a high thermal stability (m.p. 210 °C). The X-ray structure analysis reveals that the five-membered 1,3-diborolyl ring is not planar, but folded along the B...B vector (folding angle 41.3°). The Extended Hückel calculations^[46d] (Fig. 2) show that the folded structure is 9.8 kcal/mol in energy more stable than the corresponding structure with a planar diborolyl ligand, and a high-lying combination of the $\sigma(\text{B-C})$ orbitals donates two electrons to the d_{xz} orbital of Fe, thus fulfilling its 18 valence electron configuration ($\pi^5 + d^8 + \pi^3 + \sigma^2$). However, the HOMO is higher than that of ferrocene and complexes **V** are actually electron-poor 18 VE species.

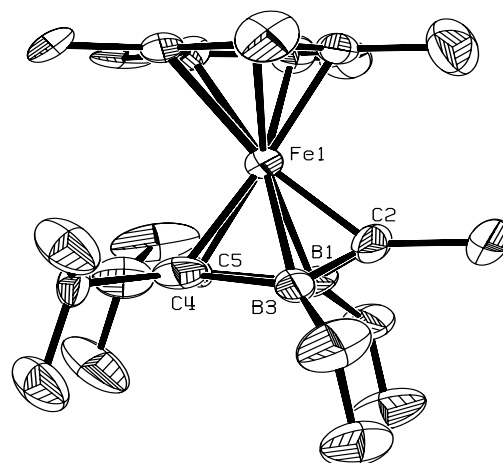


Fig. 1. The structure of sandwich **V**.

As to the electron configurations of the boron containing sandwich complexes, the 18 VE rule^[49] is well applicable for mononuclear compounds. For di- and oligonuclear compounds, the corresponding number of valence electrons is 30 (triple-decker)^[41], 42 (tetradeccker),^[50, 38a] and $12n + 6$ for oligodecker complexes^[44] (where n is the number of stacks, metal + ligand),^[45b, 50] respectively. As the number of VE of triple-decker complexes depend on the metals (FeFe^+ : 28 \rightarrow NiNi^- : 34 VE), the family of tetradecckers^[44] have related numbers (40 - 46) of VE. Alternatively, the closed-shell sandwich complexes (of 18, 30, 42 VE) can be

regarded as cluster compounds with metal complex fragments as vertices, according to the above- mentioned Wade-Mingos rules.^[6]

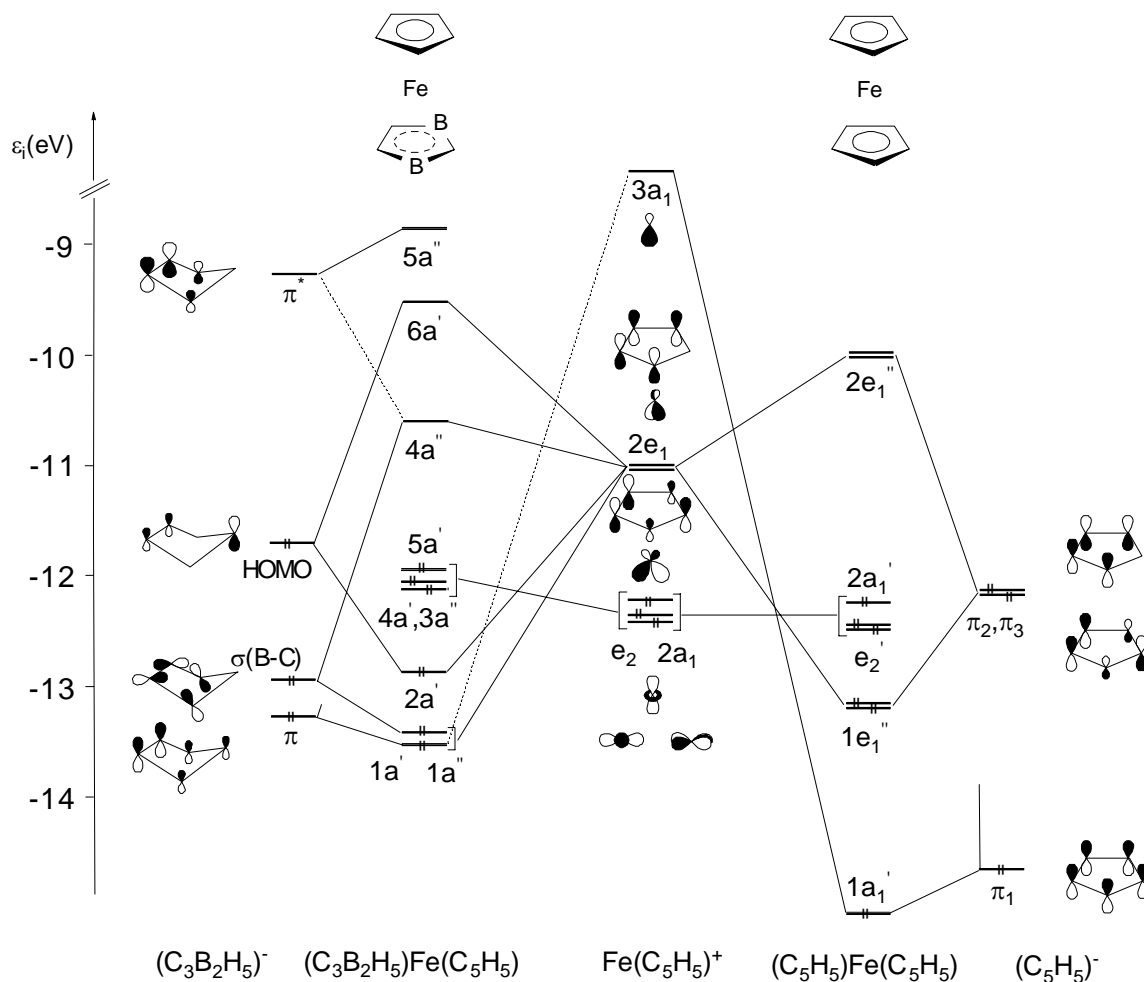
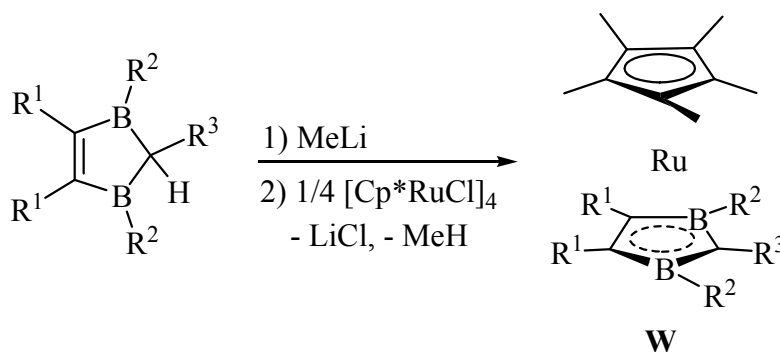


Fig. 2. Qualitative MO scheme of ferrocene and V.

2. Objectives

In this dissertation, the first objective is to study organoborane/carborane systems. To synthesize and characterize new boron-functionalized *nido*-C₄B₂H₆ (**B**) and *nido*-C₄B₄H₈ (**G**) derivatives, and their reactivities have to be studied. Possible intermediate species may be trapped, owing to the interesting transformations between classic and nonclassic structures of the unique organoborane/carborane systems. A further objective is to prepare some boron functionalized *closo*-2,3-C₂B₅H₇ (**I**) and C-borylated *o*-carborane (**J**) derivatives, and to study their reactivities.

The second is to further study the reactivities of the violet, electron-poor 2,3-dihydro-1,3-diboroly-ruthenium complexes **W**, which are isoelectronic with **V**, and synthesized by reactions of organyl-substituted 2,3-dihydro-1,3-diboroles with MeLi and [Cp*₂RuCl]₂ (Scheme 9).^[47] As has been assumed, but not confirmed, the boron heterocycle in **W** has a folding along the B...B vector similar to that in the green iron analog.^[46] The acceptor property and the folding effect lead to unique reactivities^[47] towards electron-donor ligands (CO, *t*BuNC, and phosphane), stacking metal complex fragments (CpCo, RhCl), oxidative addition (H₂, BH₃), and insertion of phosphaalkyne :P≡C*t*Bu (to form a rutenaphospha-carborane complex). One important task is to obtain crystalline species for studying the detailed structure and bonding situations in such formal 16 VE sandwich complexes **W**. The reactivities of **W** with alkynes and other unsaturated small molecules will be tested.

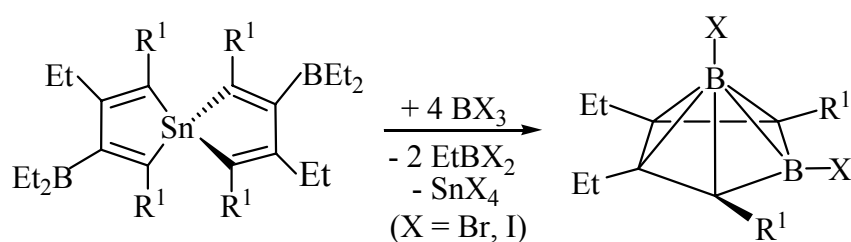


Scheme 9

3. Results and discussion

3.1 Synthesis and reactivity of 2,3,4,5-tetracarba-*nido*-hexaboranes(6)

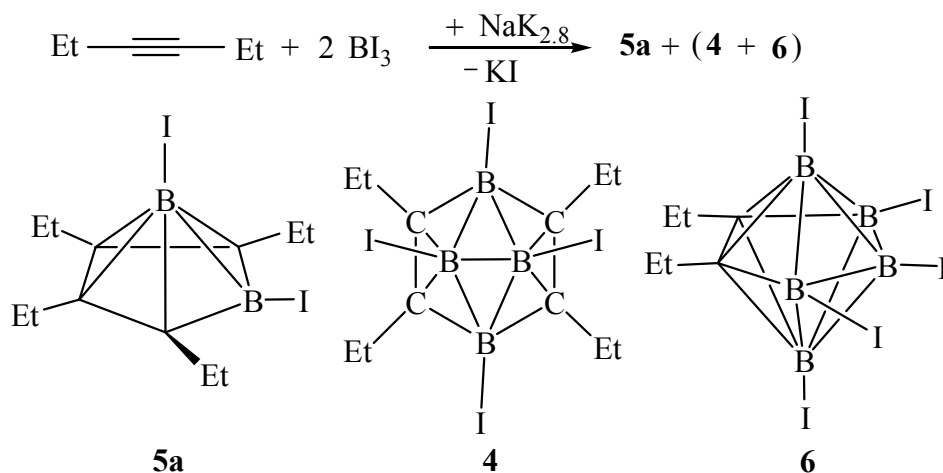
Although peralkylated 2,3,4,5-tetracarba-*nido*-hexaboranes(6)^[11c-f] (known since mid 1960s) are more stable than the parent compound C₄B₂H₆^[11a,b] and are readily available by a variety of methods, their reactivities have only recently been studied.^[11g,14,15,51] To investigate substitution reactions in C₄B₂-*nido*-carboranes, functional groups at the boron atom(s) other than alkyl groups are needed.



Scheme 10

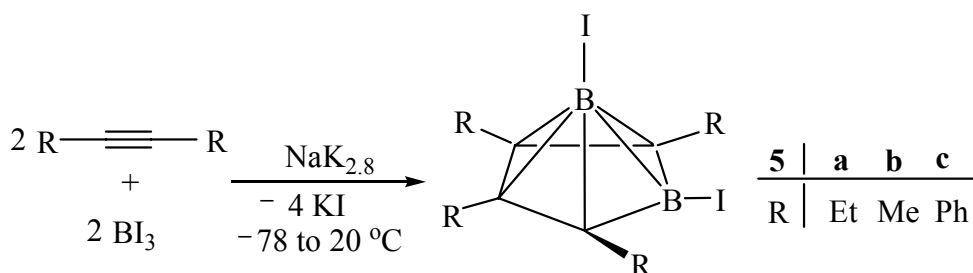
Wrackmeyer et al. were able to obtain 1,6-dibromo-2,3,4,5-tetracarba-*nido*-hexaboranes(6)^[11g] by reacting 1,4,6,9-tetraalkyl-3,8-diethyl-2,7-bis(diethylboryl)-5-stanna-spiro[4.4]nona-1,3,6,8-tetraenes with BBr₃ (Scheme 10). They also studied the reaction between peralkylated 2,3,4,5-tetracarba-*nido*-hexaboranes(6) and an excess of BBr₃, whereby the corresponding B6-bromo substituted carboranes were formed.^[51a] Nucleophiles were found to replace the basal B6-bromo atom to give the corresponding carboranes with organyl,^[51b] stannyl,^[51c] diphenylphosphanyl^[51d] as well as the N-bonded (μ-NS)Fe₂(CO)₆^[51e] group. In the 1,6-dibromo case, substitution with the N-bonded (μ-NS)Fe₂(CO)₆ cluster took place at the basal B-Br bond, an excess of the nucleophile did not induce additional substitution of the 1-position.^[51e]

In our efforts to prepare the iodo analog of the tetracarba-*nido*-octaborane(8) (EtC)₄(BCl)₄^[18b-d] we have developed a convenient one-pot route to 1,6-diiodo-2,3,4,5-tetracarba-*nido*-hexaboranes(6) involving alkynes, BI₃ and NaK_{2,8} alloy. Here, apart from the formation of the expected *nido*-(EtC)₄(BI)₄, the synthesis and characterization of the resulting C₄B₂-*nido*-carboranes are described as well as a proposed formation mechanism, and reactivity towards a variety of nucleophiles.



Scheme 12

Starting at low temperature ($-78\text{ }^{\circ}\text{C}$) the same reaction gives **5a** as the single product in 51 % yield as a yellow, sensitive and viscous oil. The yield increases to 66 % when a 1:1 ratio of 3-hexyne and BI_3 is used (Scheme 13). In the latter case a very small amount of hexaethylbenzene is also detected.



Scheme 13

The ^{11}B -NMR spectrum of **5a** exhibits two signals at $\delta = 5.5$ and -52.5 ppm. The ^1H -NMR spectrum shows an ABX_3 spin pattern for the methylene protons of the ethyl groups, and in the ^{13}C -NMR spectrum the corresponding four signals for the two different ethyl groups appear. The signal responsible for the skeletal carbon atoms non-adjacent to the basal boron is found, while the signal for the other two skeletal carbon atoms (expected at ca. $105\text{ ppm}^{[11g]}$) is not observed. It should be noted that the formation of **5a** was first detected by Wrackmeyer et al.,^[11g] as they carried out reactions on small scale for NMR studies.

The analogous reaction with 2-butyne proceeds smoothly, however, the yellowish *nido*-(MeC) $_4$ (BI) $_2$ (**5b**) is obtained only in low yield. The ^{11}B -NMR spectrum exhibits two signals at $\delta = 5.7, -48.6$ ppm and the ^1H -NMR spectrum shows two singlets for the two different methyl groups. The ^{13}C -NMR spectrum gives the corresponding signals for methyl

and the skeletal carbon atoms non-adjacent to the basal boron, while the signal for the other two skeletal carbon atoms is not observed. In the mass spectrum the molecule ion peak with the expected isotopic pattern is found.

While calculations^[57] suggest that such *nido*-carboranes carrying halogen substituents at the boron atom(s) would prefer a classic 1,4-diboracyclo-2,5-hexadiene structure, we have found that **5a** and **5b** are perfectly stable like the bromo analogs.^[11g,51a] The reaction of diphenylacetylene with BI₃/NaK_{2,8} also proceeds, however, the orange yellow *nido*-(PhC)₄(BI)₂ (**5c**) is obtained in low yield. It is characterized by ¹¹B-NMR ($\delta = 7.9, -50.1$ ppm), and HR-MS exhibits the molecule ion peak having the correct isotopic distribution. Unfortunately, the formation of significant amount of hexaphenylbenzene hampers the successful isolation and satisfactory NMR spectra. Moreover, it is found to be unstable at RT, even when stored under nitrogen, as indicated by its color turning from orange yellow to pale yellow. This instability is different from **5a** and **5b**, and reminiscent of the instability of the iodoboration product of diphenylacetylene with BI₃, which leads to a 9,10-dihydro-9-boraanthracene derivative.^[55a]

3.1.2 Crystal structure of 1,6-diiodo-2,3,4,5-tetraethyl-2,3,4,5-tetracarba-*nido*-hexaborane(6) (**5a**)

The structures of the C₄B₂-*nido*-carboranes were previously studied by electron diffraction^[58] of the hexamethyl derivative (MeC)₄(BMe)₂, and by microwave spectroscopy^[59] of the parent derivative (HC)₄(BH)₂.^[11a,b] In 1992, Berndt et al.,^[14] reported the structure of a benzo-annelated derivative, and in 1996 Herberhold, Wrackmeyer et al.^[51e] published the structure of the first example of ‘undisturbed’ pentamethyl-*nido*-C₄B₂ carborane with a N-bonded Fe₂(CO)₆(μ -NS) complex fragment in 6-position. Derivatives of a benzo compound^[14] with transition metal complex fragments coordinated to the benzene ring have also been synthesized.^[51f]

On standing at r.t., yellow crystals of **5a** were obtained, whereas all bromo compounds are oil.^[11g,51a] Its molecular structure is shown in Fig. 3, the C₄B₂ skeleton adopts the expected *nido* structure (C_s symmetry) with the six-coordinate apical boron atom. The B–B bond length

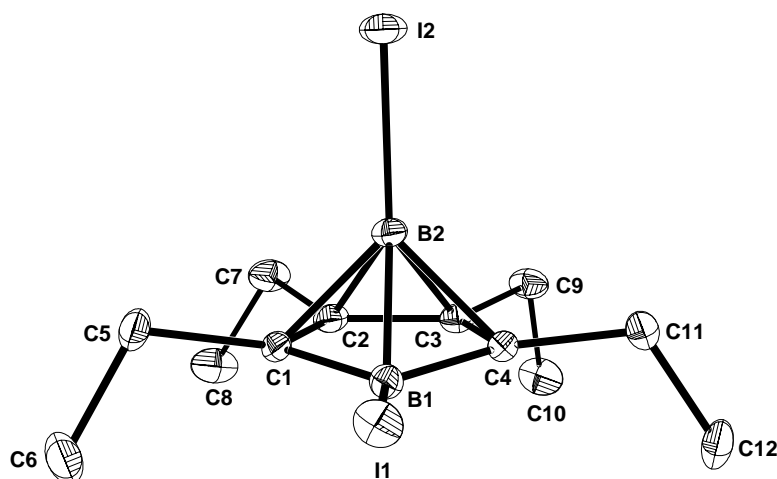
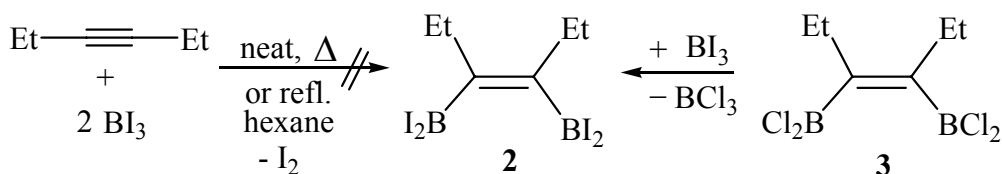


Fig. 3. Molecular structure of **5a**, hydrogen atoms omitted for clarity. Selected bond lengths [Å] and angles [°]: I1–B1 2.155(3), I2–B2 2.126(3), C1–C2 1.457(4), C2–C3 1.437(4), C3–C4 1.459(3), C1–B1 1.522(3), C4–B1 1.526(4), C1–B2 1.705(4), C2–B2 1.713(4), C3–B2 1.713(4), C4–B2 1.708(4), B1–B2 1.821(4); C2–C1–B1 108.3(2), C1–B1–C4 104.1(2), B1–C4–C3 107.9(2), C4–C3–C2 109.6(2), C3–C2–C1 109.2(2), B2–B1–I1 130.0(2), B1–B2–I2 140.1(2).

of 1.821 Å is similar to, but slightly shorter than the corresponding distances in (MeC)₄(BMe)[(B(μ-NS)Fe₂(CO)₆)]^[51e] (1.836 Å), the benzo-annelated structure^[14] (1.870 Å) and the parent derivative (HC)₄(BH)₂^[11a,b] (1.886 Å). The B2–C distances vary within a narrow range (1.705–1.713 Å), which are also slightly shorter than the values in the mentioned examples^[51e, 14] (1.720–1.743, 1.673–1.865 Å, respectively). This can be attributed to the different steric environments at the skeleton. The skeletal C–C distances are found to be almost identical (av. 1.451 Å), which are also comparable to the average of 1.438 Å, in (MeC)₄(BMe)(B(μ-SN)Fe₂(CO)₆). The four skeletal carbon atoms are in one plane, and the four *exo*-polyhedral carbon atoms C5, C7, C9, C11 are bent out of the C₄ plane towards B2 by av. 0.24 Å. The five-membered C₄B open face is not planar, with B1 lying ca. 0.15 Å below the C₄ plane, and the dihedral angle between the C₄ plane and the C₂B1 plane is ca. 9°. The B–I bond lengths are 2.126 and 2.155 Å, respectively, similar to the reported values in some B-iodinated polyhedral borane and carborane clusters, for example, av. 2.133 Å in HNB₁₁Cl₅I₆^[60] 2.09–2.17 Å in polyiodinated *p*-carboranes,^[61] and also similar to that in BI₃ [2.10(4) Å].^[62]

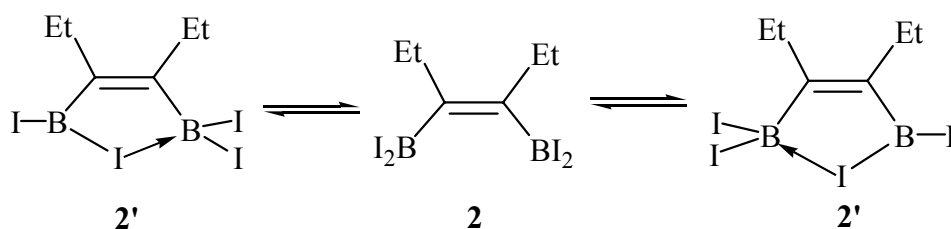
3.1.3 Formation of *nido*-(EtC)₄(BI)₄ (**4**) and crystal structure of 3,4-bis-(diiodoboryl)-3-hexene (**2**)

In order to verify the formation of compounds **4** and **6**, the independent dehalogenation of **2**^[52] is carried out. The attempts to obtain **2** (Scheme 14) via redox reaction of 3-hexyne and two equiv. of BI₃ were not successful.^[63] However, the halogen exchange reaction of **3**^[53] with BI₃ leads to **2**, a yellow crystalline solid, which is extremely sensitive to air and moisture.



Scheme 14

In solution, **2** exhibits one ¹¹B-NMR signal at $\delta = 11.8$ ppm; cooling the sample to -30 °C no change in the chemical shift is observed, only broadening of the signal. The significant shift to high field compared to **3** ($\delta = 53.9$ ppm) indicates some intra- or intermolecular interaction and suggests a fast equilibrium as shown in Scheme 15 to be present. An X-ray structure determination reveals that **2** forms an intra- molecular B-I-B bridge to yield **2'**.



Scheme 15

The molecular structure of **2** is shown in Fig. 4, the B1 and B2 groups are in *cis* position, and the I1 atom is coordinated to B1, forming a unique B–I–B bridge. The boron atom B2 is tri-coordinate, the B2–I4 bond length is 2.107 Å, typical of a I–B(sp²) distance, while B1 is four-coordinate, the B1–I2 and B1–I3 distances are 2.231 and 2.201 Å, respectively, very similar to the reported values for I–B(sp³) bonds, e.g. av. 2.21(1) Å in [Ph₂PBI₂]₂^[64] and av. 2.229 Å in (vi₃P)BI₃^[65] (where vi is vinyl). The B–I bond distances involving the bridging I1 atom are 2.160 and 2.383 Å, respectively, and the latter is longer than the sum of the covalent

radii of the two atoms, indicating the interaction between B1 and I1 is weak.

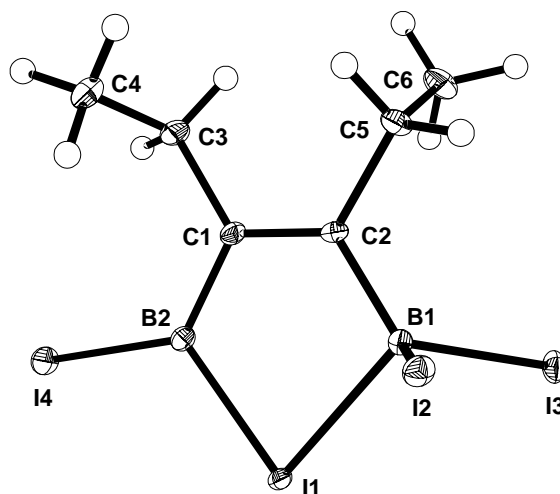
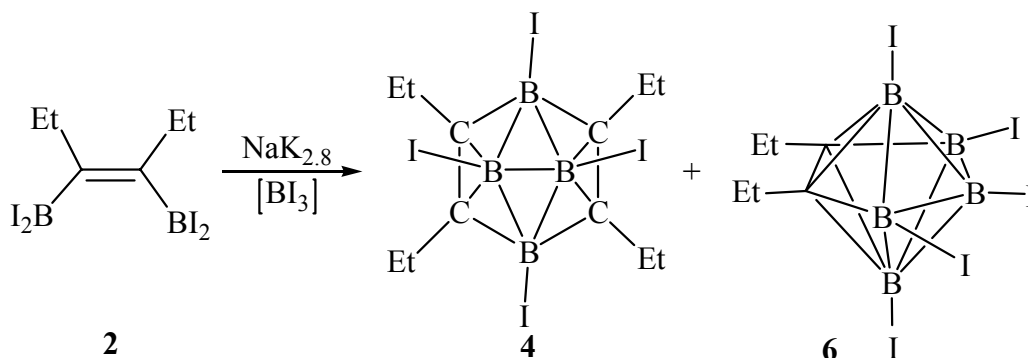


Fig. 4. Molecular structure of **2**. Selected bond lengths [\AA] and angles [$^\circ$]: I1–B2 2.160(4), I1–B1 2.383(4), I2–B1 2.231(4), I3–B1 2.201(4), I4–B2 2.107(4), B1–C2 1.571(6), B2–C1 1.510(5), C1–C2 1.371(5), B2–I1–B1 81.1(2), C2–B1–I3 117.0(3), C2–B1–I2 111.0(3), I3–B1–I2 112.25(18), C2–B1–I1 102.8(2), I3–B1–I1 105.9(2), I2–B1–I1 106.8(2), C1–B2–I4 127.7(3), C1–B2–I1 113.8(3), I4–B2–I1 118.5(2), C2–C1–B2 118.5(3), C1–C2–B1 123.5(3).

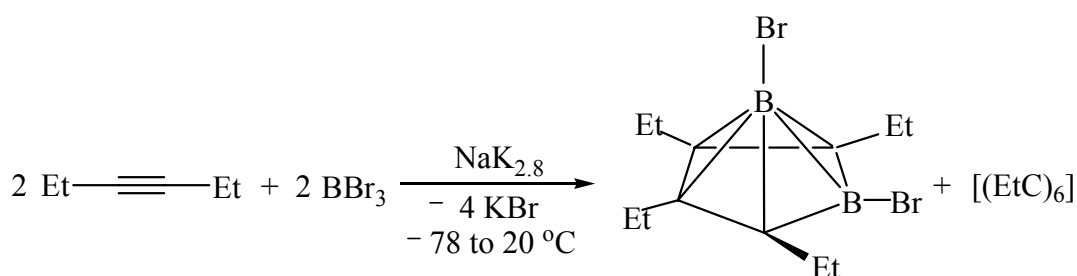
The dehalogenation of **2** starting at $-65\text{ }^\circ\text{C}$ gives compound **4** (Scheme 16) in 29 % yield; when the same reaction is carried out at room temperature, the yield is lower. Compound **4** exhibits two ^{11}B -NMR signals at $\delta = -10.5$ and -13.4 ppm, which are shifted to lower frequencies in comparison to *nido*-(EtC) $_4$ (BCl) $_4$ ^[18] ($\delta = -1.5$ and -5.5 ppm). The MS spectrum shows the molecule ion of **4** at $m/z = 716$ as the base peak, with correct isotopic pattern, while the formation of **6** is only detected by a peak at $m/z = 771$ (M^+) in low intensity.



Scheme 16

3.1.4 Scope and limitations of the one-pot method

To further study the scope and limitations, a series of other alkynes have been studied, using the same or similar procedures. In the cases of 5-decyne, di-*tert*-butylacetylene, bis(trimethylsilyl)ethyne, and di-*p*-tolylacetylene, all the reactions led to decomposition products. The debromination reaction of 3-hexyne and BBr₃ (1 equiv.) affords the known *nido*-(EtC)₄(BBr)₂^[11g] in 49 % yield, together with small amount of hexaethylbenzene (Scheme 17), while the analogous reaction using BCl₃ gives a mixture of boron-containing species, which have not yet been identified, and a significant amount of hexaethylbenzene.



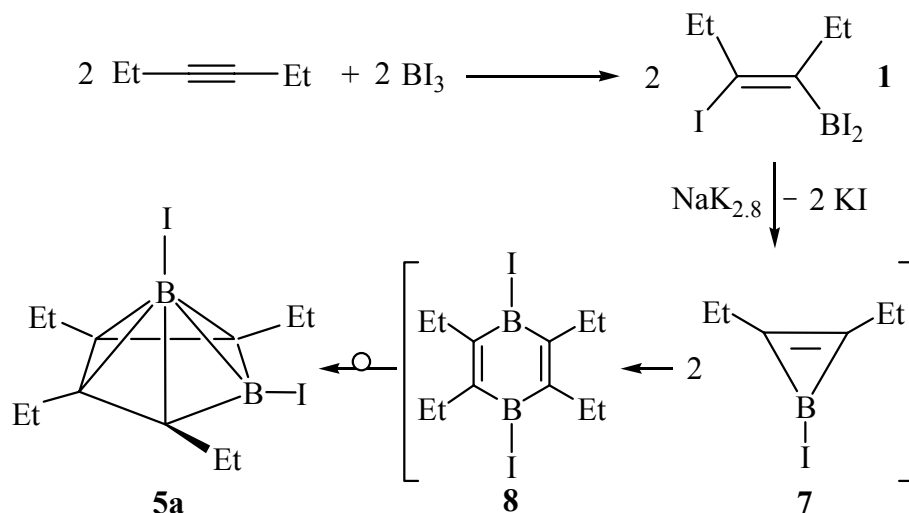
Scheme 17

Surprisingly, the reaction system of diphenylacetylene/BBr₃/NaK_{2.8} led only to decomposition, no matter if the one-pot or stepwise procedures are used. The efforts starting from ethyne and phenylacetylene, and BI₃ (or BBr₃), respectively, to produce the corresponding *nido*-C₄B₂ carboranes with CH cluster atoms were not successful. As pointed out by Wrackmeyer et al., the reaction of peralkylated *nido*-C₄B₂ carboranes with an excess of BBr₃ occurs selectively at the basal boron atom, but in the case of the carborane with two CH vertices, only the degradation of the carborane cluster is observed.^[51a]

3.1.5 Mechanistic studies on the reaction system alkynes/BI₃/NaK_{2.8}

There have been two similar dehalogenation reactions reported. One is the early studied diphenylacetylene/PhBBr₂/K system of Lappert et al.,^[66] from which they claimed to have obtained a perphenylated 1,4-diboracyclohexadiene derivative or an unknown carborane species, however, these results could not be reproduced by Eisch et al.^[67] The other system involves the alkynes/MeBBr₂/C₈K reaction reported by van der Kerk et al.,^[68] who claimed to

have obtained stable peralkylated 1,4-diboracyclohexadiene derivatives via a borylene mechanism as the main products, while Wrackmeyer et al.^[69] (in the cases of 3-hexyne and 5-decyne) obtained the corresponding C_4B_2 -*nido*-carboranes, no 1,4-diboracyclohexadiene derivatives could be detected.



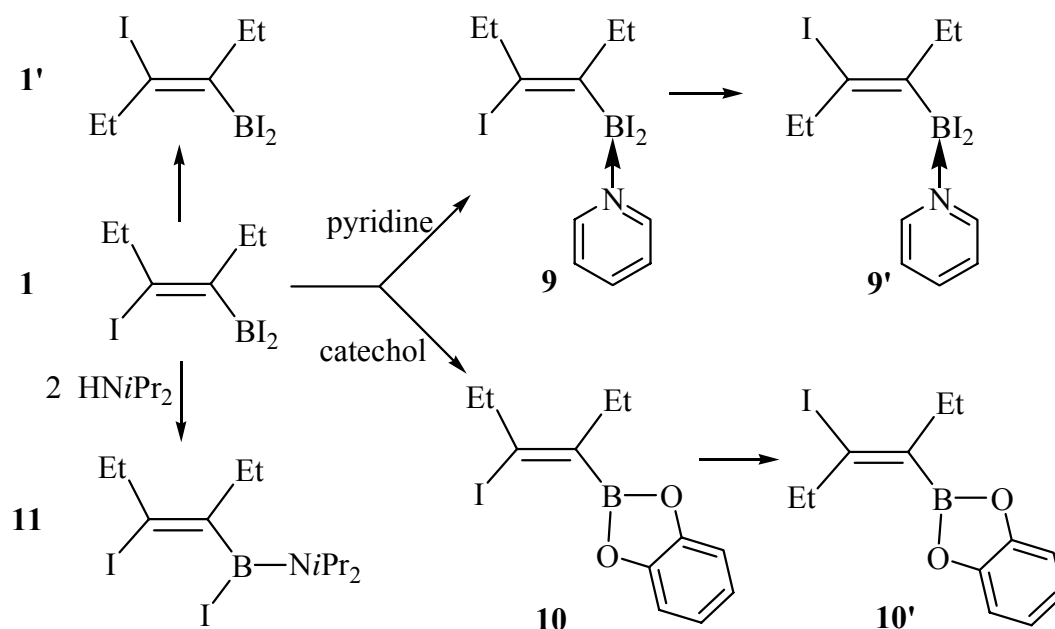
Scheme 18

In order to get insight into the formation of **5**, we selected **5a** as our target compound. A possible pathway to **5a** is proposed (Scheme 18): iodoboration of 3-hexyne with BI_3 affords **1**, its dehalogenation yields presumably the iodoborirene intermediate **7**, which might dimerize^[11h,70] to give 1,4-diboracyclohexadiene **8** or its 1,2-isomer **8'** (which may be formed by C-C and B-B coupling), as intermediates to rearrange to the carborane **5a**.

The first step is the iodoboration of 3-hexyne to yield **1**. In a study involving this step to prepare the 2,5-dihydro-1,2,5-thiadiborol,^[55a,b] the iodoboration product was reported to be a *cis/trans* mixture (ca. 2:3 *cis/trans* ratio) based on the acetolysis, which is an established method^[71] to determine the stereochemistry of haloboration products (we repeated the acetolysis reaction and a ratio of 1:1 was obtained). The problem is that at RT the 1H -NMR spectrum shows two sets of ethyl signals and the ^{13}C -NMR only six signals, whereas a *cis/trans* mixture should give more signals. Moreover, the ^{11}B -NMR spectrum exhibits only one signal at $\delta = 40$ ppm. This was noticed^[55c] and some reactions were carried out with $Fe_2(CO)_9$ and Me_2S , unfortunately neither complexation nor adduct formation took place. Later the very similar reaction of 3-hexyne and BBr_3 was studied by Wrackmeyer,^[72] the results reveal that it is a stereoselective *cis*-addition, while the fast *cis-trans* isomerization leads to a

mixture which on the other hand allows the assignment of both isomers by NMR methods.

We tried to determine the stereochemistry of the present iodoboration products using a more direct method other than acetolysis. It turned out that, in accord with Wrackmeyer's findings, the reaction of 3-hexyne and BI_3 gives the *cis* isomer **1** (Scheme 19), which undergoes a slow isomerization to the thermodynamically more stable *trans* isomer **1'**, thus allowing the characterization and even separation of both isomers. The pyridine adduct **9** and the catechol derivative **10** show much faster *cis-trans* isomerization than the parent **1**, while the amino derivative **11** does not isomerize at RT within weeks. The X-ray crystal structure analyses of **9** (*cis*) and **9'** (*trans*) unequivocally confirm the stereochemical assignments.



Scheme 19

Figs. 5 shows the structures of **9** (*cis*) and **9'** (*trans*), respectively. In both structures the boron atom is 4-coordinate, adopting slightly distorted tetrahedral geometry. The bond lengths and angles in both structures are very similar. The B-I bond lengths are 2.269 and 2.306, in **9**, and 2.275(3), 2.294(3) Å in **9'**, respectively, comparable to the corresponding values in compound **2**. The corresponding B-N distances of 1.587 in **9** and 1.596 Å, in **9'** respectively, are similar to, but slightly shorter than those found in other pyridine adducts.^[73]

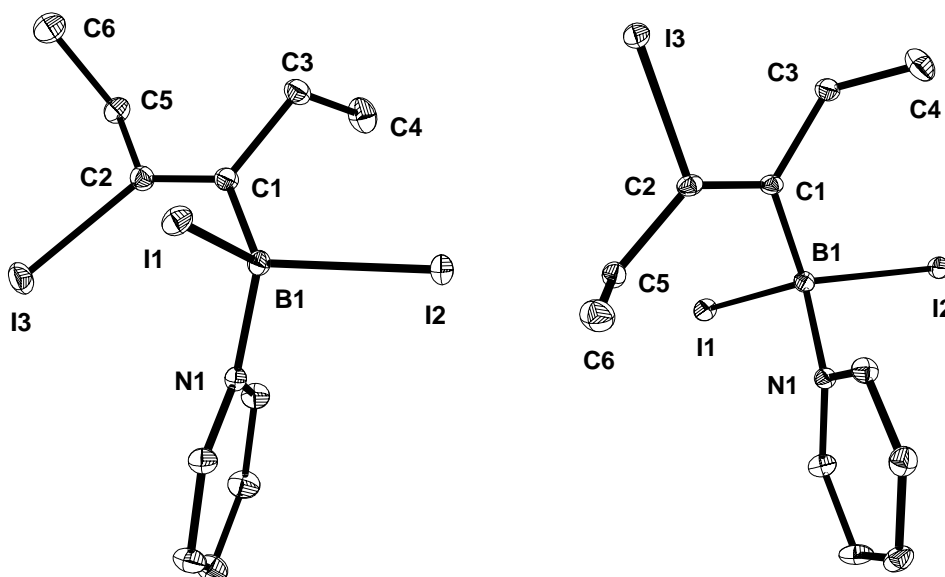
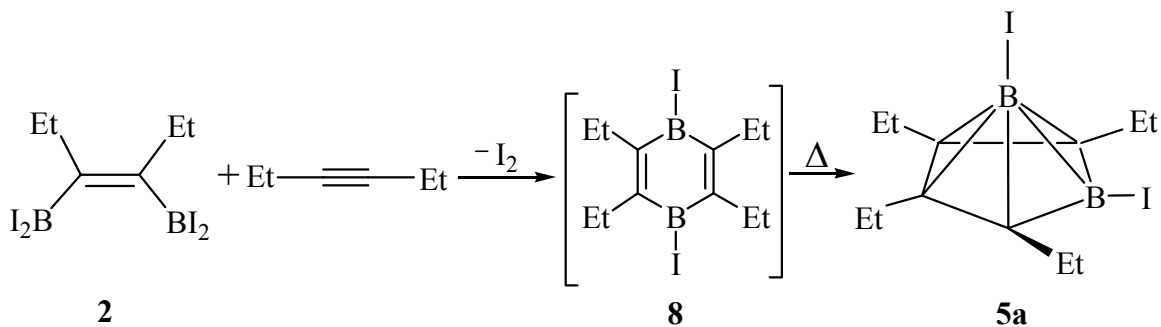


Fig. 5. Molecular structures of **9** (left) and **9'** (right). H atoms omitted for clarity. Selected bond lengths [\AA] and angles [$^\circ$]: For **9**: I1-B1 2.269(3), I2-B1 2.306(3), I3-C2 2.141(3), N1-B1 1.587(4), B1-C1 1.600(4), C1-C2 1.343(4), N1-B1-C1 114.4(2), N1-B1-I1 111.8(2), C1-B1-I1 109.2(2), N1-B1-I2 101.4(2), C1-B1-I2 113.6(2), I1-B1-I2 106.1(1). For **9'**: I1-B1 2.275(3), I2-B1 2.294(3), I3-C2 2.160(3), N1-B1 1.596(4), B1-C1 1.607(4), C1-C2 1.342(4), N1-B1-C1 114.8(2), N1-B1-I1 111.3(2), C1-B1-I1 109.7(2), N1-B1-I2 100.8(2), C1-B1-I2 114.0(2), I1-B1-I2 105.7(1).

The second step in the formation of **5a** is the dehalogenation of **1**. Apart from the one-pot reactions, the stepwise reaction also affords **5a** in a somewhat lower yield (43%). Although we do not have the direct proof for the formation of the borirene intermediate **7**, we find ^{11}B -NMR signals in the reaction mixtures which might be assigned to the corresponding 1,4-diboracyclohexadiene **8** (broad signals at ca. 68 and 67 ppm in the formation of **5a** and **5b**, respectively), near to the expected region for 1,4-diboracyclohexadienes (55-65 ppm).^[74]

The designed redox reaction of **2** with 3-hexyne as shown in Scheme 20 (in analogy to the preparation of the corresponding 1,3-diiodo-2,3-dihydro-1,3-diborole derivatives^[75] and the 1,4-diiodo-1,4-diboracyclohexene compounds^[76]) indeed affords the expected carborane **5a**. The reaction mixture shows a broad ^{11}B -NMR signal at $\delta = 66$ ppm. As suggested by Schleyer et al.^[70] the straightforward intramolecular rearrangement of 1,4-diboracyclohexa-2,5-dienes into carboranes is forbidden by symmetry, our attempts to separate **8** by distillation leads

gradually to **5a**, as characterized by ^{11}B -NMR and EI-MS. Although this redox reaction (Scheme 20) represents a new route to the corresponding 1,4-diboracyclohexadienes/ C_4B_2 -*nido*-carboranes, the difficult access to the *cis*-1,2-diborylalkene **2** prevents its practical application.



Scheme 20

3.1.6 Reactivity of 1,6-diiodo-2,3,4,5-tetraethyl-2,3,4,5-tetracarba-*nido*-hexaborane(6) (**5a**)

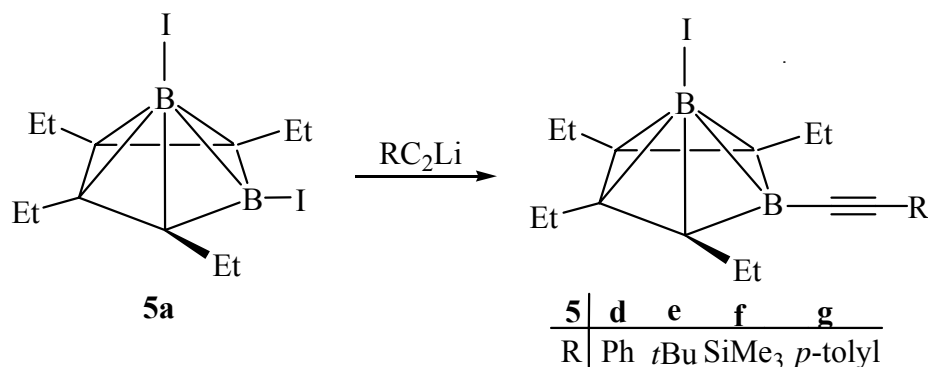
Wrackmeyer et al.^[51a-d] have demonstrated that the B-bromo *nido*- C_4B_2 carborane derivatives undergo nucleophilic substitution, (selectively in the only one dibromo case studied^[51e]) at the basal boron atom. In this part, the diiodo carborane **5a** is selected for reactivity studies because of the ease and good yield of its synthesis from the one-pot procedure described above. The reactions of **5a** towards a variety of nucleophiles lead in most of the cases to the basal substitution, however, the apical substitution has also been realized by Pd-catalyzed transformations.

3.1.6.1 Regiospecific substitution at the basal boron atom

Alkynyl compounds **5d-g**

Nucleophilic substitution reactions on **5a** with RC_2Li ($\text{R} = \text{Ph}, t\text{Bu}, \text{SiMe}_3, p\text{-tolyl}$) proceed smoothly, and the corresponding B6-alkynylated carborane derivatives **5d-g** were produced in high yields (Scheme 21). The *nido*- C_4B_2 framework is retained, as little differences have been found in the ^1H - and ^{13}C -NMR spectra when compared with that of **5a**. In the ^{11}B -NMR spectra, the basal boron atoms give rise to signals at $\delta = 9.8\text{--}10.9$ ppm, which are only slightly downfield shifted from that of **5a** (5.5 ppm), while those for the apical boron

atoms are the same as that for **5a** (– 52.5 ppm). X-ray structure analyses of **5d** and **5g** (see below) confirm the spectroscopic results. In accord with Herberhold, Wrackmeyer et al.,^[51e] excess of lithium acetylide did not effect the substitution at the apical boron atoms.



Scheme 21

The molecular structures of **5d** and **5g** are shown in Figs. 6,7, respectively. The structure of **5g** (at room temperature) is very similar to that of **5d**. In both structures, the C₄B₂-*nido*-carborane frameworks are essentially similar to that of the starting carborane **5a**. The B-I bond lengths in **5d** [2.139], **5g** [2.119Å], respectively, are very similar to the corresponding value [2.126 Å] of **5a** in spite of the B6-substitution. In the alkynyl B-C-C moieties are almost linear, the corresponding B-C-C bond angles are 177.0 in **5d**, and 173.2° for **5g**, respectively.

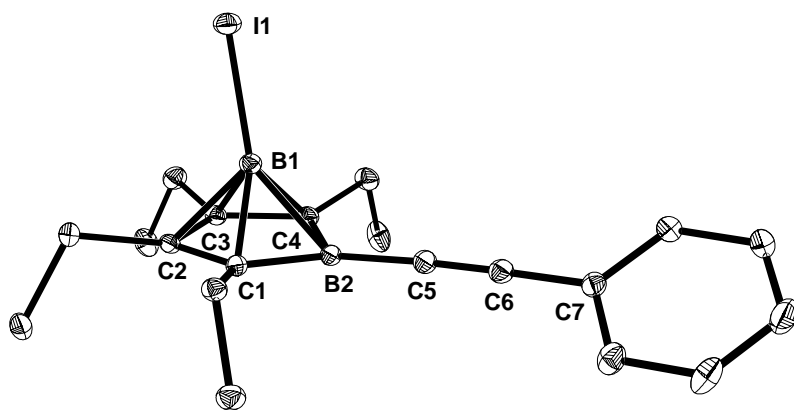


Fig. 6. Molecular structure of **5d**, hydrogen atoms omitted for clarity. Selected bond lengths [Å] and angles [°]: I(1)-B(1) 2.139(2), B(1)-C(1) 1.714(3), B(1)-C(2) 1.722(3), B(1)-C(3) 1.714(3), B(1)-C(4) 1.706(3), B(1)-B(2) 1.825(3), B(2)-C(1) 1.537(3), B(2)-C(4) 1.532(3), C(1)-C(2) 1.453(3), C(2)-C(3) 1.446(2), C(3)-C(4) 1.459(3), B(2)-C(5) 1.529(3), C(5)-C(6) 1.211(3), C(6)-C(7) 1.435(3); B(2)-B(1)-I(1) 143.3(1), C(5)-B(2)-B(1) 131.2(2), C(6)-C(5)-B(2) 177.0(2), C(5)-C(6)-C(7) 178.3(2).

The B-C and C≡C bond distances in **5d** [1.529, 1.211] and **5g** [1.530, 1.197] are similar to each other, and also in agreement with the reported values for borylacetylenes.^[77] In **5d** and **5g** the apical B-I groups are bent away by the B_{basal} group, the angle B2-B1-I being 143.3(3), 141.3(3)^o, respectively [cf. in **5a** the corresponding angle is 140.06^o].

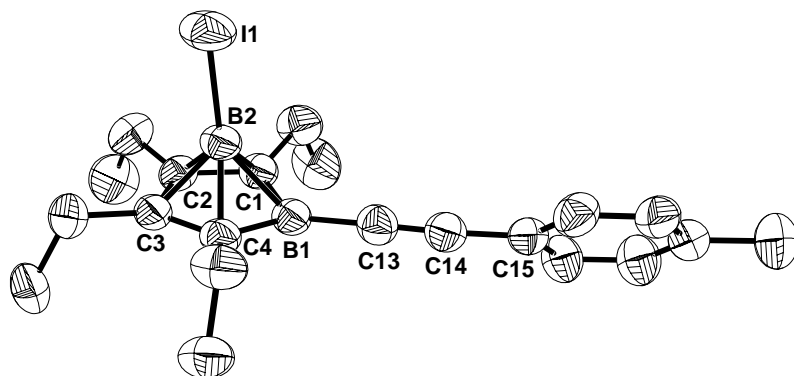
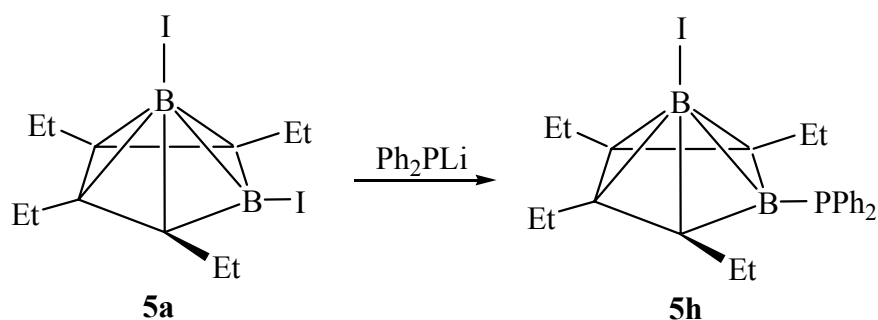


Fig. 7. Molecular structure of **5g**, hydrogen atoms omitted for clarity. Selected bond lengths [Å] and angles [^o]: I(1)-B(2) 2.119(4), B(2)-C(1) 1.694(5), B(2)-C(2) 1.712(6), B(2)-C(3) 1.709(5), B(2)-C(4) 1.696(5), B(1)-B(2) 1.825(6), B(1)-C(1) 1.517(6), B(1)-C(4) 1.528(5), C(1)-C(2) 1.447(5), C(2)-C(3) 1.429(5), C(3)-C(4) 1.448(6), B(1)-C(13) 1.530(6), C(13)-C(14) 1.197(5), C(14)-C(15) 1.438(6); (B1)-B(2)-I(1) 141.3(3), C(13)-B(1)-B(2) 132.6(3), C(14)-C(13)-B(1) 173.2(4), C(13)-C(14)-C(15) 176.6(4).

Diphenylphosphanylcarborane **5h**

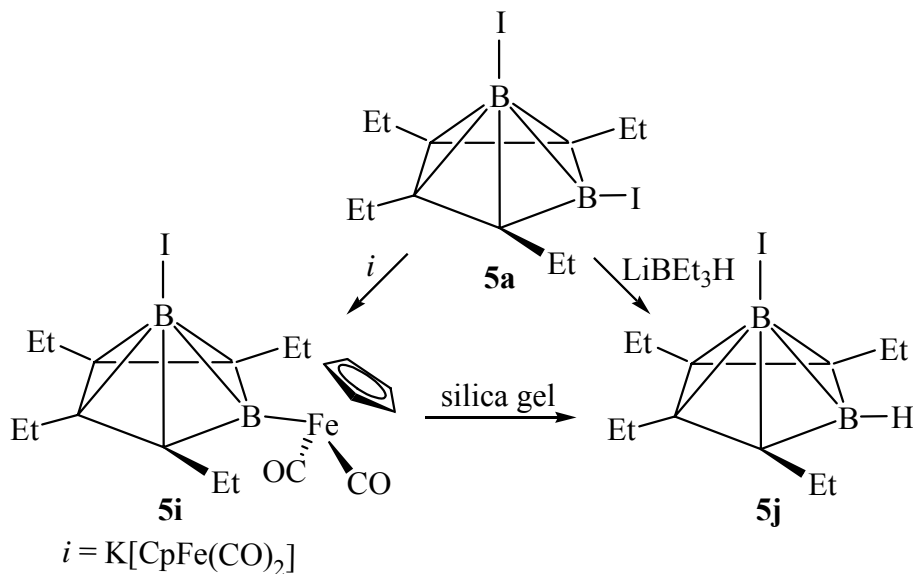
A similar result to the formation of **5d-g** is observed in the reaction of **5a** with Ph₂PLi to give the basal-substituted **5h** (Scheme 22). In the ¹¹B-NMR spectrum of **5h**, the signal of the basal boron is shifted downfield by ca. 9 ppm, while the apical boron is unaffected.



Scheme 22

Compounds with B-Fe and B-H bonds

The reaction of **5a** with $K[(\eta^5\text{-C}_5\text{H}_5)\text{Fe}(\text{CO})_2]$ ^[78] gives **5i** (Scheme 23), with regiospecific substitution at the basal position. In this case, the basal boron of the C_4B_2 -*nido*-cluster is significantly deshielded (28.6 ppm), and the signal of the apical boron is slightly shifted to -49.6 ppm. This reveals that the $\text{CpFe}(\text{CO})_2$ fragment is directly bonded to the basal boron by a Fe-B σ -bond, which is confirmed by an X-ray diffraction study (see below).



Scheme 23

Thus **5i** is the first transition metal derivative of the C_4B_2 -*nido*-carborane with direct metal-boron bonding. A few iron derivatives^[79] with other carborane or polyborane frameworks of this type have been reported having Fe-B or Fe-C bonding. Cooling the solution of the crude product in hexane resulted yellow crystals of **5i**, along with an unknown paramagnetic impurity, which makes the NMR spectra not satisfactory. The initial isolation of **5i** by column chromatography on silica gel led to cleavage of the Fe-B bond to give **5j** and paramagnetic impurities. The designed synthesis of **5j** is achieved by the separate reaction of **5a** with LiBEt_3H (Scheme 23).

The B-I bond length in **5i** [2.135 Å] is very similar to the corresponding value [2.126 Å] of **5a**, and the angle B2-B1-I is $141.9(1)^\circ$. In **5i** a $\text{CpFe}(\text{CO})_2$ fragment is directly σ -bonded to the basal boron, the Fe-B bond length is 2.069 Å, which is significantly longer than the corresponding values for iron-boryl complexes, [1.959(6)-2.034(3),^[80a,b] 1.964(8)-2.027(5)^[80c,d]] and iron-borylene complexes [2.010(3) Å^[80e]], but in the range of the reported values

for ferracarboranes (1.968–2.161 Å^[80f]). This long Fe–B distance in **5i** is also consistent with the easy cleavage of the Fe–B bond on silica gel. The iron center achieves an 18e configuration through coordination to two CO ligands (2e donor), the cyclopentadienyl group (5e donor), and the Fe–B interaction (one-electron donor).

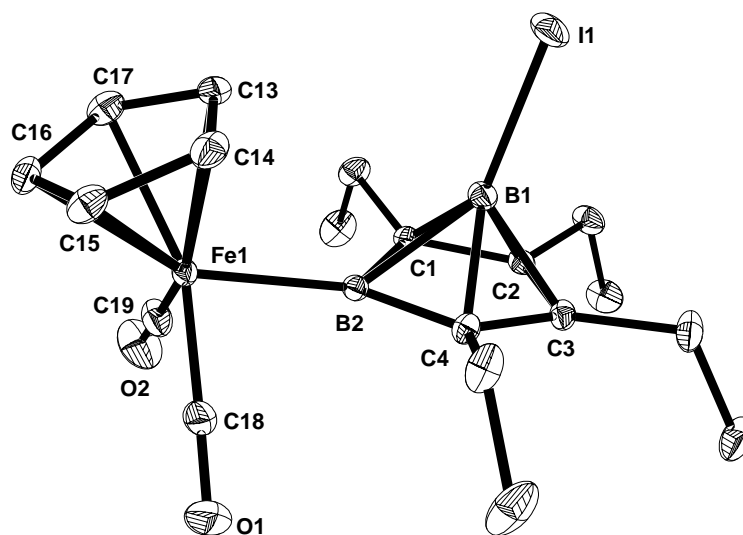
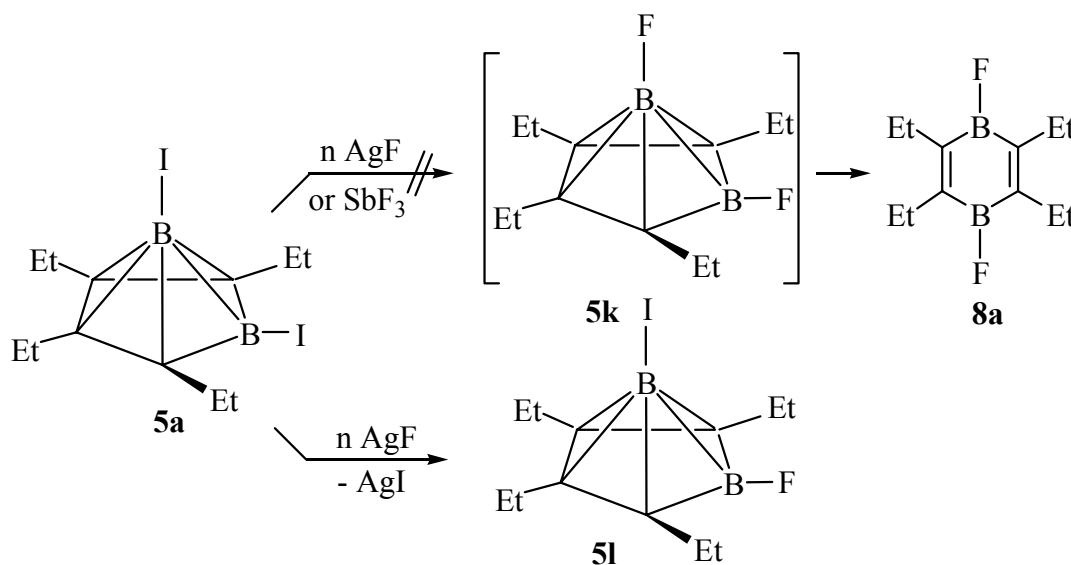


Fig. 8. Molecular structure of **5i**, H atoms omitted for clarity. Selected bond lengths [Å] and angles [°]: I(1)–B(1) 2.135(2), B(1)–C(1) 1.692(2), B(1)–C(2) 1.711(2), B(1)–C(3) 1.709(2), B(1)–C(4) 1.689(3), B(1)–B(2) 1.841(3), B(2)–C(1) 1.547(2), B(2)–C(4) 1.547(2), C(1)–C(2) 1.460(2), C(2)–C(3) 1.431(2), C(3)–C(4) 1.468(2), Fe(1)–B(2) 2.069(2), Fe(1)–C(19) 1.739(2), Fe(1)–C(18) 1.742(2), Fe(1)–C_{Cp} 2.094–2.116(2), O(1)–C(18) 1.150(2), O(2)–C(19) 1.151(2); B(2)–B(1)–I(1) 142.91(11), B(1)–B(2)–Fe(1) 133.48(11), C(19)–Fe(1)–C(18) 92.59(10), C(19)–Fe(1)–B(2) 86.26(8), C(18)–Fe(1)–B(2) 85.03(8), O(1)–C(18)–Fe(1) 178.7(2), O(2)–C(19)–Fe(1) 178.6(2).

6-Fluorocarborane **5e**

Although halogen exchange is a conventional way to functionalized organoboron compounds,^[81] it is rare in polyhedral borane and carborane chemistry. Onak et al.^[82] reported a few reactions involving halogenated *closo*-2,4-C₂B₅ carborane derivatives which resulted in halide exchange to afford products containing always smaller halogen atom(s) than the leaving halogen atom(s). Stanko et al.^[83a] described that 2-iodo-*p*-carborane was transformed to 2-chloro-*p*-carborane by treatment with CuCl, and the B–I bonds^[83b] in 10-iodo-*o*-carborane,

9-iodo-*m*-carborane, 2-iodo-*p*-carborane, respectively, participate in isotopic exchange with Na¹³¹I. Recently Grushin et al.^[84] observed that, in the presence of *n*-Bu₄NBr, 9-*I*-*m*-carborane underwent halogen exchange to give 9-Br-*m*-carborane under Pd catalysis. It was described that a 6-bromo-peralkylated *nido*-C₄B₂ carborane reacts with AgF to give the 6-F-carborane analog in the presence of a catalytic amount of Et₃N.^[85]



Scheme 24

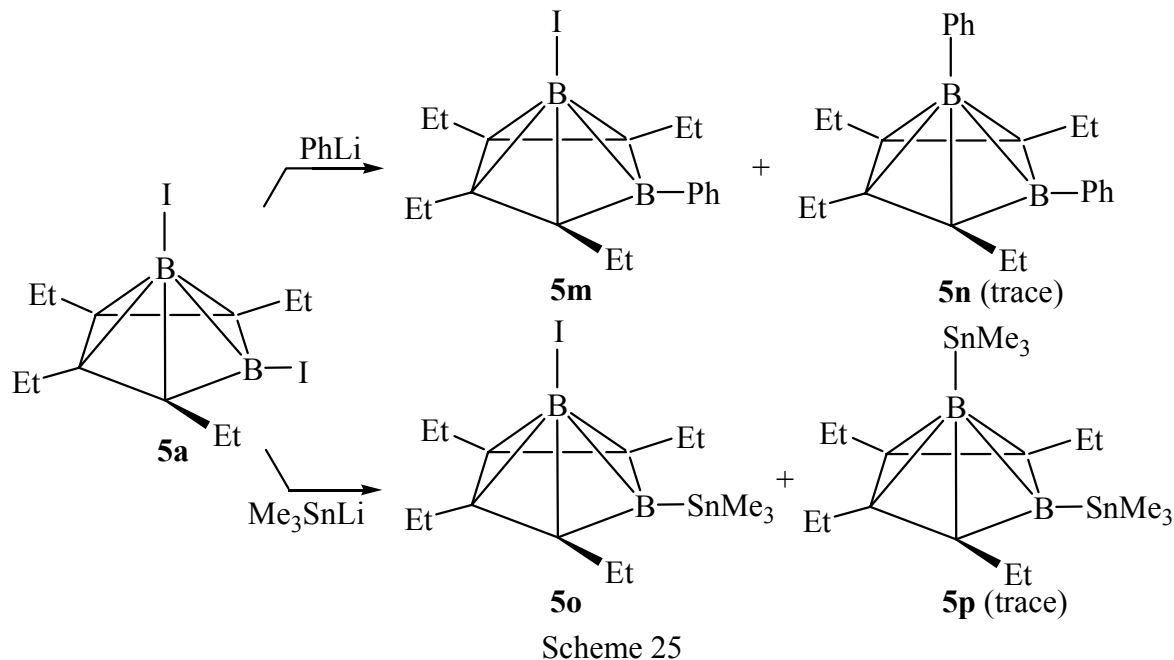
The reactions of **5a** with an excess of AgF and SbF₃, respectively, were carried out (Scheme 24) in hope to obtain the difluoro *nido*-C₄B₂ intermediate **5k**, which, as has been demonstrated by Timms,^[10a] would rearrange to give the classic structure **8a**. While no reaction was observed between **5a** and SbF₃ in hexane at room temperature, the reaction of **5a** with AgF (no catalyst) led only to the basically substituted monofluoro derivative **5l**. Compound **5l** was characterized by its ¹¹B-NMR spectrum ($\delta = 21.8, -53.1$ ppm) [cf. those of **5a**: $\delta = 5.5$ for basal boron and -52.5 ppm for apical boron], and the MS spectrum exhibits the molecule ion peak at $m/z = 332$ with the correct isotopic distribution.

3.1.6.2 Substitution reactions involving the apical boron atom

B-Phenyl and -trimethylstannyl derivatives **5m,o** and **5n,p**

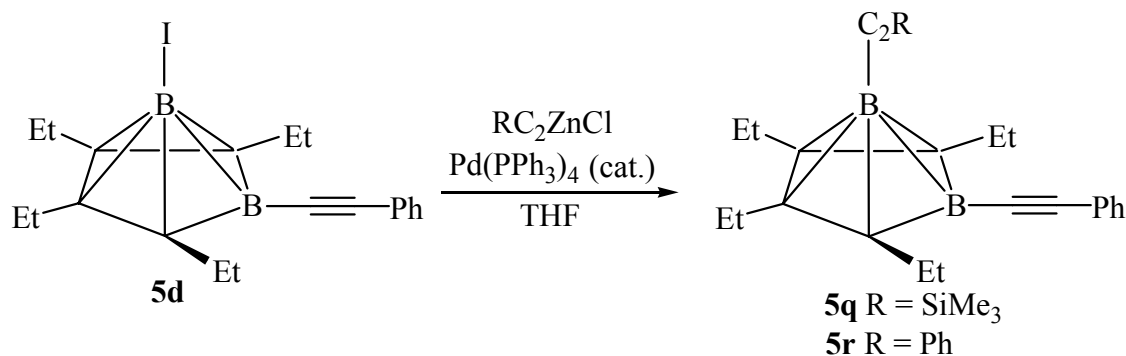
In most of the cases the apical B-I bonds are inert, however, it was found that the substitution at the apical boron atom is also possible. In the reactions of **5a** with more than two equiv. of PhLi and Me₃SnLi^[86], respectively (Scheme 25), the B6-substituted products **5m** and

5o are formed, together with trace amounts of the disubstituted species **5n** and **5p**, as detected by MS. For **5m** and **5o**, the ^{11}B -NMR signals of the basal boron atoms are shifted downfield to 17.9 and 16.1 ppm, respectively, while the signals of the apical boron atoms are unchanged.



Bis(alkynyl)-substituted *nido*- C_4B_2 -carboranes **5q** and **5r**

The substitution at the apical boron atom by alkynyl groups has been realized by a Pd(0)-catalyzed Negishi-type^[87] cross coupling reaction of **5d** and RC_2ZnCl in THF (Scheme 26). Heating the reaction mixtures for 10 days leads to yellow products **5q** and **5r**.



Interestingly, the ^{11}B -NMR signal of the substituted apical boron is only slightly downfield shifted to -50.7 (**5q**) and -49.8 ppm (**5r**). The structure is established by an X-ray diffraction analysis of **5q** (Fig. 9). The B–C≡C moieties are almost linear, the corresponding

bond angles are 177.6 (apical)/175.4° (basal), respectively. The angle B2-B1-C21 is 142.5(1)°. All these values are comparable to those for **5a**, **5d** and **5g** mentioned above.

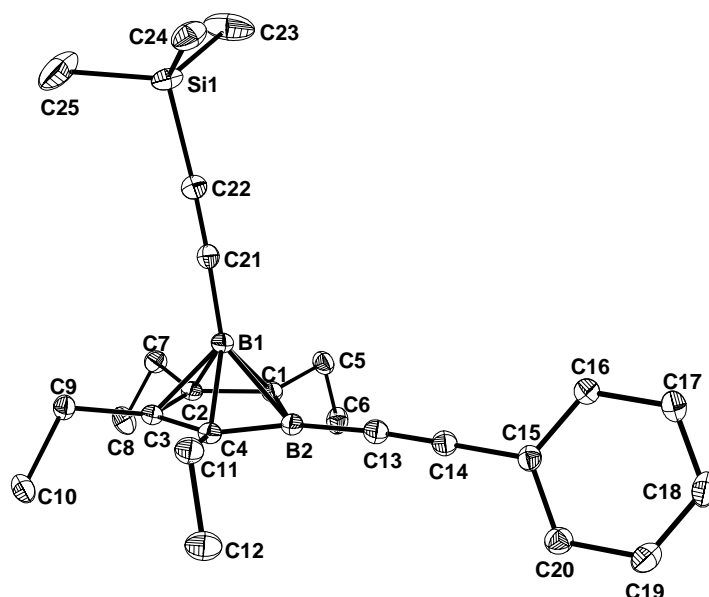
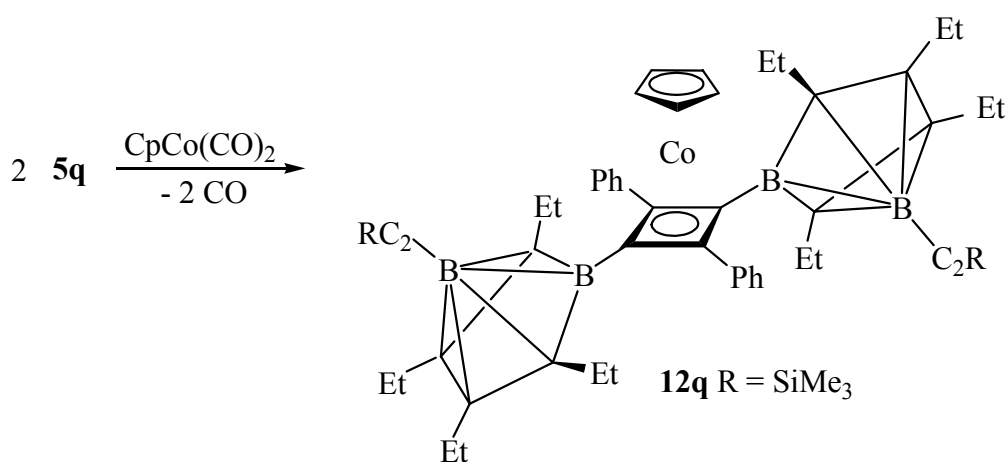


Fig. 9. Molecular structure of **5q**, hydrogen atoms omitted for clarity. Selected bond lengths [Å] and angles [°]: B(1)-C(1) 1.723(2), B(1)-C(2) 1.735(2), B(1)-C(3) 1.734(2), B(1)-C(4) 1.731(2), B(1)-B(2) 1.833(2), B(2)-C(1) 1.532(2), B(2)-C(4) 1.532(2), C(1)-C(2) 1.455(2), C(2)-C(3) 1.440(2), C(3)-C(4) 1.452(2), B(2)-C(13) 1.536(2), C(13)-C(14) 1.207(2), C(14)-C(15) 1.438(2), B(1)-C(21) 1.522(2), C(21)-C(22) 1.205(2); C(21)-B(1)-B(2) 142.49(10), C(13)-B(2)-B(1) 132.30(10), C(14)-C(13)-B(2) 175.39(13), C(13)-C(14)-C(15) 178.79(13), C(22)-C(21)-B(1) 177.62(12) C(21)-C(22)-Si(1) 175.45(12).

The mechanism of such Pd-catalyzed coupling reactions involving B-I bonds^[88] is expected to be similar to that of carbon-carbon cross coupling, however, the very first step in the catalytic cycle, i.e. the oxidative addition of the B-I group leading to a B-Pd-I species has not yet been verified. Stirring a mixture of **5d** and Pd(PPh₃)₄ in THF leads to a brown solution, its ³¹P-NMR spectrum shows a signal at $\delta = 22.4$ ppm, which is in the expected region compared to that of (PPh₃)₂Pd(I)Ph ($\delta = 22.3$ ppm).^[84] Its ¹¹B-NMR spectrum shows a signal at $\delta = -36$ ppm, which might be due to the formation of the (σ -carboranyl)palladium iodide complex. Shore et al.^[89] have studied the reaction of Pd(PPh₃)₄ with the iodoborane cluster 9-I-1,7-(SMe₂)₂B₁₂H₉ and they observed similar results ($\delta^{31}\text{P} = 24.2/24.0$ ppm).

CpCo[bis(carboranyl)cyclobutadiene] complex 12q

Recently Siebert, Goswami et al. have reported that the stoichiometric reactions of borylacetylenes with either $\text{CpCo}(\text{C}_2\text{H}_4)_2$ (“Jonas reagent”)^[90] or $\text{CpCo}(\text{CO})_2$ afford the corresponding $\text{CpCo}(\text{diboryl-cyclobutadiene})$ complexes.^[91] As part of a cooperation, a similar $\text{CpCo}[\text{bis}(\text{carboranyl})\text{cyclobutadiene}]$ complex^[91c] starting with carboranylacetylene **5d** was realized. The synthesis of an analog containing *closo*- C_2B_5 carboranyl moiety has also been achieved which will be described in Chapter 3.2. Herein the reactions of **5q** and **5r** with $\text{CpCo}(\text{C}_2\text{H}_4)_2$ or $\text{CpCo}(\text{CO})_2$ are studied.



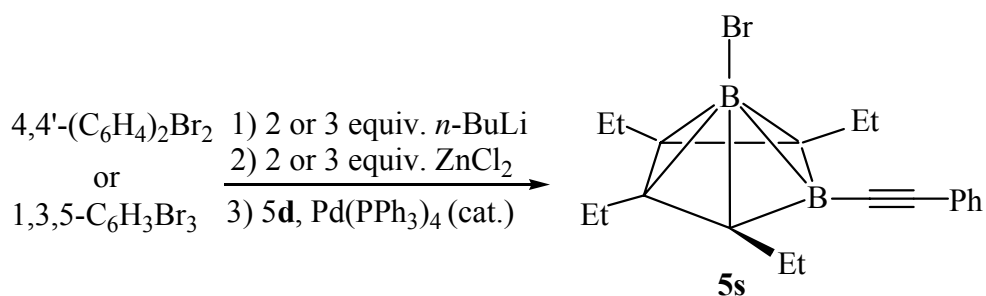
Scheme 27

The stoichiometric reaction of **5q** and $\text{CpCo}(\text{CO})_2$ in refluxing toluene gave a brown oil (Scheme 27). Its ^{11}B -NMR spectrum exhibits signals at $\delta = 15, -50.4$ ppm, with a slightly downfield shift for the apical boron compared to those for **5q**, and the HR-MS spectrum gives the molecular ion peak at $m/z = 892.4999$ for the formula $\text{CpCo}[\text{C}_4(\text{Et}_4\text{C}_4\text{B}_2\text{C}_2\text{SiMe}_3\text{Ph})_2(\text{Ph})_2]$ with correct pattern, indicating the formation of $\text{CpCo}[\text{bis}(\text{carboranyl})\text{cyclobutadiene}]$ complex **12q** occurs selectively at the basal position.

No reaction was observed between **5r** and $\text{CpCo}(\text{C}_2\text{H}_4)_2$ in refluxing toluene for a week, after which $\text{CpCo}(\text{CO})_2$ was added to the mixture and refluxed for another 5 days. After workup a brown solid was obtained which is soluble in hexane and CH_2Cl_2 . The ^{11}B -NMR spectrum shows signals at $\delta = 20, -43.9$ ppm, both are slightly shifted to downfield compared to those for **5r**. The EI-MS spectrum failed to give any clear information even when heated to 500°C .

1-Br-carborane 5s

The reactions of **5d** with aryl zinc reagents (generated in situ from 4,4'-dibromobiphenyl and 1,3,5-tribromobenzene, respectively, with the appropriate amount of *n*-BuLi and ZnCl₂) in the presence of a catalytic amount of Pd(PPh₃)₄, did not give the expected apically linked clusters, but the apically brominated product **5s** as a yellow solid (Scheme 28).



Scheme 28

The formation of **5s** was first deduced from its ¹¹B-NMR spectrum ($\delta = 10.6, -40.2$ ppm), downfield shifted relative to the signals of **5d** ($\delta = 10.3$ for B_{basal}, -52.6 ppm for B_{apical}). In addition, the MS spectrum exhibits a base peak at $m/z = 366/368$, with the correct isotopic pattern for (EtC)₄(BC₂Ph)(BBr). Based on the results described below (formation of **5u**), a very weak peak at $m/z = 388$ in the MS spectrum of **5s** is assigned to be *nido*-(EtC)₄(BC₂Ph)₂ (**5r**).

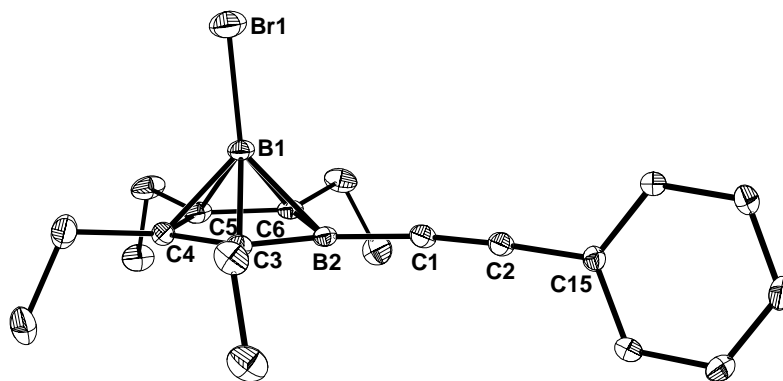
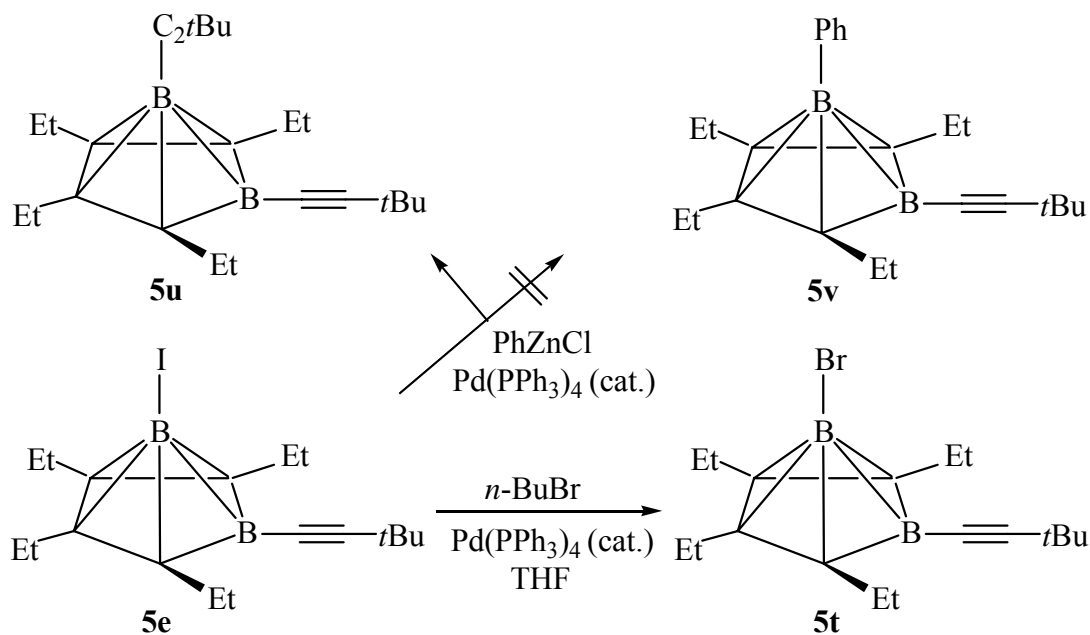


Fig. 10. Molecular structure of **5s**. hydrogen atoms omitted for clarity. Selected bond lengths [\AA] and angles [$^\circ$]: Br(1)-B(1) 1.906(3), B(1)-C(3) 1.712(3), B(1)-C(4) 1.720(4), B(1)-C(5) 1.717(3), B(1)-C(6) 1.711(4), B(1)-B(2) 1.820(4), B(2)-C(3) 1.523(3), B(2)-C(6) 1.529(3), B(2)-C(1) 1.531(3), C(3)-C(4) 1.456(3), C(4)-C(5) 1.442(4), C(5)-C(6) 1.451(3), C(1)-C(2) 1.208(3), C(2)-C(15) 1.434(3); B(2)-B(1)-Br(1) 138.76(17), C(1)-B(2)-B(1) 132.12(19), C(2)-C(1)-B(2) 174.0(2), C(1)-C(2)-C(15) 174.9(3).

The structure of **5s** (Fig. 10) was finally established by a single crystal X-ray analysis, which is very similar to that of **5d** and **5g**. The B-Br bond length is 1.906(3) Å. The alkynyl B2-C1-C2 moiety is almost linear, the corresponding B-C-C bond angle is 174.0(2)° [cf. those for 177.0° in **5d**, and 173.2° for **5g**], respectively. In **5s** the apical B-Br group is also bent away by the B_{basal} group, and the angle B2-B1-Br1 is 138.76(17)° comparable to those in **5d** and **5g** [143.3(3) and 141.3(3)°, respectively].

The formation of **5s** implies that the apically brominated *nido*-C₄B₂ carborane derivative is not suitable for the Pd catalyzed Negishi-type cross coupling with zinc reagents. Obviously the bromine source for the formation of **5s** is 4,4'-dibromodiphenyl and 1,3,5-tribromobenzene, which reacted with *n*-BuLi to generate *n*-BuBr along with the corresponding lithium reagents. The lithium reagents would further react with ZnCl₂ to produce the corresponding zinc reagents.



Scheme 29

Two control reactions were therefore carried out (Scheme 29). The reaction of **5e** with *n*-BuBr and a catalytic amount of Pd(PPh₃)₄ produced the expected product **5t**, whereas the similar reaction of **5e** with PhZnCl did not give apically phenylated product **5v**, the apically alkynylated species **5u** was detected instead, by its ¹¹B-NMR spectrum ($\delta = 8.9$, -52.6 ppm), comparable to those of **5q** ($\delta = 9.8$ for B_{basal}, -50.7 ppm for B_{apical}), and MS spectrum $m/z =$

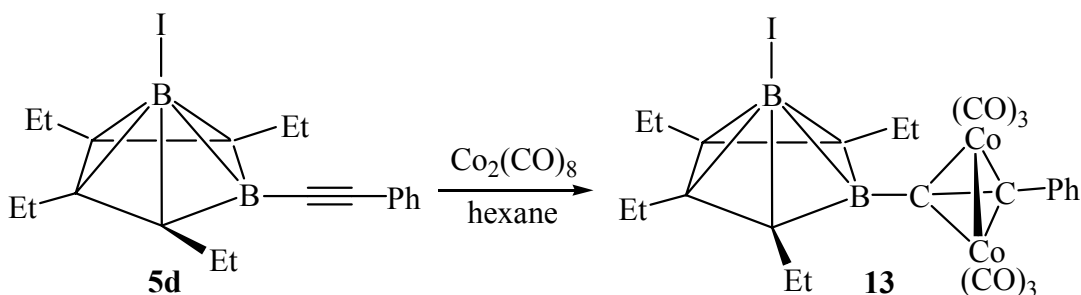
348). The formation of **5u** may be from an intermolecular reaction, in which the basal B-C_{alkynyl} bond of **5e** was cleaved and a new alkynyl zinc reagent *t*BuC≡CZnCl formed, which reacted further with the apical B–I bond of **5e** to give **5u** under Pd catalysis, as mentioned above in Scheme 26.

3.1.6.3 Cluster linkages involving 2,3,4,5-tetracarba-*nido*-hexaboranes(6)

There is current interest in cluster linkages in search of new materials, for which carborane clusters are excellent candidates, as demonstrated on the C₂B₄ system by Grimes et al.^[92] For the B-functionalized C₄B₂-*nido*-carboranes, nucleophilic substitution by the anionic cluster (μ-NS)Fe₂(CO)₆[−] has been shown to be an effective way to linked clusters.^[11g] In this context, new linked clusters involving C₄B₂-*nido*-carboranes have been synthesized, either with direct linkage or with different linkers at different positions.

nido-C₄B₂-C₂Co₂ cluster **13**

The reaction of carboranylacetylene **5d** with Co₂(CO)₈ leads to the deep brown product **13** (Scheme 30), in which the *nido*-C₄B₂ and the C₂Co₂ tetrahedrane cluster are directly linked



Scheme 30

by a B–C bond at the basal position. In the ¹¹B-NMR spectrum the signal for basal boron is shifted downfield by 6.5 ppm compared to that of **5d**, while the signal for the apical boron is only slightly shifted downfield by ca. 1.5 ppm.

The molecule structure of **13** has been confirmed by an X-ray diffraction analysis (Fig. 11). There are only a few acetylene–Co₂(CO)₆ complexes with boron groups attached to the acetylene unit,^[77a,93] and two^[77a,93b] structurally characterized examples carry B-catechol groups. In the structure of **13** (Fig. 11), the almost linear B–C≡C–C part in **5d** has been altered by the complexation with the Co₂(CO)₆ fragment, the angles are decreased to 141.07°

(B2-C13-C14) and 140.1° (C13-C14-C15). The Co1-Co2 (2.483 Å) and C13-C14 (1.348 Å) bond lengths are comparable with those in similar complexes carrying B-cat groups.^[77a,93 b]

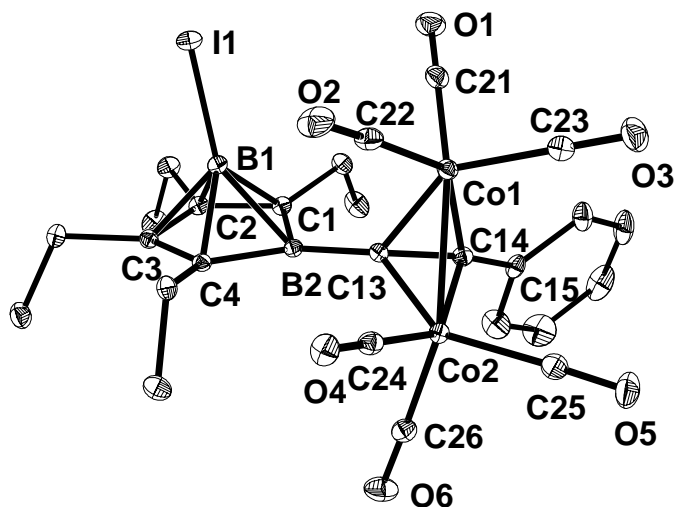
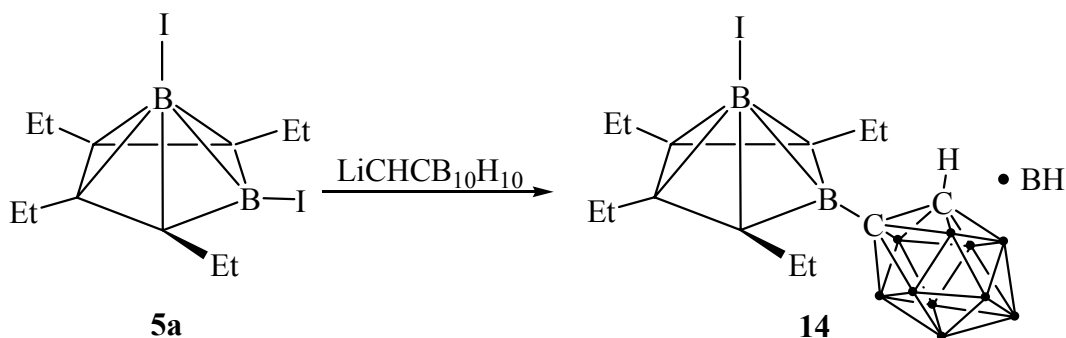


Fig. 11. Molecular structure of **13**, hydrogen atoms omitted for clarity. Selected bond lengths [Å] and angles [$^\circ$]: I(1)-B(1) 2.121(2), B(1)-C(1) 1.712(3), B(1)-C(2) 1.712(3), B(1)-C(3) 1.718(3), B(1)-C(4) 1.705(3), B(1)-B(2) 1.826(3), B(2)-C(1) 1.537(3), B(2)-C(4) 1.537(3), C(1)-C(2) 1.458(3), C(2)-C(3) 1.443(3), C(3)-C(4) 1.456(3), B(2)-C(13) 1.554(3), C(13)-C(14) 1.348(3), C(14)-C(15) 1.465(3), Co(1)-Co(2) 2.483(4), Co(1)-C(13) 1.999(2), Co(1)-C(14) 1.952(2), Co(2)-C(13) 1.990(2), Co(2)-C(14) 1.976(2); B(2)-B(1)-I(1) 140.7(2), C(13)-B(2)-B(1) 130.5(2), C(14)-C(13)-B(2) 141.1(2), C(13)-C(14)-C(15) 140.1(2).

nido-C₄B₂-*closo*-C₂B₁₀ cluster **14**

The C₄B₂-C₂B₁₀ cluster **14** is produced by the reaction of **5a** with monolithio-*o*-carborane (Scheme 31), in which the C₄B₂ cluster is directly connected to the icosahedral *o*-carborane by the B6-C bond, as confirmed by an X-ray diffraction analysis (Fig. 12).



Scheme 31

The ^{11}B -NMR signals of the basal boron atoms are shifted downfield to $\delta = 13.9$ ppm, while the apical boron atom is essentially unaffected ($\delta = -53.4$ ppm). The MS spectrum exhibits the respective molecular ion peaks with correct isotopic pattern.

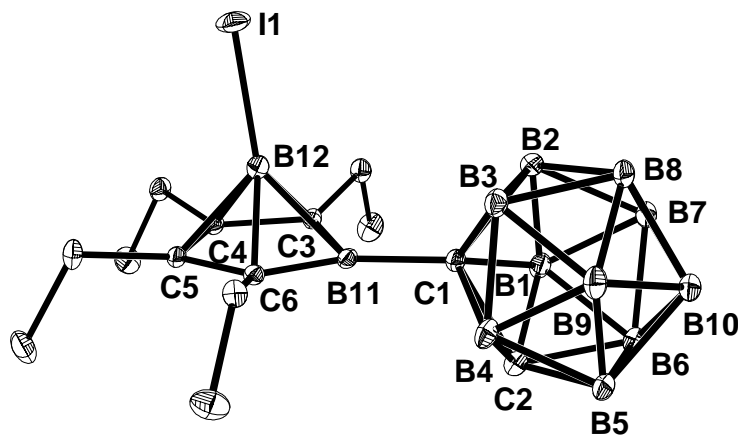
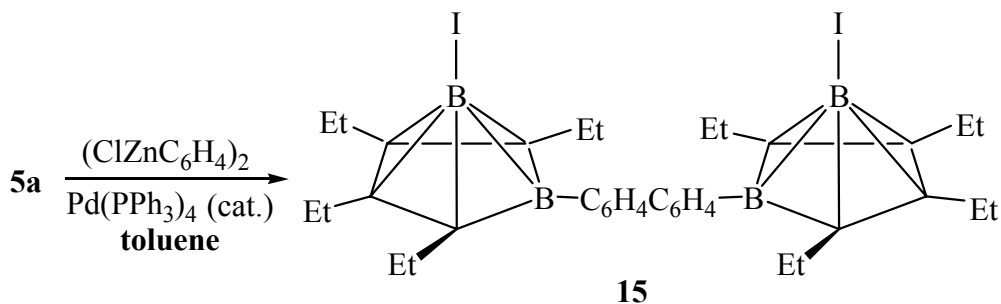


Fig. 12. Molecular structure of **14**, hydrogen atoms omitted for clarity. Selected bond lengths [\AA] and angles [$^\circ$]: I(1)-B(12) 2.125(2), B(12)-C(3) 1.708(2), B(12)-C(4) 1.731(2), B(12)-C(5) 1.731(2), B(12)-C(6) 1.710(2), B(11)-B(12) 1.817(2), B(11)-C(3) 1.543(2), B(11)-C(6) 1.541(2), B(11)-C(1) 1.595(2), C(1)-C(2) 1.687(2), B(11)-B(12)-I(1) 141.46(10), C(1)-B(11)-B(12) 132.04(12).

The structure of **14** contains the small *nido*- C_4B_2 connected to the large *o*-carboranyl cluster. Interestingly, in the asymmetric unit two cocrystallized free *o*-carborane molecules have been found without any significant intermolecular interaction among the three molecules. The B11-C1 bond length of 1.595 \AA is typical of a C-B single bond. In the *o*-carboranyl fragment the C1-C2 bond distance is 1.687 \AA , which is significantly longer than that in *o*-carborane [1.630(6) \AA].^[94] The B-B bond lengths [av. distance 1.776(2) \AA , ranging from 1.744(2) and 1.793(2) \AA] and the C-B bond lengths [av. distance 1.720(2) \AA , with a range 1.703(2) – 1.731(2) \AA] are within expected values.

C_6H_4 - C_6H_4 -linked C_4B_2 clusters **15**

Compound **15** with two C_4B_2 clusters connected via a $\text{C}_6\text{H}_4\text{C}_6\text{H}_4$ unit (Scheme 32) is obtained from the reaction of **5a** with $\text{ClZnC}_6\text{H}_4\text{C}_6\text{H}_4\text{ZnCl}$ in the presence of catalytic amount of $\text{Pd}(\text{PPh}_3)_4$.

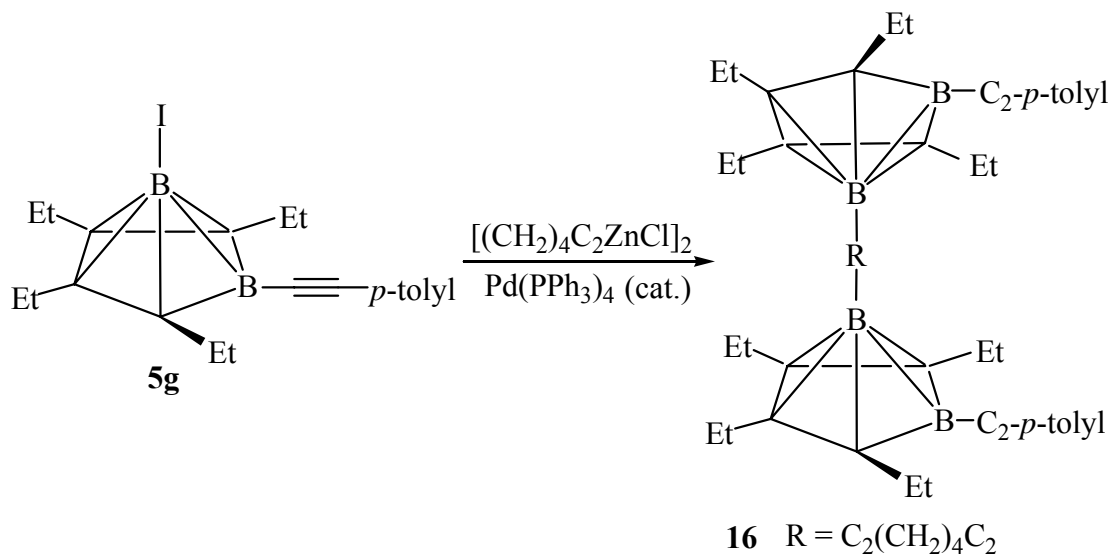


Scheme 32

In contrast, the reaction **5a** with $\text{LiC}_6\text{H}_4\text{C}_6\text{H}_4\text{Li}$ did not work. It should be noted that the reaction leading to **15** is carried out in toluene, because the basal B–I bond in **5a** is sensitive to THF, resulting first in a yellow and then a deep green solution. This is significantly different to the bromo derivatives of *nido*- C_4B_2 which have been studied in THF solution.^[51c,d,e]

$\text{C}_2(\text{CH}_2)_4\text{C}_2$ linked C_4B_2 clusters **16**

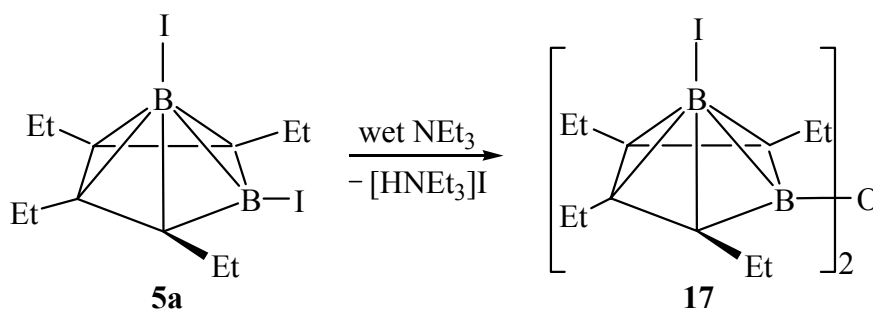
While the reaction of **5g** with the corresponding lithium reagent did not work, its reaction with the dialkynyl zinc reagent produced apically linked cluster **16** (Scheme 33) in the presence of a Pd catalyst. The yellow oil **16** exhibits in the ^{11}B -NMR spectrum two signals at $\delta = 10.2$ and -49.4 ppm. The mass spectrum shows the molecule ion peak with the correct isotopic pattern. Unexpectedly, a few colorless crystals were observed after workup and found by an X-ray structure analysis to be $\text{ZnI}_2(\text{OPPh}_3)_2$.^[95]



Scheme 33

Oxygen-bridged C₄B₂ clusters 17

The reactions of **5a** with wet Et₃N yields an oxygen-bridged species **17** (Scheme 34), formed by hydrolysis of **5a**. The formed by-product was identified by FAB-MS to be the ammonium salt [Et₃NH]I. **17** is characterized by ¹¹B-NMR ($\delta = 22.1$ and -51.9 ppm) and HR-MS which exhibits the molecule ion peak with the correct isotopic pattern.



Scheme 34

3.1.7 Conclusion

A one-pot synthesis of 1,6-diiodo-2,3,4,5-tetracarba-*nido*-hexaboranes(6) has been developed, involving disubstituted alkynes, BI₃ and NaK_{2.8}. Considering the easy availability of the starting materials and the product *nido*-(EtC)₄(BI)₂ (**5a**), it is convenient to study the reactivity of the B-functionalized carborane. Dehalogenation is a practical method for the preparation of carboranes. The formation of *nido*-(EtC)₄(BI)₄ (**4**) from dehalogenation of *cis*-I₂B(Et)C=C(Et)BI₂ (**2**) confirms that bisborylalkenes are precursors of *nido*-C₄B₄ carboranes. Such dehalogenation reactions are more complex and give lower yields at ambient temperature than at lower temperatures. A possible mechanism of the formation of C₄B₂-*nido*-hexaboranes(6) is proposed and studied using **5a** as the representative example. The stereochemistry of the iodoboration product of the alkyne has been clarified to be *cis*, using a more direct method other than acetolysis, and the *cis-trans* isomerization exists in the addition product and some of the derivatives.

The reactivity of **5a** towards various nucleophiles has been investigated. In most of the cases, the substitution with hydride, alkynyl, diphenylphosphanyl, trimethylstannyl, CpFe(CO)₂ fragment and even the bulky *o*-carboranyl group occurs regioselectively on the basal boron atom of the *nido*-C₄B₂ frameworks, while the “inert” apical iodine atom can be substituted by a

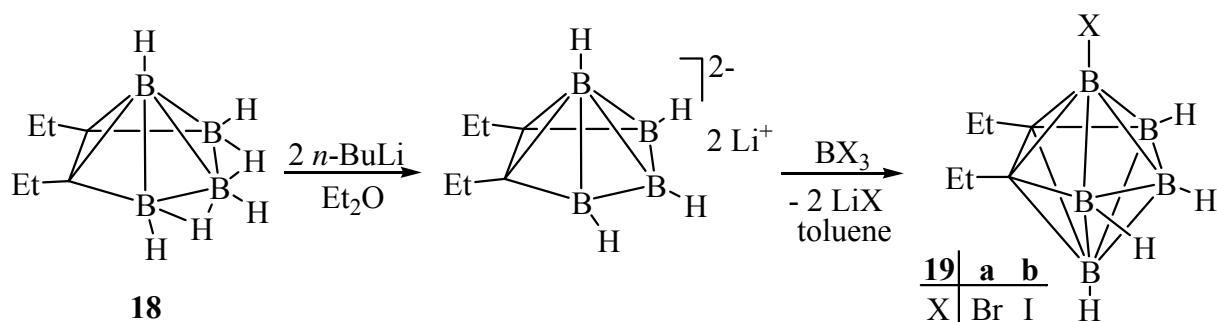
Pd(0)-catalyzed Negishi-type cross coupling reaction, as demonstrated by the synthesis of apically alkynyl-substituted compounds **5q** and **5r**. A new strategy for cluster linkages has been developed and compounds with different types of cluster linkages have been prepared, either by direct B–C bonding ($C_4B_2-C_2B_{10}$ and $C_4B_2-C_2Co_2$), or via a $C_6H_4C_6H_4$ or a $C_2(CH_2)_4C_2$ unit, at the basal boron atom of the *nido*- C_4B_2 skeletons. The reactivity of the basal B–I bond of **5a** is further shown by its sensitivity to THF and by the formation of the oxygen-bridged species $(C_4B_2)_2O$ (**17**).

3.2 Formation and properties of 2,3-dicarba-*closo*-heptaboranes(**7**)

In Chapter 3.1 the formation of *closo*-2,3- $Et_2C_2B_5I_5$ (**6**) from the reaction of 3-hexyne, BI_3 , and $NaK_{2.8}$ at r.t. has been described. Herein the synthesis of apically functionalized *closo*-2,3- C_2B_5 carboranes, and the reactions of some alkynyl-substituted derivatives towards cobalt complexes are reported.

3.2.1 Facile synthesis of apically halogenated 2,3-dicarba-*closo*-heptaboranes(**7**) (**19a,b**) from 2,3-dicarba-*nido*-hexaborane(**8**)

Boron insertion or capping reactions^[96] are a convenient pathway to functionalized carborane products. To achieve apically B-halogenated *closo*-2,3- C_2B_5 carborane derivatives, we carried out reactions of the *nido*-2,3- $Et_2C_2B_4H_4^{2-}$ dianion (formed by deprotonation of



Scheme 35

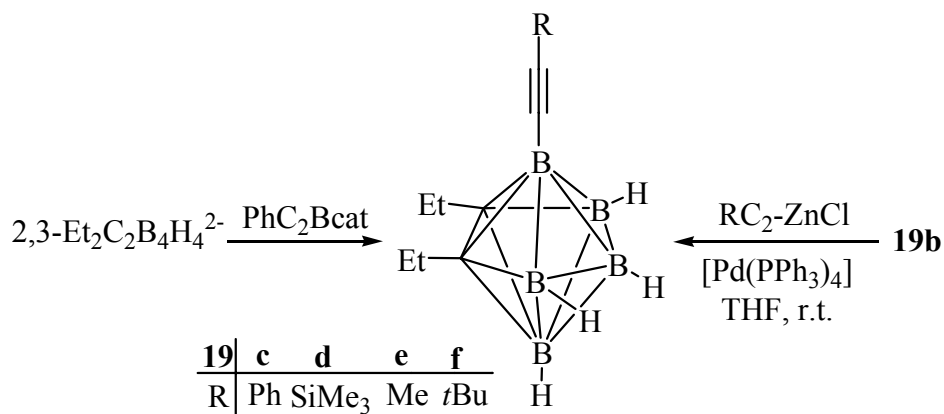
nido-2,3- $Et_2C_2B_4H_6$ ^[97] (**18**) with 2 equiv. $n-BuLi$ in diethylether) and BX_3 ($X = Br, I$) in toluene (Scheme 35), and **19a,b** were obtained as yellow oil, respectively. Their ^{11}B -NMR spectra exhibit signals at 6.3 (B4,6), 1.2 (B5), -17.4 (B1), -23.6 (B7) (**19a**), 6.7 (B4,6), 1.9 (B5), -18.3 (B7), -31.9 (B1) (**19b**) ppm, in a ratio of 2:1:1:1, respectively. The MS spectra of

19a,b give the corresponding molecular ion peaks with correct isotopic patterns.

The formation of **19a,b** is of interest, as the bromination of *closo*-2,3-Et₂C₂B₅H₅ with Br₂ or Br₂/AlBr₃ occurs selectively at the B5 position, affording 5-Br-*closo*-2,3-Et₂C₂B₅H₄ in moderate yield.^[26b] Wrackmeyer et al.^[98] studied a similar reaction of *nido*-2,4-(EtC)₂(BEt)₄H⁻Na⁺ with BBr₃ to give 1-Br-*closo*-2,4-(EtC)₂(BEt)₄B only as a side product, whereas the major product is *closo*-2,4-(EtC)₂(BEt)₄BH.

3.2.2 Alkynyl-substituted 2,3-dicarba-*closo*-heptaboranes(7) (**19c-f**) via Pd-catalyzed cross-coupling reactions

Similarly, the reaction of 2,3-Et₂C₂B₄H₄²⁻ with PhC≡CBcat^[91a] (cat = O₂C₆H₄) gave the apically alkynyl-substituted 1-PhC≡C-*closo*-2,3-Et₂C₂B₅H₄ (**19c**) as a yellow oil (Scheme 36).



Scheme 36

A more efficient way to **19d-f** was found by the Pd-catalyzed Negishi-type cross-coupling reaction of **19b** (Scheme 36). The ¹¹B-NMR spectrum of **19c** shows signals at 6.4 (B4,6), 1.8 (B5), -16.1 (B1), -18.7 (B7) ppm, in a ratio of 2:1:1:1. Similar shifts are found for **19d-f**. There appears to be no significant “anti-podal” effect of the R groups at B1 upon B7 in **19c-f**, as shown by the chemical shift for *closo*-1-butenyl-2,3-C₂B₅H₆ (B7: -25.0 ppm) compared to that of *closo*-2,3-C₂B₅H₇ (B7 -17.9 ppm).^[26e] The ¹¹B-NMR signals for B7 (**19c-f**, -18.7 to -20.3 ppm, in CDCl₃) are comparable to that of *closo*-2,3-Et₂C₂B₅H₅ (B7 -14.2 ppm).^[26]

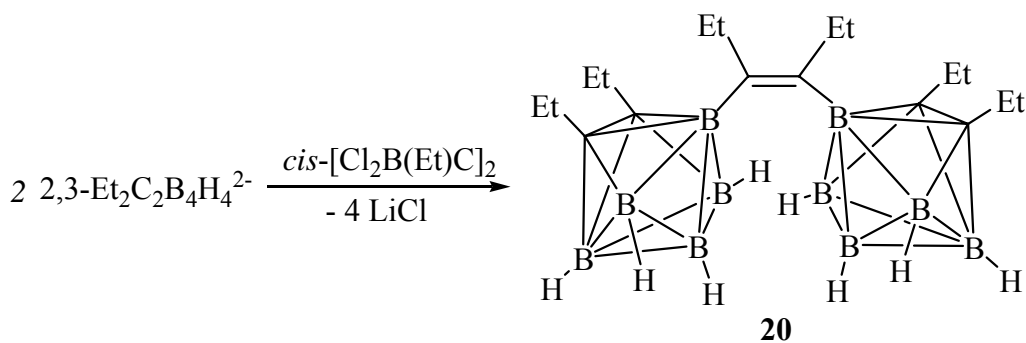
The catalytic reactions can be easily monitored by the stepwise color change and ¹¹B-NMR: the yellow solution of **19b** in THF turned to red upon addition of a catalytic amount of Pd(PPh₃)₄, and again gradually to yellow after the corresponding zinc reagents were added. It is noteworthy that the Pd-catalyzed cross-coupling in the present work was achieved at

ambient temperature (48-72 h), whereas in most of the reported Pd-catalyzed coupling reactions involving halogenated borane or other carborane clusters, either heating or longer reaction time or both are needed.^[99]

The initial attempts to obtain **19d** by heating the THF solution at reflux led only to a mixture of **19d** and other unidentified carborane species. The efforts to obtain the proposed oxidative addition intermediate $2,3\text{-Et}_2\text{C}_2\text{B}_5\text{-Pd(PPh}_3)_2\text{I}$ by reacting **19b** and $\text{Pd(PPh}_3)_4$ in THF at room temperature were not successful, instead red crystals of *trans*- $\text{Pd(PPh}_3)_2\text{I}_2$ ^[100] were identified, which were also formed in a trace amount in the preparation of **19d** at room temperature. Unexpectedly, the desilylation of **19d** with *n*- Bu_4NF in THF did not lead to a terminal carboranylacetylene, only the degradation of the cluster was observed.

3.2.3 Alkenyl-linked 2,3-dicarba-*closo*-heptaborane(7) clusters (**20**)

The similar reaction of $2,3\text{-Et}_2\text{C}_2\text{B}_4\text{H}_4^{2-}$ with *cis*- $\text{Cl}_2\text{B(Et)C=C(Et)BCl}_2$ (**3**) produced compound **20** (Scheme 37), in which two *closo*-2,3- C_2B_5 clusters are linked via a C=C double bond. Its ¹¹B-NMR spectrum exhibits broad signals at 6.2 (B4,6), 2.9 (B5), -4.7 (B1), -21.5 (B7) ppm, and the MS spectrum gives the molecular ion peak at $m/z = 362$ with correct pattern.



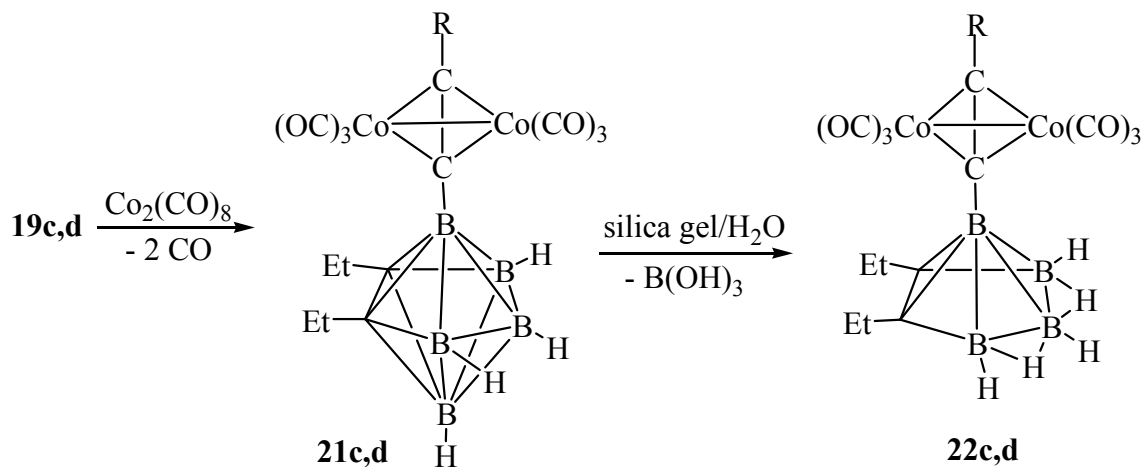
Scheme 37

3.2.4 Reactions of **19c,d** with cobalt complexes

3.2.4.1 Reactions of carboranylacetylenes **19c,d** with $\text{Co}_2(\text{CO})_8$

The reactions of carboranylacetylenes **19c,d** and $\text{Co}_2(\text{CO})_8$, respectively, afforded the dicobalttetrahedrane derivatives **21c,d** (Scheme 38) as brown oil, each having the C_2B_5 and

Co_2C_2 clusters connected by a B-C bond. Like the benzene-centered triscarboranyl compound $\text{C}_6\text{H}_3(\text{C}_2\text{B}_5)_3$ [27] our attempts to purify the products **21c,d** on column (silica gel for **21c**, and

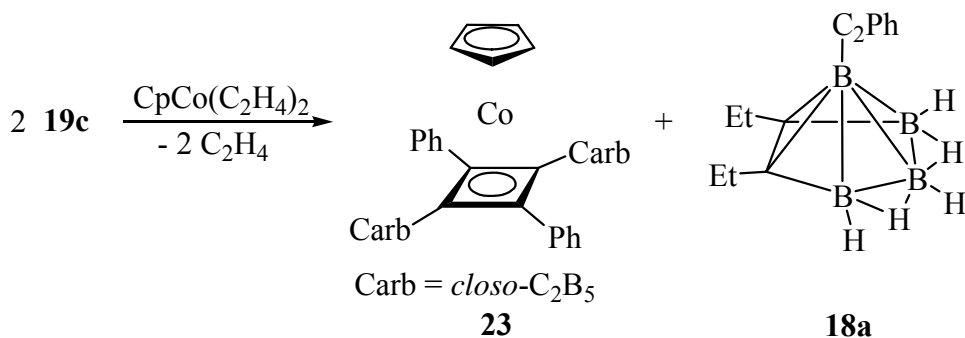


Scheme 38

seasand for **21d**) led to mixtures of **21c,d** and the *nido*- C_2B_4 -clusters **22c,d**, respectively, formed by elimination of a BH group [as $\text{B}(\text{OH})_3$ in the reaction of **21c,d** with trace amount of H_2O and production **22c,d**, a derivative of **18** [97]]. The ^{11}B -NMR spectrum of **21c** (in hexane, before column chromatography) exhibits signals at 7.2 (B4,6), 2.9 (B5), -5.6 (B1), -20.5 (B7) in a ratio of 2:1:1:1, after chromatography new signals appeared at -2.9 , -35.7 ppm, indicating the formation of **22c**. Additionally, the MS spectra of **21c,d** exhibit the molecular ion peaks, respectively, and the characteristic fragments of sequential loss of the six carbonyl ligands.

3.2.4.2 Reactions of **19c** with $\text{CpCo}(\text{C}_2\text{H}_4)_2$: formation of $\text{CpCo}(\text{dicarboranylcyclobutadiene})$ complex **23**

No reaction was observed between **19c** and $\text{CpCo}(\text{CO})_2$ in refluxing toluene for 1 week, as monitored by ^{11}B -NMR. However, similar to the $\text{CpCo}(\text{cyclobutadiene})$ complex **12q** (Chapter 3.1), adding $[\text{CpCo}(\text{C}_2\text{H}_4)_2]$ to this mixture and refluxing for additional 6 days led to a brown mixture (after filtration through a pad of sand), from which the formation of the carboranyl-substituted $\text{CpCo}(\text{cyclobutadiene})$ complex **23** and the partial degradation species **18a** (Scheme 39) was detected (^{11}B -NMR: $\delta = 6.3, 2.2, -4.0, -16.6, -19.6, -45.1$ ppm; EI-MS: $m/z = 606$ for **23** and 232 for **18a**, respectively). Compound **18a** may be formed in a way similar to **22c,d**. No evidence was found for the formation of cyclotrimerization product.



Scheme 39

3.2.5 Conclusion

Treatment of the *nido*-2,3-Et₂C₂B₄H₄²⁻ dianion with monoboron reagents BX₃ (X = Br, I) and PhC≡C_Bcat led to *closo*-2,3-Et₂C₂B₅H₄-1-R (R = Br, I, C₂Ph) (**19a-c**) derivatives, with functional substituents at the apical boron atom. Compound **20** with two C₂B₅ moieties linked via a C=C unit was obtained by a similar boron insertion reaction with *cis*-Cl₂B(Et)C=C(Et)BCl₂ (**3**). A more efficient pathway was developed by the Pd-catalyzed Negishi-type cross-coupling reactions of **19b** with R'C≡CZnCl at room temperature to give *closo*-2,3-Et₂C₂B₅H₄-1-C≡CR' (**19d-f**, R' = SiMe₃, Me, *t*Bu). The reactions of **19c,d** and Co₂(CO)₈ afforded diclusters **21c,d**, in which a *closo*-C₂B₅ and a Co₂C₂ cluster are connected by a B-C bond. Compounds **21c,d** lost the apical boron on silica gel to give the *nido*-C₂B₄-Co₂C₂ diclusters **22c,d**. The formation of carboranyl-substituted CpCo(cyclobutadiene) complex **23** was observed from the reaction of **19c** and CpCo(C₂H₄)₂.

3.3 C-Boryl-*o*-carborane compounds

While many small carboranes are known, the most intensively studied are *o*-, *m*-, *p*-carboranes, especially *o*-carborane (**24**) and its derivatives.^[30] Indeed numerous C- and B-substituted *o*-carborane clusters have been prepared and characterized, including a wide variety of organic and organometallic substituents. Surprisingly, there has been limited work on the *o*-carboranyl boron compounds, moreover, only a few of such derivatives have been structurally characterized.

In 1965, Brotherton et al.^[101] reported the bis(dimethylamino)boryl-*o*-carborane by reacting C-monolithio-*o*-carborane and (Me₂N)₂BCl, similarly B-tri(*n*-butyl-*o*-carboranyl)-

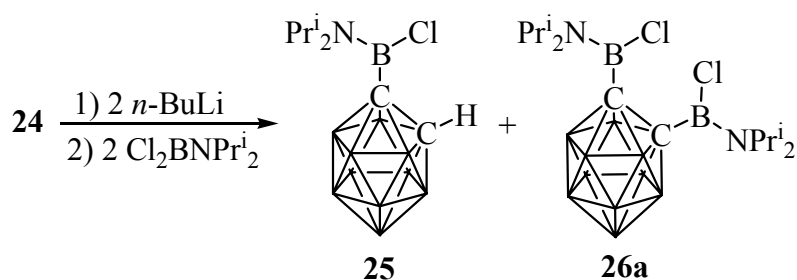
N-trimethylborazine was prepared. Mikhailov et al.^[102] described the dichloroboryl-C-alkyl-*o*-carboranes and several 1-alkyl-2-alkylboryl-*o*-carborane derivatives, as well as their transformations into the corresponding organoboryl *o*-carborane derivatives. By heating the mono-C-alkylborylated-*o*-carborane derivatives, *exo*-polyhedral boron heterocycles (five-membered rings C_{cage}-C_{cage}-B-C-C or C_{cage}-C_{cage}-B-C=C) could be formed.^[102e,f]

Hawthorne^[103] and Rudolph^[104] independently synthesized of 1-Me₃N·BH₂-*o*-carborane from Me₃N·BH₂I and monolithio-*o*-carboranes. Various ways were found by Plesek et al.^[105] to [1-H₃B-1,2-C₂B₁₀H₁₁]⁻ anion and a family of the 1-L-H₂B-1,2-C₂B₁₀H₁₁ (L = Lewis bases) adducts. Hosmane et al. reported [1,2-(H₂BX)₂-1,2-C₂B₁₀H₁₀]²⁻ and [1-R-2-H₂BX-1,2-C₂B₁₀H₁₁]⁻ (where R = Me or Ph).^[106] A type of organic-inorganic hybrid ligands has recently been realized by Xie et al., in which *o*-carborane clusters and cyclic π ligands are bridged by a boron moiety.^[107]

As part of the reactivity study on the *nido*-C₄B₂ carboranes (Chapter 3.1), a linked dicluster in which a *nido*-C₄B₂ cluster and an *o*-carborane are connected via a C-B bond has been described. In this part, the syntheses and structures of some C-boryl-*o*-carborane derivatives including *exo*-polyhedral boron heterocycles, are reported.

3.3.1 C-Aminoboryl-*o*-carborane derivatives

Deprotonation of *o*-carborane **24** with 2 equiv. of *n*-BuLi and the following treatment with 2 equiv. of Pr₂^{*i*}NBCl₂^[108] (Scheme 40) gave a colorless crystalline solid, which was identified by EI-MS to be a mixture of the monoborylated **25** and the diborylated product **26a**.

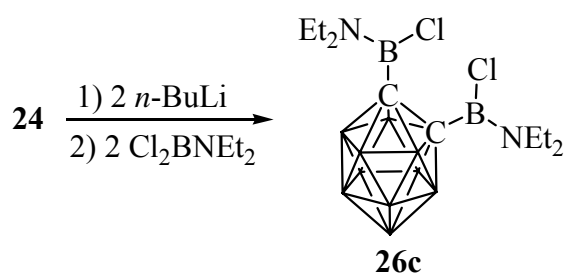


Scheme 40

The ¹¹B-NMR spectrum with six signals [δ = 31.4 ppm (exopolydral boron atom, comparable to that of Pr₂^{*i*}NBCl₂, 30.3 ppm), 0.5, - 2.5, - 7.6, - 10.9, - 12.9 ppm (skeletal boron atoms)] indicates that **25** is the predominant product, which has been structurally

characterized by an X-ray structure analysis (Fig. 13).

The formation of **25** as the dominant product may be due to the bulky isopropyl groups, as the reaction of dilithio-*o*-carborane with Et_2NBCl_2 [109] (Scheme 41) afforded the diborylated **26b** under the same conditions. The ^{11}B -NMR spectrum exhibits five signals [$\delta = 31.4$ ppm (exopolydral boron atom, comparable to that for Et_2NBCl_2 , 30.7 ppm), -2.1 , -7.1 , -10.9 , -12.4 ppm (skeletal boron atoms)] for **26b**. The EI-MS spectrum shows the molecule ion peak for **26b** with correct isotopic pattern.



Scheme 41

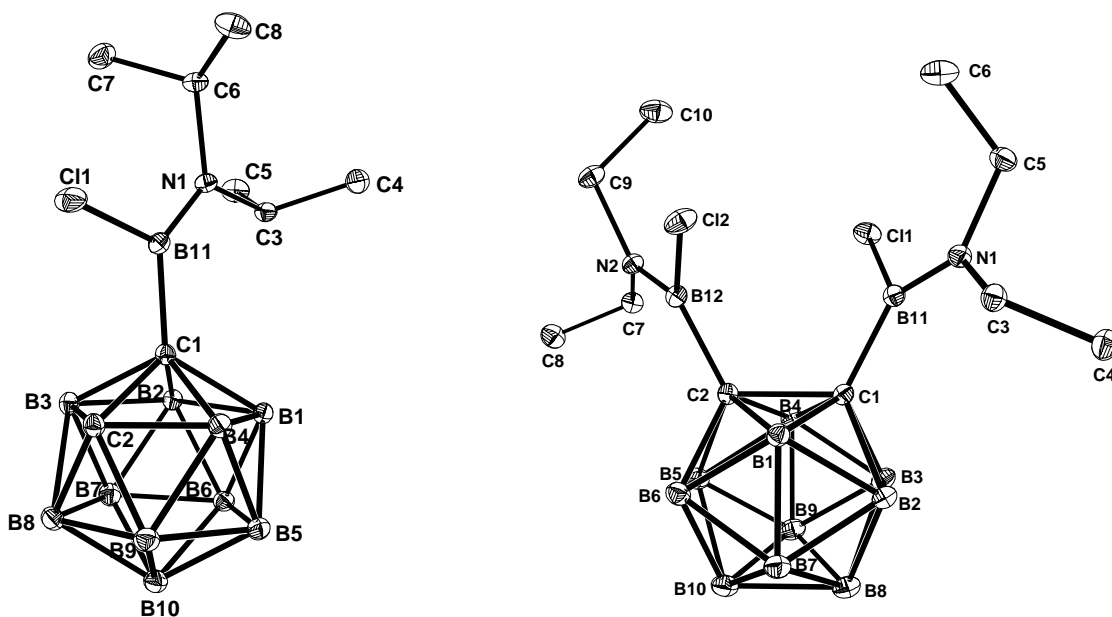


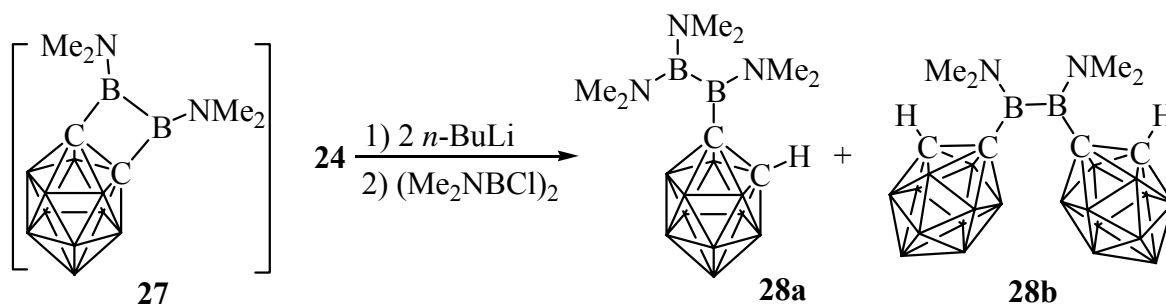
Fig. 13. Molecular structures of **25** (left) and **26b** (right), H atoms omitted for clarity. Selected bond lengths [\AA] and angles [$^\circ$]: **25**: Cl(1)-B(11) 1.798(1), N(1)-B(11) 1.387(1), B(11)-C(1) 1.617(2), C(1)-C(2) 1.673(1); N(1)-B(11)-C(1) 126.7(9), N(1)-B(11)-Cl(1) 120.13(8), C(1)-B(11)-Cl(1) 113.20(7), B(11)-C(1)-C(2) 116.21(8). **26b**: Cl(1)-B(11) 1.791(1), N(1)-B(11) 1.384(1), B(11)-C(1) 1.612(1), Cl(2)-B(12) 1.792(1), N(2)-B(12) 1.386(1), B(12)-C(2) 1.617(1), C(1)-C(2) 1.695(1); N(1)-B(11)-C(1) 127.57(8), N(1)-B(11)-Cl(1) 117.23(7), C(1)-

B(11)-Cl(1) 115.20(7), N(2)-B(12)-C(2) 127.34(8), N(2)-B(12)-Cl(2) 117.44(7), C(2)-B(12)-Cl(2) 115.21(7), B(11)-C(1)-C(2) 117.12(7), B(12)-C(2)-C(1) 117.70(7).

The molecule structures of **25** and **26b** are shown in Fig. 13. The B-N bond lengths are 1.387 Å for **25** and 1.384/1.386 Å for **26b**, respectively, indicating strong π interactions between boron and nitrogen atoms. The B-C_{cage} distances of 1.617 Å for **25** and 1.612/1.617 Å for **26b**, respectively, are typical of B-C single bonds. It has been reported that the C_{cage}-C_{cage} bond lengths in substituted *o*-carborane clusters are tunable by different substitution.^[110] In the cases of **25** and **26b**, the C1-C2 bond lengths [1.673 and 1.695 Å, respectively] are slightly longer than in *o*-carborane^[94] [1.629 Å], but fall into the range for other substituted *o*-carborane clusters [1.63- 1.72 Å].^[111] The C2-C1-B11 bond angle in **25** is 116.2°, and the two corresponding angles in **26b** are 117.1/117.7°, respectively.

3.3.2 Diborane(4)-yl-*o*-carboranes **28**

The reaction of *o*-carborane, *n*-BuLi and 1,2-dichloro-1,2-bis(dimethylamino)diborane (4)^[112] did not lead to **27** with a four-membered *exo*-cycle, but to a mixture of **28a** and **28b** (Scheme 42), the first examples of diborane(4)-yl-substituted *o*-carborane derivatives, as confirmed by an X-ray structure analysis of **28a** (see below).

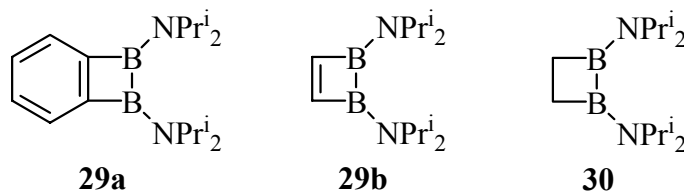


Scheme 42

The ¹¹B-NMR spectrum exhibits five signals [δ = 44.9, 34.9 (*exo*-polydral boron atoms) ppm, slightly shifted when compared with that for (Me₂NBCl)₂, 37.6 ppm), - 2.1, - 8.2, - 11.0, - 12.8 (skeletal boron atoms) ppm]. The EI-MS spectrum shows peaks at m/z = 296 for [**28a**⁺-1] and 396 for [**28b**⁺], respectively].

That the reaction favors **28** instead of **27** indicates that the ring strain is too high for the

four membered heterocycle in the latter, although the related 1,2-dihydro-1,2-diborete **29a**,^[113] **29b**^[114], and 1,2-diboretane **30**^[115] are known. The long C-C bond distance in *o*-carborane [1.629 Å]^[94] may be another factor which does not allow the formation of **27**. The formation mechanism for **28a** is not yet clear.



The structure of **28a** is shown in Fig. 14. In the diborane(4)-yl moiety, the three B-N bond lengths are 1.393, 1.423 and 1.435 Å, indicating strong boron nitrogen π interactions. The distances of B11-C1 (1.626 Å) and C1-C2 (1.667 Å) are not unusual when compared with those in **25** and **26c**, while the C2-C1-B11 bond angle of 113.7° is slightly smaller than those in **25** and **26c**, respectively.

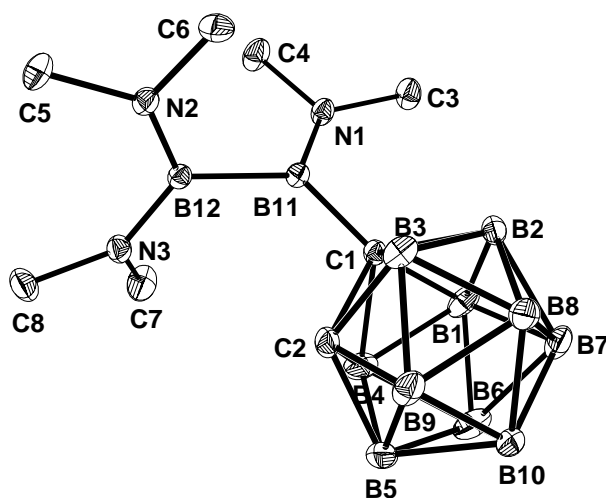
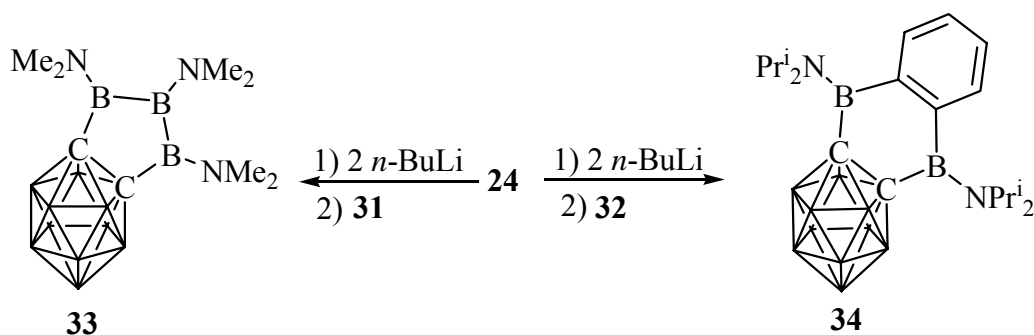


Fig. 14. Molecule structure of **28a**, H atoms omitted for clarity. Selected bond lengths [Å] and angles [°]: N(1)-B(11) 1.393(1), N(2)-B(12) 1.423(1), N(3)-B(12) 1.435(1), B(11)-C(1) 1.626(1), B(11)-B(12) 1.733(1), C(1)-C(2) 1.667(1); N(1)-B(11)-C(1) 121.50(8), N(1)-B(11)-B(12) 119.52(8), C(1)-B(11)-B(12) 118.97(8), N(2)-B(12)-N(3) 123.10(8), N(2)-B(12)-B(11) 118.09(8), N(3)-B(12)-B(11) 118.80(8), B(11)-C(1)-C(2) 113.72(7).

3.3.3 *o*-Carboranes with *exo*-cluster boron heterocycles

There are a few *o*-carborane derivatives with *exo*-polyhedral rings involving boron, and a less number of such derivatives have direct C_{cage}-B bonds. The reactions of dilithio-*o*-carborane with 1,3-dichloro-1,3,5-tris(dimethylamino)triborane(5) (**31**)^[116] and 1,2-C₆H₄-(*i*Pr₂BCl)₂ (**32**)^[113] afforded the *exo*-cyclic derivative **33** with a five-membered C-C-B-B-B ring and **34** with six-membered C-C-B-C-C-B heterocycle, respectively (Scheme 43).



Scheme 43

The ¹¹B-NMR spectra of **33** exhibits seven signals [$\delta = 53.9, 44.2$ ppm (*exo*-polydral boron atom, slightly downfield shifted when compared with that for **31**, 50.5 and 40.9 ppm), $-0.1, -2.6, -6.3, -10.5, -13.5$ ppm (skeletal boron atoms)]. The ¹¹B-NMR spectra of **34** gives five signals [$\delta = 38.5$ ppm (*exo*-polydral boron atom, comparable to that for **32**, 37.5 ppm), $1.3, -2.6, -7.8, -9.3, -13.6$ ppm (skeletal boron atoms)]. The EI-MS spectra show the molecule ion peaks for **33** and **34**, respectively, with correct isotopic patterns.

The structures of **33** and **34** have been confirmed by X-ray diffraction analyses (Fig. 15). Both the *exo*-polyhedral heterocycles are puckered. In **33**, the B-N bond lengths (av. 1.388 Å) are comparable to those in **34** (av. 1.397 Å), indicating strong B-N π interactions, as in the structures of **25**, **26c** and **28**. The C1-C2 distance in **33** (1.736 Å) is longer than that **34** (1.675 Å) and those found for **25**, **26c** and **28**. The bond angles of B11-C1-C2 and B13-C2-C1 in **33** (107.4 °) and B1-C1-C2 and B2-C2-C1 in **34** (110.5/110.2 °), respectively, are slightly smaller than those found in **25**, **26c** and **28** (113.7-117.7°) due to the formation of the *exo*-polyhedral heterocycles. In **33**, the B11-C1 and B13-C2 distances of 1.623/1.624 Å are typical of B-C single bonds. The *exo*-cyclic B-B bond lengths are 1.703/1.714 Å, and the torsion angles of

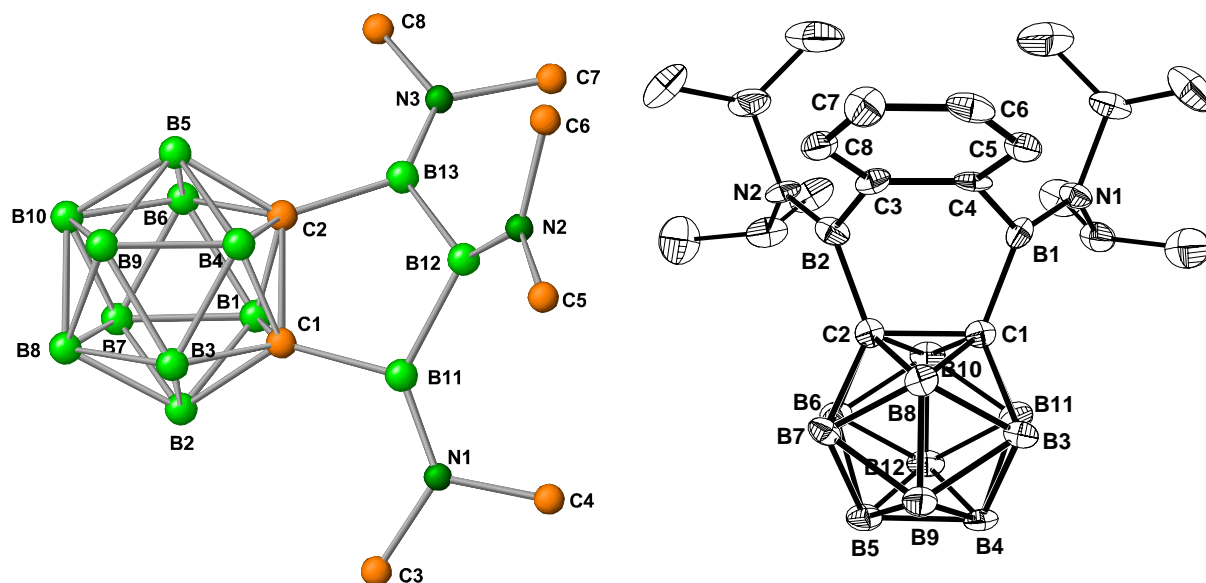


Fig. 15. Molecule structures of **33** (left) and **34** (right). H atoms omitted for clarity. Selected bond lengths [\AA] and angles [$^\circ$]: **33**: C1-C2 1.736(4), C2-B13 1.623(4), B13-N3 1.381(4), B13-B12 1.714(5), B12-N2 1.396(4), B12-B11 1.703(5), B11-N1 1.388(4), B11-C1 1.624(5); C1-C2-B13 107.4(2), C2-B13-B12 103.7(2), B13-B12-B11 104.7(2), B12-B11-C1 104.1(2), B11-C1-C2 107.4(2). For **34**: N1-B1 1.395(7), N2-B2 1.398(7), B1-C4 1.576(8), B1-C1 1.641(8), B2-C3 1.577(8), B2-C2 1.641(8), C1-C2 1.675(7), C3-C4 1.422(7); N1-B1-C4 125.6(5), N1-B1-C1 124.3(5), C4-B1-C1 109.9(5), N2-B2-C3 125.3(5), N2-B2-C2 125.3(5), C3-B2-C2 109.2(5), B1-C1-C2 110.5(4), B2-C2-C1 110.2(4), C8-C3-B2 125.3(5), C4-C3-B2 116.0(5), C5-C4-B1 123.7(5), C3-C4-B1 116.5(5).

B11-B12-B13-C2 and B12-B11-C1-C2 are calculated to be $34.7^\circ/21.30^\circ$, respectively. In **34**, the C1-B1 and C2-B2 distances of 1.641(8) \AA are longer than those for B2-C3 and B1-C4 [1.577(8) and 1.576(8), respectively], which can be attributed to the different coordination numbers of C_{cage} and C_{phenyl} atoms. The torsion angles of C3-B2-C2-C1 and B1-C1-C2-B2 are calculated to be $-51.9(5)/1.2(5)^\circ$, respectively.

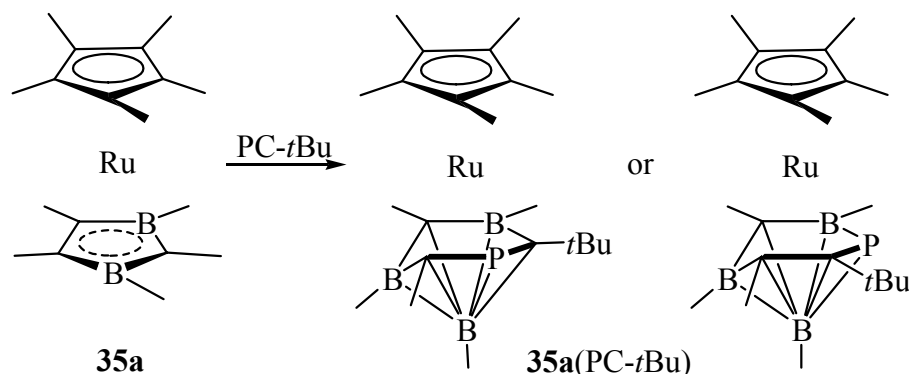
3.3.4 Conclusion

A series of C-boryl-*o*-carborane derivatives have been synthesized by reacting dilithio-*o*-carborane and the corresponding chloroboranes, respectively, which were structurally characterized. The monborylation occurs as the main reaction with $i\text{Pr}_2\text{NBCl}_2$, whereas with Et_2NBCl_2 the diborylated product 1,2-(Et_2NBCl) $_2$ -*o*- $\text{C}_2\text{B}_{10}\text{H}_{10}$ (**26b**) is obtained. The

diborane(4)-yl *o*-carboranes **28a** and **28b** were produced by the reaction involving 1,2-dichloro-1,2-bis-(dimethylamino)diborane(4). The reactions with 1,3-dichloro-1,3,5-tris(dimethylamino)triborane(5) (**31**) and 1,2-C₆H₄(*i*Pr₂BCl)₂ (**32**) afforded the *exo*-cyclic derivatives **33** with a five-membered C-C-B-B-B ring and **34** with a six-membered C-C-B-C-C-B heterocycle, respectively.

3.4 Reactivity of (η^5 -pentamethylcyclopentadienyl)(η^5 -2,3-dihydro-1,3-diboroly)ruthenium complexes

The unique reactivity of the violet, formally 16 VE sandwich complexes 2,3-dihydro-1,3-diboroly-pentamethylcyclopentadienylruthenium **35**^[47] results from the folding along the B...B vector of the heterocycle, like that in the green iron complexes (folding angle $\alpha = 41.3^\circ$).^[46c,d] Coordination of the donor ligands :CO and :CN-R at the Ru center yields yellow



Scheme 44

18 VE adducts **35**-CO, **35**-CN-R with reduced folding angles ($< 20^\circ$)^[47a] and incorporation of boranediyl ($[:\text{BH}]$ from $\text{BH}_3\cdot\text{thf}$) as well as sulfur (from H_2S) results in the formation of ruthenacarboranes^[47a] and ruthenathiacarboranes^[47b], respectively. Phosphanes and **35** form donor-acceptor complexes **35**-PH₂R (R = H, Ph), whereas triorganylphosphane adducts **35**-PR₃ (R = Me, Ph) are unstable. With *t*-butylphosphaacetylene $:\text{P}\equiv\text{C-CMe}_3$, no adduct but its incorporation into **35** is observed (Scheme 44). However, it is not yet known which of the possible isomers of the resulting ruthenaphosphacarborane **35a(PC-*t*Bu)** was formed.^[47 b]

As a continuation of the reaction with $:\text{P}\equiv\text{C-CMe}_3$ the reactivity of **35** towards alkynes is studied, which in principle should give complexes with new ligands via insertion/ring expansion. Reactions of **35** with allyl chloride are carried out to test the possibility of formation of allylruthenium compounds, which might lead to oligodecker products. First, the

long-sought crystal structure of the (η^5 -pentamethylcyclopentadienyl)(η^5 -2,3-dihydro-1,3-diborolyl)ruthenium derivative **35b** will be described. The preliminary results of DFT calculations on the electronic structures of the corresponding model complexes of ruthenium and iron, respectively, are reported (by Dr. I. Hyla-Kryspin).

3.4.1 Crystal and electronic structures of Ru and Fe complexes

3.4.1.1 Crystal structure of the B-trimethylsilylmethyl derivative **35b**

The Siebert group^[47] has been trying for years to obtain the detailed structure of a (η^5 -pentamethylcyclopentadienyl)(η^5 -2,3-dihydro-1,3-diborolyl)ruthenium sandwich complex to further understand its unique properties. Finally, compound **35b**, first isolated as a dark violet oil,^[47b] gave suitable crystals for an X-ray structure analysis on cooling in hexane. The crystal structure of **35b** (Fig. 16) confirms that the 1, 3-diborolyl ring C_3B_2 is folded by 40.7° along the B...B vector, very similar to its green iron analog.^[46c,d] The Ru-C2 bond length (2.029, cf. Fe-C 1.899 Å) is markedly shorter than the other Ru-C bond lengths of the heterocycle. Upon coordination of a donor ligand such as $Me_3C-N=C$: the folding angle along the B...B vector is reduced to $16.2/19.0^\circ$.^[47a]

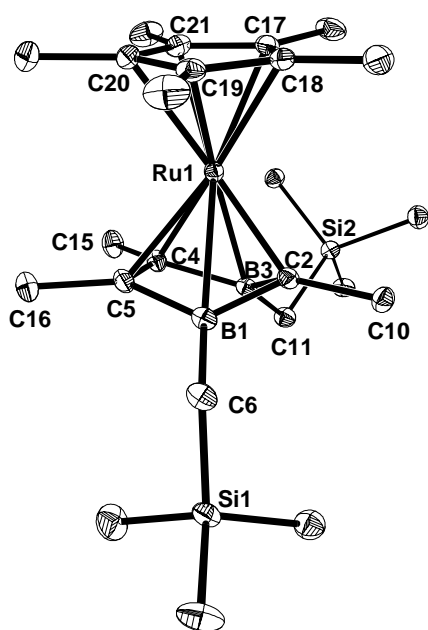


Fig. 16. (left) Molecule structure of **35b**, H atoms omitted for clarity. Selected bond lengths [Å] and angles [$^\circ$]: Ru(1)-Cp* 2.139(2)-2.219(2), Ru(1)-C(2) 2.029(2), Ru(1)-B(1) 2.359(2), Ru(1)-C(5) 2.225(2), Ru(1)-C(4) 2.221(2), Ru(1)-B(3) 2.405(3), B(1)-C(5) 1.574(3), C(4)-C(5) 1.399(3), B(3)-C(4) 1.582(3), B(3)-C(2) 1.560(3), B(1)-C(2) 1.559(3); C(2)-B(1)-C(5) $109.7(2)$, C(4)-C(5)-B(1) $105.8(2)$, C(5)-C(4)-B(3) $103.8(2)$, C(2)-B(3)-C(4) $109.6(2)$, B(1)-C(2)-B(3) $90.1(2)$.

3.4.1.2 Electronic structures of the model compounds of Ru (**35**) and Fe (**36**)

Calculations have been carried out by Dr. I. Hyla-Kryspin, University of Münster, and she has summarized the preliminary results as follows: “X-ray investigation on the 1,3-diborolyl complexes of ruthenium **35b** and iron **36b** revealed that both structures differ from other known 1,3-diborolyl sandwich structures since the diborolyl ring of (η^5 -pentamethylcyclopentadienyl)(η^5 -1,3-bis(trimethylsilylmethyl)-2,4,5-trimethyl-2,3-dihydro-1,3-diborolyl)ruthenium (**35b**) and of (η^5 -pentamethylcyclopentadienyl)(η^5 -1,3-diethyl-2-methyl-4,5-diisopropyl-2,3-dihydro-1,3-diborolyl)iron (**36b**) is largely folded along the B...B vector. Some years ago the electronic structure of complex **36** was investigated with help of semiempirical Extended-Hückel calculations.^[46d] On the basis of the qualitative interaction diagrams (Fig. 2) and the comparison with bonding properties of the cyclopentadienyl ligand as well as the 18 valence electrons rule it was possible to postulate that the folding of the diborolyl ligand of complex **36** is due to electronic factors. It is clear that a more accurate and quantitative description of the structural and electronic properties of complex **36** could not be achieved within the Extended-Hückel scheme.

Nowadays, computational transition metal chemistry is dominated by density functional theory (DFT) approaches^[117] which are able to provide good results not only for geometries and the energetics but also for spectroscopic properties, and allow for a complementary to experimental description of the investigated chemical problems. Up to now, alternative high level *ab initio* methods are either too costly for large molecules or not accurate enough.

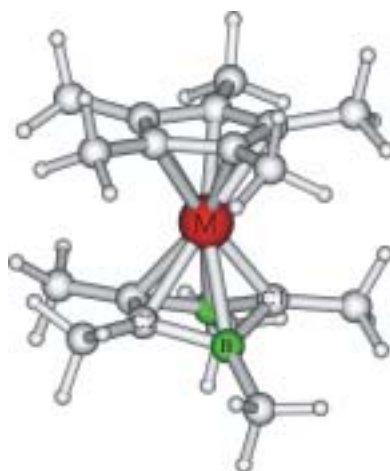


Fig. 17. Global minimum structure of the model complexes **35a** (M = Ru) and **36a** (M = Fe).

The investigation has been continued on complex **35** as well as on **36** with the DFT/B3LYP method^[118] by using valence triple- ξ basis sets augmented with polarization functions. In the case of Ru, 28 core electrons are approximated by pseudopotentials and the remaining electrons are also described by a triple- ξ basis. We started with geometry optimizations for the model complexes **35a** and **36a** with methyl substituents on both ligands (Fig. 17). In order to investigate the possible influence of the substituents on structural and electronic properties of the parent complexes **35** and **36** we continued with B3LYP calculations on the model complexes **35**, **36**, **35'** and **36'** as well as for the free 1,3-diborolyli anion (**37-H**)⁻ and the metal fragments $\text{Fe}(\text{C}_5\text{H}_5)^+$ and $\text{Ru}(\text{C}_5\text{H}_5)^+$.

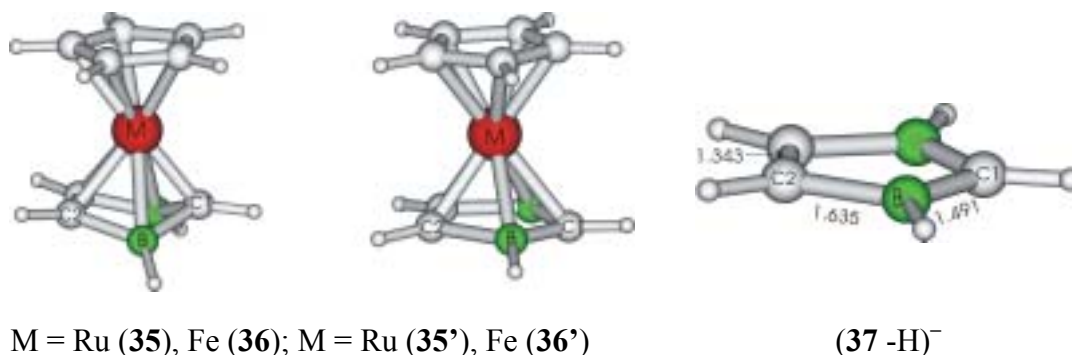


Fig. 18. Optimized structures of the model complexes **35**, **36**, and the free 1,3-diborolyli anion.

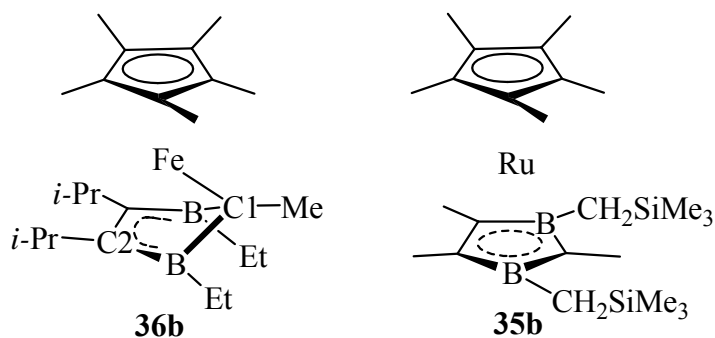
In the model complexes **35** and **36** the substituents on both ligands are hydrogen atoms. During the geometry optimization for **35'** and **36'** we required a planar structure of the diborolyli ligand (constrained geometry optimizations) (Fig. 18). In order to verify the stationarity of the optimized structures, the geometry optimization were followed by vibrational frequency analyses.

We are interested in: (i) structural, electronic and energetic properties of the optimized structures, (ii) bonding energies of the diborolyli ligand, and (iii) spectroscopic properties of the global minimum structures. Excitation energies were calculated by using the time dependend density functional theory (TD-DFT) method with the same basis sets and functionals as described above. The description of the electronic properties of the investigated complexes, metal fragments and ligands was supported by the natural bond orbital (NBO) population analyses.^[119] The preliminary calculations were carried out with the Gaussian 98

Program.^[120] For graphic displays we used MOLDEN program.^[121]

Table 1. Comparison of selected optimized parameters of the model complex **35a** and **36a** with available X-ray data of **35b** and **36b**.

Distance [Å]	36a (M = Fe) 36b		35a (M=Ru) 35b	
	Calc.	X-ray ^[46d]	Calc.	X-ray
M-C(Cp) _{avr}	2.122	2.054-2.118	2.228	2.138-2.219
M-C1	1.936	1.899	2.041	2.029
M-C2	2.143	2.116	2.247	2.223
M-B	2.288	2.248	2.399	2.382
B-C1	1.562	1.547	1.567	1.559
B-C2	1.578	1.568	1.581	1.578
C2-C2'	1.404	1.412	1.406	1.399
α [deg.]	39.6	41.3	40.8	40.7



The free diborolyl anion (**37** -H)⁻ adopts a planar structure. The distortion from the planar structures (**35'** and **36'**) to the folded one of the complexes **35** and **36** (Table 2) is an endothermic process and requires 12.6 and 11.4 kcal/mol, respectively. However, **35** and **36** are more stable than **35'** and **36'** by 24.5 and 24.9 kcal/mol, respectively.

Table 2. Relative energies, number of imaginary frequencies (NIMAG), and selected optimized parameters of the model complexes **35** and **36**.

	36 (C_s)	36' (C_s)	35 (C_s)	35' (C_s)
E_{rel} [kcal/mol]	0.00	+24.94	0.00	+24.51
NIMAG	0	3	0	3
α [$^\circ$]	41.1	0.0	41.7	0.0
Distance [\AA]				
M - C(Cp) _{avr}	2.091	2.065	2.227	2.190
M - C1	1.906	2.207	2.016	2.371
M - C2	2.096	2.084	2.221	2.252
M - B	2.251	2.150	2.382	2.314
B - C1	1.545	1.507	1.556	1.513
B - C2	1.565	1.667	1.566	1.652
C2 - C2'	1.390	1.357	1.395	1.362

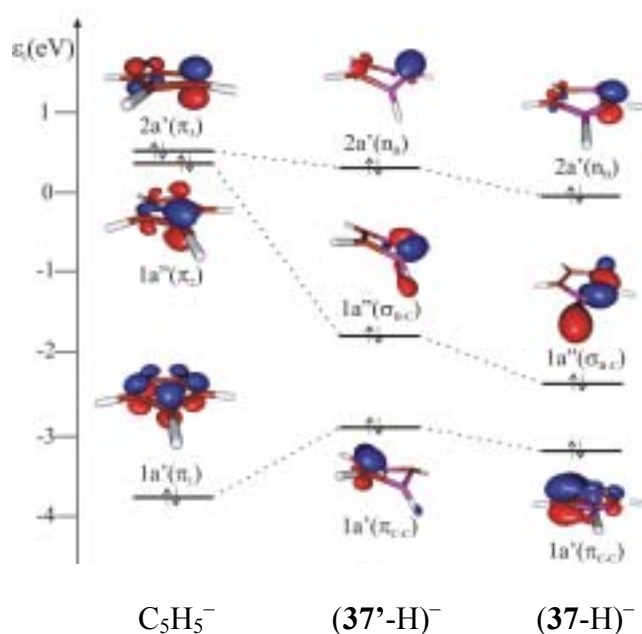


Fig. 19. (left) Comparison of the highest occupied Kohn- Sham MOs of the free diborolyl ligand in the optimized planar (**37** -H)⁻ and folded (**37'** -H)⁻ structures with those of $C_5H_5^-$.

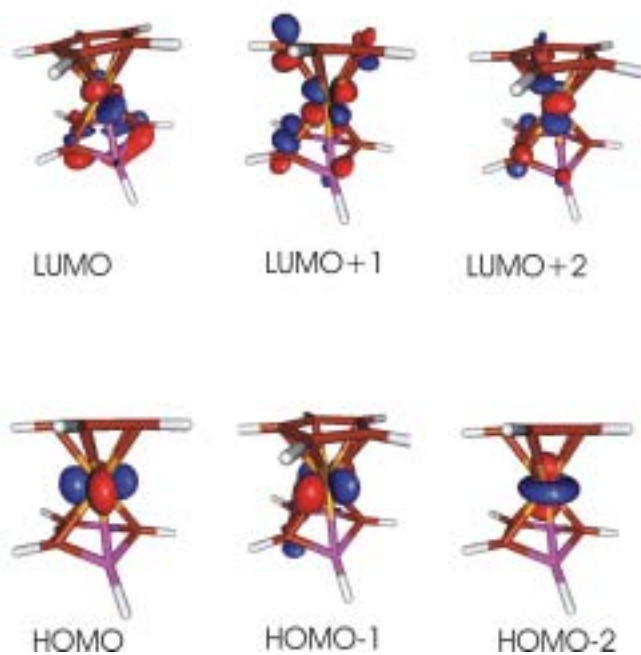


Fig. 20. Valence Kohn-Sham MOs of **35a** and **36a**.

The three highest occupied MOs can be characterized as metal “ t_{2g} ” like level. LUMO and LUMO+1 correlate with the metal “ e_g ”-like level and LUMO+2 with the $2a''(\pi^*_{C-C})$ MO of the diborolyly ligand. The HOMO-LUMO gap amounts to 3.45 eV in **36a** and 3.43eV in **35a**.

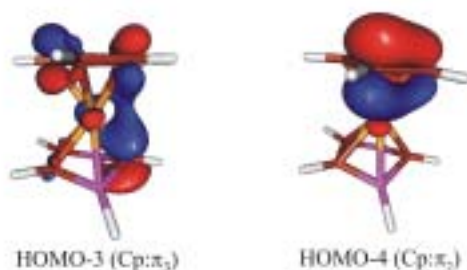


Fig.21. Kohn-Sham MOs of **35a** and **36a** with predominant Cp(π_3) and Cp(π_2) character.

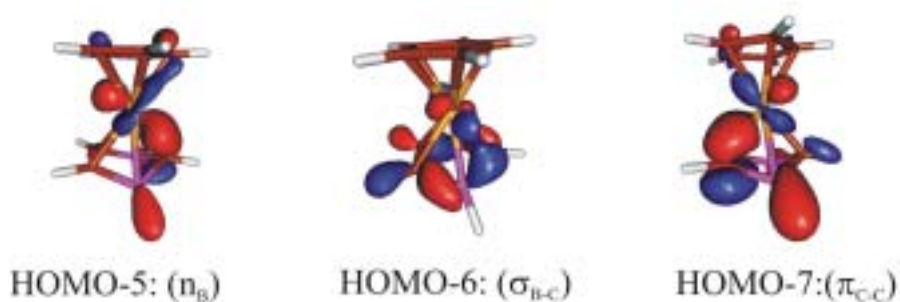


Fig. 22. Kohn-Sham MOs of **35a** and **36a** with predominant diborolyly character.

Table 3. TD-DFT calculated excitation energies and assignment for the ten lowest excited singlet states of the model iron complex **36**.

Nr.	[nm]	[eV]	f^a	Excited state	Contributing orbital excitations	Character ^{b)}
1	1059	1.17	0.0007	1A''	0.57 HOMO → LUMO	d → d
					0.15 HOMO → LUMO+2	d → d
2	850	1.46	0.0035	1A'	0.56 HOMO-1 → LUMO	d → d
					0.24 HOMO-1 → LUMO+2	d → ligand (L)
3	751	1.65	0.0000	2A''	0.58 HOMO-2 → LUMO	d → d
					0.24 HOMO-2 → LUMO+2	d → ligand (L)
4	453	2.73	0.0005	2A'	0.58 HOMO → LUMO+1	d → d
					0.31 HOMO-2 → LUMO+1	d → d
5	405	3.06	0.0011	3A''	0.59 HOMO-1 → LUMO+1	d → d
					0.26 HOMO → LUMO+2	d → ligand (L)
6	374	3.31	0.0046	4A''	0.57 HOMO-3 → LUMO	Ligand (Cp) → d
					-0.24 HOMO-5 → LUMO	Ligand (L) → d
7	360	3.44	0.0066	3A'	0.53 HOMO-2 → LUMO+1	d → d
					0.32 HOMO-1 → LUMO+2	d → ligand (L)
8	339	3.66	0.0008	5A''	0.55 HOMO → LUMO+2	d → ligand (L)
					-0.29 HOMO-3 → LUMO	Ligand (Cp) → d
9	317	3.92	0.0000	6A''	0.60 HOMO-5 → LUMO	Ligand (L) → d
					-0.19 HOMO-2 → LUMO+2	d → ligand (L)
10	310	4.00	0.0070	4A'	0.62 HOMO-4 → LUMO	Ligand (Cp) → d
					0.21 HOMO-2 → LUMO+2	d → ligand (L)

a) oscillator strength; b) L = diborolylyl, Cp = C₅H₅

TD-DFT

1. We do not consider the character of the transitions with low oscillator strength, because normally they should not appear in the spectrum.
2. The calculated transition to the excited state 1A' of the model complex **36** (850 nm; 1.46 eV, Table 3) agrees very well with that observed in the UV-spectrum of complex **36a** (750-800 nm; 1.65-1.55eV).

3. The calculated transition to the excited state 1A' of the model complex **35** (552 nm; 2.45 eV, Table 4)) agrees also very well with that observed in the UV-spectrum of complex **35a** (560-580 nm; 2.21-2.14eV).
4. Both transitions have predominant d → d character (Tables 3 and 4).

Table 4. TD-DFT calculated excitation energies and assignment for the ten lowest excited singlet states of the model ruthenium complex **35**.

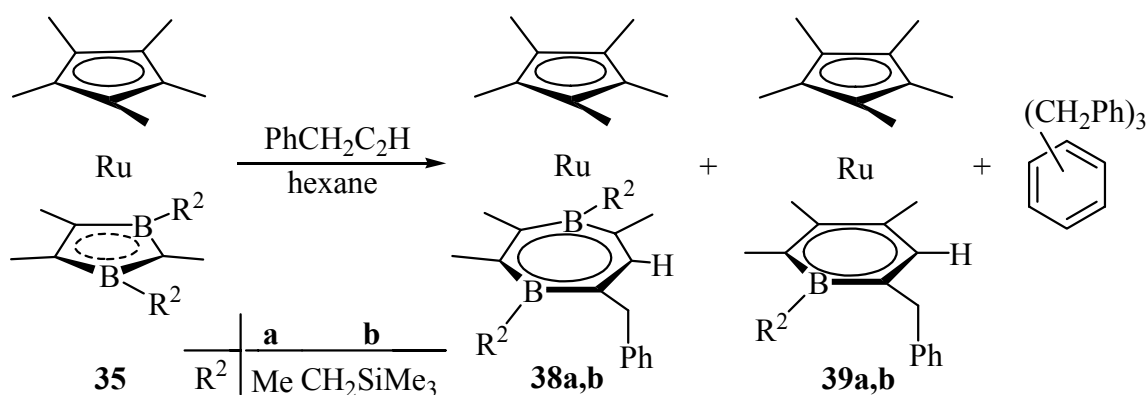
Nr.	[nm]	[eV]	f ^{a)}	Excited state	Contributing orbital	
					excitations	Character ^{b)}
1	634	1.95	0.0021	1A''	0.65 HOMO → LUMO	d → d
					-0.11 HOMO-2 → LUMO	d → d
2	622	1.99	0.0017	2A''	0.65 HOMO-2 → LUMO	d → d
					-0.13 HOMO-2 → LUMO+2	d → ligand (L)
3	552	2.45	0.0087	1A'	0.64 HOMO-1 → LUMO	d → d
					-0.13 HOMO-1 → LUMO+2	d → ligand (L)
4	385	3.22	0.0024	3A''	0.68 HOMO-3 → LUMO	Ligand (Cp) → d
5	313	3.96	0.000	2A'	0.53 HOMO → LUMO+1	d → d
					-0.37 HOMO-2 → LUMO+1	d → d
6	299	4.15	0.0014	4A''	0.53 HOMO-1 → LUMO+1	d → d
					-0.39 HOMO → LUMO+2	d → ligand (L)
7	298	4.16	0.0148	3A'	0.44 HOMO-2 → LUMO+1	d → d
					0.43 HOMO-4 → LUMO	Ligand (Cp) → d
8	293	4.24	0.0230	4A'	0.48 HOMO-4 → LUMO	Ligand (Cp) → d
					-0.38 HOMO-1 → LUMO+2	d → ligand (L)
9	288	4.30	0.0025	5A''	0.61 HOMO-2 → LUMO+2	d → ligand (L)
					0.28 HOMO → LUMO+2	d → ligand (L)
10	281	4.41	0.0045	6A''	0.41 HOMO → LUMO+2	d → ligand (L)
					0.36 HOMO-1 → LUMO+1	d → d

a) oscillator strength; b) L = diborolylyl, Cp = C₅H₅

3.4.2 Insertion of alkynes into 1,3-diborolyruthenium complexes

3.4.2.1 Formation of novel 4-borataborepine complexes **38**

Treatment of **35b** with 3-phenyl-1-propyne (Scheme 45) in hexane yields the yellow, relatively air-stable solid **38b**, which exhibits one broad signal at $\delta = 29$ ppm in the ^{11}B -NMR spectrum (downfield compared to that of **35b**, $\delta = 21.7$ ppm). The absence of a second ^{11}B -NMR signal in the high-field region indicates that the uptake of the alkyne did not give a ruthenacarborane with an apical boron atom, as observed when **35a** is reacted with diborane(6).^[47a]



Scheme 45

In the EI-MS spectra, a cutoff peak at $m/z = 630$ shows that the 1:1 product does not lose the alkyne (expected for an adduct). A weak signal at $m/z = 532$ was tentatively assigned to the Cp*Ru(boratabenzene) complex **39b**, having the same isotopic pattern as the [**38b**-BCH₂SiMe₃]⁺ fragment. In addition, tribenzylbenzene was identified by MS as a side product. The structure of **38b** (Fig. 23) established by a single-crystal X-ray diffraction analysis proves the presence of a novel sandwich complex with the 4-borataborepine ligand, as a result of the insertion of the C≡C unit of the alkyne into a B-C bond of **35b**. As B1-C2 and B3-C2 bonds in **35b** are equivalent for the insertion of a C≡C group of the alkyne, both the B-C bonds react with the alkyne yielding enantiomers, which are found in the solid state.

The seven-membered ring in **38b** exhibits a reduced folding along the B...B vector ($\alpha = 26^\circ$), and the Ru-B distances are found to be 2.527 and 2.542 Å, respectively, which are significantly elongated compared to those in **35b**. The Ru-C bond distances vary within a range of 2.203 to 2.345 Å, with Ru-C4 being the shortest of the C₅B₂ ring. Because of the

bonding between Ru and the larger ring its exocyclic α -atoms are more or less tilted towards the ruthenium, with the exception of α -carbon C16 and C20 at the boron atoms, which tilt in the opposite direction.

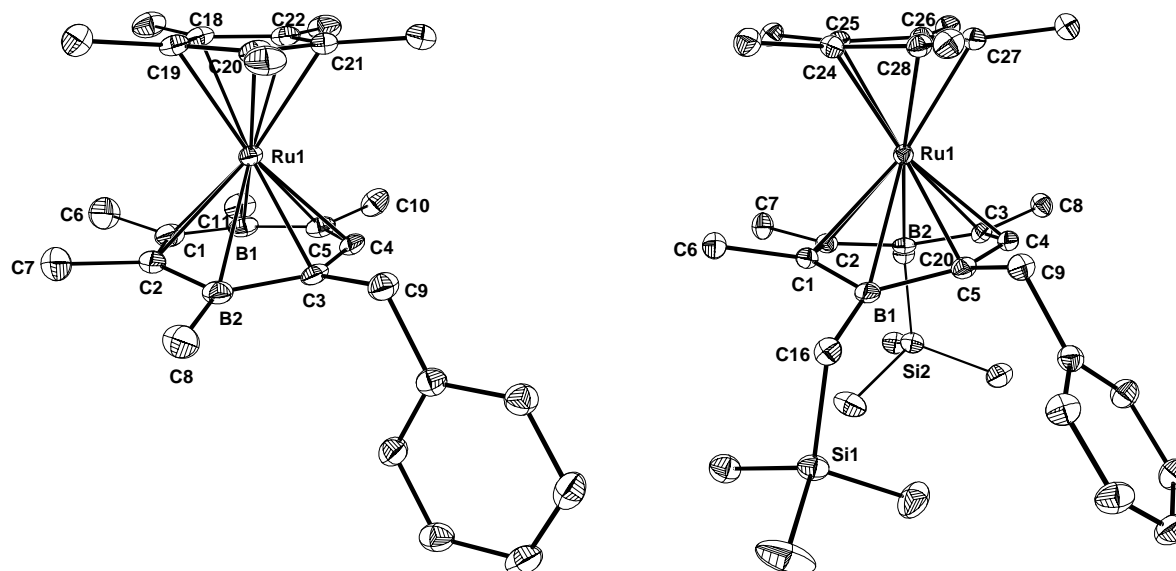
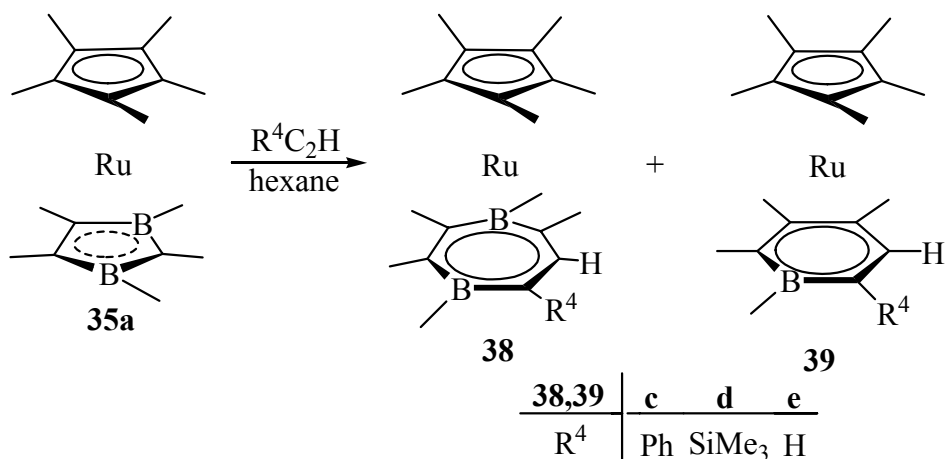


Fig. 23. Molecular structures of **38a** (left) and **38b** (right). H atoms omitted for clarity. Selected bond lengths [\AA]: **38a**: Ru-C_{Cp*} 2.178(3)-2.201(3), Ru-C2 2.332(3), Ru-B2 2.443(3), Ru-C3 2.299(3), Ru-C4 2.234(3), Ru-C5 2.315(3), Ru-B1 2.429(4), Ru-C1 2.330(3), B2-C3 1.520(5), C3-C4 1.415(4), C4-C5 1.400(4), C5-B1 1.528(5), B1-C1 1.531(5), C1-C2 1.415(5), C2-B2 1.542(5). The dihedral angle between the Cp* and C₅B₂ two best planes is 6.6°. **38b**: Ru-C_{Cp*} 2.172(3)- 2.205(3), Ru-C1 2.287(3), Ru-C2 2.345(3), Ru-B2 2.542(3), Ru-C3 2.311(3), Ru-C4 2.203(3), Ru-C5 2.303(3), Ru-B1 2.527(3), B1-C5 1.531(4), C5-C4 1.409(4), C4-C3 1.412(4), C3-B2 1.524(4), B2-C2 1.540(4), C2-C1 1.413(4), C1-B1 1.545(4).

The influence of the bulky silyl groups in **38b** is evident when compared with **38a**, obtained from the reaction of violet **35a** and 3-phenyl-1-propyne in hexane (Scheme 45). The yellow product was identified as a mixture of the expected 4-borataborepine complex **38a** and the boratabenzene compound **39a** by MS. While most of the bond lengths and angles are similar to those in **38b**, some differences arise in **38a** (Fig. 23) due to the absence of the silyl groups: the Ru-B bond lengths of 2.429 and 2.443 \AA , respectively, are significantly shorter than those in **38b**, and the folding along the B...B vector ($\alpha = 12.5^\circ$) is only half of that in **38b**. The seven-membered C₅B₂ ring is almost parallel to the Cp* ring.



Scheme 46

The reactions of **35a** with other terminal alkynes such as phenylacetylene, trimethylsilylacetylene and ethyne gave the yellow 4-borataborepine complexes **38c,d,e** respectively, and the corresponding boratabenzene complexes **39** as byproducts (Scheme 46). In the former two cases, the benzene derivatives were also detected by MS.

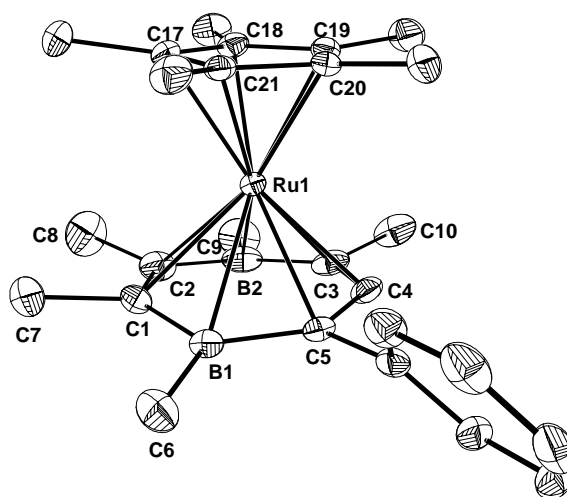
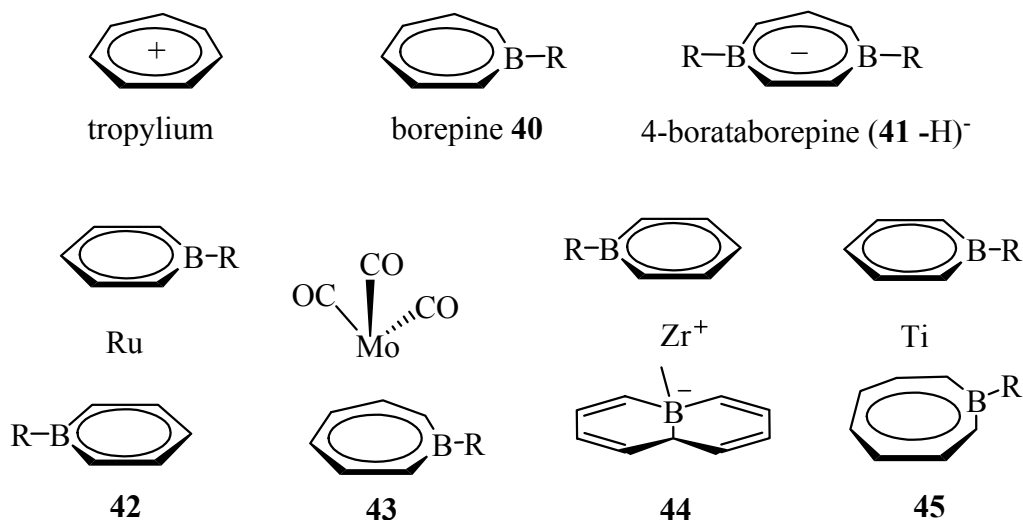


Fig. 24. Molecule structures of **38c**. H atoms omitted for clarity. Selected bond lengths [Å]: Ru-Cp* 2.184(2)-2.196(2), Ru-B(1) 2.446(3) Ru-C(1) 2.310(2), Ru-C(2) 2.333(2), Ru-B(2) 2.456(3), Ru-C(3) 2.311(2), Ru-C(4) 2.244(2), Ru-C(5) 2.319(2), B(1)-C(1) 1.524(3), C(1)-C(2) 1.412(3), B(2)-C(2) 1.525(4), B(2)-C(3) 1.513(4), C(3)-C(4) 1.413(3), C(4)-C(5) 1.417(3), B(1)-C(5) 1.519(3). C(5)-B(1)-C(1) 124.2(2), C(2)-C(1)-B(1) 129.4(2), C(1)-C(2)-B(2) 128.9(2), C(3)-B(2)-C(2) 124.5(2), C(4)-C(3)-B(2) 129.7(2), C(3)-C(4)-C(5) 130.1(2), C(4)-C(5)-B(1) 129.58(19).

The constitution of compounds **38c,d,e** follow from their NMR ($\delta^{11}\text{B} = 26.1$ for **38c**, 28.1 for **38d**, and 26.0 ppm for **38e**) and MS data, respectively, and is confirmed by an X-ray structure analysis of **38c** (Fig. 24), which is similar to those of **38a,b**. With the B-Ph group replacing the methyl or trimethylsilylmethyl substituents in **38a,b**, respectively, the folding of the 1,3-diborolyl ligand along the B...B vector is 15.2° in **38c**. It was assumed that the reaction of **35a** with ethyne could be different. However, the reaction worked similarly, producing the yellow 4-borataborepine complex **38e**. The ^1H -NMR spectrum exhibits two doublet at $\delta = 5.54$ and 4.56 ppm, indicating the two CH moieties are adjacent. The preliminary results of the X-ray analysis of **38e** supports this assignment, however, the seven-membered ring is found to be severely disordered.

In general, the above-mentioned 4-borataborepine-ruthenium complexes **38** are yellow solids, and are relatively stable in the solid state at r.t. (even in air for a short time), but will decompose to give the corresponding boratabenzene complexes **39** in solution, and such process is found to be faster when in contact with air.



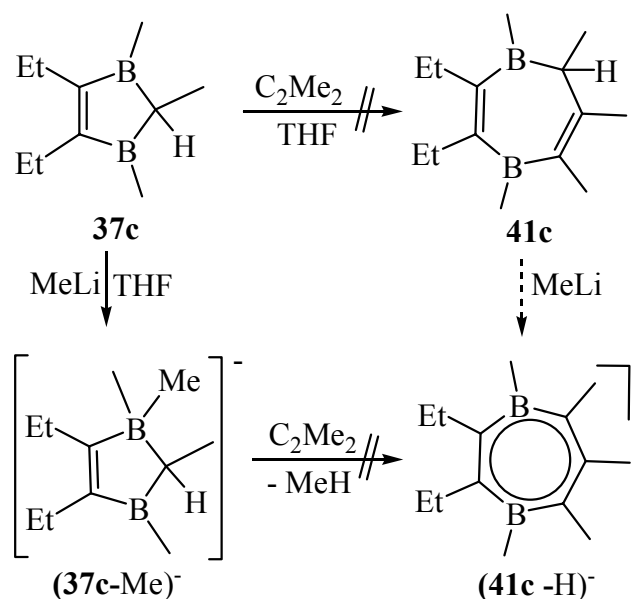
As boratabenzenes in complex **42**,^[122] the 4-borataborepines (**41 -H**)⁻ in **38a-e** function as 6e ligand, the 2e ene and the 4e allylic groups being separated by two boron atoms, but electronically connected by the p_z orbitals of boron atoms, as the short boron-carbon bond lengths indicate. The 4-borataborepine (**41 -H**)⁻ is formally derived from the tropylium ion C_7H_7^+ and the neutral borepine **40**^[123 a] (a 6e ligand in tricarbonyl(1-chloroborepine)-molybdenum **43**^[123 b]) by replacing two/one CH by two/one anionic BR^- , respectively. Thus **38** is an isomer of the bis(η^6 -boratabenzene)ruthenium **42**^[122 b] and a structural analog of (η^5 -

cyclopentadienyl)(η^7 -cycloheptatrienyl)chromium.^[124] Alternatively, according to the Wade-Mingos rules, **38** can be regarded as *nido*-ruthenapentacarbonacborane clusters with 8 vertices and 20 skeletal electrons (Cp*Ru: 1e, CR: 3e, BR: 2e).

The driving force for the alkyne insertion into the electron-poor complex **35** is the formation of the 6π electron anionic 4-borataborepine (**41** -H)⁻ in the 18 VE complexes **38**. The first insertion reactions of ethyne into one of the boratabenzene rings of bis(boratabenzene)zirconium and -titanium complexes have been reported by Ashe III et al.^[125] and Bazan et al.^[126], who obtained complexes **44** and **45** with 8a-H-4-borata-naphthalene^[125] and boratacyclooctatetraene^[126] as ligands, respectively.

3.4.2.2 Attempts to prepare 4-borataborepines from 1,3-diborole **37c**

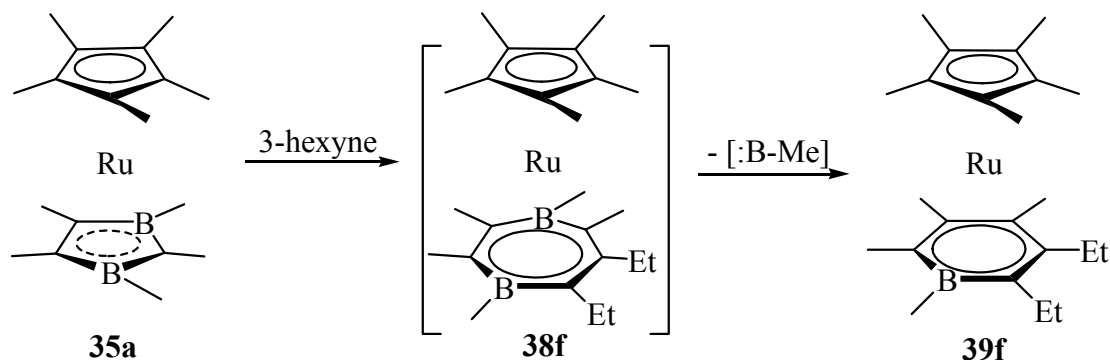
The independent preparation of the 4-borataborepine ligand is of particular interest, which would allow the complexation of a series of d-metal ions. However, first attempts did not give any positive results (Scheme 47). It was found that 2-butyne did not insert into the 1,3-diborole **37c** to give the expected product **41c**, which would produce the 4-borataborepine (**41c** -H)⁻ on deprotonation. Alternatively, no insertion of 2-butyne into the (proposed) deprotonated intermediate^[47a,127] (**37c**-Me)⁻ by elimination of Me-H was observed. In addition, the same reaction with 3-phenyl-1-propyne was also not successful.



Scheme 47

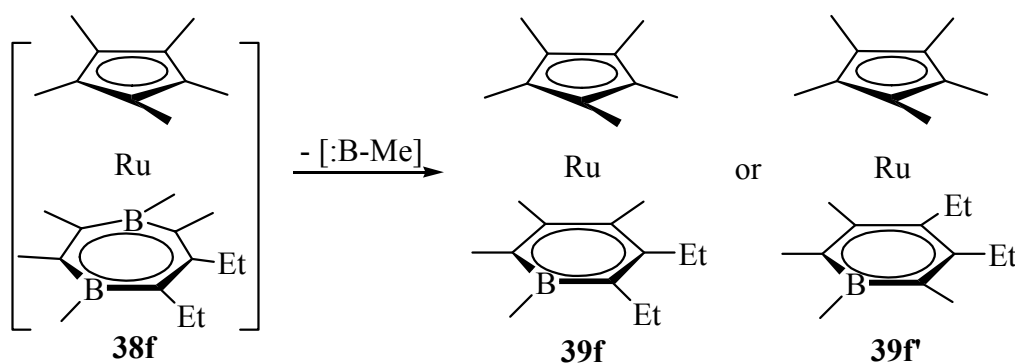
3.4.2.3 Formation of boratabenzene ruthenium complexes **39f,g**

To elucidate the unexpected formation of boratabenzene complexes **39a,b**, the stability of **38b** in solution was monitored by ^{11}B -NMR. During a period of several weeks a weak signal at $\delta = 16$ ppm increased, indicating that the boratabenzene complex **39b** was formed. In addition, the reactions of **35a** and 3-hexyne was carried out (Scheme 48), which led to the boratabenzene complexes **39f**, identified by ^{11}B -NMR ($\delta = 16.8$ ppm), HR-MS, and confirmed



Scheme 48

by a structural study. Obviously, steric requirements in the anticipated peralkylated complexes **38f** cause the fast elimination of one methylboranediyl moiety $[\text{:B-Me}]$, whereas **38a,b** eliminate $[\text{:B-R}^2]$ only slowly in solution. In principle, there may be the two isomers **39f** and **39f'** (Scheme 49), however, only **39f** was identified from the X-ray structure analysis.



Scheme 49

The structure of **39f** is shown in Fig. 25. The boratabenzene ring is essentially planar (torsion angle C13-C14-C15-B16: -1.3°), like in the reported boratabenzene complexes.^[122] The bond lengths of C11-B16/C15-B16 [1.470(4) and 1.458(4) Å, respectively] and C12-C13/C13-C14 [1.468(4) and 1.469(4) Å, respectively] are slightly longer than those of C11-C12/C14-C15 [1.436(4) and 1.436(4) Å, respectively] and that the Ru-C13/Ru-B16 bond

distances [2.262(3) and 2.257(3)Å, respectively] are comparable with those of the other Ru-C distances within the boratabenzene ring [2.220(3)-2.262(3)Å], indicating the boratabenzene ring in **39f** is disordered at the B16/C13 symmetrically equivalent positions.

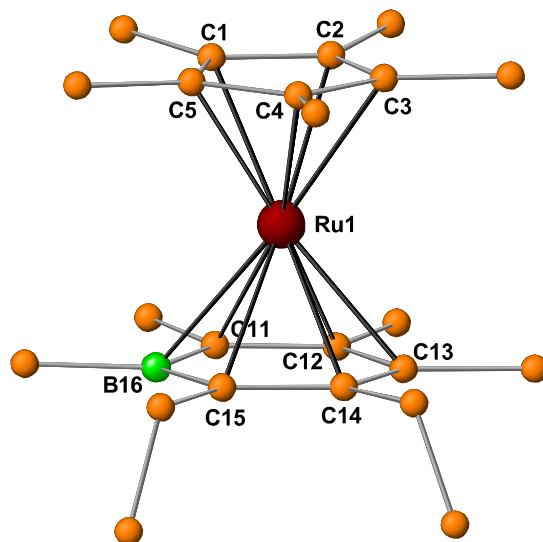
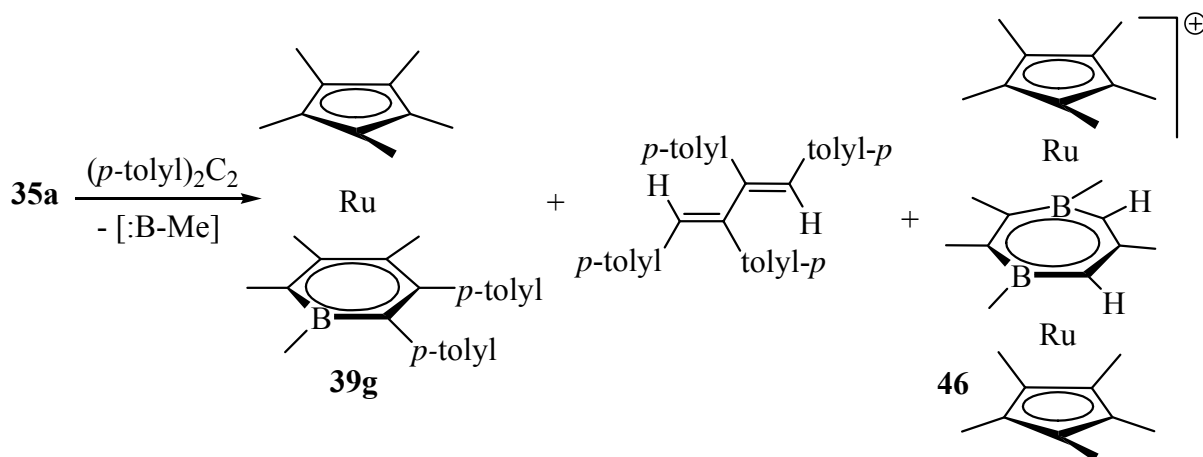


Fig. 25. Molecular structure of **39f**, H atoms omitted for clarity. Selected bond lengths [Å]: Ru1-Cp* 2.171(3)-2.181(3), Ru1-C11 2.256(3), Ru1-C12 2.262(3), Ru1-C13 2.262(3), Ru1-C14 2.220(3), Ru1-C15 2.232(3), Ru1-B16 2.257(3), C11-C12 1.436(4), C12-C13 1.468(4), C13-C14 1.469(4), C14-C15 1.436(4), C15-B16 1.458(4), C11-B16 1.470(4).

To further investigate the influence of the steric requirements on the formation of the boratabenzene complexes **39a,b,f**, the reaction of **35a** and di-*p*-tolylacetylene (Scheme 50, 1:1 molar ratio, in THF) was carried out. The reaction mixture was dried and extracted with



Scheme 50

toluene, after which the extract and trace amount of a yellow solid (see next Chapter) were

separated. The extract was found to be a mixture of the boratabenzene complex **39g**, (identified by ^{11}B -NMR and HR-MS) and (*Z,Z*)-1,2,3,4-tetratolyl-1,3-butadiene as a result of the dimerization of di-*p*-tolylacetylene.

3.4.3 Formation of the triple-decker **46** with a bridging C_5B_2 ligand

Recrystallization of the yellow solid isolated from the reaction mixture of **35a** and di-*p*-tolylacetylene (see above, Chapter 3.4.2) in CH_2Cl_2 gave yellow crystals. The X-ray structure analysis and HR-MS data showed it to be the novel triple-decker species **46** with a seven-membered ring as the bridging ligand, in which two CH groups are separated by a CMe moiety (Scheme 50). In the crystal structure (Fig. 26), the triple-decker cation with the chloride anion and a molecule of methylboronic acid are found, the latter two forming an infinite chain for the packing. The formation of **46** is not clear and no mechanism will be proposed. Most likely the recrystallization of the yellow solid in wet CH_2Cl_2 led to the cationic triple-decker **46**, and methylboronic acid.

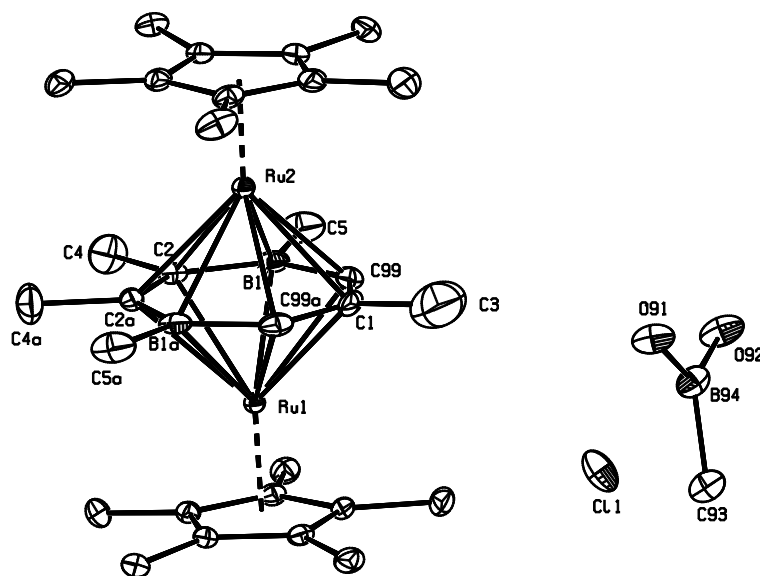
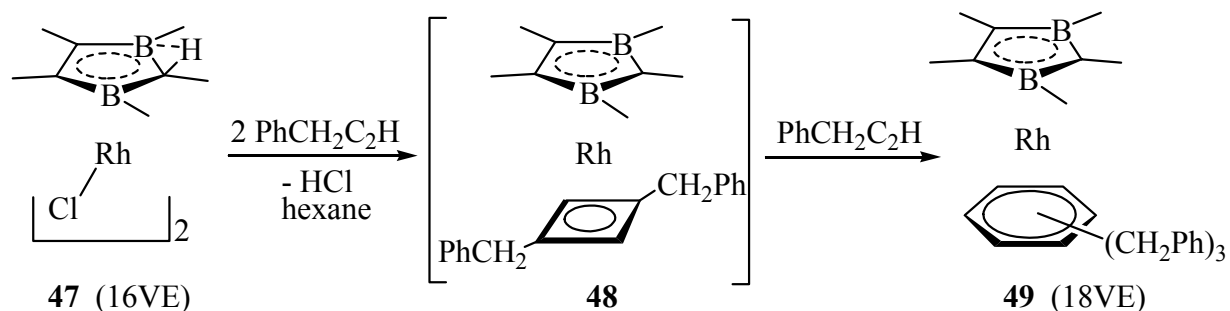


Fig. 26. Structure of **46** in the asymmetric unit, hydrogen atoms omitted for clarity.

Compound **46** is the first structurally characterized triple-decker complex to have a seven-membered ring as the bridging ligand. More experiments are needed to clarify its formation. The first example with a bridging C_5B_2 ring is a triple-decker CoCo complex^[128], which was only identified by MS from the reaction mixture of $\text{CpCo}(\text{C}_2\text{H}_4)_2$ and 1,4-dimethyl-2,3-diethyl-1,4-diboracyclohepta-2-ene.^[129]

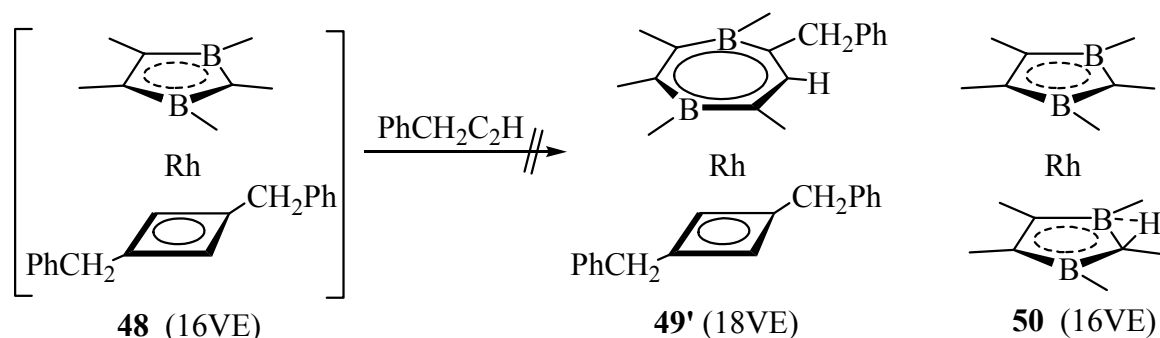
3.4.4 Interactions of η^5 -2,3-dihydro-1,3-diborole-(chloro)rhodium complexes with RCH_2C_2H and $(R_2P)_2C_2H_4$ ($R = Ph$)

In order to compare the reactivity of the Ru complexes **35** with the related dimeric chloro-rhodium species **47**^[130], its reaction with 3-phenyl-1-propyne was carried out (Scheme 51), in which the alkyne is cyclotrimerized to give **49** with a complexed tribenzylbenzene ring (and elimination of HCl).



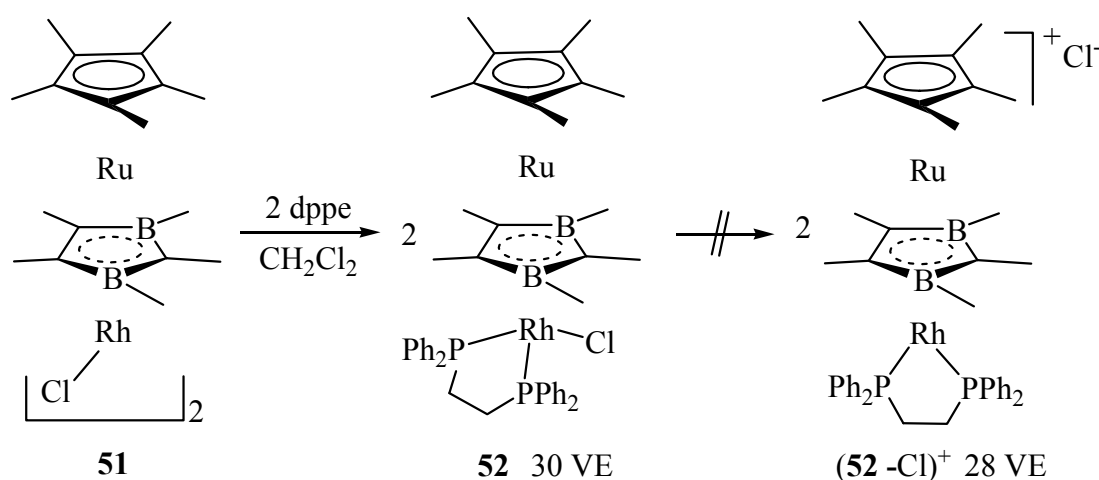
Scheme 51

The dark brown solid **49** is sparingly soluble in hexane. The ^{11}B -NMR (signal at $\delta = 32.3$ ppm, in CH_2Cl_2), and the HR-MS data ($m/z = 584.2281$) confirm the formation of **49**. The intermediate is proposed to be the $(\eta^5$ -1,3-diborolylo)(η^4 -cyclobutadiene)rhodium complex **48**, which offers two possible insertion of the third alkyne $PhCH_2C_2H$. The formation of the 18 VE complex **49** indicates, that its isomer **49'** having C_5B_2 and C_4 ligands is not favored. However, the reaction of **50**^[130] with an alkyne should give an 18 VE Rh complex with a C_5B_2 and C_3B_2 ring.



Scheme 52

The reaction of **35a** with $[\text{RhCl}(\text{C}_2\text{H}_4)_2]_2$ afforded the dimeric RuRh complex **51**.^[47b] The products obtained from **51** and PhC_2H have not yet identified. The reaction of **51** with $(\text{Ph}_2\text{PCH}_2)_2$ (dppe) produced the 30 VE triple-decker species **52** rather than the cationic $(\text{52} - \text{Cl})^+$ (Scheme 53), because the triple-decker complexes of 30 VE are close-shell species. The ^{11}B -NMR spectrum shows a signal at $\delta = 18.2$ ppm, which is slightly upfield shifted when compared with that for **51** ($\delta^{11}\text{B} = 21$ ppm). The ^{31}P -NMR spectrum ($\delta = 46.5, 47.9$ ppm) exhibits the two slightly different phosphorus atoms of the dppe ligand. The HR-MS gives the molecule ion peak with correct isotopic pattern.



Scheme 53

The structure of **52** (Fig. 27) has been established by an X-ray crystallographic study. In the asymmetric unit, a molecule of CH_2Cl_2 and half a toluene were found but the accurate assignment of the latter has not been successful. However, the main structure is solved and refined smoothly. The 1,3-diborolyll heterocycle is almost planar and parallel to the Cp^* ring, as in $[\text{Cp}^*\text{Ru}(\mu\text{-}1,3\text{-diborolyll})\text{-Rh}(2\text{-Me-}2,3,4\text{-C}_3\text{B}_7\text{H}_9)]$.^[48c] The 1,3-diborolyll ring is bifacially coordinated to Cp^*Ru and $\text{Rh}(\text{dppe})\text{Cl}$ moieties and has similar distances to the Ru and Rh atoms. In the $\text{Rh}(\text{dppe})\text{Cl}$ moiety, the Rh-Cl bond length is $2.423(1)$ Å and the angle P-Rh-P is $82.45(3)^\circ$.

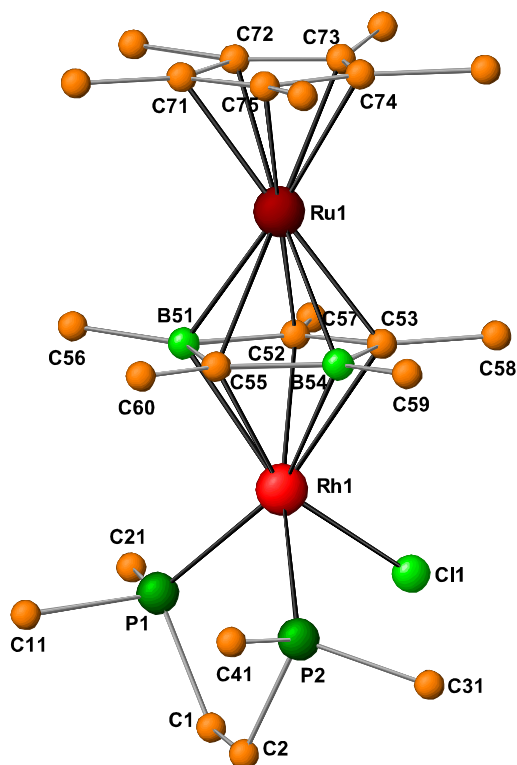
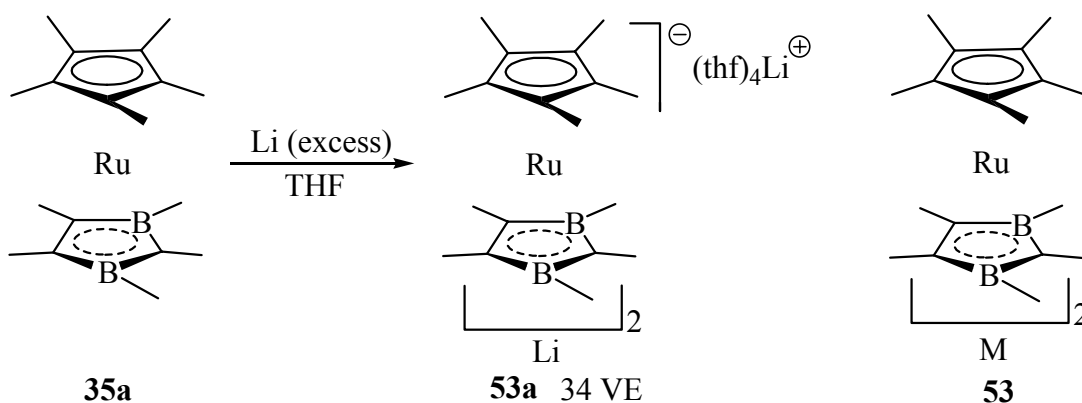


Fig. 27. (left) Molecular structure of **52**, H atoms and solvent molecules are omitted and only the *ipso* carbon atoms of the dppf moiety are shown for clarity. Selected bond lengths [Å] and angles [°]: Rh1-P1 2.323(1), Rh1-P2 2.314(1), Rh1-C11 2.423(1), Rh1-B51 2.242(3), Rh1-C52 2.181(3), Rh1-C53 2.242(3), Rh1-B54 2.297(3), Rh1-C55 2.210(3), Ru1-Cp* 2.145(4) 2.159(5), Ru1-B51 2.219(3), Ru1-C52 2.214(3), Ru1-C53 2.205(3), Ru1-B54 2.250(4), Ru1-C55 2.232(3), B51-C52 1.600(5), C52-C53 1.467(5), C53-B54 1.587(5), B54-C55 1.559(5); P2-Rh1-P1 82.45(3), P2-Rh1-C11 85.08(3), P1-Rh1-C11 86.10(3).

3.4.5 Crystal structure of the tetradecker complex **53a**

While the 2e reduction of **35c** (with two B-ethyl groups) with Li in THF occurred with the color changing from dark violet to yellow, no clear information was obtained. The same reduction of **35a** with an excess of Li (Scheme 54, the reaction was started by B. Bach^[131] but not worked up) gave a mixture, from which pieces of yellow crystals were isolated and identi-



Scheme 54

fied by an X-ray structure analysis to be the anionic tetradecker complex **53a**, in which two sandwiches (each sandwich carries a negative charge) are linked by a Li^+ cation, while the second Li^+ cation is solvated with four thf molecules and separated from the tetradecker anion.

Although the poor crystal quality did not allow the exact bond lengths to be determined, the preliminary results show (Fig. 28) that the tetradecker structure is not linear but slightly slipped (the angle Ru1-Li2-Ru2 is 177.5°). For the 1,3-diborolylyl (B11, B13) ligand, the centroid-metal distances are 1.76 Å (to Ru2) and 1.88 Å (to Li2) [metal-metal distances $\text{Ru2}\dots\text{Li2}$ 3.64 Å], and the corresponding distances for the second 1,3-diborolylyl (B21, B23) ligand are 1.78 and 1.93 Å, respectively, [$\text{Ru1}\dots\text{Li2}$ 3.72 Å]. This structure implies that a series of tetradecker complexes of type **53** may be accessible by reacting **53a** with MX_2 (M = d-metal ions, X = halide, Scheme 54).

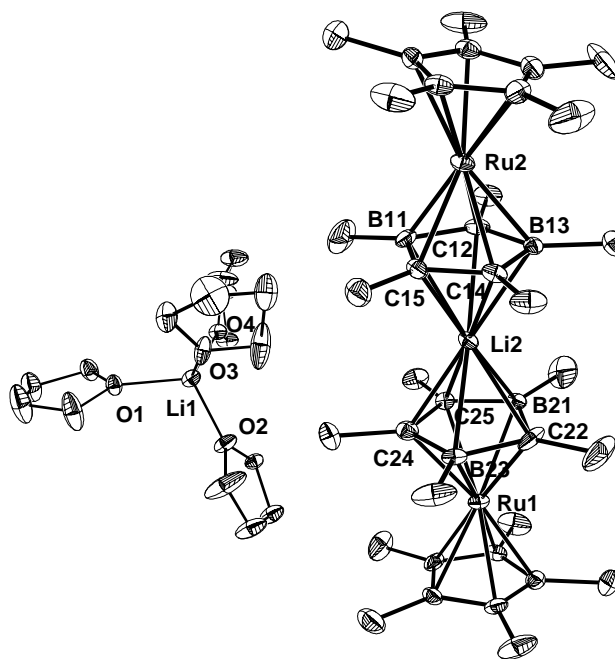
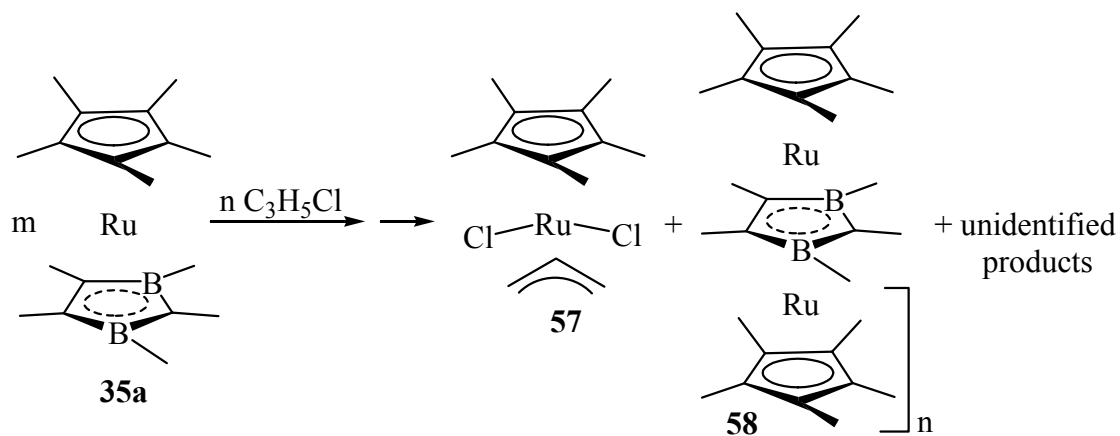


Fig. 28 Crystal structure of the tetradecker complex **53a**: $[(35a)_2\text{Li}]^-[(\text{thf})_4\text{Li}]^+$.

3.4.6 Reaction of **35a** with allylchloride: formation of “oligodecker” **58**

The only known polydecker species^[45] were made possible by polycondensation of the corresponding Ni- and Rh-sandwich precursors (Schemes 55). Interestingly, the observed electric properties of **54** and **55** are different: the nickel polydeckers **54** are semi-conductors, whereas the rhodium polydeckers **55** are insulators. The stacking unit $\text{Ni}(1,3\text{-diborolylyl})$ has 13 VE and $\text{Rh}(1,3\text{-diborolylyl})$ has 12 VE.

Ru(II) center.^[134] From the solution a yellow solid was obtained after dryness, the following recrystallization (CH₂Cl₂, r.t.) gave a mixture of **57** (small amount) as well as red crystals of **58** which were studied by X-ray diffraction analyses (see below) and a small amount of unidentified yellow oily species.



Scheme 57

The EI-MS spectrum of **58** (single crystal) exhibits isotopic pattern at peaks m/z (%) = 605 (15) [Cp*₃Ru(C₃B₂Me₅)RuCp*], 590 (20) [Cp*₃Ru(C₃B₂Me₅)RuCp* -15], 398 (50) [Cp*₂Ru(C₃B₂Me₅)₂], 383 (100) [Cp*₂Ru(C₃B₂Me₅)₂Me]. The isotopic patterns at peaks $m/z > 800$ (intensity < 1) [m/z = 847[Cp*₄Ru₃], 843[Cp*₃Ru₃(C₃B₂Me₅)] (**58**, n = 2), 833[Cp*₄Ru₃ -14], 828 [Cp*₃Ru₃(C₃B₂Me₅) -15] confirm, that Cp*₃Ru fragments and the triple-decker species [Cp*₃Ru(C₃B₂Me₅)RuCp*] (**58** (n = 1), **62**, see below) were combined to form **58** (n = 2). These findings indicate not only the formation of the tetradecar fragments with mixed-ligand stacking in the ratio 3:1, but also for the first time the homo-ligand tetradecar [Cp*₄Ru₃] fragment.

The preliminary results of the X-ray structure analyses on **58** (cell: a = b = 15.000(2), c = 3.600(7) Å, α = β = 90°, γ = 120°, apparent space group R-3m) reveal that it has a one-dimensional oligomeric/polymeric structure. The Ru...Ru distances are found to be 3.600 Å (Fig. 29). The rhombohedral space group imposes an apparent threefold symmetry on the stacks (Fig. 29 a,b, Dr. Hu, Aachen) which could be explained by extensive rotational disorder (Fig. 29 c,d, Prof. Wadepohl, Heidelberg). Alternatively, tripling of the crystals may well pretend the threefold crystallographic symmetry which is not compatible with the molecular

structure. Interestingly, Cp*Li crystallizes in a very similar cell. Its polymeric structure^[135], which has been solved by powder diffraction methods, has been modelled by rotational disorder similar to that in Fig. 29.

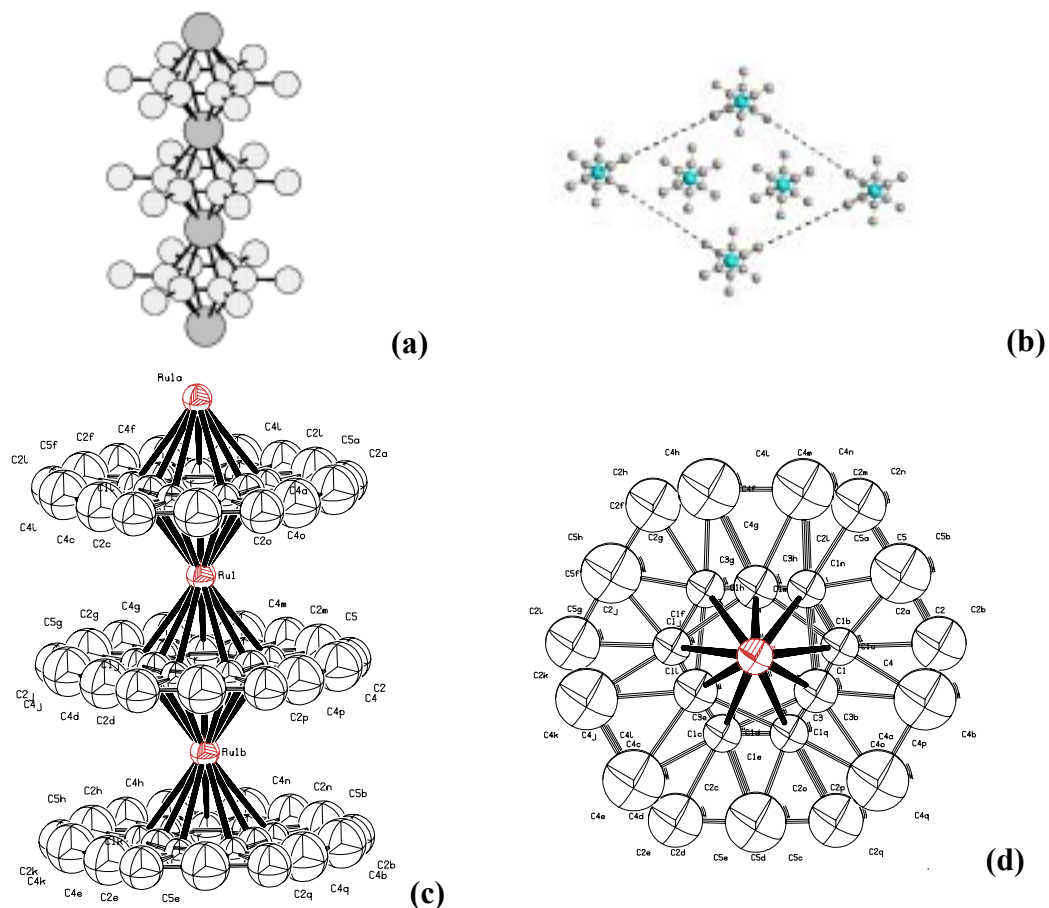
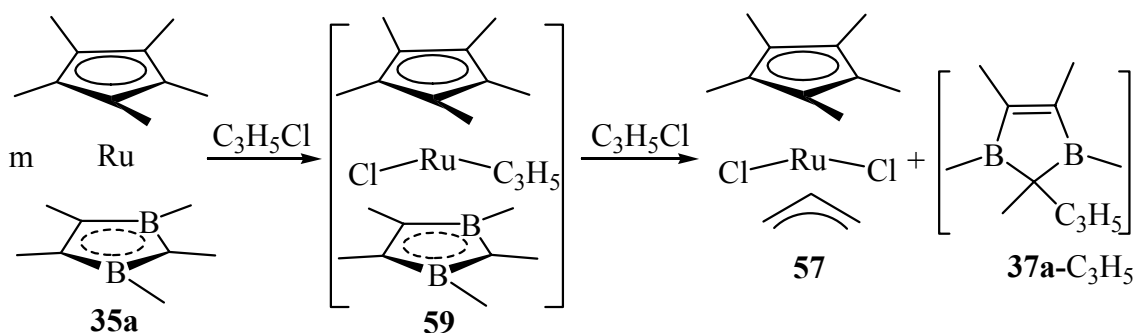


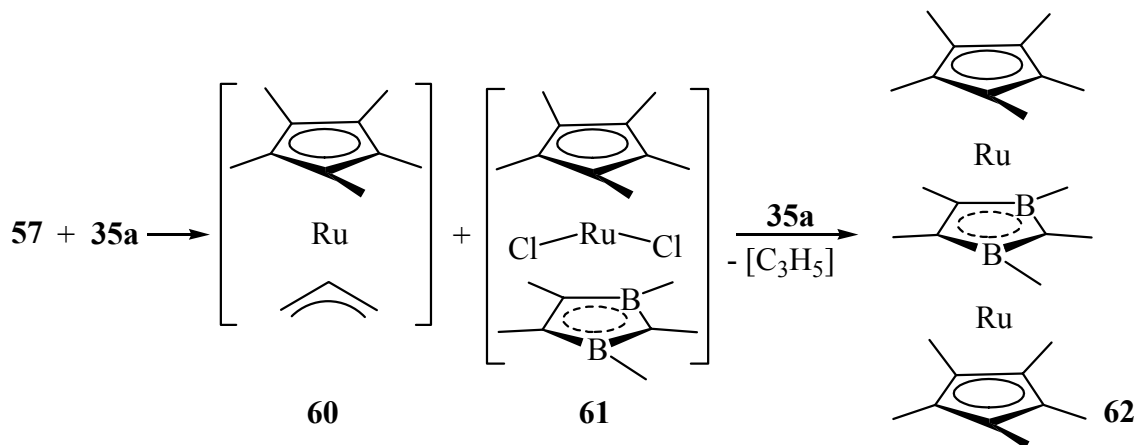
Fig. 29 Unsolved structure of **58**. **a** and **c** are side-views of the stacking. The crystal packing **b** along the *c* axis displaces the stacking. **c** and **d** demonstrate the disorder in detail.



Scheme 58

The reaction in CH_2Cl_2 is much faster and complete within 30 min., with **57** being the only identified product. The formation mechanism of **58** is not yet clear, however, a plausible

pathway is proposed, part of which is shown in Scheme 58. **35a** reacts with allylchloride to form the oxidative addition product **59** (an 18 VE species), which reacts further with C_3H_5Cl to give **57** as the most favored product and the 2,3-dihydro-1,3-diborole derivative **37a**- C_3H_5 .



Then **57** interacts with another molecule of **35a** (Scheme 59) to produce the dichloro complex **61** and the $Cp^*Ru(allyl)$ intermediate **60**, which reacts as precursor for the stacking unit (Cp^*Ru) with **35a** to form an oligodecker product.

The separate reaction of **57** and **35a** in a ratio of 2:3 only gave the triple-decker species **62** (Scheme 59), as identified by MS $m/z = 605$. No high-field signal in the 1H -NMR spectrum for Ru-bound hydrogen atom is observed, in contrast to $Cp^*Ru(C_3B_2Me_5)RuHCp^{*[46b]}$. It does provide hints for the stacking of **35a** with $[Cp^*Ru]$ unit to form **58**. More experiments are needed to fully explore this highly interesting formation of the oligomeric species.

3.4.7 Conclusion

The long-sought crystal structure of the $(\eta^5\text{-pentamethylcyclopentadienyl})(\eta^5\text{-2,3-dihydro-1,3-diboroly})ruthenium$ derivative **35b** is described and the folding along the B...B vector (40.7°) is finally confirmed. The electronic structures of the corresponding model sandwiches of Ru and Fe have been studied by Dr. I. Hyla-Kryspin. The DFT calculations indicate that the folding of the 1,3-diboroly ligands is of electronic origin, and the structures with a folded 1,3-diboroly ligand are more stable in energy than those with a planar ligand in **35** and **36**.

The reactivity of **35** is further studied with respect to insertion of terminal alkynes into

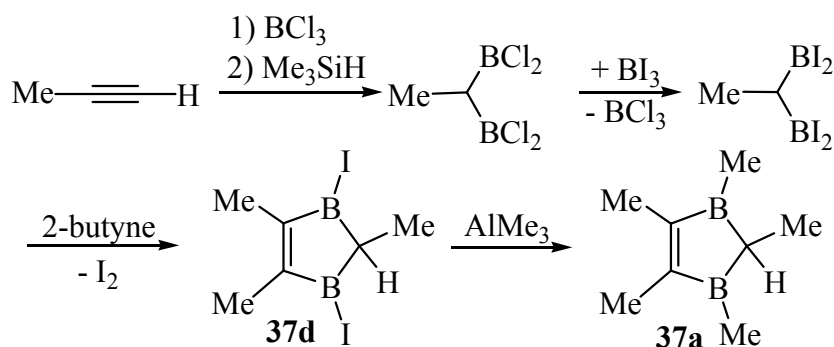
the C₃B₂ heterocycle of **35** which results in novel 18 VE boron-containing ruthenocene analogs **38**. The new 4-borataborepine in **38** function as 6e ligand in classic bonding.^[136] Besides the main product **38**, the formation of boratabenzene complexes **39** is observed, which are formed as the only boron-containing products in the reactions with disubstituted alkynes. In a comparative study on the reactivity towards terminal alkyne, it has been found that [(1,3-diborole)RhCl]₂ dimer **48** cyclotrimerizes PhCH₂C₂H to give a (1,3-diboroly)Rh(arene) complex. Attempts to synthesize the free 4-borataborepine ligand were not yet successful, which would allow the preparation of a series of sandwich complexes with two 4-borataborepine ligands.

The reduction of **35a** with an excess of lithium produces the anionic tetradecker species **53a**, in which one Li cation bridges two sandwich anions of **35a**. The second Li cation is solvated and separated from the tetradecker moiety. A novel triple-decker complex **46** with a seven-membered C₃B₂ ring as the bridging ligand has been structurally characterized, which was formed as a side-product from the reaction of **35a** with di-*p*-tolylacetylene. More experiments are needed to clarify its formation.

The reaction of **35a** with allylchloride in hexane afforded a novel oligodecker complex **58**, its identity and mechanism of formation are not yet fully known. The isolation of the triple-decker **62** from a separate reaction of **35a** with the main reaction product Cp*₂Ru(C₃H₅)Cl₂ (**57**) indicates, that most likely stacking of **62** with Cp*₂Ru units [from the intermediate Cp*₂Ru(C₃H₅)] leads to **58**. The preliminary results (from MS and X-ray diffraction analyses) support the formation of an oligodecker complex containing both Cp* and 1,3-diboroly ligands.

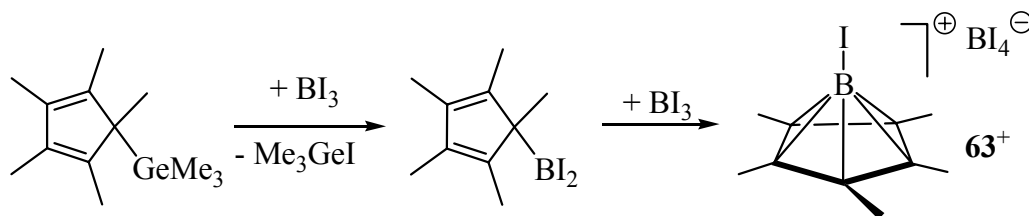
3.5 Synthesis of the 1,3-diiodo-1,3-diborole **37d** and formation of the 2,3,4,5,6-pentacarba-*nido*-hexaborane(6) cation (**63**⁺)

In the preparation of the ligand precursor 1,3-diiodo-2,3-dihydro-1,3-diborole **37d**^[75] (Scheme 60) for the (1,3-diboroly)Ru complexes **35** (Chapter 3.4), we have observed the unexpected formation of the known 2,3,4,5,6-pentamethyl-2,3,4,5,6-pentacarbahexaborane(6) cation **63**⁺, first synthesized by Jutzi (Scheme 61).^[19]



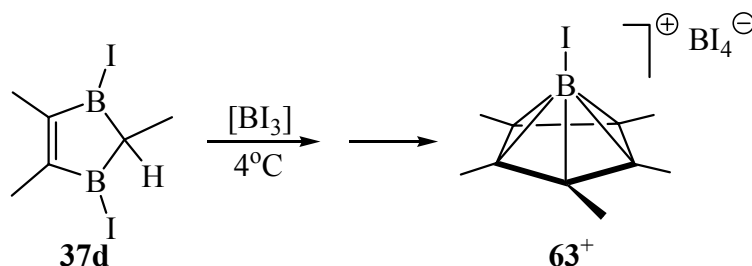
Scheme 60

The oily compound **37d** (with some BI_3 present) was stored at 4°C for ca. one year, during which time a small amount of red brown solid was formed, which was isolated and purified by repeated washing with hexane, and characterized by spectroscopic and X-ray methods as $[\text{C}_5\text{Me}_5\text{BI}]^+\text{BI}_4^-$ (**63⁺**). It is insoluble in pentane or hexane, but soluble in CH_2Cl_2 .



Scheme 61

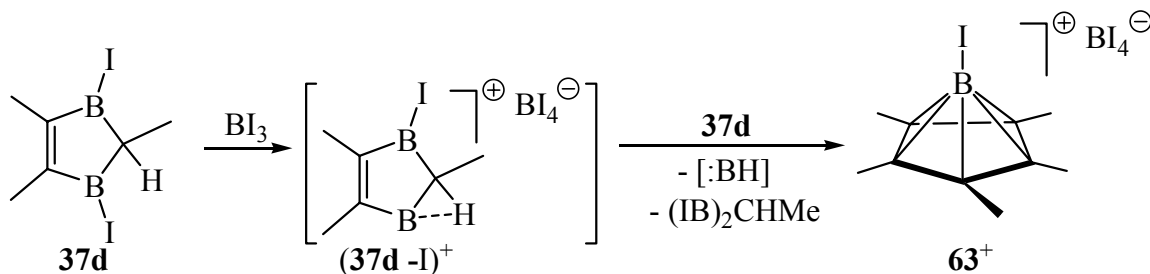
In the $^1\text{H-NMR}$ spectrum, it exhibits a quartet at $\delta = 2.29$ ppm ($J = 2.2$ Hz) for the methyl protons. The $^{11}\text{B-NMR}$ spectrum shows two signals at $\delta = -51.8$ ppm for the apical boron atom (similar to those found for the apical boron atoms of the *nido*- C_4B_2 carborane derivatives, Chapter 3.1), and at $\delta = -120$ ppm for the boron atom in the BI_4^- moiety. The ESI-MS spectrum shows a peak at $m/z = 273$ for the carborane cation. All data are consistent to those reported by Jutzi.^[19]



Scheme 62

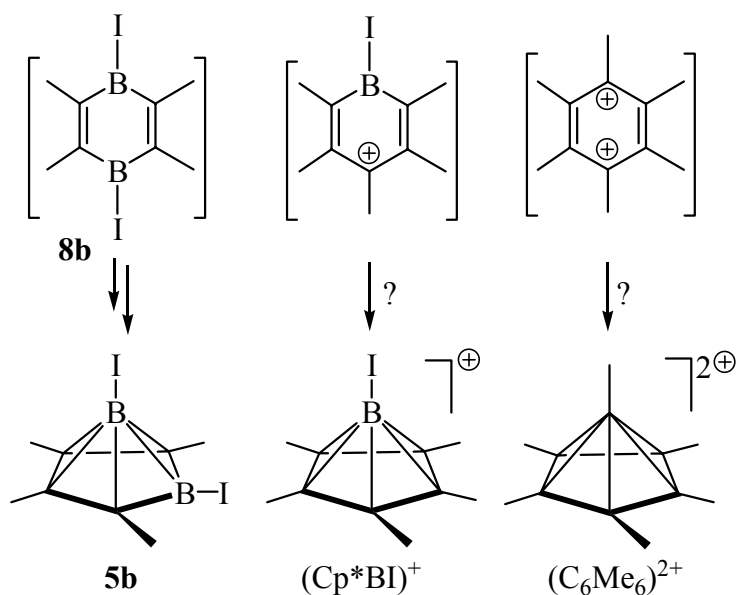
The formation of **63⁺** is not yet clear. Presumably **37d** reacts with BI_3 leading to a strong Lewis acidic species (**37d** -I)⁺ (Scheme 63), which might abstract a $\text{MeC}=\text{CMe}$ fragment from another molecule of **37d**, forming **63⁺** with the formal elimination of a boranediyl $[\text{:BH}]$ and

the reactive 1,3-diborirane $(\text{IB})_2\text{CHMe}$. As a result of this postulated intermediate of two **37d** with BI_3 the formation of *cyclo*- $(\text{C}_5\text{Me}_5\text{BI})^+$ (Scheme 64) could occur, which then transforms into *nido*- $(\text{C}_5\text{Me}_5\text{BI})^+$ (**63**⁺).



Scheme 63

Similarly, the possible intermediate 1,4-diboracyclohexa-2,5-diene **8b** (Scheme 64, by analogy to compound **8a** in Schemes 18 and 20, Chapter 3.1) could rearrange into the corresponding *nido*- $(\text{MeC})_4(\text{BI})_2$ (**5b**), which was prepared via the one-pot procedure. The unknown isoelectronic species *cyclo*- $\text{C}_6\text{Me}_6^{2+}$ could be a precursor of the known^[137] polyhedral $\text{C}_6\text{Me}_6^{2+}$.



Scheme 64

The structure (Fig. 30) was confirmed by an X-ray diffraction analysis to be the carborane species *nido*- $(\text{Me}_5\text{C}_5\text{BI})^+$ (**63**⁺) and BI_4^- . The study showed that two modifications are present: $a = 15.6827(11) \text{ \AA}$, $b = 16.3559(11)$, $c = 46.4819(33) \text{ \AA}$, $V = 11922.8 \text{ \AA}^3$, space group $Pna2(1)$; and $a = 49.14$, $b = 11.63$, $c = 10.39 \text{ \AA}$, $V = 5936 \text{ \AA}^3$, space group $Pnma$. With the first modification, relatively better results were obtained. For the refinement the final R

values are $R1 = 0.0825$ for 14880 unique reflections [$F_o > 4\sigma(F_o)$] and 0.1376 for all 23651 reflections, respectively. In the asymmetric unit there are six separated ion pairs, with most iodine atoms seriously disordered. The B1-I1 bond length is 2.12 Å, similar to those in isoelectronic C_4B_2 -*nido*-carboranes (Chapter 3.1). The B-C bond distances vary within a range of 1.63-1.75 Å.

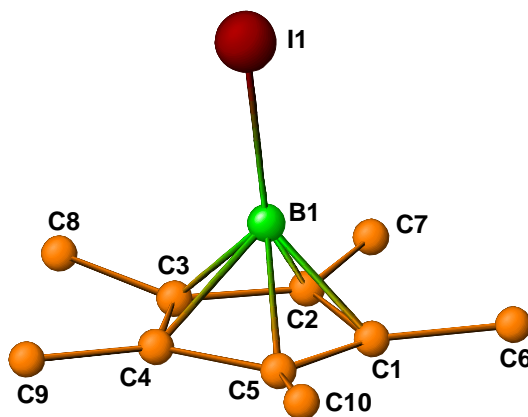
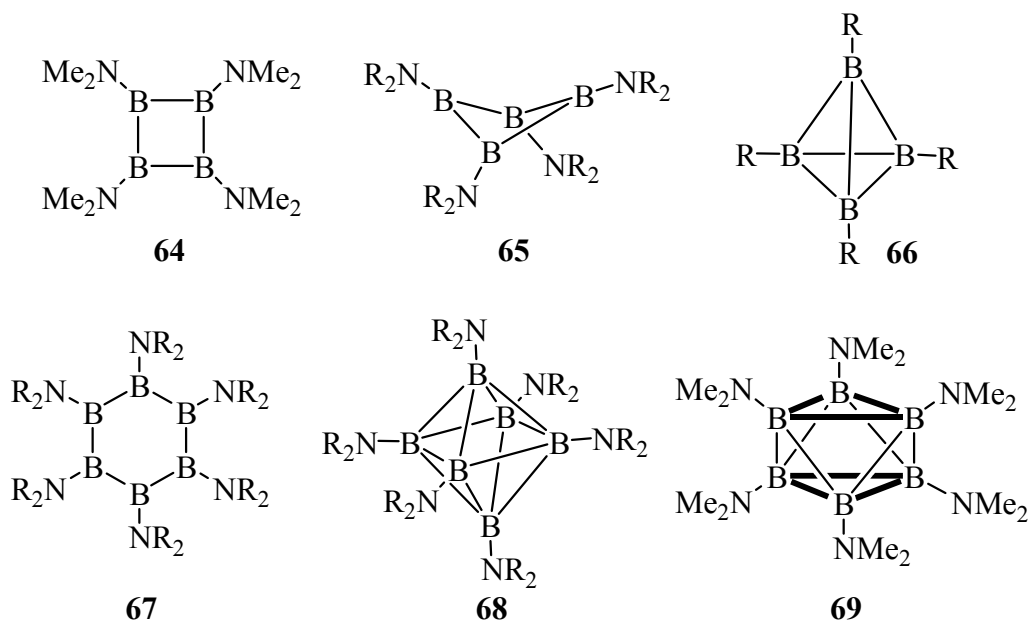


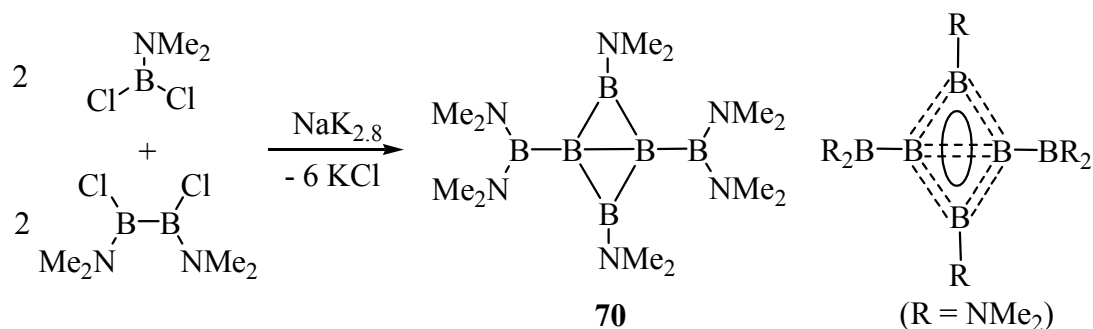
Fig. 30 Crystal structure of the carborane cation **63**⁺.

3.6 Synthesis and properties of some aminoborane derivatives

The chemistry of small boranes shows a unique structural interplay between *cyclo*- and polyboron compounds.^[18d] Reports on the *cyclo*-tetraborane(4) **64**^[138] with a planar structure has not yet been confirmed, and attempts^[18c] to obtain analogs of **64** by dehalogenation of diborane(4) derivatives $R(Cl)B-B(Cl)R$ ($R = NMe_2$,^[112] NEt_2 ^[139,18c]) with Na/K alloy were not successful, instead, the formation of the orange red *cyclo*-hexaborane **67a** ($R = Me$)^[18c] in low yield was observed, which was first reported as a side product in 1980^[140] by dehalogenation of $(Me_2N)_2BCl$. MO studies^[141] have indicated that planar B_4 rings are unstable. Ten years later the corresponding diethylamino derivative **67b** ($R = Et$) was described. On standing in solution the orange red color of **67b** changed to green.^[142] The resulting isomer **68b** is a cluster with 2n SE. However, the disorder of the crystal of **68b** did not allow the exact bond lengths to be determined. On heating **68b** is transformed into **67b**.^[142] The dehalogenation^[18c] of $R(Cl)B-B(Cl)R$ ($R = NEt_2$) leads to the green isomer **68b** in 40% yield. However, it was not possible to obtain better crystals than those reported previously.



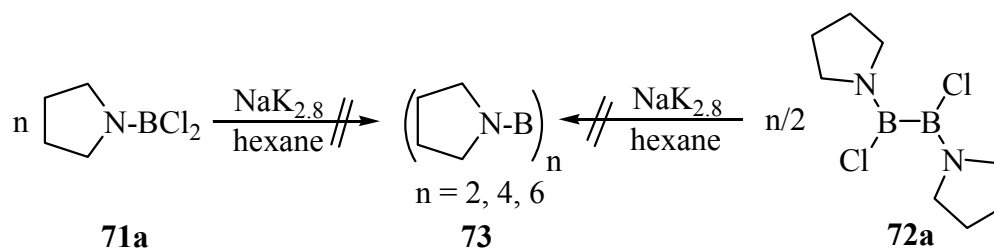
By reacting the more sterically hindered diisopropylamino derivative $R(Cl)B-B(Cl)R$ ($R = NiPr_2$) the blue folded **65a** was isolated, and in the case of the corresponding 2,2,6,6-tetramethylpiperidino (tmp) derivative yellow tetraboratetrahedrane **66a** was produced.^[143] Tetraboratetrahedranes **66** with other substituents on boron ($R = Cl$ ^[144], CMe_3 ^[145]) are long known. In an attempt to obtain the corresponding *cyclo*-triborane(3) and/or -pentaborane(5) by dehalogenating a 1:1 mixture of Me_2NBCl_2 and $Me_2N(Cl)B-B(Cl)NMe_2$ (Scheme 64), colorless crystals of **70**^[146a] were isolated in low yield. An X-ray diffraction analysis proved the presence of a planar, diamond-shaped B_4 ring with a short diagonal [$1.633(2)\text{\AA}$].



Scheme 64

The four boron atoms of the B_4 frame of **70** supply only eight electrons therefore the non-classical bonding (Scheme 64, a simple description) is required, which is supported by calculations^[146a] that the bonding in the B_4 frame may be described by two $3c,2e$ σ bonds (shown as triangular dashed lines), one $4c,2e$ π bond (ellipsoid), and an additional $4c,2e$ bond (dashed diamond).

Berndt *et al.* have shown that the dehalogenation of 1,3-dichloro-1,3,5-tris(dimethylamino)triborane(5) (**31**)^[116] with NaK_{2.8} leads to **70**^[146b] in 40-50% yield, together with a dianionic *closo*-**69**²⁻,^[147a] which gives the neutral **69** on oxidation with dibromoethane. Compound **69** adopts the trigonal antiprism geometry, as confirmed by X-ray studies. On heating^[147a] **69** was transformed into the cyclic isomer **67a**. Very little is known of the reactivity of **70**. Berndt *et al.* studied the reduction^[147b] of **70** by lithium which afforded the folded product **65b**²⁻ (R = Me).

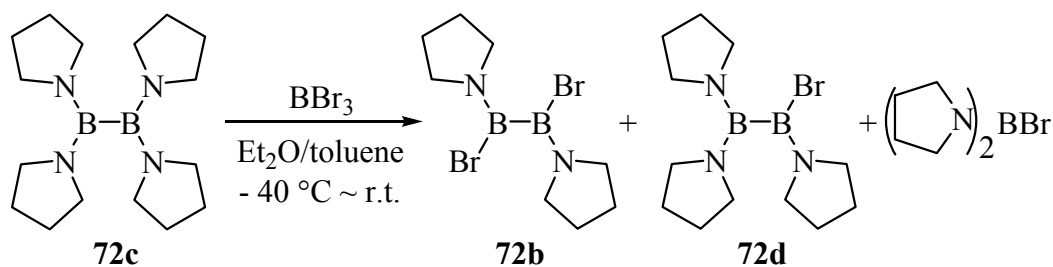


Scheme 65

Considering the similarity between pyrrolidino, dimethylamino and diethylamino groups, one might think that the dehalogenation of pyrrolidinoboranes **71a** and **72a**, respectively, would give cyclic or polyhedral aminoboranes (C₄H₈NB)_n **73** (n = 2, 4, 6). Unfortunately, neither reaction gave definite products (Scheme 65).^[18c] It was anticipated that the dehalogenation of the more reactive pyrrolidinodibromoborane (C₄H₈N)BBR₂ (**71b**)^[148] and 1,2-dibromo-1,2-dipyrrolidinodiborane(4) (**72b**) could work better. Herein the synthesis and dehalogenation of **72b** will be described, as well as the reactivity study on **70**.

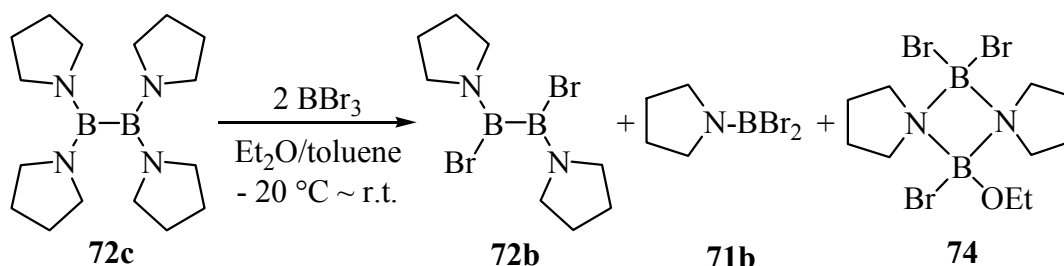
3.6.1 1,2-Dibromo-1,2-dipyrrolidinodiborane(4) (**72b**)

To obtain **72b**, we started from tetrapyrrolidinodiborane(4) (**72c**), which was prepared in a high yield (90%) by a combination of the literature procedures^[149] through the reaction of the more reactive species (C₄H₈N)₂BBr and NaK_{2.8} alloy. The reaction of **72c** and 1 equiv. of BBr₃ did not afford pure **72b**, instead a mixture of **72b** and a monobromodiborane(4) species **72d** was obtained (Scheme 66), which was characterized by ¹¹B-NMR (δ = 36 ppm, br.) and MS, which gives the molecular ion peaks for **72b** and **72d**, respectively. This indicates that, in contrast to the literature method^[150] involving tetrakis(dimethylamino)diborane(4), 1 equiv. of BBr₃ in the present case is not enough to completely replace two pyrrolidino groups in **72c**.



Scheme 66

When 2 equiv. of BBr_3 were used (Scheme 67), colorless **72b** was obtained in 69% yield. A very small amount of a dimeric compound **74** was also formed, its structure has been confirmed by an X-ray structure analysis.



Scheme 67

The formation of **74** results obviously from the presence of Et_2O , which can react with the formed $(\text{C}_4\text{H}_8\text{N})\text{BBr}_2$ (**71b**), produced in the reaction (identified by MS), to give $[(\text{C}_4\text{H}_8\text{N})\text{B}(\text{OEt})\text{Br}]$ as an intermediate, which further reacts with another molecule of **71b** to afford the dimeric **74**. Another pathway could be that **71b** dimerizes to form $[(\text{C}_4\text{H}_8\text{N})\text{BBr}_2]_2$,^[148] which reacts with Et_2O to give **74**. The same reaction without ether only afforded **72b** in similar yield (64%).

It is interesting that under different recrystallization conditions **72b** grow different types of crystals: on cooling **72b'** crystallizes in orthorhombic space group $P2_12_12$; while from a hexane/toluene solution ($-28\text{ }^\circ\text{C}$) **72b''** crystallizes in triclinic, space group $P-1$, indicating polymorphism or dimorphism of **72b**. **72b'** was determined at 103(2) K, while **72b''** was analyzed at 293(2) K. Both structures (Fig. 31) are essentially the same with respect to bond lengths and angles, but differ in conformation. The B-Br bond lengths [1.981(2) in **72b'** and 1.978(2) Å in **72b''**] are similar to those in $\text{B}_2(\text{NMe})_2\text{Br}_2$ [1.979(13) Å].^[151] The B-B bond distances [1.696(4) in **72b'**, 1.684(3) in **72b''** Å] are similar to that in $\text{B}_2(\text{NMe})_2\text{Br}_2$ [1.682(16) Å],^[151] but shorter than that in the starting compound **72c** [1.739 Å]. The shorter B-N bond

lengths [1.381(2) in **72b'**, 1.371(2) in **72b''**, cf. 1.424/1.427 Å in **72c**] indicate stronger B-N π interaction in **72b** than in **72c** with the introduction of two bromine atoms, which is consistent with the results in 1,3-dichloro-1,3,5-tris(dimethylamino)triborane(5) (**31**)^[116] and the corresponding bromine and iodine triboranes(5). The torsion angles of Br1-B1-B1A-Br1A and N1-B1-B1A-N2 in **72b'** are $-122.8(2)$ and $-122.8(3)^\circ$, respectively, while the corresponding values in **72b''** are $-86.3(15)$ and $-82.9(19)^\circ$, respectively.

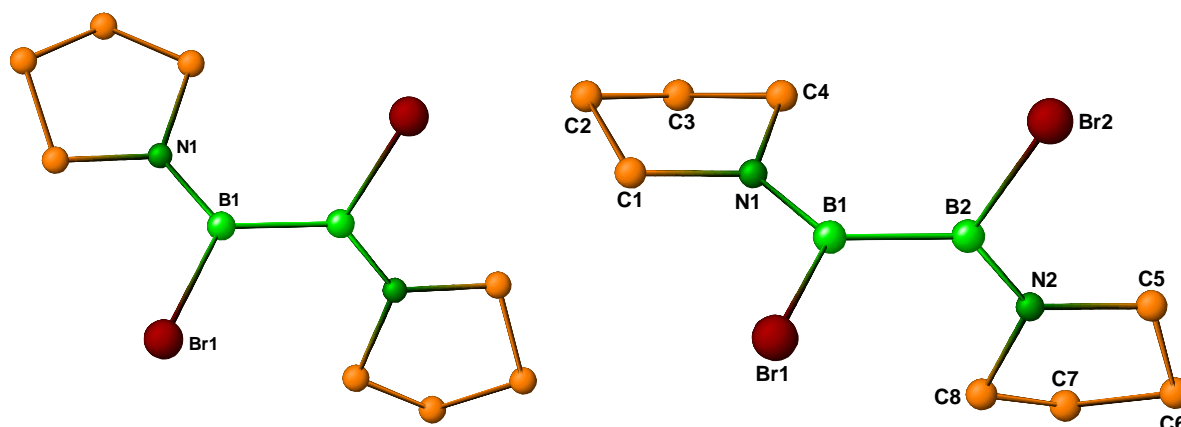


Fig. 31. Molecular structures of the two types of crystals for **72b'** (left) and **72b''** (right). selected bond lengths [Å]: for **72b'**: Br1-B1 1.981(2), N1-B1 1.381(2), B1-B1A 1.696(4); for **72b''**: Br(1)-B(1) 1.978(2), Br(2)-B(2) 1.978(2), N(1)-B(1) 1.370(2), N(2)-B(2) 1.371(2) B(1)-B(2) 1.684(3).

The structure **74** is shown in Fig. 32. The four-membered B-N-B-N ring is not planar but folded (the torsion angle of B1-N2-B2-N1 12.5°). The B2-Br3 bond length of 2.045 Å is slightly longer than those in **72b**, also longer than the B1-Br1 and B1-Br2 distances [2.012/2.013], which is due to the different orientations of the pyrrodo rings and steric requirement of the OEt group. The presence of the OEt group also influences the B-N bond lengths: the distances of B2-N1 and B2-N2 [1.655/1.618 Å, respectively] are longer than those involving B1 atom [1.578/1.580 Å, respectively]. However, the B-Br and B-N bond lengths in **74** are similar to those in the related structure [C₄H₈BBR₂]₂ [av. B-Br distance 1.999, B-N 1.603Å].^[152]

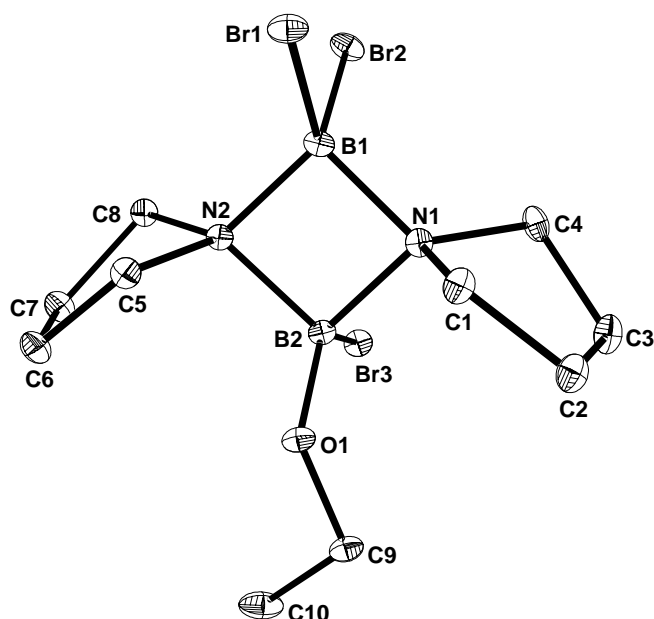
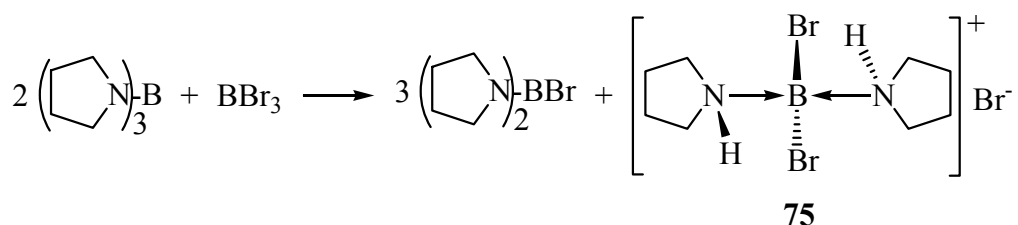


Fig. 32. Molecular structure of **74**, hydrogen atoms omitted for clarity. Selected bond lengths [Å] and angles [°]: Br1-B1 2.012(3), Br2-B1 2.013(3), Br3-B2 2.045(3), N1-B1 1.578(4), N1-B2 1.655(3), N2-B1 1.580(3), N2-B2 1.618(3), O(1)-B(2) 1.375(3); B1-N1-B2 86.7(4), B1-N2-B2 88.0(2), N2-B2-N1 89.1(2), N1-B1-N2, 93.3(2).

It turned out, that the dehalogenation of **71b** with $\text{NaK}_{2.8}$ in hexane or toluene afforded a mixture, from which **72c** was identified to be the main component and confirmed by the comparison of the NMR and HR-MS with the authentic sample. A very minor product is assigned to be a hexamer $(\text{C}_4\text{H}_8\text{NB})_6$ (**73a**) as indicated by HR-MS. In both the dehalogenation of **72b** and the codehalogenation of **71b** and **72b**, **72c** was the only identifiable boron-containing species.



Scheme 68

In the course of the preparation of $(\text{C}_4\text{H}_8\text{N})_2\text{BBr}$, the starting compound of **72c**, we obtained the unexpected bispyrrolidine boronium salt **75**, the details are reported in the following (Scheme 68). The reaction of tripyrrolidinoborane $(\text{C}_4\text{H}_8\text{N})_3\text{B}$ and BBr_3 has been

reported to be sensitive to the reaction conditions: a) 2:1 ratio, pentane, $-50\sim -40\text{ }^{\circ}\text{C}$,^[149b] the product is isolated as $(\text{C}_4\text{H}_8\text{N})_2\text{BBr}$, which can serve as the precursor of **72c**; b) 1:2 ratio, pentane, $0\text{ }^{\circ}\text{C}$,^[152] the product is characterized to be the dimeric $[\text{C}_4\text{H}_8\text{BBr}_2]_2$. We observed that the reaction of $(\text{C}_4\text{H}_8\text{N})_3\text{B}$ and BBr_3 (2:1 ratio, pentane, $-50\sim -40\text{ }^{\circ}\text{C}$, two separate reactions) gave, along with the main product $(\text{C}_4\text{H}_8\text{N})_2\text{BBr}$, an orange precipitate, which was not mentioned in the published papers.^[149b,152] The precipitate is partly soluble in toluene and soluble in CH_2Cl_2 . After workup a colorless product was isolated. The colorless crystal obtained from an NMR tube after ca. two months was found by an X-ray structure analysis to be the pyrrolidine boronium salt **75**. Although many boronium salts of the formula $[\text{L}_2\text{BX}_2]^+\text{X}^-$ (L = H, amino or amine, X = halide) are known,^[153] **75** is the one of the few structurally characterized amine boronium salts.

The formation of **75** is not yet clear, however, slow changes have been observed as monitored by ^1H - and ^{11}B -NMR of the original product. The ^1H -NMR spectrum exhibits two sets of signals corresponding to two different types of pyrrolidino rings, and one set of signals gradually disappears. In the ^{11}B -NMR spectrum one signal at $\delta = 23.5$ ppm and broad signal(s) at $\delta = 6.7$ ppm are found, the former gradually disappears. This suggests that the colorless product isolated is a mixture, and **75** may be formed in the NMR tube via hydrolysis.

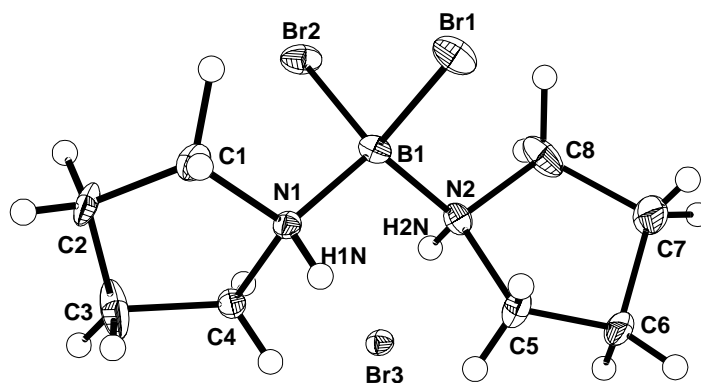


Fig. 35. Crystal structure of **75**, with the chloroform solvent omitted. Selected bond lengths [\AA] and angles [$^{\circ}$]: B1-Br2 2.008(3), B1-Br1 2.016(3), B1-N2 1.562(4), B1-N1 1.568(4), N(2)-B(1)-N(1) 110.4(2), N(2)-B(1)-Br(2) 108.0(2), N(1)-B(1)-Br(2) 109.0(2), N(2)-B(1)-Br(1) 109.4(2), N(1)-B(1)-Br(1) 108.3(2), Br(2)-B(1)-Br(1) 111.8(2).

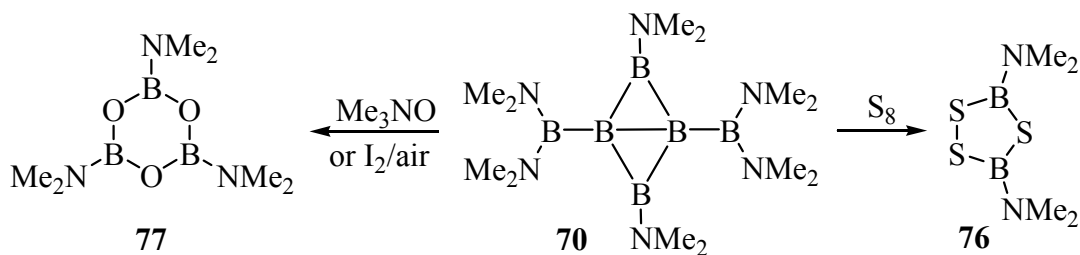
The structure of **75** is shown in Fig. 34. The feature is that the pyrrolidiniumboronium cation has connections to the Br⁻ anion via two N-H...Br hydrogen bonds. The N1...Br3 and N2...Br3 distances are 3.284 and 3.268 Å, respectively, and the N1-H1N...Br3 and N2-H2N...Br3 angles are 163.0, 168.41°, respectively. The four-coordinate boron atom adopts a slightly distorted tetrahedral geometry. The B-Br bond lengths of 2.008 and 2.016 Å are similar to those in **74**. The two B-N bond distances [1.562/1.568 Å] are similar to, but slightly shorter than those in **74**.

3.6.2 Properties of (Me₂N)₂B₄[B(NMe₂)₂]₂ (**70**)

The novel rhombohedral B₄ unit in compound **70** has attracted recent interest in theoretical studies.^[146,154] However, the reactivity of **70** remains largely unknown. Herein the reactions of **70** with elemental sulfur (S₈) and trimethylamine N-oxide (Me₃NO), respectively, will be studied, in which the rhombohedral B₄ is cleaved, forming known boron heterocycles. The rearrangement of **70** into its cyclic isomer **67a** will also be described.

3.6.2.1 Reactions with S₈ and Me₃NO

The reaction of **70** with S₈ in hexane (Scheme 69) gave the known colorless boron-sulfur heterocycle **76**^[155], which was characterized by ¹¹B-NMR (δ = 44.7 ppm) and MS. The reaction of **70** with either Me₃NO or I₂ (with participation of air) produced the known colorless boroxine **77**^[156]. The constitution of **77** follows from its ¹¹B-NMR (δ = 21.3 ppm) and MS, and confirmed by an X-ray diffraction analysis.



Scheme 69

The X-ray structure of **77** is shown in Fig. 36. The six-membered ring is almost planar, with all the angles inside the ring being nearly 120°. The average B-O and B-N bond lengths are 1.389(3) and 1.402(3) Å, respectively, indicating π interactions is mainly concentrated in the BN bonds.

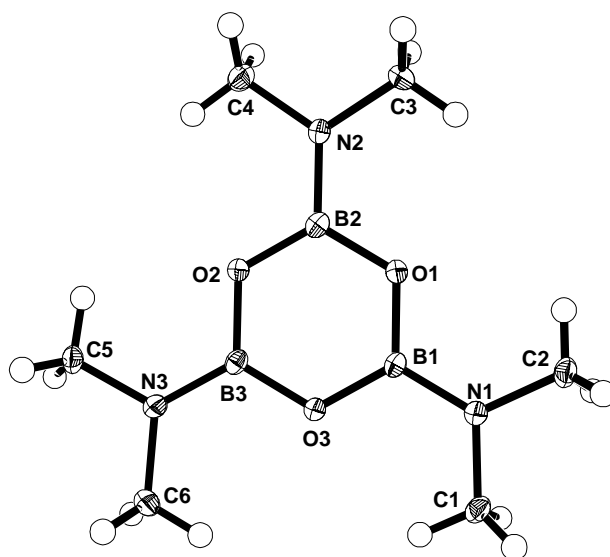
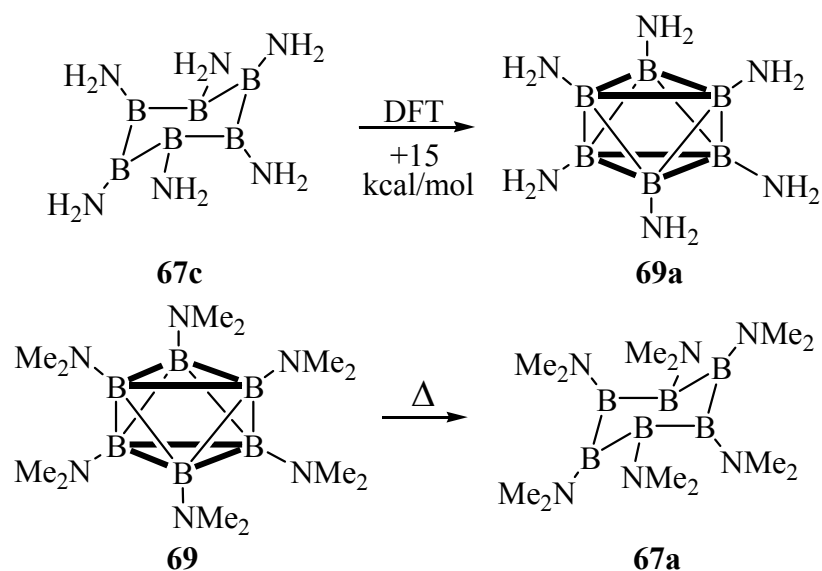


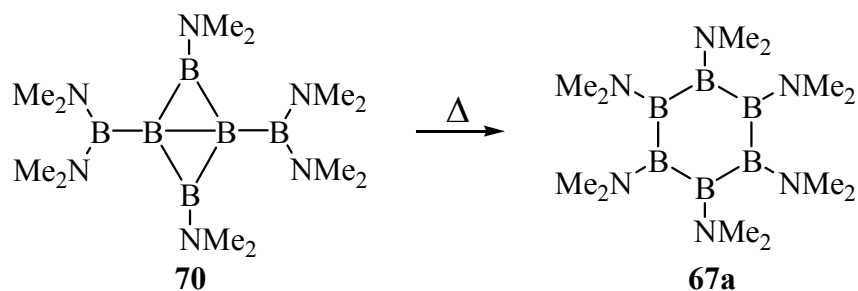
Fig. 36. Molecular structure of 77.

3.6.2.2 Rearrangement of 70 into the *cyclo*-B₆ isomer 67a

According to the calculations^[141] on the polyborane B_n(NH₂)_n (n = 4-6), the classic *cyclo*-isomers are predicated to be more stable than the nonclassic cages. In the case of B₆(NH₂)₆, the *cyclo*-isomer **67c** is 15.0 kcal/mol more stable in energy than the trigonal antiprism **69a** (Scheme 70), which has been confirmed experimentally^[147a] by heating **69** (>200°C), whereby the transformation to **67a** was achieved.



Scheme 70

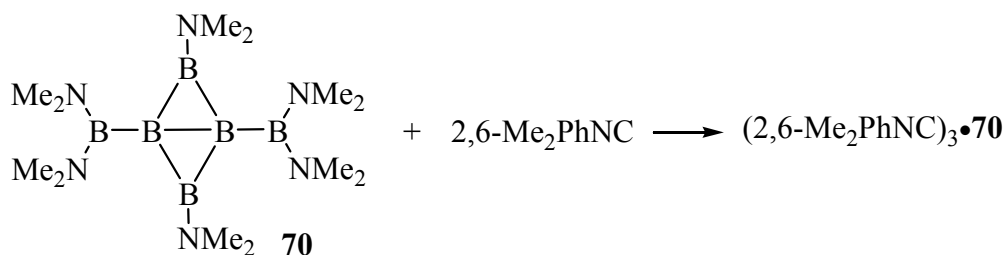


Scheme 71

We have found the rearrangement of **70** into **67a** (Scheme 71), although no calculation on this transformation has been done so far. No reaction was observed between **70** and 3-hexyne in hexane at room temperature, heating at reflux for ca. 7 days led to a complicated mixture [^{11}B -NMR: $\delta = 63.1$ (br.), 36.3, 36.5, 28.0, 21.1, 0.4, -10.0 ppm], from which the signal at $\delta = 63$ ppm was tentatively assigned to the cyclic isomer **67a**, which was confirmed by an X-ray diffraction analysis (cell parameters) on the orange red crystals grown from the reaction mixture. The same rearrangement was also observed when we repeated the preparation of **70** by dehalogenation^[146b] of 1,3-dichloro-1,3,5-tris(dimethylamino)triborane(5) (**31**)^[116] with $\text{NaK}_{2.8}$ in hexane at 55~60 °C for 1 day. While **70** (^{11}B -NMR: $\delta = 64.1, 42.1, 6.9$ ppm) was obtained in good yield, orange red crystals were grown from the same NMR tube at r.t. and tested by an X-ray diffraction analysis (cell parameters) to be **67a**.

3.6.2.3 Reactions with isonitriles

The reaction of **70** with *t*BuNC in hexane (Scheme 72) immediately gave a deep red solution, the red oily residue separated gradually solidified, which is partly soluble in hexane but soluble in chloroform. In the ^{11}B -NMR spectrum it exhibits broad signals at $\delta = 36.2, 27.3, 20.1$ ppm. Similarly, the reaction of **70** with 2,6-Me₂PhNC produced a red brown solution.



Scheme 72

The ^{11}B -NMR spectrum shows broad signals at $\delta = 30.6, 26.9$ ppm. The HR-MS spectrum of the red brown solid obtained shows a peak at $m/z = 723$, corresponding to the constitution for $[\mathbf{70}\cdot 3(2,6\text{-Me}_2\text{PhNC})]$, however, the structure of this product is not yet clear.

3.6.3 Conclusion

The reactions of tetrapyrrolidinodiborane(4) (**72c**) and BBr_3 have been studied. With a **72c** : BBr_3 ratio of 1:1, a mixture of $[(\text{C}_4\text{H}_8\text{N})_2\text{B}_2\text{Br}_2]$ (**72b**) and the monobromodiborane(4) **72d** was obtained; while in a ratio of 1:2 **72b** was isolated as the main product, along with a small amount of the dimeric $[(\text{C}_4\text{H}_8\text{NB})_2\text{Br}_3\text{OEt}]$ (**74**) because of the Et_2O used as solvent. The crystal structures of **72b** show interesting dimorphism. The formation of the pyrrolidine boronium salt $[(\text{C}_4\text{H}_8\text{NH})_2\text{BBr}_2]^+\text{Br}^-$ (**75**) was observed in the reaction of $(\text{C}_4\text{H}_8\text{N})_3\text{B}$ and BBr_3 , caused by the presence of moisture. The reactivity of $(\text{Me}_2\text{N})_2\text{B}_4[\text{B}(\text{NMe}_2)_2]_2$ (**70**) which has a novel rhombohedral B_4 unit is studied. It has been found that in both the reactions with S_8 and Me_3NO , respectively, the rhombohedral B_4 is cleaved and 1,2,4,3,5-trithiadiborolane **76** and boroxine **77** are formed. On heating the rearrangement of **70** into its cyclic isomer **67a** was observed, suggesting that the classic cyclic isomer is more stable than the nonclassic isomer.

4. Experimental section

4.1 General: All reactions and manipulations were performed in dry glassware under argon or nitrogen using standard Schlenk techniques. Solvents were dried, distilled, and saturated with nitrogen.

NMR spectra were recorded on a Bruker DRX 200 spectrometer (operators: Mrs. B. Termin and D. Gutruf), ^1H : 200.13 MHz, ^{11}B : 64.21 MHz, ^{13}C : 50.32 MHz, ^{31}P : 80.92 MHz, ^{29}Si : 39.7 MHz, ^{119}Sn : 74.5 MHz. $\text{Et}_2\text{O}\cdot\text{BF}_3$ was used as the external standard for ^{11}B -NMR, as internal references for ^1H - and ^{13}C -NMR, the signals of the deuterated solvents (C_6D_6 , CDCl_3 , CD_2Cl_2) were used and calculated relative to TMS. The external standards for ^{31}P -NMR, ^{29}Si -NMR and ^{119}Sn -NMR are H_3PO_4 (85 %), TMS and SnMe_4 , respectively.

MS spectra were recorded by Mr. T. Jannack and Dr. A. Mohkir (Institute of Inorganic Chemistry, University of Heidelberg), using EI and ESI ionization techniques, respectively. and by Dr. J. Gross, Mrs. A. Seith and Mr. N. Nieth (Institute of Organic Chemistry, University of Heidelberg), on a ZAB-2F VH Micromass CTD spectrometer, and a JEOL MS Station JMS 700 spectrometer, using the EI, CI, FAB, and ESI ionization techniques.

X-ray structures were determined by Dr. H. Pritzkow, Dr. T. Oeser (Institute of Organic Chemistry), Dr. C.-H Hu (Institute of Inorganic Chemistry, RWTH Aachen), Prof. Dr. H. Wadepohl, using Bruker AXS Smart CCD diffractometer, or Apex Smart CCD diffractometer. Mo- K_α radiation, $\lambda = 0.71073 \text{ \AA}$, graphite monochromator, ω -scans. Data were corrected for Lorentz polarization and absorption effects. The structures were solved by direct methods and refined by least-squares methods based on F^2 with all measured reflections. All non-hydrogen atoms are refined anisotropically.

IR was recorded on a BioRad spectrometer. Elemental analyses were conducted by the Microanalysis Laboratory, Institute of Organic Chemistry, University of Heidelberg (operators: Mrs. U. Gaetner, Mrs. C. Vetter and Mr. F. Liebscher) on a Heraeus C,H,N,O-Rapid. Melting points (uncorrected) were measured with a Büchi apparatus, using capillaries which were filled under nitrogen and sealed.

4.2 Starting materials

The following starting materials were either prepared according to the literature methods, or supplied by the coworkers[#] in this group otherwise stated.

BI ₃ ^[56]	B ₂ Cl ₄ ^[56]
Me ₃ SnLi ^[86]	3,4-bis(dichloroboryl)-3-hexene (3) ^[53]
CpCo(C ₂ H ₄) ₂ ^[90]	K[(η ⁵ -C ₅ H ₅)Fe(CO) ₂] ^[78]
1,2-C ₆ H ₄ (Pr ⁱ BCl) ₂ [#] (32) ^[113]	Pr ⁱ ₂ NBCl ₂ [#] ^[108]
Et ₂ NBCl ₂ [#] ^[109]	Cl(Me ₂ N)B-B(NMe ₂)Cl [#] ^[112]
(C ₄ H ₈ N)BBR ₂ ^[148]	(C ₄ H ₈ N) ₄ B ₂ ^[149]
PhC≡CBcat [#] ^[91a] (A. Goswami)	70 ^[146]
Allyl chloride (Dr. I. Kaifer, AK Prof. Huttner)	[Cp*Ru(C ₃ H ₅)Cl ₂] ^[134]
(η ⁵ -pentamethylcyclopentadienyl)(η ⁵ -pentamethyl-2,3-dihydro-1,3-diborolyl)ruthenium (35a) [#] ^[47a]	
(η ⁵ -pentamethylcyclopentadienyl)(η ⁵ -1,3-bis(trimethylsilylmethyl)-2,4,5-trimethyl-2,3-dihydro-1,3-diborolyl)ruthenium (35b) [#] ^[47a]	
(η ⁵ -pentamethylcyclopentadienyl)(η ⁵ -2-methyl-1,3,4,5-tetraethyl-2,3-dihydro-1,3-diborolyl)-ruthenium (35c) [#] ^[46d]	
1,2,3-trimethyl-4,5-diethyl-2,3-dihydro-1,3-diborole 37c ^[75]	
1,3-diiido-2,4,5-trimethyl-2,3-dihydro-1,3-diborole 37d ^[75]	
1,3-dichloro-1,3,5-tris(dimethylamino)triborane(5) (31) ^[116] (Prof. A. Berndt, Marburg).	
<i>nido</i> -2,3-Et ₂ C ₂ B ₄ H ₆ ^[97] (Prof. R. N. Grimes, Charlottesville, USA)	
2,3-dihydro-1,3-diborole-rhodium dimer 48 [#] ^[130]	
Cp*Ru(μ-1,3-diborolyl)RhCl dimer 50 [#] ^[47a] ,	

4.3 Experimental details

1.) 1,6-Diiodo-2,3,4,5-tetraethyl-2,3,4,5-tetracarba-*nido*-hexaborane(6) (**5a**): formation from 3-hexyne, BI₃ (1 equiv.) and NaK_{2.8}

a) One-pot procedure: To a solution of BI₃ (872 mg, 2.23 mmol) in 40 mL of hexane at – 78 °C was added 3-hexyne (190 mg, 2.3 mmol) dropwise, and then NaK_{2.8} (0.9 mL, excess) was added via a syringe. The mixture was stirred at that temperature for ca. 15 min., and the cooling bath was removed. The reaction mixture was allowed to warm to r.t. and stirred overnight, then filtered (G4 frit) and the residue washed with hexane (2 × 15 mL). The solvent of the yellow filtrate was removed *in vacuo*, leaving a yellow viscous oil. Distillation at 80 °C/ 2 × 10^{–3} torr gave **5a** (326 mg, 66%) as a yellow, air-sensitive oil, which slowly solidified.

For reactions with up to 28 mmol of BI₃, longer reaction times (1 week) are needed (av. yield > 60 %, m.p. 52 °C). ¹H-NMR (CDCl₃): δ = 1.20 (t, 6 H, ³J_{H,H} = 7.6 Hz, CH₃), 1.26 (t, 6 H, ³J_{H,H} = 7.6 Hz, CH₃), 1.87– 2.04 (m), 2.11– 2.38(m) (8H, CH₂). ¹¹B-NMR (CDCl₃): δ = 5.5 (s, B_{basal}, 1 B), – 52.5 (s, B_{apical}, 1 B). ¹¹B-NMR (C₆D₆): δ = 5.9 (s, B_{basal}, 1 B), – 52.4 (s, B_{apical}, 1 B). ¹³C-NMR (CDCl₃): δ = 13.5, 14.2 (CH₃), 18.9, 20,4 (CH₂), 114.2 (skeletal carbon atoms non-adjacent to the basal boron), the signals for the other basal carbon atoms not observed. EI-MS: *m/z* (%) = 440 (100) [M⁺], 313 (20.3) [M⁺ – I]. HR-MS (EI): *m/z* = 439.9842 [M⁺]; Calcd. For ¹²C₁₂¹H₂₀¹¹B₂¹²⁷I₂ 439.9840 (Δ*m* = 0.2 mmu).

b) Stepwise procedure: To a solution of BI₃ (2.165 g, 5.53 mmol) in 50 mL of hexane was added dropwise 3-hexyne (470 mg, 5.7 mmol) at – 50 °C, and the solution was allowed to warm up to r.t.. The resulting red solution (¹¹B-NMR: δ = 40.5 ppm) was cooled to – 60 °C again and NaK_{2.8} (2 mL) was added via a syringe. The following workup was similar to that of the one-pot reaction to yield **5a** (520 mg, 43 %).

2.) Reactions of 3-hexyne with BI₃ (2 equiv.) and NaK_{2.8} at different temperatures

a) A solution of BI₃ (858 mg, 2.19 mmol) in 35 mL of hexane was added dropwise to a mixture of 3-hexyne (90 mg, 1.1 mmol) and NaK_{2.8} (0.9 mL) at RT. The reaction mixture became gray in ca. 20 min., and was stirred for 1 day, then filtered (G4 frit), the residue washed with hexane (2 × 15 mL), and the slight pink filtrate was dried *in vacuo*, leaving a

red-brown oil (238 mg), which is a mixture of **5a**, **4** and **6**. EI-MS: m/z (%) = 440 (100) (**5a**), 716(3.35) (**4**), and 771 (44.83) (**6**). HR-MS (EI): m/z = 439.9847 (**5a**); Calcd. for $^{12}\text{C}_{12}^{1}\text{H}_{20}^{11}\text{B}_2^{127}\text{I}_2$ 439.9840 ($\Delta m = 0.6$ mmu), m/z = 715.8150 (**4**); Calcd. for $^{12}\text{C}_{12}^{1}\text{H}_{20}^{11}\text{B}_4^{127}\text{I}_4$ 715.8116 ($\Delta m = 3.4$ mmu), m/z = 715.6464 (**6**); Calcd. for $^{12}\text{C}_6^1\text{H}_{10}^{11}\text{B}_5^{127}\text{I}_5$ 715.6472 ($\Delta m = -0.8$ mmu).

b) To a solution of BI_3 (3.126 g, 7.98 mmol) in 30 mL of hexane at -78 °C was added 3-hexyne (332 mg, 4.04 mmol) dropwise, the mixture immediately became yellow brown, and then $\text{NaK}_{2.8}$ (2 mL) was added via a syringe. The reaction mixture was stirred at -78 °C for ca. 10 min., the cooling bath was removed, and the mixture was allowed to warm to r.t. and stirred for 1 day, then filtered (G4 frit), and the residue washed with hexane (2×15 mL). The yellow filtrate was dried *in vacuo*, leaving a yellow viscous oil, which was distilled to give **5a** (455 mg, 51 %) as the single carborane product. In this case, no hexaethylbenzene was detected.

3.) *cis*-3,4-Bis(diiodoboryl)-3-hexene (**2**)^[52a]

A portion of 3,4-bis(dichloroboryl)-3-hexene (**3**) (2.13 g, 8.7 mmol) was added to BI_3 (4.653 g, 11.9 mmol) at RT, the resulting dark brown solution was stirred at r.t. for ca. 2.5 h. The reaction flask was connected to a condensation apparatus, the trap cooled to -78 °C, and the system was kept at ca. 60 mbar overnight. Then all volatiles were removed under high vacuum, and the resulting dark brown residue was recrystallized five times with hexane (ca. 20 ml), four times at -84 °C, and the last time at -28 °C. Compound **2** (2.53 g, 47.5 %) was obtained as a yellow crystalline solid, which can be kept at -28 °C for a long time, m.p. 70 – 72 °C. $^1\text{H-NMR}$ (C_6D_6): $\delta = 1.02$ (t, 6 H, $^3J_{\text{H,H}} = 7.5$ Hz, CH_3), 2.29 (q, 4 H, $^3J_{\text{H,H}} = 7.5$ Hz, CH_2). $^{11}\text{B-NMR}$ (C_6D_6): $\delta = 11.8$. $^{13}\text{C-NMR}$ (C_6D_6): $\delta = 14.8$ (CH_3), 26.2 (CH_2), 178.4 ($\text{C}=\text{C}$). EI-MS: m/z (%) = 485 (100) [$\text{M}^+ - \text{I}$], HR-MS (EI): m/z = 484.8128 [$\text{M}^+ - \text{I}$]; Calcd. For $^{12}\text{C}_6^1\text{H}_{10}^{11}\text{B}_2^{127}\text{I}_3$ 484.8103 ($\Delta m = 2.5$ mmu).

4.) Formation of **5a** from the redox reaction of 3-hexyne and **2**

3-Hexyne (196 mg, 2.3 mmol) was added dropwise to a solution of **2** (1.357 g, 2.22 mmol) in hexane (25 mL) at -60 °C. The mixture was allowed to warm to r.t., it became deep brown indicating the formation of I_2 . The $^{11}\text{B-NMR}$ spectrum showed a signal at $\delta = 66$ ppm. All the

volatiles were removed *in vacuo* and the resulting red oil was distilled at 71 °C/ 8×10^{-2} torr to give a yellowish oil (533 mg, 55 %), which gradually became deep red. The ^{11}B -NMR (C_6D_6 , 64 MHz) data of the original distillate: $\delta = 57.6$ (s), 45.7, 5.9, -9.0 (BI_3), -52.4 ppm; after three days, the corresponding signals were: $\delta = 57$ (s), 32, 5.9, -52.4 ; after three weeks, there were only two ^{11}B -NMR signals: $\delta = 5.9$, -52.4 ppm (**5a**). The EI-MS spectrum was identical to that of authentic **5a**.

5.) 1,6-Diiodo-2,3,4,5-tetramethyl-2,3,4,5-tetracarba-*nido*-hexaborane(6) (**5b**)

Same procedures as described for **5a**, 2-butyne (426 mg, 7.9 mmol), BI_3 (3.09 g, 7.9 mmol), $\text{NaK}_{2.8}$ (2 mL). The final yellow viscous oil was distilled at 95 °C/ 3×10^{-2} torr to give **5b** (225 mg, 15 %) as a yellowish solid. (m. p. 92–94 °C). ^1H -NMR (CDCl_3): $\delta = 1.72$ (s, 6 H, CH_3), 1.87 (s, 6H CH_3). ^{11}B -NMR (CDCl_3): $\delta = 5.7$ (s, B_{basal}), -48.6 (s, B_{apical}). ^{13}C -NMR (CDCl_3): $\delta = 11.29$, 12.55 (CH_3), 110.7 (skeletal carbon atoms non-adjacent to basal boron), the signals for the other basal carbon atoms not observed. EI-MS: m/z (%) = 384 (94) [M^+], 257 (100) [$\text{M}^+ - \text{I}$]. HR-MS (EI): $m/z = 383.9218$ [M^+]; Calcd. for $^{12}\text{C}_8^1\text{H}_{12}^{11}\text{B}_2^{127}\text{I}_2$ 383.9215 ($\Delta m = 0.3$ mmu).

6.) 1,6-Diiodo-2,3,4,5-tetraphenyl-2,3,4,5-tetracarba-*nido*-hexaborane(6) (**5c**)

Same procedures as described for **5a**, diphenylacetylene (1.38 g, 7.7 mmol), BI_3 (3.03 g, 7.7 mmol), $\text{NaK}_{2.8}$ (1.6 mL). The yellow filtrate was cooled, and some yellow solid (mainly hexaphenylbenzene) was filtered, and the yellow filtrate was dried *in vacuo* to give **5c** (147 mg, ca. 5 %) and small amount of hexaphenylbenzene as an orange yellow solid. ^{11}B -NMR (CD_2Cl_2): $\delta = 7.9$ (s, B_{basal}), -50.1 (s, B_{apical}), ($\delta = 8.2$ and -49.6 in CDCl_3). EI-MS: m/z (%) = 632 (100) [M^+], 505 (69.6) [$\text{M}^+ - \text{I}$]. HR-MS (EI): $m/z = 631.9855$ [M^+]; Calcd. for $^{12}\text{C}_{28}^1\text{H}_{20}^{11}\text{B}_2^{127}\text{I}_2$ 631.9841 ($\Delta m = 1.4$ mmu).

7.) Tetraethyltetraiodotetracarba-*nido*-octaborane(8) (**4**)

To a solution of **2** (2.3 g, 3.76 mmol) in 40 mL of hexane at -65 °C was added $\text{NaK}_{2.8}$ (1.5 mL, excess) dropwise via a syringe, after ca. 1 h, the cooling bath was removed, and the reaction mixture was warmed to r.t., and stirred for 3 days. Then the reaction mixture was filtered (G4

frit) and the residue washed with hexane (2×15 mL), the light yellow filtrate dried *in vacuo*, leaving a yellow viscous oil which slowly solidified, containing **4** (385 mg, 28.6 %) and trace amount of **6**. ^{11}B -NMR (CDCl_3 , 64 MHz): $\delta = -10.5$ (s, 2B), -13.4 (s, 2 B). EI-MS: m/z (%) = 716 (100) [M^+] (**4**), 589 (91.7) [$\text{M}_1^+ - \text{I}$]. 771(4.3) [M^+] (**6**). HR-MS (EI): $m/z = 715.8112$ [M_1^+]; Calcd. For $^{12}\text{C}_{12}\text{H}_{20}\text{B}_4\text{I}_4$ 715.8117 ($\Delta m = -0.5$ mmu). $m/z = 771.6440$ [M_2^+]; Calcd. For $^{12}\text{C}_6\text{H}_{10}\text{B}_5\text{I}_5$ 771.6471 ($\Delta m = -3.1$ mmu).

8.) *cis*-3-Diiodoboryl-4-iodo-3-hexene (**1**)^[55]

The procedure in the literature was slightly modified. To a solution of BI_3 (3.245 g, 8.3 mmol) in 50 mL of pentane was added 3-hexyne (681 mg, 8.3 mmol) dropwise at -25 °C. The red mixture was warmed to r.t. and the deep pink solution was transferred to another flask, leaving a little black solid on the wall of the original flask. The solution was dried *in vacuo* to give analytically pure **1** almost quantitatively as a deep red liquid. ^1H -NMR (CDCl_3): $\delta = 1.08$ (t, 3 H, $^3J_{\text{H,H}} = 7.4$ Hz, CH_3), 1.22 (t, 3 H, $^3J_{\text{H,H}} = 7.6$ Hz, CH_3), 2.15 (q, 2 H, $^3J_{\text{H,H}} = 7.6$ Hz, CH_2), 2.62 (q, 2 H, $^3J_{\text{H,H}} = 7.4$ Hz, CH_2). ^{11}B -NMR (CDCl_3): $\delta = 40.0$. ^{13}C -NMR (CDCl_3): $\delta = 14.2$, 15.0 (CH_3), 24.7, 33.3 (CH_2), 106.4 (=C-I), 157.6 (br., =C-B).

9.) *trans*-3-Diiodoboryl-4-iodo-3-hexene (**1'**)

Slow isomerization of **1** (*cis*) at room temperature afforded **1'** (not complete within 5 weeks as indicated by NMR in a CDCl_3 solution, with partial decomposition). ^1H -NMR: $\delta = 1.08$ (t, 3 H, $^3J_{\text{H,H}} = 7.2$ Hz, CH_3), 1.15 (t, 3 H, $^3J_{\text{H,H}} = 6.7$ Hz, CH_3), 2.2 (q, 2 H, $^3J_{\text{H,H}} = 7.2$ Hz, CH_2), 2.61 (q, 2 H, $^3J_{\text{H,H}} = 6.7$ Hz, CH_2). ^{11}B -NMR: $\delta = 43.5$. ^{13}C -NMR: $\delta = 12.8$, 14.0 (CH_3), 33.6, 39.1 (CH_2), 114.6 (=C-I), 158.1 (br., =C-B).

10.) *cis*-3-Diiodoboryl-4-iodo-3-hexene-pyridine adduct (**9**)

Pyridine (223 mg, 2.8 mmol) was added dropwise to a solution of **1** (1.33 g, 2.8 mmol) in 25 mL of hexane at -25 °C. The color immediately turned to deep red and then a yellow precipitate appeared. The mixture was warmed to r.t., the solvent was removed *in vacuo*, and an orange yellow powder **9** was obtained quantitatively. The X-ray quality crystals were grown from a toluene solution at -28 °C. m. p. 30 °C. ^1H -NMR (CDCl_3): $\delta = 1.05$ (t, 3 H, $^3J_{\text{H,H}} = 7.4$

Hz, CH₃), 1.29 (t, 3 H, ³J_{H,H} = 7.4 Hz, CH₃), 2.77 (q, 2 H, ³J_{H,H} = 7.4 Hz, CH₂), 2.86 (q, 2 H, ³J_{H,H} = 7.4 Hz, CH₂), 7.70 (m), 8.19(m), 9.39 (m) (py-H). ¹¹B-NMR (CDCl₃): δ = - 13.9. ¹³C-NMR (CDCl₃): δ = 14.4, 14.9 (CH₃), 32.4, 39.5 (CH₂), 115.2 (=C-I), 126.6, 142.4, 147.6 (py-C), the signal for the boron-bound carbon n.o..

11.) *trans*-3-Diiodoboryl-4-iodo-3-hexene-pyridine adduct (9')

Slow isomerization of **9** (*cis*) at room temperature afforded **9'** within one week as yellow crystals from a CH₂Cl₂ solution. (m. p. 108–110 °C, decom.). ¹H-NMR (CDCl₃): δ = 0.74 (t, 3 H, ³J_{H,H} = 7.4 Hz, CH₃), 1.25 (t, 3 H, ³J_{H,H} = 7.4 Hz, CH₃), 1.94 (q, 2 H, ³J_{H,H} = 7.2 Hz, CH₂), 2.98 (q, 2 H, ³J_{H,H} = 7.4 Hz, CH₂), 7.76 (m), 8.26(m), 9.47 (m) (py-H). ¹¹B-NMR (CDCl₃): δ = - 20.8. ¹³C{¹¹B}-NMR (CDCl₃): δ = 12.9, 13.7 (CH₃), 38.8, 45.3 (CH₂), 120.0 (=C-I), 126.4, 142.9, 146.9 (py-C), 147.9 (C=C-B). The EI-MS failed to give definite information.

12.) *cis*-3-(1,3,2-Benzodioxaborol-2-yl)-4-iodo-3-hexene (10)

A solution of **1** (730 mg, 1.54 mmol) in 10 mL of CH₂Cl₂ was added dropwise to a solution of catechol (169 mg, 1.54 mmol) in CH₂Cl₂ (15 mL) at - 45 °C. The reaction mixture was warmed to r.t. and the solvent removed *in vacuo* to give 455 mg (90 %) of **10** as a deep red liquid. ¹H-NMR (CDCl₃): δ = 1.10 (t, 3 H, ³J_{H,H} = 7.6 Hz, CH₃), 1.17 (t, 3 H, ³J_{H,H} = 7.4 Hz, CH₃), 2.43 (q, 2 H, ³J_{H,H} = 7.6 Hz, CH₂), 2.73 (q, 2 H, ³J_{H,H} = 7.4 Hz, CH₂), 7.10- 7.33 (m, 4H, C₆H₄). ¹¹B-NMR (CDCl₃): δ = 31.1. ¹³C-NMR (CDCl₃): δ = 12.9, 14.4 (CH₃), 26.7, 35.7 (CH₂), 110.1 (=C-I), 112.7, 122.8, 147.9 (C₆H₄), the signals for boron-bound carbon n.o.. EI-MS: *m/z* (%) = 328 (50.6) [M⁺], 246 (100) [M⁺ - C₆H₁₀], 201 (99.8) [M⁺ - I]. HR-MS (EI): *m/z* = 328.0116 [M⁺]; Calcd. For ¹²C₁₂¹H₁₄¹¹B¹²⁷I¹⁶O₂ 328.0131 (Δ*m* = - 1.5 mmu).

13.) *trans*-3-(1,3,2-Benzodioxaborol-2-yl)-4-iodo-3-hexene (10')

The isomerization of **10** (*cis*) at room temperature afforded **10'** within ca. 3 weeks (as indicated by NMR in a CDCl₃ solution). ¹H-NMR: δ = 1.12 (t, 3 H, ³J_{H,H} = 7.6 Hz, CH₃), 1.27 (t, 3 H, ³J_{H,H} = 7.4 Hz, CH₃), 2.60 (q, 2 H, ³J_{H,H} = 7.4 Hz, CH₂), 3.22 (q, 2 H, ³J_{H,H} = 7.6 Hz, CH₂), 7.12- 7.33 (m, 4H, C₆H₄). ¹¹B-NMR: δ = 29.1. ¹³C-NMR: δ = 13.3, 15.6 (CH₃), 36.6, 39.9 (CH₂), 112.2 (=C-I), 112.6, 122.9, 147.9 (C₆H₄), the signals for boron-bound carbon n.o..

14.) *cis*-3-Diisopropylaminoiodoboryl-4-iodo-3-hexene (11)

Diisopropylamine (1.07 g, 10.6 mmol) was added dropwise to a solution of **1** (2.45 g, 5.2 mmol) in hexane (50 mL) at $-40\text{ }^{\circ}\text{C}$. The mixture was warmed to r.t. and filtered, the light yellow filtrate was dried *in vacuo* to give a red oil, which was distilled at $82\text{ }^{\circ}\text{C}/5.9 \times 10^{-2}$ torr to give yellow **11** (1.8 g, 76 %). $^1\text{H-NMR}$ (CDCl_3): $\delta = 1.04$ (t, 3 H, $^3J_{\text{H,H}} = 7.3$ Hz, Et- CH_3), 1.14 (t, 3 H, $^3J_{\text{H,H}} = 7.6$ Hz, Et- CH_3), 1.24 (d, 3H, $^3J_{\text{H,H}} = 6.7$ Hz, *iPr*- CH_3), 1.30 (d, 3H, $^3J_{\text{H,H}} = 6.7$ Hz, *iPr*- CH_3), 1.49 (d, 3H, $^3J_{\text{H,H}} = 7.2$ Hz, *iPr*- CH_3), 1.54 (d, 3H, $^3J_{\text{H,H}} = 7.2$ Hz, *iPr*- CH_3), 2.10 (m, 1 H, Et- CH_2), 2.31 (m, 1 H, Et- CH_2), 2.53 (q, 2H, $^3J_{\text{H,H}} = 7.4$ Hz, Et- CH_2), 3.53 (sept, 1H, *iPr*-CH), 3.95 (sept, 1H, *iPr*-CH). $^{11}\text{B-NMR}$ (CDCl_3): $\delta = 28.1$. $^{13}\text{C-NMR}$ (CDCl_3): $\delta = 14.2, 14.3$, (Et- CH_3), 21.0, 22.1, 23.0, 24.0 (*iPr*- CH_3), 25.5, 34.2 (Et- CH_2), 47.8, 53.9 (*iPr*-CH), 110.1 (=C-I), the boron-bound carbon n.o.. EI-MS: m/z (%) = 447 (2.4) [M^+], 320 (100) [$\text{M}^+ - \text{I}$], 238 (39.8) [$\text{M}^+ - \text{I} - 2\text{C}_3\text{H}_5$]. HR-MS (EI): $m/z = 447.0079$ [M^+]; Calcd. For $^{12}\text{C}_{12}^{1}\text{H}_{24}\text{N}^{11}\text{B}^{127}\text{I}_2$ 447.0091 ($\Delta m = -1.2$ mmu).

15.) 1-Iodo-6-phenylalkynyl-2,3,4,5-tetraethyl-2,3,4,5-tetracarba-nido-hexaborane(6) (5d)

To a solution of phenylacetylene (507 mg, 5 mmol) in hexane (30 mL) was added *n*BuLi (2.5 M in hexanes, 2 mL) at $-50\text{ }^{\circ}\text{C}$, the mixture was stirred for 30 min., and then warmed up to r.t.. The resulting white suspension was cooled to $-60\text{ }^{\circ}\text{C}$, and added via syringe to a solution of **5a** (900 mg, 2.05 mmol) in hexane (30 mL). The mixture was warmed to room temperature and stirred for 2 days. Filtration (G4 frit) gave light yellow filtrate, which was dried *in vacuo* to give **5d** as a yellow powder (746 mg, 88 %), m.p. $74\text{ }^{\circ}\text{C}$. Crystals suitable for X-ray diffraction analysis were grown from a toluene/hexane solution at $-28\text{ }^{\circ}\text{C}$. $^1\text{H-NMR}$ (CDCl_3): $\delta = 1.25$ (t, 6 H, $^3J_{\text{H,H}} = 7.6$ Hz, CH_3), 1.33 (t, 6 H, $^3J_{\text{H,H}} = 7.6$ Hz, CH_3), 2.0 (m), 2.38(m) (8H, CH_2), 7.27-7.48 (m, Ph). $^{11}\text{B-NMR}$ (CDCl_3): $\delta = 10.3$ (s, B_{basal}), -52.6 (s, B_{apical}). $^{13}\text{C-NMR}$ (CDCl_3): $\delta = 13.4, 14.3$ (CH_3), 18.4, 19.8 (CH_2), 104.4 (br., boron-bound basal carbon atoms), 113.0 (skeletal carbon atoms non-adjacent to the basal boron), 124.6, 127.6, 128.1, 131.7 (Ph), alkynyl carbon atoms n.o.. -EI-MS: m/z (%) = 414 (100) [M^+], 287 (14.6) [$\text{M}^+ - \text{I}$]. HR-MS (EI): $m/z = 414.1224$ [M^+]; calcd. for $^{12}\text{C}_{20}^{1}\text{H}_{25}^{11}\text{B}_2^{127}\text{I}$ 414.1187 ($\Delta m = 3.7$ mmu).

16.) 1-Iodo-6-tert-butylalkynyl-2,3,4,5-tetraethyl-2,3,4,5-tetracarba-nido-hexa-

borane(6) (5e)

Similar procedures as described for **5d**. *t*BuC≡CLi (750 mg, 8.5 mmol), **5a** (528 mg, 1.2 mmol), hexane (50 mL). **5e** (450 mg, 95 %) was obtained as a yellow oil. ¹H-NMR (CDCl₃): δ = 1.20 (br., 6 H, CH₃), 1.25 (br., 6 H, CH₃), 1.25 (s, 9 H, *t*Bu-H), 1.91 (m), 2.28(m) (8H, CH₂). ¹¹B-NMR (CDCl₃): δ = 10.8 (s, B_{basal}), - 52.6 (s, B_{apical}). ¹³C-NMR (CDCl₃): δ = 13.4, 14.0 (CH₃), 18.3, 19.6 (CH₂), 30.8 (C(CH₃)₃), 31.2 (C(CH₃)₃), boron-bound basal carbon atoms n.o., 112.3 (skeletal carbon atoms non-adjacent to the basal boron), alkynyl carbon atoms n.o.. -EI-MS: *m/z* (%) = 394 (100) [M⁺], 267 (10.8) [M⁺ - I]. HR-MS (EI): *m/z* = 394.1517 [M⁺]; calcd. for ¹²C₁₈¹H₂₉¹¹B₂¹²⁷I 394.1500 (Δ*m* = 1.7 mmu).

17.) 1-Iodo-6-trimethylsilylalkynyl-2,3,4,5-tetraethyl-2,3,4,5-tetracarba-*nido*-hexaborane(6) (5f)

Similar procedures as described for **5d**. Me₃SiC≡CH (310 mg, 3.16 mmol), *n*-BuLi (2.5 M in hexanes, 3 mmol), **5a** (634 mg, 1.44 mmol), hexane (50 mL). **5f** (536 mg, 91 %) was obtained as a yellow oil. ¹H-NMR (CDCl₃): δ = 0.18 (s, SiMe₃), 1.21 (t, 6 H, ³J_{H,H} = 7.6 Hz, CH₃), 1.26 (t, 6 H, ³J_{H,H} = 7.6 Hz, CH₃), 1.94 (m), 2.29(m) (8H, CH₂). ¹¹B-NMR (CDCl₃): δ = 9.8 (s, B_{basal}), - 52.8 (s, B_{apical}). ¹³C-NMR (CDCl₃): δ = 0.18 (SiMe₃), 13.3, 14.1 (CH₃), 18.3, 19.7 (CH₂), 105.2 (boron-bound basal carbon atoms), 112.8 (skeletal carbon atoms non-adjacent to the basal boron), alkynyl carbon atoms n.o.. ²⁹Si-NMR (CDCl₃, 39.7 MHz): δ = - 19.8 -EI-MS: *m/z* (%) = 410 (100) [M⁺], 283 (13.5) [M⁺ - I]. HR-MS (EI): *m/z* = 410.1265 [M⁺]; calcd. for ¹²C₁₇¹H₂₉¹¹B₂¹²⁷I 410.1269 (Δ*m* = - 0.4 mmu).

18.) 1-Iodo-6-*p*-tolylalkynyl-2,3,4,5-tetraethyl-2,3,4,5-tetracarba-*nido*-hexaborane(6) (5g)

Similar procedures as described for **5d**. *p*-Tolylacetylene (431 mg, 3.72 mmol), **5a** (264 mg, 0.6 mmol), hexane (50 mL). **5g** (247 mg, 96 %) was obtained as a yellow solid, m.p. 81 °C. Crystals suitable for X-ray analysis were grown from a toluene solution at - 28°C. ¹H-NMR (CDCl₃): δ = 1.24 (t, 6 H, ³J_{H,H} = 7.6 Hz, CH₃), 1.31 (t, 6 H, ³J_{H,H} = 7.6 Hz, CH₃), 1.97 (m), 2.29(m) (8H, CH₂), 2.32 (s, 3 H, *p*-tolyl-CH₃), 7.08 (d, ³J_{H,H} = 7.94 Hz, C₆H₄), 7.38 (d, ³J_{H,H} = 7.94 Hz, C₆H₄). ¹¹B-NMR (CDCl₃): δ = 10.9 (B_{basal}), - 52.6 (s, B_{apical}). ¹³C-NMR (CDCl₃): δ = 13.3, 14.2 (CH₃), 18.4, 19.7 (CH₂), 21.4 (*p*-tolyl-CH₃), boron-bound basal carbon atoms n.o.,

112.9 (skeletal carbon atoms non-adjacent to the basal boron), 121.6, 128.8, 131.6, 137.6 (C₆H₄), alkynyl carbon atoms n.o.. -EI-MS: m/z (%) = 428 (100) [M⁺], 301 (13.6) [M⁺ - I]. HR-MS (EI): m/z = 428.1360 [M⁺]; calcd. for ¹²C₂₁¹H₂₇¹¹B₂¹²⁷I 428.1344 (Δm = 1.6 mmu).

19.) 1-Iodo-6-diphenylphosphanyl-2,3,4,5-tetraethyl-2,3,4,5-tetracarba-*nido*-hexaborane(6) (5h)

A suspension of Ph₂PLi (170 mg, 0.88 mmol, prepared *in situ* from HPPH₂ and n-BuLi in hexane) in hexane (5 mL) was cooled to -60°C, and added to a solution of **5a** (194 mg, 0.44 mmol) in hexane (10 mL). The mixture was allowed to warm to r.t., stirred overnight and filtered. The yellow filtrate was dried *in vacuo* to give **5h** (158 mg, 72 %) as a yellow oil. ¹H-NMR (CDCl₃): δ = 0.99 (t, 6 H, ³J_{H,H} = 7.6 Hz, CH₃), 1.37 (t, 6 H, ³J_{H,H} = 7.6 Hz, CH₃), 1.94 (m), 2.36 (m) (8H, CH₂), 7.37-7.56 (m, 10 H, aromatic). ¹¹B-NMR (CDCl₃): δ = 14.8 (br., B_{basal}), -52.8 (s, B_{apical}). ¹³C-NMR (CDCl₃): δ = 13.7, 15.1 (CH₃), 18.8, 19.2 (CH₂), boron-bound basal carbon atoms n.o., 116.1 (skeletal carbon atoms non-adjacent to the basal boron), 127.2, 128.5, 134.4, 138.2 (aromatic), alkynyl carbon atoms n.o.. ³¹P{¹H}-NMR (CDCl₃, 80.92 MHz): δ = -40.1 -EI-MS: m/z (%) = 498 (59.1) [M⁺], 371 (9.8) [M⁺ - I], 186 (100) [HPPH₂]. HR-MS (EI): m/z = 498.1307 [M⁺]; calcd. for ¹²C₂₄¹H₃₀¹¹B₂¹²⁷I³¹P 498.1316 (Δm = -0.9 mmu).

20.) 1-Iodo-6-[(η^5 -cyclopentadienyl)dicarbonyliron]-2,3,4,5-tetraethyl-2,3,4,5-tetracarba-*nido*-hexaborane(6) (5i)

A solution of **5a** (317 mg, 0.72 mmol) in hexane (10 mL) was added to a suspension of K[(η^5 -C₅H₅)Fe(CO)₂] (395 mg, 1.8 mmol) in toluene (30 mL) at r.t.. The mixture was stirred for 4 days and filtered. The deep red filtrate was concentrated and cooled to -28°C, yellow crystals were formed after one week (258 mg, 73 %), m.p. 132 °C. ¹H-NMR (CDCl₃): δ = 1.2 (br., 6 H, CH₃), 1.3 (br., 6 H, CH₃), 1.93 (m), 2.22 (m) (8H, CH₂), 4.8 (s, Cp). ¹¹B-NMR (CDCl₃): δ = 28.6 (br., B_{basal}), -49.6 (s, B_{apical}). ¹³C-NMR (CDCl₃): δ = 13.6, 14.1 (CH₃), 19.3, 21.7 (CH₂), 88.1 (Cp), 106.5 (boron-bound basal carbon atoms), 117.9 (skeletal carbon atoms non-adjacent to the basal boron), 217.2 (CO), alkynyl carbon atoms n.o.. ν_{co} (hexane) = 1998.1 (s), 1942.4 (s) cm⁻¹. -EI-MS: m/z (%) = 490 (4.2) [M⁺], 462 (24.1) [M⁺ - CO], 434 (100) [M⁺ -

2CO], 405 (7.3) [$M^+ - 2CO - Et$], 307 (22.9) [$M^+ - 2CO - I$]. HR-MS (EI): $m/z = 490.0431$ [M^+]; calcd. for $^{12}C_{19}H_{25}O_2^{11}B_2Fe^{127}I$ 490.0435 ($\Delta m = -0.4$ mmu).

21.) 1-Iodo-6-hydrido-2,3,4,5-tetraethyl-2,3,4,5-tetracarba-*nido*-hexaborane(6) (**5j**)

a) from decomposition of 5i: In an attempt to separate **5i** by column chromatography on silica gel, the crude product was eluted with hexane, however, only decomposition was observed. Compound **5j** and paramagnetic impurities were formed, as indicated by the NMR.

b) from the reaction of 5a and LiBEt₃H: To a solution of **5a** (194 mg, 0.44 mmol) in hexane (5 mL) was added dropwise a solution of LiBEt₃H (1.0 M in THF, 0.4 mmol) at $-65^\circ C$. A white precipitate was formed, the mixture was allowed to warm to RT and filtered. The colorless filtrate was dried *in vacuo* to give **5j** (123 mg, 89 %) as a colorless oil. 1H -NMR (CDCl₃): $\delta = 1.2$ (br., 6 H, CH₃), 1.2 (br., 6 H, CH₃), 2.04 (m), 2.21 (m) (8H, CH₂). ^{11}B -NMR (CDCl₃): $\delta = 11.5$ (d, $J_{B,H} = 148.3$ Hz, B_{basal}), -53.8 (s, B_{apical}). ^{13}C -NMR (CDCl₃): $\delta = 13.1$, 14.3 (CH₃), 18.5, 20.1 (CH₂), 106.3 (boron-bound basal carbon atoms), 114.8 (skeletal carbon atoms non-adjacent to the basal boron). -EI-MS: m/z (%) = 314 (100) [M^+], 187 (10) [$M^+ - I$]. HR-MS (EI): $m/z = 314.0893$ [M^+]; calcd. for $^{12}C_{12}H_{21}^{11}B_2^{127}I$ 314.0874 ($\Delta m = 1.9$ mmu).

22.) 1-Iodo-6-fluoro-2,3,4,5-tetraethyl-2,3,4,5-tetracarba-*nido*-hexaborane(6) (**5l**)

a) reaction of 5a with SbF₃: A solution of **5a** (145 mg, 0.33 mmol) in hexane (3 mL) was added dropwise to a suspension of SbF₃ (600 mg, 3.4 mmol) in hexane (2 mL) at r.t.. The mixture was stirred for one week. The starting compound **5a** remained unreacted in the light yellow solution part checked by ^{11}B -NMR ($\delta = 6.5, -52.3$).

b) reaction of 5a with AgF: A solution of **5a** (145 mg, 0.33 mmol) in hexane (3 mL) was added dropwise to a suspension of AgF (180 mg, 1.4 mmol) in hexane (7 mL) at r.t. in dark. The mixture was stirred overnight and a colorless solution was obtained after filtration, which was dried to give **5l** (60 mg, 56 %) as a colorless oil. 1H -NMR (CDCl₃): $\delta = 1.18$ (br., 6 H, CH₃), 1.26 (br., 6 H, CH₃), 2.08 (m), 2.33 (m) (8H, CH₂). ^{11}B -NMR: $\delta = 21.9$ (br., B_{basal}), -53.1 (s, B_{apical}). ^{13}C -NMR: $\delta = 13.3, 14.1$ (CH₃), 18.5, 20.1 (CH₂), 106.1 (boron-bound basal carbon atoms), the signals for the other skeletal carbon atoms non-adjacent to the basal boron n.o.. -EI-MS: m/z (%) = 332 (100) [M^+], 205 (67) [$M^+ - I$]. HR-MS (EI): $m/z = 332.0782$ [M^+];

calcd. for $^{12}\text{C}_{12}^{1}\text{H}_{20}^{19}\text{F}^{11}\text{B}_2^{127}\text{I}$ 332.0780 ($\Delta m = 0.2$ mmu).

23.) 1-Iodo-6-phenyl-2,3,4,5-tetraethyl-2,3,4,5-tetracarba-*nido*-hexaborane(6) (**5m**)

A suspension of PhLi (dried from a solution (1.6 M) in ether/cyclohexane, 1 mmol) in hexane (5 mL) was cooled to -60°C and added to a solution of **5a** (194 mg, 0.44 mmol) in hexane (10 mL). The mixture was allowed to warm to RT, stirred overnight and filtered. The slight yellow filtrate was dried *in vacuo* to give **5m** (150 mg, 87 %) as a colorless oil, and trace amount of **5n**. $^1\text{H-NMR}$ (CDCl_3): $\delta = 1.19$ (t, $^3J_{\text{H,H}} = 7.6$ Hz, 6 H, CH_3), 1.4 (t, $^3J_{\text{H,H}} = 7.6$ Hz, 6 H, CH_3), 2.08 (m), 2.36(m) (8H, CH_2), 7.40-7.55 (m, Ph). $^{11}\text{B-NMR}$ (CDCl_3): $\delta = 17.9$ (s, B_{basal}), -52.4 (s, B_{apical}). $^{13}\text{C-NMR}$ (CDCl_3): $\delta = 13.7$, 14.2 (CH_3), 18.5, 19.0 (CH_2), 103.4 (br., boron-bound basal carbon atoms), 112.9 (skeletal carbon atoms non-adjacent to the basal boron), 126.8, 127.2, 128.8, 133.2, 141.3 (Ph). -EI-MS: m/z (%) = 390 (100) [M^+], 361 (10.8) [$\text{M}^+ - \text{Et}$], 263 (5.9) [$\text{M}^+ - \text{I}$]. HR-MS (EI): $m/z = 390.1188$ [M^+]; Calcd. for $^{12}\text{C}_{18}^{1}\text{H}_{25}^{11}\text{B}_2^{127}\text{I}$ 390.1187 ($\Delta m = 0.1$ mmu); $m/z = 340.2532$ (**5n**) $^+$; calcd. for $^{12}\text{C}_{24}^{1}\text{H}_{30}^{11}\text{B}_2$ 340.2534 ($\Delta m = -0.2$ mmu).

24.) 1-Iodo-6-trimethylstannyl-2,3,4,5-tetraethyl-2,3,4,5-tetracarba-*nido*-hexaborane(6) (**5o**)

A solution of **5a** (194 mg, 0.44 mmol) in hexane (10 mL) was added to a suspension of Me_3SnLi (1 mmol) in hexane (20 mL) at -60°C . The mixture was allowed to warm to r.t., stirred for 3 days and filtered. The slight yellow filtrate was dried *in vacuo* to give **5o** (170 mg, 81 %) as a yellow oil, and trace amount of **5p**. $^1\text{H-NMR}$ (CDCl_3): $\delta = 0.3$ (s, 9 H, SnMe_3), 1.2 (br., 6 H, CH_3), 1.3 (br., 6 H, CH_3), 2.11 (m), 2.24 (m) (8H, CH_2). $^{11}\text{B-NMR}$ (CDCl_3): $\delta = 16.1$ (br., B_{basal}), -52.6 (s, B_{apical}). $^{13}\text{C-NMR}$ (CDCl_3): $\delta = -6.0$ (SnMe_3), 13.5, 14.1 (CH_3), 19.2, 22.2 (CH_2), boron-bound basal carbon atoms n.o., 118.6 (skeletal carbon atoms non-adjacent to the basal boron). $^{119}\text{Sn-NMR}$ (CDCl_3 , 74.5 MHz): $\delta = -97.9$. -EI-MS: m/z (%) = 463 (100) [$\text{M}^+ - \text{CH}_3$], 499 (68.5) [**5p** $^+$ - CH_3]. HR-MS (EI): $m/z = 463.0254$ [$\text{M}^+ - \text{CH}_3$]; calcd. for $^{12}\text{C}_{14}^{1}\text{H}_{26}^{11}\text{B}_2^{127}\text{I}^{120}\text{Sn}$ 463.0288 ($\Delta m = -3.4$ mmu). $m/z = 501.0996$ [**5p** $^+$ - CH_3]; calcd. for $^{12}\text{C}_{17}^{1}\text{H}_{35}^{11}\text{B}_2^{120}\text{Sn}_2$ 501.0968 ($\Delta m = 2.8$ mmu).

25.) 1-Trimethylsilylalkynyl-6-phenylalkynyl-2,3,4,5-tetraethyl-2,3,4,5-tetracarba-*nido*-

hexa-borane(6) (5q)

A portion of lithium trimethylsilylacetylide (138 mg, 1.33 mmol) was dissolved in THF (15 mL) at r.t., and ZnCl₂ (180 mg, 1.33 mmol) was added and stirred for 3 h, the solution was then added into a mixture of **5d** (146 mg, 0.35 mmol) and Pd(PPh₃)₄ (20 mg, 0.017 mmol). The resulting yellow mixture was stirred for 3 days and heated at reflux for 10 days. The solvent was removed, the black residue was extracted with hexane (2 x 20 mL) and filtered. The yellow filtrate was dried *in vacuo* to give a yellow viscous oil. A minimum amount of hexane was added and on cooling to -28 °C yellow crystals of **5q** (115 mg, 85 %) were grown, m.p. 72 °C. ¹H-NMR (CDCl₃): δ = 0.08 (SiMe₃), 1.22 (t, 6 H, ³J_{H,H} = 7.6 Hz, CH₃), 1.30 (t, 6 H, ³J_{H,H} = 7.6 Hz, CH₃), 2.22 (m), 2.35(m) (8H, CH₂), 7.27-7.50 (m, 5 H, Ph). ¹¹B-NMR (CDCl₃): δ = 9.8 (s, B_{basal}), -50.7 (s, B_{apical}). ¹³C-NMR (CDCl₃): δ = 0.01 (SiMe₃), 13.6, 14.7 (CH₃), 17.4, 19.1 (CH₂), 104.4 (boron-bound basal carbon atoms), 112.4 (skeletal carbon atoms non-adjacent to the basal boron), 125.0, 127.4, 128.0, 131.7 (Ph), alkynyl carbon atoms n.o.. ²⁹Si-NMR (CDCl₃): δ = -19.4. -EI-MS: *m/z* (%) = 384 (100) [M⁺]. HR-MS (EI): *m/z* = 384.2621 [M⁺]; calcd. for ¹²C₂₅¹H₃₄¹¹B₂²⁸Si 384.2616 (Δ*m* = 0.5 mmu).

26.) 1,6-Bis(phenylethynyl)-2,3,4,5-tetraethyl-2,3,4,5-tetracarba-*nido*-hexa-borane(6) (5r)

To a solution of phenylacetylene (146 mg, 1.43 mmol) in THF (10 mL) was added *n*BuLi (2.5 M in hexanes, 0.6 ml, 1.6 mmol) at -40 °C, the mixture was stirred at that temperature for 30 min., ZnCl₂ (218 mg, 1.6 mmol) in a solution of THF (5 ml) was then added and the resulting yellow solution was warmed up and stirred for 2 h. The solution was transferred to a mixture of **5d** (436 mg, 1.1 mmol) and Pd(PPh₃)₄ (61 mg, 0.05 mmol). The resulting yellow mixture was heated at reflux for 7 days. The solvent was removed, the yellow brown oily residue was extracted with hexane (2 x 20 mL) and filtered. The yellow filtrate was dried *in vacuo* to give **5r** (350 mg, 86 %) as a yellow oil. ¹H-NMR (CDCl₃): δ = 1.28 (t, 6 H, ³J_{H,H} = 7.5 Hz, CH₃), 1.38 (t, 6 H, ³J_{H,H} = 7.5 Hz, CH₃), 2.31 (m), 2.48 (m) (8H, CH₂), 7.24-7.58 (m, 5 H, Ph). ¹¹B-NMR (CDCl₃): δ = 9.9 (s, B_{basal}), -49.8 (s, B_{apical}). ¹³C-NMR (CDCl₃): δ = 13.8, 14.9 (CH₃), 17.5, 19.3 (CH₂), 104.4 (boron-bound basal carbon atoms), 112.7 (skeletal carbon atoms non-adjacent to the basal boron), 127.5, 128.0, 131.8, 132.1 (Ph), alkynyl carbon atoms

n.o.. -EI-MS: m/z (%) = 388 (100) [M^+]. HR-MS (EI): m/z = 388.2519 [M^+]; calcd. for $^{12}C_{28}^{1}H_{30}^{11}B_2$ 388.2534 ($\Delta m = -1.5$ mmu).

**27.) 1-Bromo-6-phenylethynyl-2,3,4,5-tetraethyl-2,3,4,5-tetracarba-*nido*-hexa- borane(6)
(5s)**

A portion of *n*BuLi (2.5 M in hexanes, 1.2 ml, 3 mmol) was added into a solution of 1,3,5-tribromobenzene (254 mg, 0.8 mmol) in THF (15 mL) at -60 °C, and slowly warmed up. To this solution was added ZnCl₂ (340 mg, 2.5 mmol) at r.t. and stirred for 3 h, the resulting light yellow solution was then added to a mixture of **5d** (240 mg, 0.56 mmol) and Pd(PPh₃)₄ (80 mg, 0.07 mmol). The mixture was heated at reflux for 7 days. All volatiles were removed, the black oily residue was extracted with hexane (30 mL) and filtered. The light yellow filtrate was dried *in vacuo* to give **5s** (201 mg, ca. 94 %) as a slight yellow oil. A tiny amount of **5r** was identified by MS to be byproduct. Suitable crystals for X-ray analysis was obtained by cooling a pure sample at 4 °C. ¹H-NMR (C₆D₆): 0.92 (t, 6 H, ³J_{H,H} = 7.6 Hz, CH₃), 1.37 (t, 6 H, ³J_{H,H} = 7.6 Hz, CH₃), 2.15 (m), 2.50(m) (8H, CH₂), 7.50 (m, 5 H, Ph). ¹¹B-NMR(C₆D₆): δ = 10.8 (s, B_{basal}), -39.9 (s, B_{apical}). ¹³C-NMR(C₆D₆): δ = 13.8, 14.2 (CH₃), 17.6, 19.4 (CH₂), 104.9 (br., boron-bound basal carbon atoms), 112.8 (skeletal carbon atoms non-adjacent to the basal boron), 124.9, 125.7, 131.7 (Ph), alkynyl carbon atoms n.o.. -EI-MS: m/z (%) = 366 (100) [M^+], 388 (3) [**5r**⁺]. HR-MS (EI): m/z = 366.1330 [M^+]; calcd. for $^{12}C_{20}^{1}H_{25}^{11}B_2^{79}Br$ 366.1326 ($\Delta m = 0.4$ mmu); m/z = 388.2556 [**5r**⁺]; calcd. for $^{12}C_{28}^{1}H_{30}^{11}B_2$ 388.2533 ($\Delta m = 2.3$ mmu).

**28.) 1-Bromo-6-*tert*-butylethynyl-2,3,4,5-tetraethyl-2,3,4,5-tetracarba-*nido*-hexaborane(6)
(5t)**

A portion of *n*BuBr (130 mg, 0.95 mmol) was added to a mixture of **5e** (180 mg, 0.46 mmol) and Pd(PPh₃)₄ (30 mg, 0.026 mmol) in THF (15 mL) at r.t.. The yellow mixture was stirred overnight and then heated at reflux for 5 days. The solvent was removed, the yellow brown residue was extracted with hexane (2 x 20 mL) and filtered. The filtrate was dried *in vacuo* to give **5t** (136 mg, 85 %) as a red orange oil. ¹H-NMR (C₆D₆): δ = 1.01 (br., 6 H, CH₃), 1.27 (s, 9 H, *t*Bu-H), 1.33 (br., 6 H, CH₃), 1.97 (m), 2.33(m) (8H, CH₂). ¹¹B-NMR((C₆D₆)): δ = 11.1 (s, B_{basal}), -40.0 (s, B_{apical}). ¹³C-NMR(C₆D₆): δ = 13.0, 14.0 (CH₃), 17.6, 19.3 (CH₂), 29.8

(C(CH₃)₃), 31.1 (C(CH₃)₃), 102.8 (br., boron-bound basal carbon atoms), 112.7 (skeletal carbon atoms non-adjacent to the basal boron), alkynyl carbon atoms n.o.. -EI-MS: m/z (%) = 348 (100) [M⁺]. HR-MS (EI): m/z = 346.1644 [M⁺]; calcd. for ¹²C₁₈¹H₂₉¹¹B₂⁷⁹Br 348.1638 (Δm = 0.6 mmu).

29.) 1,6-Bis(*tert*-butylethynyl)-2,3,4,5-tetraethyl-2,3,4,5-tetracarba-*nido*-hexaborane(6) (5u)

ZnCl₂ (235 mg, 1.72 mmol) was added to a solution of PhLi (1.8 M in cyclohexane/ether, v/v = 70/30, 1.62 mmol, predried) in THF (10 mL) at 0 °C, and stirred for 3 h. To the light yellow solution was added **5e** (180 mg, 0.46 mmol) and Pd(PPh₃)₄ (28 mg, 0.024 mmol). The resulting yellow mixture was heated at reflux for 7 days. The solvent was removed, the dark brown residue was extracted with hexane (2 x 20 mL) and filtered. The filtrate was dried *in vacuo* to give **5u** (60 mg, 37.5 % based on **5e** used) as a slight yellow oil. ¹H-NMR (CD₂Cl₂): 1.25 (br., 6 H, CH₃), 1.28 (br., 6 H, CH₃), 1.36 (s, 9 H, *t*Bu-H), 1.37 (s, 9 H, *t*Bu-H), 2.22 (m), 2.37(m) (8H, CH₂). ¹¹B-NMR(CD₂Cl₂): δ = 8.9 (s, B_{basal}), - 52.7 (s, B_{apical}). ¹³C-NMR: δ = 13.9, 14.4 (CH₃), 17.3, 19.0 (CH₂), 29.8 (C(CH₃)₃), 30.8, 31.1 (C(CH₃)₃), 103.1 (boron-bound basal carbon atoms), 111.9 (skeletal carbon atoms non-adjacent to the basal boron). -EI-MS: m/z (%) = 348 (100) [M⁺]. HR-MS (EI): m/z = 348.3153 [M⁺]; calcd. for ¹²C₂₄¹H₃₈¹¹B₂ 348.3160 (Δm = - 0.7 mmu).

30.) CpCo[bis(carboranyl)cyclobutadiene] 12q

To a solution of **5q** (53 mg, 0.14 mmol) in toluene (8 ml) was added a portion of CpCo(CO)₂ (40 mg, 0.22 mmol) at r.t.. The deep red reaction mixture was then heated at reflux for 9 days. The brown reaction mixture was cooled and filtered through a pad of seasand, the yellow brown filtrate was dried *in vacuo* to give a brown oil (56 mg). ¹¹B-NMR (CDCl₃): δ = 15, (br., B_{basal}), - 50.4 (s, B_{apical}). -EI-MS: m/z (%) = 892 (100) [M⁺], HR-MS (EI): m/z = 892.4999 [M⁺]; calcd. for ¹²C₅₅¹H₇₃¹¹B₄Co²⁸Si₂ 892.4955 (Δm = 4.4 mmu).

31.) 3-Carboranyl-4-phenyl-1,2-bis(tricarbonylcobalta)tetrahedrane (13)

A solution of **5d** (193 mg, 0.47 mmol) in hexane (15 mL) was added to a solution of Co₂(CO)₈

(178 mg, 0.52 mmol) in hexane (15 mL) at $-40\text{ }^{\circ}\text{C}$. The mixture was allowed to warm to r.t. and stirred for 4 days until the reaction was complete. The solvent was removed *in vacuo* and the black residue was extracted with dichloromethane (2 mL) and separated by column chromatography ([®]Florisil) with hexane. After small amount of unreacted $\text{Co}_2(\text{CO})_8$, a deep brown band was eluted. The solution was concentrated and cooled to $-28\text{ }^{\circ}\text{C}$, black crystals of **13** (170 mg, 52 %) were formed, m.p. $140\text{-}141\text{ }^{\circ}\text{C}$ (decomp.). ¹H-NMR (CDCl_3): $\delta = 1.09$ (br., 6 H, CH_3), 1.35 (br., 6 H, CH_3), 1.84 (br.), 2.28 (br.) (8H, CH_2), $7.26\text{-}7.51$ (m, 5H, Ph). ¹¹B-NMR (CDCl_3): $\delta = 16.3$ (br., B_{basal}), -51.1 (s, B_{apical}). ¹³C-NMR (CDCl_3): $\delta = 13.6$, 14.1 (CH_3), 18.6 , 19.0 (CH_2), 102.6 (boron-bound basal carbon atoms), 114.0 (skeletal carbon atoms non-adjacent to the basal boron), 127.2 , 128.4 , 129.7 (Ph), 200.4 (CO). -EI-MS: m/z (%) = 672 (13.0) [$\text{M}^+ - \text{CO}$], 644 (12.1) [$\text{M}^+ - 2\text{CO}$], 616 (19.0) [$\text{M}^+ - 3\text{CO}$], 588 (28.2) [$\text{M}^+ - 4\text{CO}$], 560 (11.7) [$\text{M}^+ - 5\text{CO}$], 532 (100) [$\text{M}^+ - 6\text{CO}$], 473 (20.6) [$\text{M}^+ - 6\text{CO} - 2\text{Et}$]. HR-MS (EI): $m/z = 671.9595$ [$\text{M}^+ - \text{CO}$]; calcd. for $^{12}\text{C}_{25}^{1}\text{H}_{25}\text{O}_5^{11}\text{B}_2\text{Co}_2^{127}\text{I}$ 671.9596 ($\Delta m = -0.1$ mmu). $\text{C}_{26}\text{H}_{25}\text{B}_2\text{IO}_6\text{Co}_2$ (699.9): calcd. C 44.62, H 3.60; found C 44.08, H 3.98.

32.) 1-Iodo-6-*o*-carboranyl-2,3,4,5-tetraethyl-2,3,4,5-tetracarba-*nido*-hexaborane(6) (**14**)

To a solution of *o*-carborane (126 mg, 0.875 mmol) in toluene (15 mL) was added *n*BuLi (2.5 M in hexanes, 0.4 mL, 1 mmol) at $-65\text{ }^{\circ}\text{C}$. The colorless mixture was allowed to warm to r.t. and stirred overnight. The resulting white suspension was cooled to $-65\text{ }^{\circ}\text{C}$ and a solution of **5d** (264 mg, 0.58 mmol) in hexane (7 mL) was added. The mixture was warmed to r.t. and heated at reflux overnight, and filtered. The colorless filtrate was dried *in vacuo* to give a solid. A minimum amount of CDCl_3 was added and on cooling to $-28\text{ }^{\circ}\text{C}$ colorless crystals of **14** (200 mg, 76 %) were obtained, m.p. $108\text{ }^{\circ}\text{C}$. ¹H-NMR (CDCl_3): $\delta = 1.20$ (t, 6 H, $^3J_{\text{H,H}} = 7.6$ Hz, CH_3), 1.28 (t, 6 H, $^3J_{\text{H,H}} = 7.6$ Hz, CH_3), 1.93 (m), 2.25 (m) (8H, CH_2), $3.3\text{-}3.8$ (m, *o*-carborane). ¹¹B{¹H}-NMR (CDCl_3): $\delta = 13.9$ (s, B_{basal}), -2.4 (2B), -9.2 (2B), -13.6 (4B), -14.8 (2B), -53.4 (s, B_{apical}). ¹³C-NMR: $\delta = 13.6$, 14.7 (CH_3), 17.4 , 19.1 (CH_2), 59.6 (C_{cage}), 102.3 (br., boron-bound basal carbon atoms), 114.5 (skeletal carbon atoms non-adjacent to the basal boron). -EI-MS: m/z (%) = 456 (100) [M^+]. HR-MS (EI): $m/z = 458.2604$ [M^+]; calcd. for $^{12}\text{C}_{14}^1\text{H}_{31}^{11}\text{B}_{12}^{127}\text{I}$ 458.2587 ($\Delta m = 1.7$ mmu).

33.) C₆H₄C₆H₄-linked C₄B₂-carboranes 15

*n*BuLi (2.5 M in hexanes, 0.6 mL, 1.5 mmol) was added to a solution of 4,4'-dibromobiphenyl (164 mg, 0.53 mmol) in THF (15 mL) at – 65 °C, and stirred at that temp. for 2h. To the resulting white suspension ZnCl₂ (150 mg, 1.1 mmol) was added in one portion. The mixture was allowed to warm to r.t. to form a cloudy mixture, which was dried and to the resulting solid, dry toluene (25 mL), **5a** (200 mg, 0.45 mmol, in 5 mL of hexane) and Pd(PPh₃)₄ (60 mg, 0.052 mmol) were added. The resulting yellow mixture was stirred at RT for 3 days and filtered. The slight yellow filtrate was dried *in vacuo*, the residue was extracted with hexane (2 x 20 mL) and filtered. The colorless filtrate was dried *in vacuo* to give **15** as an oil (90 mg, 50 %). ¹H-NMR (CDCl₃): δ = 1.2 (br., 6 H, CH₃), 1.3 (br., 6 H, CH₃), 2.10 (m), 2.32(m) (8H, CH₂), 7.41 (d, J = 8 Hz, 4 H), 7.48 (d, J = 8 Hz, 4 H, C₆H₄C₆H₄). ¹¹B-NMR (CDCl₃): δ = 22.0 (br., 2B, B_{basal}), – 52.4 (s, 2B, B_{apical}). ¹³C-NMR (CDCl₃): δ = 13.4, 14.3 (CH₃), 18.4, 19.8 (CH₂), 104.4 (boron-bound basal carbon atoms), 113.0 (skeletal carbon atoms non-adjacent to the basal boron), 124.6, 127.6, 128.1, 131.7 (C₆H₄C₆H₄). – FAB-MS: *m/z* (%) = 778 (100) [M⁺]. HR-MS (FAB): *m/z* = 778.2294 [M⁺]; calcd. for ¹²C₃₆¹H₄₈¹¹B₄¹²⁷I₂ 778.2217 (Δ*m* = 7.7 mmu).

34.) Apically C₂(CH₂)₄C₂-linked dicluster 16

*n*BuLi (2.5 M in hexanes, 0.65 mL, 1.62 mmol) was added to a solution of 1,7-octadiyne (86 mg, 0.81 mmol) in THF (15 mL) at – 60 °C, and stirred at that temp. for 2h. To the resulting white suspension ZnCl₂ (220 mg, 1.62 mmol) was added in one portion. The mixture was stirred for additional 2 h and half of the white suspension added to a mixture of **5g** (231 mg, 0.54 mmol) and Pd(PPh₃)₄ (30 mg, 0.026 mmol) in 10 mL of THF. The resulting mixture was heated at reflux for 7 days. The solvent was removed, the dark brown residue was extracted with hexane (2 x 25 mL) and filtered. The slight yellow filtrate was dried *in vacuo* to give **16** (95 mg, ca. 67 %) as a yellow oil. On standing at r.t., a few colorless crystals were observed and found by an X-ray structure analysis to be ZnI₂(OPPh₃)₂. ¹H-NMR (C₆D₆): δ = 1.00 (br., 12 H, CH₃), 1.25 (br., 12 H, cage-CH₂), 1.44 (br., 4 H, CH₂CH₂), 2.03 (br., 4 H, ≡CCH₂), 2.23 (m), 2.53(m) (16 H, CH₂). ¹¹B-NMR (C₆D₆): δ = 10.4 (s, 2 B, B_{basal}), – 50.0 (s, 2 B, B_{apical}).

^{13}C -NMR (C_6D_6): $\delta = 13.6, 14.0$ (CH_3), $17.4, 19.5$ (cage- CH_2), 20.9 ($\equiv\text{C}\underline{\text{C}}\text{H}_2$), 27.3 (CH_2CH_2), 104.9 (boron-bound basal carbon atoms), 111.9 (skeletal carbon atoms non-adjacent to the basal boron), alkynyl carbon atoms n.o.. -EI-MS: m/z (%) = 706 (46) [M^+]. HR-MS (EI): $m/z = 706.5247$ [M^+]; calcd. for $^{12}\text{C}_{50}^1\text{H}_{62}^{11}\text{B}_4$ 706.5224 ($\Delta m = 2.3$ mmu).

35.) Oxygen-bridged carborane 17

Wet Et_3N (92 mg, 0.91 mmol) was added to a solution of **5a** (198 mg, 0.45 mmol) in hexane (5 mL) at -60 °C. The mixture was allowed to warm to r.t. and stirred overnight, after filtration the colorless filtrate and the white precipitate were separated. The filtrate was dried *in vacuo* to give **17** as an oil (100 mg, 69 %). ^{11}B -NMR (CDCl_3): $\delta = 22.1$ (br., B_{basal} , 2 B), -51.9 (s, B_{apical} , 2 B). -EI-MS: m/z (%) = 642 (100) [M^+], 613 (61.2) [$\text{M}^+ - \text{Et}$], 515 (48.6) [$\text{M}^+ - \text{I}$]. HR-MS (EI): $m/z = 642.1533$ (100) [M^+]; Calcd. for $^{12}\text{C}_{24}^1\text{H}_{40}^{11}\text{B}_4^{127}\text{I}_2^{16}\text{O}$ 642.1541 ($\Delta m = -0.8$ mmu). Negative FAB-MS of the white precipitate exhibited peaks at $m/z = 356$ [$\text{Et}_3\text{NH}]\text{I}_2^-$, 483 [$\text{Et}_3\text{NH}]\text{I}_3^-$, 584.9 [$\text{Et}_3\text{NH}]\text{I}_2^-$, indicating its identity is [$\text{Et}_3\text{NH}]\text{I}$.

36.) Reaction of 5a with MeSSMe

A portion of MeSSMe (100 mg, 1.1 mmol) was added to a solution of **5a** (425 mg, 0.97 mmol) in hexane (10 mL) at -50 °C. The mixture was warmed to r.t. and stirred for additional two days. No redox reaction was observed (checked by ^{11}B -NMR) and the starting **5a** was recovered in 85 % yield.

37.) 1-Bromo-2,3-diethyl-2,3-dicarbaheptaborane(7) (19a)

2,3- $\text{Et}_2\text{C}_2\text{B}_4\text{H}_6$ (250 mg, 1.91 mmol) in diethyl ether (30 ml) was treated with *n*BuLi (2.5 M in hexane, 1.55 ml, 3.8 mmol) at -65 °C. The solution was stirred for 4h at room temperature, then the solvent removed *in vacuo*, and the residue dissolved with toluene (15 ml) and cooled to -20 °C, to which a solution of BBr_3 (550 mg, 2.2 mmol) in toluene (15 ml) was added dropwise. The reaction mixture was warmed up to r.t. and stirred overnight. All volatiles were removed, the white residue was extracted with hexane (30 mL) and filtered to give a slight yellow filtrate, which was dried *in vacuo* to leave **19a** as a yellow oil (298 mg, 71 %). $^1\text{H}\{^{11}\text{B}\}$ -NMR (CDCl_3): $\delta = 1.36$ (t, 6 H, $^3J_{\text{H,H}} = 7.6$ Hz, CH_3), 2.64 (q, 4 H, $^3J_{\text{H,H}} = 7.6$ Hz,

CH₂), 3.4 (br., 1 H, B5-H), 4.2 (br., 2 H, B4,6-H), the signal for B7-H n.o.. ¹¹B-NMR (CDCl₃): δ = 6.3 (d, *J*_{B,H} = 170 Hz, B4,6), 1.2 (d, *J*_{B,H} = 170 Hz, B5), – 17.4 (s, B1), – 23.6 (d, *J*_{B,H} = 180 Hz, B7). ¹³C-NMR: δ = 13.2 (CH₃), 22.1 (CH₂), 113.5 (br., C_{cage}), the signals for C≡C moiety n.o.. -EI-MS: *m/z* (%) = 220 (100) [M⁺], 205 (36) [M⁺ – Me]. HR-MS (EI): *m/z* = 220.0751 [M⁺]; calcd. for ¹²C₆¹H₁₄¹¹B₅⁷⁹Br 200.0744 (Δ*m* = 0.7 mmu).

38.) 1-Iodo-2,3-diethyl-2,3-dicarbaheptaborane(7) (19b)

Similar procedures as described for **19a**. 2,3-Et₂C₂B₄H₆ (165 mg, 1.26 mmol), *n*-BuLi (2.5 M in hexane, 1 ml, 2.5 mmol), BI₃ (498 mg, 1.27 mmol). **19b** was obtained as a yellow oil (320 mg, 95 %). ¹H-NMR (CDCl₃): δ = 1.38 (t, 6 H, ³*J*_{H,H} = 7.8 Hz, CH₃), 2.61 (q, 4 H, ³*J*_{H,H} = 7.8 Hz, CH₂). ¹¹B-NMR (CDCl₃): δ = 6.7 (d, *J*_{B,H} = 173 Hz, B4,6), 1.9 (d, *J*_{B,H} = 173 Hz, B5), – 18.3 (d, *J*_{B,H} = 180 Hz, B7), – 31.9 (s, B1). ¹³C-NMR: δ = 13.3 (CH₃), 22.4 (CH₂), 113.9 (br., C_{cage}), the signals for the other carbon atoms n.o.. -EI-MS: *m/z* (%) = 267 (100) [M⁺], 112 (28) [M⁺ – I – C₂H₄].

39.) 1-Phenylethynyl-2,3-diethyl-2,3-dicarbaheptaborane(7) (19c)

Similar procedures as described for **19a**. 2,3-Et₂C₂B₄H₆ (340 mg, 2.6 mmol), *n*-BuLi (2.5 M in hexane, 2.1 ml, 5.25 mmol), PhC≡CBCat (570 mg, 2.6 mmol). **19c** was obtained as an orange red oil (393 mg, 63 %). ¹H-NMR (CDCl₃): δ = 1.48 (t, 6 H, ³*J*_{H,H} = 7.6 Hz, CH₃), 2.82 (q, 2 H, ³*J*_{H,H} = 7.6 Hz, CH₂), 2.82 (q, 2 H, ³*J*_{H,H} = 7.4 Hz, CH₂), 7.37 (m, 5 H, Ph). ¹¹B-NMR (CDCl₃): δ = 6.4 (br., B4,6), 1.8 (br., B5), – 16.1 (s, B1), – 18.7 (br., B7). ¹³C-NMR: δ = 13.6 (CH₃), 22.5 (CH₂), 94.1 (PhC≡), 115.1 (br., C_{cage}), 122.5, 128.2, 128.7, 132.0 (Ph), the signals for C_{sp} carbon of C≡C moiety n.o.. -EI-MS: *m/z* (%) = 241 (100) [M⁺], 226 (34) [M⁺ – Me]. HR-MS (EI): *m/z* = 242.1986 [M⁺]; calcd. for ¹²C₁₄¹H₁₉¹¹B₅ 242.1952 (Δ*m* = 3.4 mmu).

40.) 1-Trimethylsilylethynyl-2,3-diethyl-2,3-dicarbaheptaborane(7) (19d)

In a 50-ml flask, a solution of Me₃SiC≡CLi (preformed from Me₃SiC≡CH and *n*-BuLi, 218 mg, 2.1 mmol) in THF (1 ml) was treated with a solution of ZnCl₂ (286 mg, 2.1 mmol) in THF (6.5 ml) at – 10 °C, and stirred at room temperature for 2h. In another flask, a solution of **19b** (534 mg, 2 mmol) in THF (10 ml) was added to a solution of Pd(PPh₃)₄ (75 mg, 0.065 mmol)

in THF (10 ml), to the resulting red solution the above-mentioned zinc reagent was added at room temperature. The reaction mixture gradually became yellow in 1h. After completion all volatiles were removed *in vacuo*, the brown residue was extracted with hexane (40 mL) and filtered. The yellow filtrate was dried to give **19d** as an orange red oil (340 mg, 72 %). After NMR measurement in CDCl₃, pieces of red crystals were formed, which were identified by X-ray analysis to be *trans*-Pd(PPh₃)₂I₂. ¹H{¹¹B}-NMR (CDCl₃): δ = 0.02 (s, SiMe₃), 1.36 (t, 6 H, ³J_{H,H} = 7.6 Hz, CH₃), 2.71 (q, 4 H, ³J_{H,H} = 7.6 Hz, CH₂), 3.7 (br., 1 H, B5-H), 4.2 (br., 2 H, B4,6-H), the signal for B7-H n.o.. ¹¹B-NMR (CDCl₃): δ = 6.3 (br., B4,6), 1.5 (br., B5), - 17.4 (s, B1), - 19.1 (br., B7). ¹³C-NMR: δ = - 0.39 (SiMe₃), 13.4 (CH₃), 22.4 (CH₂), 102.4 (Me₃SiC≡), 114.8 (br., C_{cage}), the signals for alkynyl C_{sp} atom n.o.. ²⁹Si-NMR (CDCl₃): δ = - 19.4. -EI-MS: *m/z* (%) = 237 (16) [M⁺], 222 (100) [M⁺ - Me]. HR-MS (EI): *m/z* = 238.2050 [M⁺]; calcd. for ¹²C₁₁¹H₂₃¹¹B₅²⁸Si 238.2035 (Δ*m* = 1.5 mmu).

41.) 1-Methylethynyl-2,3-diethyl-2,3-dicarbaheptaborane(7) (19e)

Similar procedures as described for **19d**. MeC≡CLi (115 mg, 2.5 mmol), ZnCl₂ (240 mg, 2.5 mmol), **19b** (534 mg, 2 mmol), Pd(PPh₃)₄ (40 mg, 0.035 mmol). **19e** was obtained as a yellow oil (297 mg, 85 %). ¹H{¹¹B}-NMR (CDCl₃): δ = 1.37 (t, 6 H, ³J_{H,H} = 7.7 Hz, CH₃), 1.63 (s, Me), 2.70 (q, 2 H, ³J_{H,H} = 7.7 Hz, CH₂), 2.71 (q, 2 H, ³J_{H,H} = 7.7 Hz, CH₂), 3.7 (br., 1 H, B5-H), 4.2 (br., 2 H, B4,6-H), the signal for B7-H n.o.. ¹¹B-NMR (CDCl₃): δ = 6.3 (d, J_{B,H} = 165 Hz, B4,6), 2.2 (d, J_{B,H} = 170 Hz, B5), - 16.3 (s, B1), - 20.3 (d, J_{B,H} = 168 Hz, B7). ¹³C-NMR: δ = 4.2 (Me), 13.5 (CH₃), 22.3 (CH₂), 102.4 (MeC≡), 114.7 (br., C_{cage}), the signals for the alkynyl C_{sp} atom n.o.. -EI-MS: *m/z* (%) = 179 (100) [M⁺], 164 (82) [M⁺ - Me]. HR-MS (EI): *m/z* = 180.1801 [M⁺]; calcd. for ¹²C₉¹H₁₇¹¹B₅ 180.1796 (Δ*m* = 0.5 mmu).

42.) 1-*Tert*-butylethynyl-2,3-diethyl-2,3-dicarbaheptaborane(7) (19f)

Similar procedures as described for **19d**. *t*BuC≡CH (175 mg, 2.1 mmol), *n*BuLi (2.5 M in hexane, 0.9 ml, 22 mmol), ZnCl₂ (299 mg, 2.5 mmol), **19b** (534 mg, 2 mmol), Pd(PPh₃)₄ (75 mg, 0.065 mmol). **19f** was obtained as a yellow oil (292 mg, 66 %). ¹H{¹¹B}-NMR (CDCl₃): δ = 1.05 (s, *t*Bu), 1.36 (t, 6 H, ³J_{H,H} = 7.6 Hz, CH₃), 2.71 (q, 2 H, ³J_{H,H} = 7.6 Hz, CH₂), 3.74 (br., 1 H, B5-H), 4.22 (br., 2 H, B4,6-H), the signal for B7-H n.o.. ¹¹B-NMR (CDCl₃): δ = 6.4 (d,

$J_{B,H} = 159$ Hz, B4,6), 1.3 (d, $J_{B,H} = 199$ Hz, B5), -15.9 (s, B1), -20.2 (d, $J_{B,H} = 169$ Hz, B7). $^{13}\text{C-NMR}$: $\delta = 13.3$ (CH_3), 22.3 (CH_2), 29.7, 30.6 (*t*Bu), 104.2 (*t*Bu $\underline{\text{C}}\equiv$), 114.6 (br., C_{cage}), the signals for alkynyl C_{sp} atom n.o.. -EI-MS: m/z (%) = 221 (39) [M^+], 206 (100) [$\text{M}^+ - \text{Me}$]. HR-MS (EI): $m/z = 222.2273$ [M^+]; calcd. for $^{12}\text{C}_{12}^1\text{H}_{23}^{11}\text{B}_5$ 222.2265 ($\Delta m = 0.8$ mmu).

43.) 3,4-Bis[1'-2',3'-diethyl-2',3'-dicarbaheptaboranyl(7)]-3-hexene (20)

Similar procedures as described for **19a**. 2,3-Et₂C₂B₄H₆ (241 mg, 1.84 mmol), *n*-BuLi (2.5 M in hexane, 1.5 ml, 3.75 mmol), *cis*-3,4-bis(dichloroboryl)-3-hexene (227 mg, 0.92 mmol). **20** was obtained as a yellow oil (300 mg, 90 %). $^1\text{H-NMR}$ (CDCl_3): $\delta = 0.61$ (t, 6 H, $^3J_{H,H} = 7.5$ Hz, Et-CH₃), 1.23 (t, 6 H, $^3J_{H,H} = 7.5$ Hz, Cage-CH₃), 1.47 (q, 4 H, $^3J_{H,H} = 7.5$ Hz, Et-CH₂), 2.63 (q, 2 H, $^3J_{H,H} = 7.5$ Hz, Cage-CH₂), 2.67 (q, 2 H, $^3J_{H,H} = 7.6$ Hz, Cage-CH₂). $^{11}\text{B-NMR}$ (CDCl_3): $\delta = 6.2$ (br., B4,6), 2.9 (br., B5), -4.7 (s, B1), -21.5 (br., Hz, B7). $^{13}\text{C-NMR}$: $\delta = 13.9$, 14.1 (CH_3), 22.9, 26.5 (CH_2), 114.6 (br., C_{cage}), 144 (br., C=C). -EI-MS: m/z (%) = 362 (100) [M^+], 333 (680) [$\text{M}^+ - \text{Et}$]. HR-MS (EI): $m/z = 364.3893$ [M^+]; calcd. for $^{12}\text{C}_{18}^1\text{H}_{38}^{11}\text{B}_{10}$ 364.3904 ($\Delta m = -1.1$ mmu).

44.) Diclusters **21c/22c**:

A solution of **19c** (196 mg, 0.81 mmol) in hexane (15 ml) was added to a solution of $\text{Co}_2(\text{CO})_8$ (276 mg, 0.81 mmol) in hexane (15 ml) at -40 °C. The reaction mixture was warmed up to r.t. and stirred for 5 days to give a deep red solution. The transformation was complete as monitored by $^{11}\text{B-NMR}$. The solvent was removed, the dark brown residue was taken up with CH_2Cl_2 (2 mL) and chromatographed (Florisil[®], hexane). A brown fraction was obtained and dried to give a brown oil (302 mg), which was identified to be a mixture of **21c** and **22c** (ca. 4 : 1). **21c**: $^1\text{H-NMR}$ (CDCl_3): $\delta = 1.31$ (br., 6 H, CH_3), 2.75 (br., 4 H, CH_2), 7.33 (br., 5 H, Ph). $^{11}\text{B}\{^1\text{H}\}$ -NMR (hexane): $\delta = 7.2$ (B4,6), 2.9 (B5), -5.6 (B1), -20.5 (B7); $^{11}\text{B-NMR}$ (CDCl_3): $\delta = 6.7$ (br., B4,6), 2.1 (br., B5), -6.3 (B1), -21.1 (d, $J_{B,H} = 150$ Hz, B7). $^{13}\text{C-NMR}$ (CDCl_3): $\delta = 14.0$ (CH_3), 22.2 (CH_2), 115.5 (br., C_{cage}), 128.0, 128.8, 129.4, 137.7 (Ph), 199.2 (CO). -EI-MS: m/z (%) = 527 (2) [M^+], 499 (5) [$\text{M}^+ - \text{CO}$], 471 (3) [$\text{M}^+ - 2\text{CO}$], 443 (12) [$\text{M}^+ - 3\text{CO}$], 415 (42) [$\text{M}^+ - 4\text{CO}$], 387 (28) [$\text{M}^+ - 5\text{CO}$], 359 (37) [$\text{M}^+ - 6\text{CO}$], 241 (100) [$\text{M}^+ - 6\text{CO} - 2\text{Co}$]. HR-MS (EI): $m/z = 528.0262$ [M^+]; calcd. for $^{12}\text{C}_{20}^1\text{H}_{19}^{11}\text{B}_5\text{Co}_2\text{O}_6$ 528.0311 ($\Delta m = -4.9$ mmu).

mmu); **22c**: $^1\text{H-NMR}$ (CDCl_3): $\delta = -1.22$ (br., 2H, BHB), 0.88 (br., 6 H, CH_3), 2.40 (br., 4 H, CH_2), 7.42 (br., 5 H, Ph). $^{11}\text{B-NMR}$ (CDCl_3): $\delta = 6.7$ (br.), -2.8 (br.), -35.6 (apical boron). $^{13}\text{C-NMR}$ (CDCl_3): $\delta = 14.9$ (CH_3), 24.5 (CH_2), the signals for the other carbon atoms are weaker and overlapped or identical with those for **21c**. -EI-MS: m/z (%) = 517 (2) [M^+], 489 (5) [$\text{M}^+ - \text{CO}$], 461 (5) [$\text{M}^+ - 2\text{CO}$], 434 (12) [$\text{M}^+ - 3\text{CO}$], 406 (10) [$\text{M}^+ - 4\text{CO}$], 378 (15) [$\text{M}^+ - 5\text{CO}$], 350 (18) [$\text{M}^+ - 6\text{CO}$], 231 (100) [$\text{M}^+ - 6\text{CO} - 2\text{Co}$].

45.) Diclusters **21d/22d**:

Similar procedures as described for **21c/22c**. **19d** (196 mg, 0.81 mmol), $\text{Co}_2(\text{CO})_8$ (324 mg, 0.95 mmol). A mixture of **21d/22d** (ca. 7 : 1) was obtained as a brown oil (300 mg, ca. 57 %) when the reaction mixture was filtered on a pad of sand. **21d**: $^1\text{H-NMR}$ (C_6D_6): $\delta = 0.2$ (br., SiMe_3), 1.3 (br., CH_3), 2.2-2.4 (br., CH_2). $^{11}\text{B}\{^1\text{H}\}$ -NMR (hexane): $\delta = 7.2$ (B4,6), 2.5 (B5), -6.4 (B1), -20.9 (B7); $^{11}\text{B-NMR}$ (C_6D_6): $\delta = 6.8$ (br. d, $J_{\text{B,H}} = 135$ Hz, B4,6), 1.2 (br., B5), -6.9 (B1), -21.4 (br. d, $J_{\text{B,H}} = 179$ Hz, B7). $^{13}\text{C-NMR}$ (C_6D_6): $\delta = -0.30$ (SiMe_3), 13.6 (CH_3), 21.8 (CH_2), 115.5 (br., C_{cage}), 200.3 (CO). $^{29}\text{Si-NMR}$ (CDCl_3): $\delta = 38.3$. -EI-MS: m/z (%) = 523 (2) [M^+], 495 (12) [$\text{M}^+ - \text{CO}$], 467 (6) [$\text{M}^+ - 2\text{CO}$], 439 (20) [$\text{M}^+ - 3\text{CO}$], 411 (51) [$\text{M}^+ - 4\text{CO}$], 383 (41) [$\text{M}^+ - 5\text{CO}$], 355 (46) [$\text{M}^+ - 6\text{CO}$]. HR-MS (EI): $m/z = 524.0362$ [M^+]; calcd. for $^{12}\text{C}_{17}^{1}\text{H}_{23}^{11}\text{B}_5\text{Co}_2\text{O}_6^{28}\text{Si}$ 524.0393 ($\Delta m = -3.1$ mmu); **22d**: $^{11}\text{B-NMR}$ (C_6D_6): $\delta = 6.8$ (br.), -2.9 (br.), -36.5 (apical boron). $^{13}\text{C-NMR}$ (C_6D_6): $\delta = 13.9$ (CH_3), 21.9 (CH_2), other signals are overlapped or identical with those for **21d**. -EI-MS: m/z (%) = 514 (1) [M^+], 486 (15) [$\text{M}^+ - \text{CO}$], 458 (9) [$\text{M}^+ - 2\text{CO}$], 430 (16) [$\text{M}^+ - 3\text{CO}$], 402 (6) [$\text{M}^+ - 4\text{CO}$], 374 (13) [$\text{M}^+ - 5\text{CO}$], 346 (15) [$\text{M}^+ - 6\text{CO}$]. HR-MS (EI): $m/z = 514.0335$ [M^+]; calcd. for $^{12}\text{C}_{17}^{1}\text{H}_{24}^{11}\text{B}_4\text{Co}_2\text{O}_6^{28}\text{Si}$ 514.0378 ($\Delta m = -4.3$ mmu);

46.) (Cyclopentadienyl)[bisdicarbaheptaboranyl(7)cyclobutadiene]cobalt complex **23**

To a solution of **19c** (195 mg, 0.81 mmol) in toluene (20 ml) was added a portion of $\text{CpCo}(\text{CO})_2$ (81 mg, 0.45 mmol) at r.t.. The deep red mixture was heated at reflux and monitored by $^{11}\text{B-NMR}$. After one week, $\text{CpCo}(\text{C}_2\text{H}_4)_2$ (100 mg, 0.55 mmol) was added and the resulting mixture was again heated at 70 °C (oil bath) for 6 days. The brown mixture was dried to give a brown residue, which was extracted with hexane and filtered through a pad of

dry sand. The deep red filtrate was dried *in vacuo*, giving a dark brown oily residue. ^{11}B -NMR (toluene): $\delta = 6.3, 2.2, -4.0, -16.6, -19.6, -45.1$ ppm. EI-MS: m/z (%) = 606 (10) [$\mathbf{23}^+$], 597 (100) [$\mathbf{23}^+ - \text{BH} + 2$], 365 ($\mathbf{27}$) [$\mathbf{23}^+ - \mathbf{19c}$], 232 (32) [$\mathbf{18a}^+$]. HR-MS (EI): $m/z = 608.3672$ [$\mathbf{23}^+$]; calcd. for $^{12}\text{C}_{33}\text{H}_{43}^{11}\text{B}_{10}\text{Co}$ 608.3627 ($\Delta m = 4.5$ mmu); $m/z = 232.1932$ [$\mathbf{18a}^+$]; calcd. for $^{12}\text{C}_{14}\text{H}_{20}^{11}\text{B}_4$ 232.1932 ($\Delta m = -0.5$ mmu).

47.) Monoborylated *o*-carborane **25**

A portion of *t*BuLi (1.7 M in pentane, 2 ml, 3.4 mmol) was added to a suspension of *o*-carborane (243 mg, 1.69 mmol) in toluene (25 ml) at -60 °C. The mixture was warmed to r.t. and stirred for 2h. Then the resulting white suspension was cooled to -60 °C and treated with $\text{Pr}^i_2\text{NBCl}_2$ (612 mg, 3.37 mmol). It was stirred for 2 days, then heated at reflux for 2 days. After cooling it was filtered and the yellow filtrate was dried to give a colorless solid, which was identified to be a mixture of **25** and **26a** by MS. Single crystals of **25** (410 mg, ca. 84 %) suitable for an X-ray analysis were obtained by cooling a toluene solution at -28 °C. m.p. 116 °C. ^1H -NMR (CD_2Cl_2): $\delta = 1.19$ (d, $^3J_{\text{H,H}} = 7.0$ Hz, 6 H, CH_3), 1.41 (d, $^3J_{\text{H,H}} = 7.0$ Hz, 6 H, CH_3), 3.53 (m, 1 H, NCH), 4.37 (s, cage-CH), 4.67 (m, 1 H, NCH). ^{11}B -NMR (CD_2Cl_2): $\delta = 31.4$ (exopolydral boron atom), 0.5 (1B), -2.5 (1B), -7.6 (2B), -10.9 (2B), -12.9 (4B) ppm. ^{13}C -NMR (CD_2Cl_2): $\delta = 20.3, 20.7, 22.2, 22.5$ (CH_3), 48.2, 50.2 (NCHMe₂), 63.1(cage carbon). EI-MS: m/z (%) = 420 (1) [$\mathbf{18a}^+ - \text{Me}$], 289 (1) [$\text{M}^+ - 1$], 274 (100) [$\text{M}^+ - \text{CH}_4$], 258 (34) [$\text{M}^+ - 2\text{Me} - 1$]. HR-MS (EI): $m/z = 436.3479$ (3) [$\mathbf{18a}^+$]; Calcd. for $^{12}\text{C}_{14}\text{H}_{38}^{11}\text{B}_{12}^{35}\text{Cl}_2\text{N}_2$ 436.3528 ($\Delta m = -4.9$ mmu), $m/z = 291.2713$ [M^+]; Calcd. for $^{12}\text{C}_8\text{H}_{25}^{11}\text{B}_{11}^{35}\text{ClN}$ 291.2699 ($\Delta m = 1.4$ mmu).

48.) Diborylated *o*-carborane **26b**

A portion of *n*BuLi (2.5 M in pentane, 2.1 ml, 5.25 mmol) was added to a suspension of *o*-carborane (314 mg, 2.18 mmol) in toluene (25 ml) at -60 °C. The mixture was warmed to r.t. and stirred for 2h, the resulting white suspension was cooled to -60 °C and treated with Et_2NBCl_2 (670 mg, 4.36 mmol). The mixture was stirred at r.t. for 2 days and filtered. The light yellow filtrate was concentrated and cooled at -28 °C to give colorless crystals of **26b** (450 mg, 54 %). ^1H -NMR (CDCl_3): $\delta = 1.02$ (t, $^3J_{\text{H,H}} = 7.1$ Hz, 3 H, CH_3), 1.08 (t, $^3J_{\text{H,H}} = 7.1$

Hz, 3 H, CH₃), 1.12 (t, ³J_{H,H} = 7.1 Hz, 3 H, CH₃), 1.14 (t, ³J_{H,H} = 7.1 Hz, 3 H, CH₃), 2.96-3.15 (m, 4 H, CH₂), 3.27 (q, ³J_{H,H} = 7.1 Hz, 2 H, CH₂), 3.46 (q, ³J_{H,H} = 7.1 Hz, 2 H, CH₂). ¹¹B-NMR (CDCl₃): δ = 31.4 (exopolydral boron atom), - 2.1, - 7.1, - 10.9, - 12.4 ppm (skeletal boron atoms). ¹³C-NMR (CDCl₃): δ = 11.2 (CH₃), 42.2 (CH₂), the signal for the cage carbon n.o.. -EI-MS: *m/z* (%) = 379 (9) [M⁺], 363 (97) [M⁺ - CH₄], 309 (100) [M⁺ - Cl₂ + 1]. HR-MS (EI): *m/z* = 380.2942 [M⁺]; Calcd. for ¹²C₁₀¹H₃₀¹¹B₁₂³⁵Cl₂N₂ 380.2902 (Δ*m* = 4.0 mmu).

49.) Formation of the diborane(4)yl *o*-carboranes **28a** and **28b**

A portion of *n*BuLi (2.5 M in pentane, 2 ml, 5.0 mmol) was added to a suspension of *o*-carborane (359 mg, 2.5 mmol) in toluene (20 ml) at - 65 °C. The mixture was stirred at r.t. for 2h, and the resulting white suspension and treated with Cl(Me₂N)B-B(NMe₂)Cl (440 mg, 2.4 mmol) at - 65 °C. It was stirred for one day at r.t. and then filtered. The colorless filtrate was dried to give a colorless solid (559 mg), which was identified to be a mixture of **28a** and **28b** by MS. X-ray quality crystals of **28a** were obtained by cooling a CH₂Cl₂ solution at - 28 °C. ¹¹B-NMR (CDCl₃): δ = 44.9, 34.9 (exopolydral boron atoms), - 2.1, - 8.2, - 11.0, - 12.8 ppm (skeletal boron atoms). -EI-MS: *m/z* (%) = 296 (96) [**28a**⁺ - 1], 253 (100) [**28a**⁺ - NMe₂], 396 (100) [**28b**⁺], 381 (28) [**28b**⁺ - Me].

50.) *Exo*-cyclic *o*-carborane **33**

A portion of *n*BuLi (2.5 M in pentane, 1.7 ml, 4.2 mmol) was added to a suspension of *o*-carborane (249 mg, 1.73 mmol) in toluene (25 ml) at - 60 °C. The mixture was stirred overnight at r.t. and the resulting white suspension was treated with Cl(NMe₂)B-B(NMe₂)-B(NMe₂)Cl (410 mg, 1.74 mmol) at - 60 °C. The mixture was stirred for one day at r.t., then filtered. The colorless filtrate was concentrated and cooled at - 28 °C to give colorless crystals of **33** (400 mg, 75 %, based on *o*-carborane). ¹H-NMR (CD₂Cl₂): δ = 2.93 (s, 3 H, CH₃), 2.99 (s, 6 H, CH₃), 3.70 (s, 1 H, cage CH). ¹¹B-NMR (CD₂Cl₂): δ = 53.9, 44.2 (exopolydral boron atoms, - 0.1, - 2.6, - 6.3, - 10.5, - 13.5 ppm (skeletal boron atoms)]. ¹³C-NMR (CD₂Cl₂): δ = 39.5, 46.2, 46.9 (CH₃), 62.3 (Cage carbon). -EI-MS: *m/z* (%) = 307 (100) [M⁺], 292 (22) [M⁺ - CH₃]. HR-MS (EI): *m/z* = 309.3505 [M⁺]; calcd. for ¹²C₈¹H₂₈¹¹B₁₃N₃ 309.3493 (Δ*m* = 1.2 mmu).

51.) Exo-cyclic *o*-carborane 34

A portion of *t*BuLi (1.7 M in pentane, 3.2 ml, 5.4 mmol) was added to a suspension of *o*-carborane (384 mg, 2.67 mmol) in toluene (20 ml) at $-60\text{ }^{\circ}\text{C}$. The mixture was stirred for 2h at r.t., the resulting white suspension was treated with and 1,2- $\text{C}_6\text{H}_4(\text{Pr}^i\text{N}(\text{B}(\text{Cl}))_2)$ (984 mg, 2.67 mmol) at $-60\text{ }^{\circ}\text{C}$. The reaction mixture was stirred for 2 days at r.t., then heated at reflux for 1 day. After cooling and filtration, the yellow filtrate was concentrated and cooled at $-28\text{ }^{\circ}\text{C}$, then at $2\text{ }^{\circ}\text{C}$ to give colorless crystals (750 mg, 64 %, based on *o*-carborane). ^1H -NMR (CD_2Cl_2): $\delta = 1.3$ (br., 24 H, CH_3), 3.53 (s, cage-CH), 3.95 (br., 2 H, NCH), 4.67 (m, 2 H, NCH). ^{11}B -NMR (CD_2Cl_2): $\delta = 38.5$ (exopolydral boron atom, 1.3, -2.6 , -7.8 , -9.3 , -13.6 ppm (skeletal boron atoms). ^{13}C -NMR (CD_2Cl_2): $\delta = 22.5$, 24.0, 25.2, 27.2 (CH_3), 49.4, 50.2 (NCHMe_2), 125.3, 127.2, 128.2, 129.0, 131.0 (aromatic), the signal for the cage carbon n.o.. EI-MS: m/z (%) = 440 (3) [M^+], 425 (100) [$\text{M}^+ - \text{CH}_3$], 380 (15) [$\text{M}^+ - \text{CH}_3 - \text{Pr}^i$], 330 (32) [$\text{M}^+ - \text{Pr}^i$]. HR-MS (EI): $m/z = 442.4442$ [M^+]; Calcd. for $^{12}\text{C}_{20}^{1}\text{H}_{42}^{11}\text{B}_{12}\text{N}_2$ 442.4465 ($\Delta m = -2.3$ mmu).

52.) (η^5 -Pentamethylcyclopentadienyl)[η^7 -1,4-bis(trimethylsilylmethyl)-2,3,5-trimethyl-7-benzyl-4-borataborepine]ruthenium (38b)

3-Phenyl-1-propyne (82 mg, 0.7 mmol) in hexane (5 mL) was added to a violet solution of **35b** (244 mg, 0.47 mmol) in hexane (10 mL) at $-45\text{ }^{\circ}\text{C}$. After 30 min the cooling bath was removed and the reaction mixture warmed to r.t., during which the solution turned yellow. After filtration, the filtrate was dried *in vacuo*, and the resultant oily residue purified by column chromatography on silica gel. First eluted with hexane and then with hexane/ CH_2Cl_2 (4:1) gave a yellow elute, which was dried *in vacuo* resulting a yellow solid (100 mg, 34 %). Crystals suitable for X-ray analysis were grown from a CH_2Cl_2 solution at r.t.. Slow decomposition of **38b** to give **39b** was monitored in a C_6D_6 solution at r.t.. m.p. $175\text{ }^{\circ}\text{C}$; ^1H NMR (CDCl_3): $\delta = 7.39$ - 7.17 (m, 5 H; Ph), 5.41 (s, 1 H; allyl), 3.86 (d, 1 H; $^2J_{\text{H,H}} = 14.3$ Hz, CH_2Ph), 3.07 (d, 1 H; $^2J_{\text{H,H}} = 14.3$ Hz, CH_2Ph), 1.94 (s, 3 H; BCCH_3CH), 1.85 (s, 3 H; $=\text{CCH}_3$), 1.80 (s, 3 H; $=\text{CCH}_3$), 1.57 (s, 15 H; $\text{C}_3(\text{CH}_3)_5$), 0.15 (s, 18 H; SiMe_3), -0.28 (s, 2 H; BCH_2), -0.51 (s, 2 H; BCH_2) ppm; ^{11}B NMR (CDCl_3): $\delta = 34$ (br.) ppm; ^{11}B NMR (CD_2Cl_2):

$\delta = 29$ (br.) ppm; ^{13}C NMR (CDCl_3): $\delta = 143.3, 128.8, 128.0, 125.4$ (Ph), 117.4 (allyl moiety, center carbon), 86.1 ($\text{C}_5(\text{CH}_3)_5$), 47.7 (CH_2Ph), 28.7 (BCCH_3CH), 19.8, 18.3 ($\text{BC}=\text{CCH}_3$), 9.7 ($\text{C}_5(\text{CH}_3)_5$), 1.02 (SiMe_3) ppm. The signals for the boron-bound carbon atoms of the allyl moiety, for $\text{BCH}_2\text{SiMe}_3$ and for the two $=\text{CMe}$ moieties n.o.; EI-MS: m/z (%) = 630 [M^+] (57), 615 [$\text{M}^+ - \text{CH}_3$] (11), 557 [$\text{M}^+ - \text{SiMe}_3$] (32), 532 [$\text{M}^+ - \text{SiMe}_3 - \text{BCH}_2$] (66), 446 [$\text{M}^+ - 2\text{SiMe}_3 - \text{BCH}_2 - \text{CH}$] (100). HR-MS: m/z calcd for $^{12}\text{C}_{33}^{1}\text{H}_{54}^{28}\text{Si}_2^{11}\text{B}_2^{102}\text{Ru}$: 630.2993, found: 630.2996, $\Delta = 0.3$ mmu. For **39b**: ^{11}B NMR (C_6D_6): $\delta = 29$ (br.) ppm.

53.)(η^5 -Pentamethylcyclopentadienyl)(η^7 -1,2,3,4,5-pentamethyl-7-benzyl-4-borata-borepine)ruthenium (38a)

Obtained analogously to **38b**. 3-phenyl-1-propyne (58 mg, 0.5 mmol) in hexane, **35a** (140 mg, 0.38 mmol) in hexane (20 mL) gave a yellow reaction mixture. After filtration a yellow residue was obtained (40 mg), which is a mixture of **38a**, **39a** and tribenzylbenzene (detected by MS). The filtrate gave a yellow solid (150 mg), a mixture of **38a** and **39a** (detected by MS), which was recrystallized in CH_2Cl_2 at r.t. to give **38a** (81 %), m.p. 203-205 °C; ^1H NMR (CDCl_3): $\delta = 7.09$ -7.36 (m, 5 H; Ph), 5.54 (s, 1 H; allyl), 3.97 (d, 1 H; $^2J_{\text{H,H}} = 14.7$ Hz, CH_2Ph), 3.02 (d, 1 H; $^2J_{\text{H,H}} = 14.7$ Hz, CH_2Ph), 1.97 (s, 3 H; BCCH_3CH), 1.92 (s, 3 H; $=\text{CCH}_3$), 1.88 (s, 3 H; $=\text{CCH}_3$), 1.57 (s, 15 H; $\text{C}_5(\text{CH}_3)_5$), 0.68 (s, 3 H; BCH_3), 0.61 (s, 3 H; BCH_3) ppm. ^{11}B NMR (CDCl_3): $\delta = 26$ (br.) ppm. ^{13}C NMR (CDCl_3): $\delta = 142.9, 128.7, 127.9, 125.3$ (Ph), 118.5, (allyl moiety, center carbon), 86.3 ($\text{C}_5(\text{CH}_3)_5$), 46.5 (CH_2Ph), 27.9 (BCCH_3CH), 22.2, 22.1 ($\text{BC}=\text{CCH}_3$), 9.5 ($\text{C}_5(\text{CH}_3)_5$) ppm. The signals for the boron-bound carbon atoms of the allyl moiety, for BCH_3 and for the two $=\text{CMe}$ moieties n.o. observed. EI-MS: m/z (%) = 486 [M^+] (54), 444 [$\text{M}^+ - \text{BCH}_3 - \text{CH}_4$] (41), [$\text{M}^+ - \text{CH}_2\text{Ph}$] (100). HR-MS: m/z calcd. for $^{12}\text{C}_{27}^{1}\text{H}_{38}^{11}\text{B}_2^{102}\text{Ru}$: 486.2203, found: 486.2218, $\Delta = 1.5$ mmu.

54.)(η^5 -Pentamethylcyclopentadienyl)(η^7 -1,2,3,4,5-pentamethyl-7-phenyl-4-borata-borepine)ruthenium (38c)

Phenylacetylene (65 mg, 0.64 mmol) in hexane (5 mL) was added to a violet solution of **35a** (180 mg, 0.49 mmol) in hexane (10 mL) at -60 °C. Within 10 min. the reaction mixture turned to a orange red solution, the mixture was warmed to r.t., and a yellow precipitate

appeared formed which was separated by filtration. The yellow filtrate was dried *in vacuo* to yield a yellow solid, recrystallization in CH₂Cl₂ at r.t. gave yellow crystals of **38c** (164 mg, 71%). The yellow precipitate (ca. 15 mg) was identified by EI-MS to be boratabenzene complex **39c**. ¹H NMR (CDCl₃): δ = 7.19-7.42 (m, 5 H; Ph), 5.80 (s, 1 H; allyl), 2.04 (s, 3 H; 3 H; =CCH₃), 2.02 (s, 3 H; =CCH₃), 1.97 (s, 3 H; BCCH₃CH), 1.53 (s, 15 H; C₅(CH₃)₅), 0.68 (s, 3 H; BCH₃), 0.62 (s, 3 H; BCH₃) ppm. ¹¹B NMR (CDCl₃): δ = 26 (br.) ppm. ¹³C NMR (CDCl₃): δ = 130.8, 129.7, 126.9, 124.8 (Ph), 114.9, (allyl moiety, center carbon), 86.5 (C₅(CH₃)₅), 21.7 (BCCH₃CH), 9.7 (C₅(CH₃)₅) ppm. The signals for the boron-bound carbon atoms of the allyl moiety, of BCH₃ and of the two =CMe moieties were not observed. EI-MS: *m/z* (%) = 471 [M⁺] (30), 446 [M⁺ – BCH₃ + 1] (100). HR-MS: *m/z* calcd. for ¹²C₂₆¹H₃₆¹¹B¹⁰²Ru: 472.2048, found: 472.2049, Δ = 0.1 mmu.

EI-MS for **39c**: *m/z* (%) = 446 [M⁺] (100). HR-MS: *m/z* calcd for ¹²C₂₅¹H₃₃¹¹B¹⁰²Ru: 446.1719, found: 446.1739, Δ = 2.0 mmu.

55.) (η⁵-Pentamethylcyclopentadienyl)(η⁷-1,2,3,4,5-pentamethyl-7-trimethylsilyl-4-borataborepine)ruthenium (38d**)**

A solution of trimethylsilylacetylene (43 mg, 0.44 mmol) in hexane (10 mL) was added to a solution of **35a** (140 mg, 0.38 mmol) in hexane (10 mL) at – 60 °C. In ca. 1h no color change was observed, the mixture was warmed to r.t., during which time the solution turned from violet to brown and finally to yellow, and a very small amount of yellow precipitate appeared. After filtration, the yellow filtrate was dried *in vacuo* to give a yellow solid, identified to be a mixture of **38d** and **39d** (byproduct), recrystallization in CH₂Cl₂ at r.t. gave crystalline **38d** (160 mg, ca. 89.5 %). The EI-MS of yellow precipitate (ca. 10 mg) did not provide any clear information. ¹H NMR (CD₂Cl₂): δ = 5.82 (s, 1 H; allyl), 1.97 (s, 3 H; BCCH₃CH), 1.89 (s, 6 H; =CCH₃), 1.54 (s, 15 H; C₅(CH₃)₅), 0.74 (s, 3 H; BCH₃), 0.60 (s, 3 H; BCH₃), 0.11 (s, 18 H; SiMe₃) ppm; ¹¹B NMR (CD₂Cl₂): δ = 28.1 (br.) ppm; ¹³C NMR (CD₂Cl₂): δ = 115.7 (allyl moiety, center carbon), 86.5 (C₅(CH₃)₅), 27.9 (BCCH₃CH), 21.7, 21.3 (=CCH₃), 9.8 (C₅(CH₃)₅), 0.7 (SiMe₃) ppm. The signals for the boron-bound carbon atoms of the allyl moiety n.o.; ²⁹Si-NMR (CD₂Cl₂, 39.7 MHz): δ = – 21.7. EI-MS: *m/z* (%) = 467 [**38d**⁺] (42), 394 [**38d**⁺ – SiMe₃] (100), 379 [**38d**⁺ – SiMe₃-Me] (39); 442 [**39d**⁺] (100), 427 [**39d**⁺ – CH₃]

(22), 369 [**39d**⁺ – SiMe₃] (39). HR-MS: m/z calcd for ¹²C₂₃¹H₄₀²⁸Si¹¹B₂¹⁰²Ru: 468.2129, found: 468.2133, Δ = 0.4 mmu; m/z calcd. for ¹²C₂₂¹H₃₇¹¹B²⁸Si¹⁰²Ru: 442.1801, found: 442.1802, Δ = 0.1 mmu. For **39d**: **38d** in a CH₂Cl₂ solution at r.t. slowly transformed into **39d**. ¹H NMR (CD₂Cl₂): δ = 4.90 (s, 1 H; aromatic), 1.95 (s, 3 H; BCCH₃), 1.64 (s, 15 H; C₅(CH₃)₅), 1.58 (s, 6 H; BCCH₃), 0.42 (s, 3 H; BCH₃), 0.08 (s, 18 H; SiMe₃) ppm; ¹¹B NMR (CD₂Cl₂): δ = 17.5 (br.) ppm; ¹³C NMR (CD₂Cl₂): δ = 109.4, 101.5, 95.3, 87.7 (boratabenzene ring carbon atoms), 85.9 (C₅(CH₃)₅), 19.6 (BCCH₃), 16.2 (BCCCH₃), 10.1 (C₅(CH₃)₅), 0.7 (SiMe₃) ppm. The signals for the other carbon atoms n.o..

56.)(η^5 -Pentamethylcyclopentadienyl)(η^7 -1,2,3,4,5-pentamethyl-4-borataborepine) ruthenium (38e**)**

Acetylene was bubbled into a solution of **35a** (143 mg, 0.39 mmol) in hexane (10 mL) at –60°C. In a few seconds the solution turned from violet to yellow with the formation of a small amount of precipitate. It was stirred at that temperature for 15 min. and then the reaction mixture was warmed to r.t.. The yellow solution and the yellow precipitate were isolated by filtration. The solution was dried *in vacuo* to give a yellow solid, which was identified to be a mixture of **38e** and **39e** (byproduct). Recrystallization in CH₂Cl₂ at r.t. gave yellow crystals of **38e** (130 mg, 86 %). The yellow precipitate (ca. 15 mg) was dissolved in minimum CH₂Cl₂ at r.t., and some yellow crystals were grown and identified by EI-MS to be the boratabenzene complex **39e**. The cell parameter determination indicates that it is different from that of **38e**, however, the quality of the crystal was not good enough for the data collection, the. ¹H NMR (CD₂Cl₂): δ = 5.54 (d, ²J(H,H) = 10.4 Hz, 1 H; CH), 4.56 (d, ²J(H,H) = 10.6 Hz, 1 H; CH), 1.97 (s, 3 H; BCCH₃), 1.90 (s, 3 H, =CCH₃), 1.89 (s, 3 H, =CCH₃), 1.58 (s, 15 H; C₅(CH₃)₅), 0.71 (s, 3 H; BCH₃), 0.68(s, 3 H; BCH₃) ppm. ¹¹B NMR (CD₂Cl₂): δ = 26.0 (br.) ppm. ¹³C NMR (CD₂Cl₂): δ = 115.1 (CH, allyl moiety), 86.8 (C₅(CH₃)₅), 26.9 (BCCH₃CH), 22.0, 20.8 (BC=CCH₃), 9.2 (C₅(CH₃)₅) ppm. The signals for the boron-bound ring carbon atoms n.o.. EI-MS: m/z (%) = 395 [M⁺] (100), 355 [M⁺ – BCH₃ – CH₂] (74). HR-MS: m/z calcd. for ¹²C₂₀¹H₃₂¹¹B₂¹⁰²Ru: 396.1733, found: 396.1747, Δ = 1.4 mmu. HR-MS for **39e**: m/z calcd. for ¹²C₁₉¹H₂₉¹¹B¹⁰²Ru: 370.1406, found: 370.1428, Δ = 2.2 mmu.

57.) Attempts to prepare 4-borataborepines from 1,3-diborole 37c**a) From 37c and 2-butyne**

2-Butyne (54 mg, 1 mmol) was added to a solution of **37c** (134 mg, 0.83 mmol) in THF (10 mL) at $-60\text{ }^{\circ}\text{C}$, the colorless mixture was slowly warmed to r.t. and stirred for 3 days. The ^{11}B -NMR spectrum of the solution showed signals at $\delta = 69.8$ (s, **37c**), 57.3 (w), 31.8 (w) ppm. The planned product was not formed.

b) From 37c, MeLi, and 2-butyne

A solution of MeLi (1.6 M in Et_2O , 0.55 ml, 0.88 mmol) was added to a solution of **37c** (136 mg, 0.84 mmol) in THF (10 mL) at $-60\text{ }^{\circ}\text{C}$ and stirred at that temperature for 20 min., the ^{11}B -NMR spectrum of this colorless solution showed signals at $\delta = 76.4$ (w), -10.8 ppm. Then 2-butyne (60 mg, 1.1 mmol) was added to above-mentioned solution at $-60\text{ }^{\circ}\text{C}$ and the mixture was slowly warmed to r.t. and stirred for additional 2h. The ^{11}B -NMR spectrum of the solution did not exhibit any change.

c) From 37c and 3-Phenyl-1-propyne

3-Phenyl-1-propyne (100 mg, 0.86 mmol) was added to a solution of **37c** (120 mg, 0.74 mmol) in hexane (5 mL) at $-45\text{ }^{\circ}\text{C}$, the colorless mixture was slowly warmed to r.t. and stirred for 5 days. The ^{11}B -NMR spectrum of the solution showed signals at $\delta = 71.1$ (s, **37c**), 59.7 (w), 54.3 (w), 48.3 (w), 33.6 ppm. EI-MS failed to give any clear information.

58.) (η^5 -Pentamethylcyclopentadienyl)(η^6 -1,2,3,4-tetramethyl-5,6-diethylboratabenzene) ruthenium (39f**)**

A solution of 3-hexyne (75 mg, 0.91 mmol) in hexane (10 mL) was added to a solution of **35a** (179 mg, 0.49 mmol) in hexane (6 mL) at $-60\text{ }^{\circ}\text{C}$. The mixture was warmed to r.t. and stirred for additional 2 h, no clear color change was observed. The solution was cooled to $-50\text{ }^{\circ}\text{C}$ and another portion of 3-hexyne (80 mg, 0.98 mmol) was added, the reaction mixture was warmed up and stirred overnight, during which time it became a light red solution. The solution was dried *in vacuo* to give a yellow brown oily residue, recrystallization in CH_2Cl_2 at r.t. gave crystalline **39f** (180 mg, 87 %). ^1H NMR (C_6D_6): $\delta = 4.25$ (s, 1 H, aromatic), 2.25 (m, 4 H;

CH₂), 1.9 (m, 4 H; CH₂), 1.75 (s, 6 H, BCCH₃), 1.65 (s, 3 H, EtCCH₃), 1.45 (s, 15 H; C₅(CH₃)₅), 0.80 (s, 3 H; BCH₃) ppm; ¹¹B NMR (C₆D₆): δ = 16.4 (br.) ppm. ¹³C NMR (C₆D₆): δ = 86.3 (C₅(CH₃)₅), 25.0 (BCCH₃), 17.4, 16.4, 15.4, 15.0, 14.8 (Et and EtCCH₃), 9.5 (C₅(CH₃)₅) ppm. The signals for the boratabenzene ring carbon n.o.. EI-MS: *m/z* (%) = 425 [M⁺] (100), 410 [M⁺ – CH₃] (12), 395 [M⁺ – 2CH₃] (15). HR-MS: *m/z* calcd for ¹²C₂₃¹H₃₇¹¹B₂¹⁰²Ru: 426.2031, found: 426.2023, Δ = – 0.8 mmu.

59.) Reaction of **35a** with di-*p*-tolylacetylene

A solution of di-*p*-tolylacetylene (78 mg, 0.38 mmol) in THF (5 mL) was added to a solution of **35a** (140 mg, 0.38 mmol) in hexane/THF (4 + 3 mL) at – 50 °C. The mixture was warmed to r.t. and stirred overnight, no clear color change was observed (¹¹B NMR: δ = 20.9 for **35a**, 31.5 ppm). The reaction mixture was stirred for 2 days. The resulting deep red solution was dried and the dark brown oil obtained was extracted with dry toluene and filtered. The yellow solid residue (ca. 10 mg) was recrystallized from CH₂Cl₂ at r.t. to give crystalline **46**. The yellow filtrate was dried to give a yellow oil (160 mg, during this time the peak at δ¹¹B = 31.5 ppm gradually disappeared and new peaks appeared at δ = 14.6 (**39g**) and ca. – 0.1 ppm). In addition, the dimerization product (*Z,Z*)-1,2,3,4-tetratolyl-1,3-butadiene was characterized X-ray analysis after recrystallization from CH₂Cl₂ at r.t.. For **39g**: ¹¹B-NMR (δ = 14.6 ppm); EI-MS: *m/z* (%) = 549 [M⁺] (100). HR-MS: *m/z* calcd. for ¹²C₃₃¹H₄₁¹¹B¹⁰²Ru: 550.2345, found: 550.2338, Δ = – 0.7 mmu. For **46**: HR-MS (EI): *m/z* (%) = 633.1968 [M⁺] (100). calcd. for ¹²C₃₀¹H₄₇¹¹B₂¹⁰²Ru₂: 633.1952. Replacement of the two ring CH groups by either two oxygen atoms or one CH, one oxygen atom has the following formulae (calcd. formula weight): ¹²C₂₈¹H₄₅¹¹B₂¹⁶O₂¹⁰²Ru₂ (639.1693); ¹²C₂₉¹H₄₆¹¹B₂¹⁶O¹⁰²Ru₂ (636.1822). The comparison helped the X-ray crystallographic analysis to assign the two CH groups, since the alternative assignments did not find suitable HR-MS peaks within experimental error.

60.) Reactions of 1,3-diborol(yl)rhodium complexes with terminal alkynes

a) (η⁵-Pentamethyl-2,3-dihydro-1,3-diborolyl)(η⁶-tribenzylbenzene)rhodium (**49**)

3-Phenyl-1-propyne (54 mg, 0.47 mmol) in hexane (3 mL) was added to a red solution of **48** (71 mg, 0.13 mmol) in hexane (3 mL) at – 55 °C. After 30 min the cooling bath was removed

and the solution stirred for 3 h at r.t.. It turned orange red (^{11}B NMR: $\delta = 33.6$ ppm) and a black precipitate formed. After filtration, the filtrate was dried in vacuo to give a yellow oily residue (20 mg). The precipitate (25 mg) was soluble in CH_2Cl_2 (^{11}B NMR: $\delta = 32.3$ ppm). The EI-MS spectra of both species gave same information: m/z (%) = 584 [49^+] (33), 348 [tribenzylbenzene] (100). HR-MS: m/z calcd for $^{12}\text{C}_{35}\text{H}_{39}\text{B}_2\text{Rh}$: 584.2293, found: 584.2281, $\Delta = -1.2$ mmu.

b) Reaction of RuRh dimer **50** with PhC_2H

Phenylacetylene (50 mg, 0.49 mmol) was added to a solution of **50** (76 mg, 0.075 mmol) in CH_2Cl_2 (5 mL) at -50 °C. The reaction mixture was stirred at r.t. for 2 days. It turned deep brown (^{11}B NMR: $\delta = 26.6$ ppm). The solution was concentrated and chromatographed on silica gel (CH_2Cl_2), and a yellow brown eluent was obtained. The product was not identified.

61.) Dinuclear RuRh-dppe complex **51**

A portion of dppe (57 mg, 0.14 mmol) in CH_2Cl_2 (3 mL) was added to a solution of **50** (70 mg, 0.07 mmol) in CH_2Cl_2 (2 mL) at -30 °C. The mixture was warmed to r.t. and stirred for 3 days. The reaction mixture was concentrated and the resulting deep red brown solution was subjected to column chromatography (silica gel). With toluene a first light yellow band was eluted (a very small amount, not identified); this was continued with CH_2Cl_2 to give a dark brown band. The elute was concentrated and cooled at -25 °C, dark brown crystals of **51** (70 mg, 56 %) were grown. ^1H NMR (CD_2Cl_2): $\delta = 7.85\text{-}7.127$ (m, 20 H; aryl), 2.83 (m, 2 H; CH_2), 2.18 (m, 2 H; CH_2), 1.89 (s, 3 H; $=\text{CCH}_3$), 1.87 (s, 3 H; $=\text{CCH}_3$), 1.52 (s, 15 H; $\text{C}_5(\text{CH}_3)_5$), 1.56 (s, 3 H; BCCH_3), 0.87 (s, 3 H; BCH_3), 0.76 (s, 2 H; BCH_3) ppm; ^{11}B NMR (CD_2Cl_2): $\delta = 18$ (br.) ppm; ^{13}C NMR (CD_2Cl_2): $\delta = 134.8, 134.4, 134.1, 133.6, 130.1, 128.0, 127.7, 127.4$ (Ph), 77.6 ($\text{C}_5(\text{CH}_3)_5$), 29.7 (BCCH_3), 28.5 (CH_2), 16.8, 16.1 ($=\text{CCH}_3$), 10.1 ($\text{C}_5(\text{CH}_3)_5$) ppm. The signals for the boron-bound ring carbon atoms n.o.; ^{31}P -NMR (CD_2Cl_2): $\delta = 47.9, 46.5$ ppm. EI-MS: m/z (%) = 906 [M^+] (70), 891 [$\text{M}^+ - \text{CH}_3$] (20), 870 [$\text{M}^+ - \text{Cl}$] (100). HR-MS: m/z calcd for $^{12}\text{C}_{44}\text{H}_{54}\text{B}_2\text{Cl}^{31}\text{P}_2\text{Ru}^{103}\text{Rh}$: 906.1673, found: 906.1714, $\Delta = 4.1$ mmu.

62.) Reactions of 35a with allylchloride**a) Initial NMR tube reaction**

A portion of allylchloride (90 mg, 1.2 mmol) was added to a solution of **35a** (ca. 20 mg, 0.05 mmol) in hexane (0.5 mL) in an NMR tube at r.t.. The mixture turned from violet to deep red, with the formation of a small amount of precipitate. ^{11}B NMR (64 MHz): $\delta = 74.9$ (w), 71.7 (s, indicating a diborole), 59.9 (w), 54.1(w), 47.8 (w), 33.7 (s), 28.8 (w), 21.0 (w) ppm. The solution was transferred, dried and the resulting yellow solid was dissolved in minimum CH_2Cl_2 (in a flask with septum). Orange red crystals were formed by slow evaporation through the septum at r.t., which were studied (Dr. Hu, Aachen) by X-ray diffraction and identified to be **58**. After several months, the sample was found to be well soluble in CH_2Cl_2 and showed ^{11}B NMR signals at $\delta = 32.6, 28.5, 0.65$ ppm, indicating that the signal at $\delta = 71.7$ ppm no longer was present. The signal at $\delta = 32.6$ ppm may result from oxidation products.

b) Reactions of 35a with allylchloride in hexane

Allylchloride (336 mg, 4.4 mmol) was added to a solution of **35a** (140 mg, 0.38 mmol) in hexane (10 mL) at $-30\text{ }^\circ\text{C}$ without stirring. The mixture was slowly warmed to r.t., no color change was observed (^{11}B NMR: $\delta = 33.8, 20.9$). During one day at r.t., a red solution [^{11}B NMR: $\delta = 55.3$ (w), 48.3 (w), 33.7 ppm] and an orange red precipitate were formed. The precipitate was identified as $\text{Cp}^*\text{Ru}(\text{allyl})\text{dichloride}$ (**57**). The red solution was transferred, dried (all volatiles were collected, $\delta\ ^{11}\text{B} = 55.3, 48.3, 33.7$ ppm), and the resulting yellow residue (yellow solid and a little yellow oil, ca. 20 mg) was dissolved in minimum of CH_2Cl_2 (^{11}B NMR: $\delta = 27.5, 8.4$ ppm). Orange red crystals were grown out at r.t. by slow evaporation of the CH_2Cl_2 solution through the septum. The crystals were identified (Prof. Wadepohl) to be a mixture of **57** and **58**. EI-MS of **58** (single crystal): m/z (%) = 605 (15) [62^+], 590 (205) [$62^+ -15$], 398 (50) [35aMe_2], 383 (100) [35aMe]; peaks at $m/z > 800$ (intensity < 1): $m/z = 847$ [Cp^*_4Ru_3], 843 [$\text{Cp}^*_3\text{Ru}_3(\text{C}_3\text{B}_2\text{Me}_5)$] (**58**, $n = 2$), 833 [$\text{Cp}^*_4\text{Ru}_3 -14$], 828 [$\text{Cp}^*_3\text{Ru}_3(\text{C}_3\text{B}_2\text{Me}_5) -15$].

c) The reaction of **35a** and allylchloride (in a molar ratio of 1:11) under the same conditions gave **57** (ca. 80 % yield).

d) The reaction of **35a** and allylchloride (in 1:1 ratio) under the same conditions yielded (among unidentified species) **62**, which was identified by HR-MS (EI): m/z calcd. for $^{12}\text{C}_{28}^{1}\text{H}_{45}^{11}\text{B}_2^{102}\text{Ru}_2$: 607.1795, found: 607.1733, $\Delta = -6.2$ mmu.

63.) Reaction of 35a with Cp*Ru(C₃H₅)Cl₂ (57)

A solution of **35a** (32 mg, 0.09 mmol) in hexane/CH₂Cl₂ (2 ml/1 ml) was added to a flask containing **57** (22 mg, 0.06 mmol) at r.t. The mixture was allowed to stand for 4 days, and a yellow brown solution (¹¹B NMR: $\delta = 55.2, 48.6, 33.6, -0.4$ ppm) was formed, which was dried *in vacuo* to give a red brown solid and little oily product. EI-MS of both fractions exhibit $m/z = 605$ (100) [**62**⁺].

64.) Formation of [C₅Me₅BI]⁺BI₄⁻ (63⁺) from diborole 37d

Formation of **63**⁺ has been described in Chapter 3.5. ¹H NMR (CD₂Cl₂): $\delta = 2.29$ ppm (q, $J = 2.2$ Hz, CH₃). ¹¹B NMR (CD₂Cl₂): $\delta = -51.8$ (apical boron), -120 ppm (BI₄⁻ moiety). Negative ESI-MS: $m/z = 273$ (**63**⁺).

65.) 1,2-Dipyrrolidino-1,2-dibromo-diborane(4) (72b)

a) From (C₄H₈N)₄B₂ and BBr₃ (1:1)

A solution of (C₄H₈N)₄B₂ (3.2 g, 10.6 mmol) in Et₂O (20 mL) was cooled to -40 °C, and a solution of BBr₃ (2.7g, 10.7 mmol) in toluene (15 mL) was added in 20 min.. The mixture was kept at that temperature for 4 h, then warmed to r.t. and stirred overnight. After the removal of the solvents under reduced pressure, the yellow residue was distilled to give a colorless liquid [(C₄H₈N)₂BBr, 2.1g] at 70 °C/ 5×10^{-2} torr, and a colorless oil (2.0g) at 100 °C/ 6×10^{-2} torr, which was identified to be a mixture of **72b** and **72d**. ¹H-NMR (CDCl₃): $\delta = 1.6$ (br., NCH₂CH₂), 1.8 (br., NCH₂CH₂), 3.3 (br., NCH₂CH₂), 3.5 (br., NCH₂CH₂). ¹¹B-NMR (CDCl₃): $\delta = 36.2$ (br.); ¹³C-NMR (CDCl₃): $\delta = 25.6, 25.8, 26.7, 27.1$ (NCH₂CH₂), $49.5, 49.8, 50.6, 51.4$ (NCH₂). EI-MS: m/z (%) = 322 (22) [**72b**⁺], 311 (32) [**72d**⁺], 241 (53) [**72b**⁺- Br], 232 (80) [**72d**⁺- Br], 163 (32) [**72b**⁺- 2Br + 1], 151 (100) [**72d**⁺- 2Br],. HR-MS (EI): $m/z = 311.1325$ [**72d**⁺]; Calcd. For $^{12}\text{C}_{12}^{1}\text{H}_{24}^{11}\text{B}_2^{79}\text{Br}^{14}\text{N}_3$ 311.1340 ($\Delta m = -1.5$ mmu).

b) From (C₄H₈N)₄B₂ and BBr₃ (1:2)

Same procedures as described above. (C₄H₈N)₄B₂ (3.3 g, 10.9 mmol), BBr₃ (5.5g, 21.9 mmol). the colorless residue was distilled to give a colorless liquid (1.62 g) as the first fraction at 30 °C/ 2×10^{-1} torr, which was identified to be a mixture of (C₄H₈N)BBr₂ and very small amount of **74**, after a second fraction at 90 °C/ 7×10^{-2} torr (1.08 g) which contained a mixture of (C₄H₈N)BBr₂ and **72b**, gave the third fraction at 110 °C/ 7×10^{-2} torr as a colorless oil, which was identified to be **72b** (2.44 g, 69 %). ¹H-NMR (CDCl₃): 1.82 (t, ³J_{H,H} = 6.8 Hz, 2 H, NCH₂CH₂), 1.85 (t, ³J_{H,H} = 6.8 Hz, 4 H, NCH₂CH₂), 3.33 (t, ³J_{H,H} = 6.8 Hz, 4 H, NCH₂), 3.46 (t, ³J_{H,H} = 6.8 Hz, 4 H, NCH₂). ¹³C-NMR (CDCl₃): δ = 25.6, 27.1 (NCH₂CH₂), 50.6, 51.4 (NCH₂). ¹¹B-NMR (C₆D₆): δ = 35.8. EI-MS: *m/z* (%) = 322 (43) [M⁺], 241 (100) [M⁺ – Br]. HR-MS (EI): *m/z* = 319.9820 [M⁺]; Calcd. For ¹²C₈¹H₁₆¹¹B₂⁷⁹Br₂¹⁴N₂ 319.9866 (Δ*m* = – 4.7 mmu). On cooling the first fraction (ca. – 40°C) colorless crystals of **74** were formed, its structure was determined at low temperature, but attempts to measure the melting point was not successful because of the presence of (C₄H₈N)BBr₂ (a liquid) at ambient temperature. Different types of crystals of **72b** (m.p. 78-80°C) were obtained by cooling either the pure compound or a hexane/toluene (1:1, v/v) solution at – 28 °C.

66.) Pyrrolidinoborondibromide (71b)^[148]

A solution of pyrrolidine (3.11 g, 44 mmol) in toluene (100 ml) was added to a solution of BBr₃ (11.15 g, 44 mmol) in toluene (50 ml) at – 10 °C in 15 min., to the resulting crystalline suspension was added a solution of Et₃N (4.4 g, 44 mmol) in toluene (20 ml). The reaction mixture was stirred at r.t. overnight and filtered. The light yellow filtrate was evaporated at reduced pressure to remove the solvent, and distilled to give **71b** (6.47 g, 64%) at 70 °C/ 20 mbar as a colorless liquid, which on cooling solidified. The yellow brown residue (ca. 2.7 g) was dissolved in dichloromethane and colorless crystals were grown out at –20 °C, which was identified by an X-ray analysis (cell determination) to be the dimer (C₄H₈NBBR₂)₂.^[148,152] ¹H-NMR (CDCl₃): δ = 1.97 (t, ³J_{H,H} = 6.9 Hz, 4 H, NCH₂CH₂), 3.52 (t, ³J_{H,H} = 6.9 Hz, 4 H, NCH₂CH₂) ppm. ¹³C-NMR (CDCl₃): δ = 26.8 (NCH₂CH₂), 52.2 (NCH₂) ppm. ¹¹B-NMR

(CDCl₃): δ = 23.5 ppm. EI-MS: m/z (%) = 241 (M^+ , 31), 160 ($M^+ - Br - 1$, 100). HR-MS: m/z (%) = ¹²C₄¹H₈¹¹B⁷⁹Br₂ [M^+] Calcd. 238.9116; found 238.9086; Δm = - 3.0 mmu.

The NMR data for (C₄H₈NBBr₂)₂ are in agreement with the literature^[152], except for ¹¹B-NMR: (CDCl₃): δ = 4.5 ppm (s), whereas the authors reported it to be at 23.23 ppm; CI-MS (gas isobutane): m/z (%) = 401 ($M^+ - Br$, 100), 321 ($M^+ - 2Br$, 5), 240 ($M^+ - 3Br - 1$, 33), 160 ($M^+ - 4Br - 1$, 52).

67.) Dehalogenation of 71b

A solution of **71b** (1066 mg, 4.43 mmol) in 15 mL of hexane was added dropwise to a suspension of NaK_{2.8} (2 mL) in hexane (25 mL) at r.t.. The mixture was stirred for 5 days and filtered (G4 frit), and the black residue was washed with hexane (2 x 15 ml). The combined yellow filtrate was dried *in vacuo* to give a yellow oil (60 mg), which was identified to be **72c**, by ¹¹B-NMR (C₆D₆): δ = 33.1 ppm, and EI-MS: m/z = 302. The data were compared with those of the authentic sample of **72c**. The black residue was washed with toluene (30 ml) and filtered. The yellow filtrate obtained was dried to leave a yellow solid (68 mg), a mixture of **73a** and unidentified species. ¹¹B-NMR (C₆D₆): δ = 54.7 (w), 37.9, 20.5 ppm. EI-MS: m/z (%) = 486 (37) [**73a**⁺]. HR-MS (EI): m/z = 486.4521 [**73a**⁺]; Calcd. For ¹²C₂₄¹H₄₈¹¹B₆¹⁴N₆ 486.4499 (Δm = 2.2 mmu).

68.) Formation of the pyrrolidine boronium salt 75

The reaction of (C₄H₈N)₃B (21.44 g, 97 mmol) and BBr₃ (12.65g, 50 mmol) was carried out in pentane at - 40 °C, according to the literature method^[152]. The expected product (C₄H₈N)₂BBr was obtained in 60 % yield, together with an unexpected orange precipitate (5.5 g). In contact with air the precipitate became pale yellow. It was then dissolved with dichloromethane to give a red brown solution (¹¹B-NMR: δ = 23.4, 6.7, 2.2 ppm), which was filtered and the filtrate was concentrated and cooled at - 28 °C. The suitable crystals were obtained in an NMR tube. ¹H-NMR (CDCl₃): δ = 1.9 (br., 8 H, NCH₂CH₂), 3.3 (br., 8 H, NCH₂CH₂), 8.8 (br., 2 H, NH). ¹¹B-NMR (CDCl₃): δ = 3.5. ¹³C-NMR (CDCl₃): δ = 23.8 (NCH₂CH₂), 45.3 (NCH₂).

69.) Reaction of 70 with sulfur

A portion of elemental sulfur (60 mg, 1.88 mmol) was added to a solution of **70** (79 mg, 0.24 mmol) in hexane (5 ml) at r.t. and stirred for 3 days. The mixture was filtered and the light yellow filtrate dried to give a yellow solid, which was identified to be a mixture of **75** and unreacted sulfur. For **75**: $^{11}\text{B-NMR}$ (CDCl_3): $\delta = 44.7$ ppm. EI-MS: m/z (%) = 206 (M^+ , 100).

70.) Reaction of 70 with Me_3NO and I_2

A mixture of **70** (40 mg, 0.12 mmol) and Me_3NO (38 mg, 0.5 mmol) in hexane (1 ml) was stirred at r.t. for 3 days. The mixture was filtered and the filtrate was dried *in vacuo* to give **76** as a colorless solid (40 mg, 75%). $^{11}\text{B-NMR}$ (hexane): $\delta = 21.3$ ppm. EI-MS: m/z (%) = 212 (M^+ , 100).

A solution of iodine (60 mg, 0.24 mmol) in hexane (2 ml) was added to a solution of **70** (79 mg, 0.24 mmol) in hexane (4 ml) at r.t., which immediately resulted in an orange precipitate (small amount) and a colorless solution. From the solution the boroxine **76** was identified by $^{11}\text{B-NMR}$ and EI-MS. X-ray quality crystals were obtained by cooling a hexane solution at -25 °C.

71.) Rearrangement of 70 into 67a

a) A solution of **70** (79 mg, 0.24 mmol) and 3-hexyne (84 mg, 1 mmol) in hexane (5 ml) was stirred at r.t. overnight, and no reaction was observed as monitored by $^{11}\text{B-NMR}$. The mixture was then heated at reflux for 3 days. The $^{11}\text{B-NMR}$ spectrum of the resulting solution showed signals at $\delta = 63.1$ (br.), 31.8 (br.), 19.4, 9.4 (w), -1.6 (w), -16.2 (w) ppm. On cooling at -20 °C several orange red crystals were grown. The cell parameter determination indicated its identity to be **67a**.

b) Compound **70** was prepared according to Berndt's procedures^[146b] (here slightly modified). A mixture of $\text{Cl}(\text{NMe}_2)\text{B-B}(\text{NMe}_2)\text{-B}(\text{NMe}_2)\text{Cl}$ (4.53 g, 19.2 mmol) and $\text{NaK}_{2.8}$ alloy (5 ml) in hexane (90 ml) was heated at $55 \sim 60$ °C for ca. 1 day. The mixture was filtered and the brown filtrate was dried to give a yellow solid of **70** (1.93 g, ca. 60 %). $^{11}\text{B-NMR}$ (hexane): $\delta = 64.1$, 42.1, 6.9 ppm. On standing at r.t., some orange red crystals formed in the same NMR tube. The cell parameter determination indicated its identity to be **67a**.

72.) Reactions of 70 with isonitriles**a) with 2,6-Me₂PhNC**

2,6-Me₂PhNC (94 mg, 1.66 mmol) was dissolved in CDCl₃ (0.5 ml) and added to a solution of **70** (79 mg, 0.24 mmol) in 0.5 ml of CDCl₃ in an NMR tube at r.t.. The solution turned red immediately. The solution was dried to give a red orange solid. ¹H-NMR: δ = 2.38 (s, 2,6-Me₂), 2.48 (s, NMe₂), 2.57(s, NMe₂), 6.90, 7.08 (m, C₆H₃). ¹³C-NMR: δ = 134.8, 128.6, 127.7, 41.1, 39.4, 18.8. ¹¹B-NMR: δ = 36.4 (br.), 26.5 (br.). EI-MS: *m/z* (%) = 722.5 (100).

b) with *t*BuNC

t-BuNC (176 mg, 2.1 mmol) was added dropwise to a solution of **70** (79 mg, 0.24 mmol) in hexane (6 ml) at - 40 °C, immediately the mixture turned from yellow to deep red brown. The mixture was warmed to r.t. and filtered, the deep red filtrate dried to give a dark red oily residue (ca. 80 mg) of. ¹H-NMR (CDCl₃): δ = 1.22 (s, *t*Bu), 2.47 (s, NMe₂), 2.59(s, NMe₂), 2.61 (s, NMe₂). ¹¹B-NMR (CDCl₃): δ = 36.4 (br.), 27.0, 19.6 (br.), - 0.8 ppm. EI-MS failed to give definite information.

5. References

- [1] a) A. Stock, C. Massenez, *Ber.*, **1912**, *45*, 3539;
b) A. Stock, *Hydrides of Boron and Silicon*, Cornell University Press, Ithaca, New York, **1933**;
c) N. N. Greenwood, A. Earnshaw, *Chemistry of the Elements*. Pergamon Press, Oxford, **1984**, 155.
- [2] a) C. Elschenbroich, *Organometallchemie*, 4th Ed. Chapter 7, p. 84, B. G. Teubner Verlag, 2003;
b) R. N. Grimes, *Carboranes*, Academic Press, New York, **1970**;
c) E. L. Muetterties, *Boron Hydride Chemistry*, Academic Press, New York, **1975**.
- [3] a) W. N. Lipscomb, *Boron Hydrides*, Benjamin Press, New York, **1963**;
b) R. B. King, P. v. R. Schleyer, in *Molecular Clusters of the Main Group Elements*, Ed. M. Driess, H. Nöth, Wiley-VCH, **2004**.
- [4] a) J. Plesek, *Chem. Rev.*, **1992**, *92*, 269;
b) R. N. Grimes, *J. Chem. Edu.*, **2004**, *81*, 657.
- [5] H. C. Longuet-Higgins, R. P. Bell, *J. Chem. Soc.*, **1943**, 250.
- [6] a) K. Wade, *J. Chem. Soc., Chem. Commun.*, **1971**, 792; *Adv. Inorg. Chem. Radiochem.*, **1976**, *18*, 1;
b) D. M. P. Mingos, *Nat. Phys. Sci.*, **1972**, *99*, 236; *Acc. Chem. Res.*, **1984**, *17*, 311;
c) R. E. Williams, *Adv. Inorg. Chem. Radiochem.*, **1976**, *18*, 67;
d) R. W. Rudolph, *Acc. Chem. Res.*, **1976**, *9*, 446.
- [7] a) R. Köster, M. A. Grassberger, *Angew. Chem.*, **1967**, *79*, 197; *Angew. Chem. Int. Ed. Engl.*, **1967**, *6*, 218;
b) T. Onak, in *Comprehensive Organometallic Chemistry*, Vol. 1, p. 411, G. Wilkinson, F. G. A. Stone, E. W. Abel (eds), Pergamon Press, Oxford, **1982**;
c) T. Onak, in *Comprehensive Organometallic Chemistry*, Vol. 1, p. 217, E. W. Abel, F. G. A. Stone, G. Wilkinson (eds), Pergamon, Oxford, **1995**.
- [8] a) R. E. Williams, *J. Am. Chem. Soc.*, **1962**, *84*, 3837;

- b) R. E. Williams, *J. Am. Chem. Soc.*, **1963**, *85*, 3167;
c) R. E. Williams, *Adv. Organomet. Chem.*, **1994**, *36*, 1.
- [9] A. Berndt, M. Hofmann, W. Siebert, B. Wrackmeyer, in *Molecular Clusters of the Main Group Elements*, Ed. M. Driess, H. Nöth, Wiley-VCH, **2004**, p. 267.
- [10] a) P. L. Timms, *Acc. Chem. Res.*, **1973**, *6*, 118. and refs. therein;
b) G. E. Herberich, B. Hessner, *J. Organomet. Chem.*, **1978**, *161*, C36;
c) G. E. Herberich, B. Hessner, *Chem. Ber.*, **1982**, *115*, 3115.
- [11] a) T. P. Onak, G. T. F. Wong, *J. Am. Chem. Soc.*, **1970**, *92*, 5226;
b) V. R. Miller, R. N. Grimes, *Inorg. Chem.*, **1972**, *11*, 862;
c) P. Binger, *Tetrahedron Lett.*, **1966**, 2675;
d) P. Binger, *Angew. Chem.* **1968**, *80*, 288; *Angew. Chem. Int. Ed. Engl.* **1968**, *7*, 286;
e) L. Killian, B. Wrackmeyer, *J. Organomet. Chem.*, **1977**, *132*, 213;
f) H. O. Berger, H. Nöth, B. Wrackmeyer, *Chem. Ber.*, **1979**, *112*, 2884;
g) B. Wrackmeyer, G. Kehr, *J. Organomet. Chem.*, **1995**, *501*, 87;
h) B. Wrackmeyer, G. Kehr, *Polyhedron*, **1991**, *10*, 1497.
- [12] G. Herberich, H. Ohst, H. Mayer, *Angew. Chem.*, **1984**, *96*, 975; *Angew. Chem. Int. Ed. Engl.*, **1984**, *23*, 969.
- [13] a) M. Enders, H. Pritzkow, W. Siebert, *Angew. Chem.*, **1992**, *104*, 628; *Angew. Chem. Int. Ed. Engl.*, **1992**, *31*, 606;
b) J. Hauss, A. Krämer, H. Pritzkow, W. Siebert, *Z. Naturforsch.*, **1994**, *49b*, 1677.
- [14] H. Michel, D. Steiner, S. Wocadlo, J. Allwohn, N. Stamatis, W. Massa, A. Berndt, *Angew. Chem.*, **1992**, *104*, 629; *Angew. Chem. Int. Ed. Engl.*, **1992**, *31*, 607.
- [15] C. Balzereit, H.-J. Winkler, W. Massa, A. Berndt, *Angew. Chem.*, **1994**, *106*, 2394; *Angew. Chem. Int. Ed. Engl.*, **1994**, *33*, 2306.
- [16] a) T. P. Fehlner, *J. Am. Chem. Soc.*, **1977**, *99*, 8355 and **1980**, *102*, 3424;
b) M. G. L. Mirabelli, L. G. Sneddon, *Organometallics*, **1986**, *5*, 1510;
c) E. Boring, M. Sabat, M. G. Finn, R. N. Grimes, *Organometallics*, **1998**, *17*, 3865.
- [17] a) B. Wrackmeyer, H.-J. Schanz, W. Milius, *Angew. Chem.*, **1997**, *109*, 1145; *Angew. Chem. Int. Ed. Engl.*, **1997**, *36*, 1117.

- b) B. Wrackmeyer, H.-J. Schanz, M. Hofmann, P. v. R. Schleyer, R. Boese, *Eur. J. Inorg. Chem.*, **1999**, 533.
- [18] a) W. Siebert, M. E. M. El-Essawi, *Chem. Ber.*, **1979**, *112*, 1480;
b) M. Hildenbrand, *Ph. D. Thesis*, University of Heidelberg, **1986**;
c) A. Maier, *Ph. D. Thesis*, University of Heidelberg, **2002**;
d) C.-J. Maier, A. Maier, P. Greiwe, M. J. Bayer, M. Hofmann, H. Pritzkow, W. Siebert, *Pure Appl. Chem.*, **2003**, *75*, 1277.
- [19] a) P. Jutzi, A. Seufert, *Angew. Chem.*, **1977**, *89*, 339; *Angew. Chem. Int. Ed. Engl.*, **1977**, *16*, 330;
b) P. Jutzi, A. Seufert, W. Buchner, *Chem. Ber.*, **1979**, *112*, 2488;
- [20] C. Dohmeier, R. Koepe, C. Robl, H. Schnöckel, *J. Organomet. Chem.*, **1995**, *487*, 127.
- [21] a) A. H. Cowley, V. Lomeli, A. Voigt, *J. Am. Chem. Soc.*, **1998**, *120*, 6401;
b) C. L. B. MacDonald, A. H. Cowley, *J. Am. Chem. Soc.*, **1999**, *121*, 12113.
- [22] P. Greiwe, A. Bethaeuser, H. Pritzkow, T. Kuehler, P. Jutzi, W. Siebert, *Eur. J. Inorg. Chem.*, **2000**, 1927.
- [23] B. Stibr, *Chem. Rev.*, **1992**, *92*, 225.
- [24] M. L. McKee, *J. Am. Chem. Soc.*, **1988**, *110*, 5317, and references therein.
- [25] R. R. Rietz, R. Schaeffer, *J. Am. Chem. Soc.*, **1971**, *93*, 1263.
- [26] a) J. S. Beck, A. P. Kahn, L. G. Sneddon, *Organometallics*, **1986**, *5*, 2552;
b) J. S. Beck, L. G. Sneddon, *Inorg. Chem.*, **1990**, *29*, 295;
c) J. S. Beck, W. Quintana, L. G. Sneddon, *Organometallics*, **1988**, *7*, 1015;
d) K. Su, P. J. Fazen, P. J. Carrol, L. G. Sneddon, *Organometallics*, **1992**, *11*, 2715;
e) J. W. Bausch, D. J. Matoka, P. J. Carrol, L. G. Sneddon, *J. Am. Chem. Soc.*, **1996**, *118*, 11423, and references therein.
- [27] M. Bluhm, H. Pritzkow, W. Siebert, R. N. Grimes, *Angew. Chem.*, **2000**, *112*, 4736;
Angew. Chem. Int. Ed. Engl., **2000**, *39*, 4562.
- [28] a) D. Grafstein, J. Dvorak, *Inorg. Chem.*, **1963**, *2*, 1128;
b) S. Papetti, T. L. Heying, *J. Am. Chem. Soc.*, **1964**, *86*, 2295.
- [29] A. I. Shatenshtein, L. I. Zakharkin, E. S. Petrov, E. A. Yakoleva, F. S. Yakushin, Z.

- Vukmirovich, G. G. Isaeva, V. N. Kalinin, *J. Organomet. Chem.*, **1970**, *23*, 313.
- [30] V. I. Bregadze, *Chem. Rev.*, **1992**, *92*, 209.
- [31] a) A. Burke, D. Ellis, B. T. Giles, B. E. Hodson, S. A. Macgregor, G. M. Rosair, A. J. Welch, *Angew. Chem.*, **2003**, *115*, 235; *Angew. Chem. Int. Ed.*, **2003**, *42*, 225;
b) R. N. Grimes, *Angew. Chem. Int. Ed.*, **2003**, *42*, 1198, and refs. therein.
- [32] a) T. J. Kealy, P. L. Pauson, *Nature*, **1951**, *168*, 1039;
b) S. A. Miller, J. A. Tebboth, J. F. Tremaine, *J. Chem. Soc.*, **1952**, 632.
- [33] a) G. Wilkinson, M. Rosenblum, M. C. Whiting, R. B. Woodward, *J. Am. Chem. Soc.*, **1952**, *74*, 2125;
b) E. O. Fischer, W. Pfab, *Z. Naturforsch. B*, **1952**, *7*, 377.
- [34] a) J. Goubeau, R. Epple, *Ber.*, **1957**, *90*, 171;
b) R. Koester, G. Benedikt, *Angew. Chem.*, **1963**, *75*, 346;
c) R. Koester, G. Benedikt, *Angew. Chem.*, **1964**, *76*, 650.
- [35] a) M. F. Hawthorne, D. C. Young, P. A. Wegner, *J. Am. Chem. Soc.*, **1965**, *87*, 1818;
b) K. P. Callahan, M. F. Hawthorne, *Adv. Organomet. Chem.*, **1976**, *14*, 145.
- [36] a) G. E. Herberich, J. Hengesbach, U. Koeller, W. Oschmann, *Angew. Chem.*, **1977**, *89*, 43; *Angew. Chem. Int. Ed. Engl.*, **1977**, *16*, 42;
b) W. Siebert, M. Bochmann, *Angew. Chem.*, **1977**, *89*, 483; *Angew. Chem. Int. Ed. Engl.*, **1977**, *16*, 468.
c) R. N. Grimes, D. C. Beer, L. G. Sneddon, V. R. Miller, R. Weiss, *Inorg. Chem.*, **1974**, *13*, 1138.
- [37] a) For metallaboranes, J. D. Kennedy, *Prog. Inorg. Chem.*, **1984**, *32*, 519 and **1986**, *34*, 211;
b) For metallacarboranes, R. N. Grimes, *Coord. Chem. Rev.*, **2000**, *200-202*, 77
- [38] a) W. Siebert, *Adv. Organomet. Chem.*, **1980**, *18*, 301;
b) W. Siebert, *Adv. Organomet. Chem.*, **1993**, *35*, 187;
c) R. N. Grimes, *Chem. Rev.*, **1992**, *92*, 251;
d) G. E. Herberich, in *Comprehensive Organometallic Chemistry*, Vol. 1, Chapter 5, p.197, E. W. Abel, F. G. A. Stone, G. Wilkinson (eds), Pergamon, Oxford, **1995**.

- [39] a) H. Werner, A. Salzer, *Synth. React. Inorg. Met.-Org. Chem.*, **1972**, 2, 239;
b) H. Werner, *Angew. Chem.*, **1977**, 89, 1; *Angew. Chem. Int. Ed. Engl.*, **1977**, 16, 1.
- [40] D. C. Beer, V. R. Miller, L. G. Sneddon, R. N. Grimes, M. Matthew, G. J. Palenik, *J. Am. Chem. Soc.*, **1973**, 95, 3046.
- [41] J. W. Lauher, M. Elian, R. H. Summerville, R. Hoffmann, *J. Am. Chem. Soc.*, **1976**, 98, 3219.
- [42] W. Siebert, T. Renk, K. Kinberger, M. Bochmann, C. Krüger, *Angew. Chem.*, **1976**, 88, 850; *Angew. Chem. Int. Ed. Engl.*, **1976**, 15, 779;
- [43] G. E. Herberich, D. P. J. Koeffler, K. M. Peters, *Chem. Ber.*, **1991**, 124, 1947.
- [44] W. Siebert, *Angew. Chem.*, **1985**, 97, 924; *Angew. Chem. Int. Ed. Engl.*, **1985**, 24, 943.
- [45] a) T. Kuhlmann, S. Roth, J. Roziere, W. Siebert, *Angew. Chem.*, **1986**, 98, 87; *Angew. Chem. Int. Ed. Engl.*, **1986**, 25, 105;
b) T. Kuhlmann, S. Roth, J. Roziere, W. Siebert, U. Zenneck, *Synth. Met.*, **1987**, 19, 757;
c) U. Fenner, T. Kuhlmann, G. Brodt, J. Roziere, W. Siebert, *Z. Naturforsch.*, **1993**, 48b, 1512.
d) W. Siebert, *Pure Appl. Chem.*, **1988**, 60, 1345.
- [46] a) H. Wadepohl, *Ph. D. Thesis*, Universität Marburg, **1982**;
b) J. Edwin, M. C. Böhm, N. Chester, D. M. Hoffman, R. Hoffmann, H. Pritzkow, W. Siebert, K. Stumpf, H. Wadepohl, *Organometallics*, **1983**, 2, 1666;
c) W. Siebert, R. Hettrich, H. Pritzkow, *Angew. Chem.*, **1994**, 106, 215; *Angew. Chem. Int. Ed. Engl.*, **1994**, 33, 203;
d) R. Hettrich, M. Kaschke, H. Wadepohl, W. Weinmann, M. Stephan, H. Pritzkow, W. Siebert, I. Hyla-Kryspin, R. Gleiter, *Chem. Eur. J.*, **1996**, 2, 487.
- [47] a) T. Müller, M. Kaschke, M. Strauch, A. Ginsberg, H. Pritzkow, W. Siebert, *Eur. J. Inorg. Chem.*, **1999**, 1685;
b) B. Bach, Y. Nie, H. Pritzkow, W. Siebert, *J. Organomet. Chem.*, **2004**, 689, 429.
c) M. Kaschke, *Ph. D. Thesis*, Universität Heidelberg, **1995**;
d) T. Müller, *Ph. D. Thesis*, Universität Heidelberg, **1999**;
e) B. Bach, *Ph. D. Thesis*, Universität Heidelberg, **2003**.

- [48] a) A. Fessenbecker, M. D. Atwood, R. F. Bryan, R. N. Grimes, M. K. Woode, M. Stephan, U. Zenneck, W. Siebert, *Inorg. Chem.*, **1990**, *29*, 5157.
b) A. Fessenbecker, M. Stephan, R. N. Grimes, H. Pritzkow, U. Zenneck, W. Siebert, *J. Am. Chem. Soc.*, **1991**, *113*, 3061.
c) T. Müller, D. E. Kadlecek, P. J. Carroll, L. G. Sneddon, *J. Organomet. Chem.*, **2000**, *614-615*, 125, and refs. therein.
- [49] a) N. V. Sidgwick, *Trans. Faraday. Soc.*, **1923**, *19*, 469;
b) D. P. Graig, D. Doggett, *J. Chem. Soc.*, **1963**, 4189;
c) P. R. Mitchell, P. V. Parish, *J. Chem. Edu.*, **1969**, *46*, 811.
- [50] E. D. Jemmis, A. C. Reddy, *J. Am. Chem. Soc.*, **1990**, *112*, 722.
- [51] a) B. Wrackmeyer, A. Glöckle, *Z. Naturforsch.*, **1996**, *51b*, 859;
b) B. Wrackmeyer, G. Kehr, unpublished results, cited in ref. 51a;
c) B. Wrackmeyer, A. Glöckle, *Main Group Metal Chem.*, **1997**, *20*, 181;
d) B. Wrackmeyer, G. Kehr, A. Glöckle, *Phosphorus, Sulfur, and Silicon*, **1997**, *131*, 25.
e) M. Herberhold, U. Bertholdt, W. Milius, A. Glöckle, B. Wrackmeyer, *Chem. Commun.*, **1996**, 1219;
f) B. Deobald, J. Hauss, H. Pritzkow, D. Steiner, A. Berndt, W. Siebert, *J. Organomet. Chem.* **1994**, *481*, 205.
- [52] a) S. Schwiegk, *Master Degree Thesis*, University of Heidelberg, **1988**;
b) Y. Nie, S. Schwiegk, H. Pritzkow, W. Siebert, *Eur. J. Inorg. Chem.*, **2004**, 1630.
- [53] W. Siebert, M. Hildenbrand, P. Hornbach, G. Karger, H. Pritzkow, *Z. Naturforsch.*, **1989**, *44b*, 1179.
- [54] P. L. Timms, *J. Chem. Soc., Dalton Trans.*, **1972**, 830.
- [55] a) R. Full, *Ph. D. Thesis*, University of Würzburg, **1976**;
b) W. Siebert, R. Full, J. Edwin, K. Kinberger, *Chem. Ber.*, **1978**, *111*, 823;
c) K. Kinberger, *Ph. D. Thesis*, University of Würzburg, **1976**.
- [56] T. Renner, *Angew. Chem.*, **1957**, *69*, 478.
- [57] T. Onak, M. Diaz, M. Barfield, *J. Am. Chem. Soc.*, **1995**, *117*, 1403.
- [58] J. Haase, *Z. Naturforsch.*, **1973**, *28a*, 785.

- [59] J. P. Pasinski, R. A. Beaudet, *Chem. Commun.*, 1973, 928.
- [60] H.-J. Yao, C.-H. Hu, P. Paetzold, *Z. Anorg. Allg. Chem.*, 2001, 627, 2477.
- [61] W. Jiang, C. B. Knobler, C. E. Curtis, M. D. Mortimer, F. Hawthorne, *Inorg. Chem.*, **1995**, 34, 3491.
- [62] M. A. Ring, J. D. H. Donnay, W. S. Koski, *Inorg. Chem.*, **1962**, 1, 109.
- [63] Houben-Weyl, Methoden der Organischen Chemie, Band 13/3a; R. Köster (Ed.), **1982**, p. 468. Information regarding the formation of *cis*-3,4-bis(diiodoboryl)-3-hexene is not correct. The redox reaction only works when Et₂C₂ is reacted with RHC(BI₂)₂ to give the corresponding 1,3-diiodo-4,5-diethyl-2,3-dihydro-1,3-diboroles (p. 401).
- [64] G. J. Bullen, P. R. Mallinson, *J. Chem. Soc., Dalton Trans.*, **1972**, 1143.
- [65] U. Monkowius, S. Nogai, H. Schmidbaur, *J. Chem. Soc., Dalton Trans.*, **2003**, 987.
- [66] F. Joy, M. F. Lappert, B. Prokai, *J. Organomet. Chem.*, **1966**, 5, 506.
- [67] J. J. Eisch, H. P. Becker, *J. Organomet. Chem.*, **1979**, 171, 141.
- [68] a) S. M. van der Kerk, A. C. M. van Eekeren, G. J. M. van der Kerk, *J. Organomet. Chem.*, **1980**, 190, C8.
b) S. M. van der Kerk, P. H. M. Budzelaar, A. C. M. van Eekeren, G. J. M. van der Kerk, *Polyhedron*, **1984**, 3, 271.
- [69] R. Schlögl, B. Wrackmeyer, *Polyhedron*, **1985**, 4, 885.
- [70] P. H. M. Budzelaar, S. M. van der Kerk, K. Krogh-Jespersen, P. v. R. Schleyer, *J. Am. Chem. Soc.*, **1986**, 108, 3960.
- [71] a) H. C. Brown, *Hydroboration*. **1962**, Benjamin, New York.
b) M. F. Lappert, B. Prokai, *J. Organomet. Chem.*, **964**, 1, 384.
c) J. R. Blackborow, *J. Chem. Soc., Perkin Trans. 2*, **1973**, 1989.
d) J. R. Blackborow, *J. Organomet. Chem.*, **1977**, 128, 161.
- [72] B. Wrackmeyer, *Polyhedron*, **1986**, 5, 1709.
- [73] a) A. Maderna, H. Pritzkow, W. Siebert, T. Sommerfeld, L. S. Cederbaum, *Z. Naturforsch.*, **1997**, 52b, 1315.
b) M. Bayer, H. Pritzkow, W. Siebert, *Z. Naturforsch.*, **2002**, 57b, 295.
- [74] B. Wrackmeyer, R. Köster, Houben-Weyl, Methoden der Organischen Chemie, Vol.

- 13/3c, pp. 373. Thieme Verlag, Stuttgart, **1984**.
- [75] W. Siebert, U. Ender, W. Herter, *Z. Naturforsch.*, **1985**, 40b, 326.
- [76] J.-K. Uhm, H. Roemich, H. Wadepohl, W. Siebert, *Z. Naturforsch.*, **1988**, 43b, 306.
- [77] a) Y. Gu, H. Pritzkow, W. Siebert, *Eur. J. Inorg. Chem.*, **2001**, 373.
b) H. Schulz, G. Gabert, H. Pritzkow, W. Siebert, *Chem. Ber.*, **1993**, 126, 1593.
- [78] J. E. Ellis, E. A. Flom, *J. Organomet. Chem.*, **1975**, 99, 263.
- [79] a) L. I. Zakharkin, L. V. Orlova, B. V. Lokshin, L. A. Fedorov, *J. Organomet. Chem.*, **1972**, 40, 15. and refs. therein.
b) F. Sato, T. Yamamoto, J. R. Wilkinson, L. J. Todd, *J. Organomet. Chem.*, **1975**, 86, 243.
c) M. B. Fischer, D. F. Gaines, J. A. Ulman, *J. Organomet. Chem.*, **1982**, 231, 55.
- [80] a) J. F. Hartwig, S. Huber, *J. Am. Chem. Soc.*, **1993**, 115, 4908;
b) X. He, J. F. Hartwig, *Organometallics*, **1996**, 15, 400;
c) H. Brauschweig, C. Kollann, U. Englert, *Eur. J. Inorg. Chem.*, **1998**, 465;
d) H. Brauschweig, M. Colling, C. Kollann, U. Englert, *J. Chem. Soc., Dalton Trans.*, **2002**, 2289;
e) A. Cowley, V. Lomeli, A. Voigt, *J. Am. Chem. Soc.*, **1998**, 120, 6401;
f) J. Spencer, *Inorg. Chem.*, **1992**, 31, 1731.
- [81] Houben-Weyl, Methoden der Organischen Chemie, Band 13/3a; R. Köster, W. Siebert (Eds.), **1982**; and 13/3b, 1982.
- [82] a) K. Fuller, T. Onak, *J. Organomet. Chem.*, **1983**, 249, C6.
b) B. Ng, T. Onak, *J. Fluorine Chem.*, **1985**, 27, 119.
c) B. Ng, T. Onak, K. Fuller, *Inorg. Chem.*, **1985**, 24, 4371.
- [83] a) V. I. Stanko, Y. V. Gol'tyanin, *Zhu. Obsh. Khim.*, **1970**, 40, 127. (*Russ. J. Gen. Chem.*, **1970**, 40, 115.).
b) V. I. Stanko, N. G. Iroshnikova, *Zhu. Obsh. Khim.*, **1970**, 40, 311. (*Russ. J. Gen. Chem.*, **1970**, 40, 281.).
- [84] W. J. Marshall, R. J. Young, Jr., V. V. Grushin, *Organometallics*, **2001**, 20, 523.
- [85] A. D. Glöckle, *Ph. D. Thesis*, University of Bayreuth, **1998**.

- [86] C. Tamborski, F. E. Ford, E. J. Soloski, *J. Org. Chem.*, **1963**, 28, 237.
- [87] for a recent review: E.-C. Nigishi, L. Anastasia, *Chem. Rev.*, **2003**, 103, 1979.
- [88] T. Peymann, C. B. Knobler, M. F. Hawthorne, *Inorg. Chem.*, **1998**, 37, 1544.
- [89] R. G. Kultyshev, S. Liu, H. T. Leung, J. Liu, S. G. Shore, *Inorg. Chem.*, **2003**, 42, 3199.
- [90] a) K. Jonas, E. Deffense, D. Habermann, *Angew. Chem.*, **1983**, 22, 716; *Angew. Chem. Suppl.*, **1983**, 1005;
b) J. K. Cammack, S. Jalisatgi, A. J. Matzger, A. Negron, K. P. C. Vollhardt, *J. Org. Chem.*, **1996**, 61, 4798.
- [91] a) A. Goswami, C.-J. Maier, H. Pritzkow, W. Siebert, *Eur. J. Inorg. Chem.*, **2004**, 2635.
b) A. Goswami, T. Oeser, H. Pritzkow, F. Rominger, W. Siebert, *Eur. J. Inorg. Chem.*, **2004**, 4223.
c) A. Goswami, *Ph. D. Thesis*, University of Heidelberg, **2005**.
- [92] R. N. Grimes, *Pure & Appl. Chem.*, **2003**, 75, 1211.
- [93] a) P. Galow, A. Sebald, B. Wrackmeyer, *J. Organomet. Chem.*, **1983**, 259, 253.
b) Ch. Ester, A. Maderna, H. Pritzkow, W. Siebert, *Eur. J. Inorg. Chem.*, **2000**, 1177.
c) H. Yao, M. Sabat, R. N. Grimes, P. Zanello, F. Fabrizi de Biani, *Organometallics*, **2003**, 22, 2581.
- [94] M. G. Davidson, T. G. Hibbert, J. A. K. Howard, A. Mackinnon, K. Wade, *Chem. Commun.*, **1996**, 2285.
- [95] G. B. Deacon, J. H. S. Green, *Chemistry & Industry* (London, United Kingdom, **1965**, 1031.
- [96] M. F. Hawthorne, *J. Am. Chem. Soc.*, **1968**, 90, 896.
- [97] a) R. B. Maynard, L. Borodinsky, R. N. Grimes, *Inorg. Synth.*, **1983**, 22, 211.
b) N. S. Hosmane, R. N. Grimes, *Inorg. Chem.* **1979**, 18, 3294.
- [98] B. Wrackmeyer, H.-J. Schanz, W. Milius, C. McCammon, *Collect. Czech. Chem. Commun.* **1999**, 64, 977.
- [99] a) L. I. Zakharkin, L. V. Orlova, B. V. Lokshin, L. A. Fedorov, *J. Organomet. Chem.* **1972**, 40, 15.
b) T. Peymann, C. B. Knobler, M. F. Hawthorne, *Inorg. Chem.* **1998**, 37, 1544.

- c) L. Eriksson, I. P. Beletskaya, V. I. Bregadze, I. B. Sivaev, S. Sjöberg, *J. Organomet. Chem.* **2002**, 657, 267.
- d) H. Yao, M. Sabat, R. N. Grimes, P. Zanello, F. Fabrizi de Biani, *Organometallics*, **2003**, 22, 2581.
- e) R.G. Kultyshev, S. Liu, H. T. Leung, J. Liu, S. G. Shore, *Inorg. Chem.* **2003**, 42, 3199.
- f) Y. Nie, H. Pritzkow, W. Siebert, *Eur. J. Inorg. Chem.* 2004, 2425.
- g) I. P. Beletskaya, V. I. Bregadze, V. A. Ivushkin, P. V. Petrovskii, I. B. Sivaev, S. Sjöberg, G. G. Zhigareva, *J. Organomet. Chem.* **2004**, 689, 2920.
- [100] M. Kubota, S. Ohba, Y. Saito, *Acta Crystallogr. Section C*, **1991**, 47, 1727.
- [101] J. L. Boone, R. J. Brotherton, L. L. Peterson, *Inorg. Chem.* **1965**, 4, 910.
- [102] a) B. M. Mikhailov, E. A. Shagova, T. V. Potapova, *Izv. Akad. Nauk SSSR Ser. Khim.*, **1970**, 2048.(CA, 75:36201d)
- b) B. M. Mikhailov, E. A. Shagova, *Russ. J. Gener. Chem.*, **1972**, 1221
- c) B. M. Mikhailov, E. A. Shagova, *Bull. Acad. Sci. USSR, Div. Chem. Sci.*, **1979**, 1250; translated from *Izv. Akad. Nauk SSSR Ser. Khim.*, **1979**, 1337.
- d) B. M. Mikhailov, E. A. Shagova, *Bull. Acad. Sci. USSR, Div. Chem. Sci.*, **1979**, 549; (*Izv. Akad. Nauk SSSR Ser. Khim.*, **1979**, 595).
- e) B. M. Mikhailov, E. A. Shagova, *Izv. Akad. Nauk SSSR Ser. Khim.*, **1972**, 1450;
- f) B. M. Mikhailov, E. A. Shagova, *Russ. J. Gener. Chem.*, **1975**, 45, 1052; (*Zh. Obshch. Khim.*, **1975**, 1039).
- [103] G. B. Dunks, R. J. Wiersema, M. F. Hawthorne, *J. Am. Chem. Soc.*, **1973**, 95, 3174.
- [104] D. N. Rai, C. R. Venkatachelam, R. W. Rudolph, *Synth. React. Inorg. Met.-Org. Chem.*, **1973**, 3, 129.
- [105] J. Plešek, T. Jelinek, S. Hermanek, B. Stibr, *Collect. Czech. Chem. Commun.*, **1986**, 51, 81.
- [106] B. F. Spielvogel, G. Rana, K. Vyakaranam, K. Grell, K. E. Dicke, B. D. Dolash, S. Li, C. Zheng, J. A. Maguire, M. Takagaki, N. S. Hosmane, *Collect. Czech. Chem. Commun.*, **2002**, 676, 1095.
- [107] G. Zi, H. Li, Z. Xie, *Organometallics*, **2002**, 21, 1136.

- [108] W. Gerrard, H. R. Hudson, E. F. Mooney, *J. Chem. Soc.*, **1960**, 5168; **1962**, 113.
- [109] M. Baudler, A. Marx, *Z. Anorg. Allg. Chem.*, **1981**, 474, 18.
- [110] F. Teixidor, C. Vinas, A. Demonceau, R. Nunez, *Pure & Appl. Chem.*, **2003**, 75, 1305.
- [111] X. Yang, C. B. Knobler, Z. Zheng, M. F. Hawthorne, *J. Am. Chem. Soc.*, **1994**, 116, 7142.
- [112] a) H. Nöth, W. Meister, *Z. Naturforsch.*, **1962**, 17b, 714.
b) M. J. G. Lesley, N. C. Norman, C. R. Rice, *Inorg. Synth.*, **2004**, 34, 1.
- [113] D. Kaufmann, R. Boese, A. Scheer, *Chem. Ber.*, **1994**, 127, 2349.
- [114] M. Hildenbrand, H. Pritzkow, W. Siebert, *Angew. Chem.*, **1985**, 97, 769; *Angew. Chem. Int. Ed. Engl.*, 24, 759.
- [115] A. Krämer, J.-K. Uhm, S. E. Garner, H. Pritzkow, W. Siebert, *Z. Naturforsch.*, **1990**, 45b, 1019.
- [116] G. Linti, D. Loderer, H. Nöth, K. Polborn, W. Rattay, *Chem. Ber.*, **1994**, 127, 1909.
- [117] G. Frenking, T. Wagener, In *Encyclopedia of Computational Chemistry*; P. v. R. Schleyer, Ed.; Wiley: New York, **1998**; pp 3073-3084.
- [118] (a) A. D. Becke, *J. Chem. Phys.* **1993**, 98, 5648;
(b) S. H. Vosko, L. Wilk, M. Nusair, *Can. J. Phys.* **1980**, 58, 1200;
(c) C. Lee, W. Yang, R. G. Parr, *Phys. Rev. B* **1988**, 37, 785.
- [119] (a) J. P. Foster, F. Weinhold, *J. Am. Chem. Soc.* **1980**, 102, 7211;
(b) A. E. Reed, F. Weinhold, *J. Chem. Phys.* **1983**, 78, 4066;
(c) A. E. Reed, R. B. Weinstock, F. Weinhold, *J. Chem. Phys.* **1985**, 83, 735;
(d) A. E. Reed, L. A. Curtiss, F. Weinhold, *Chem. Rev.* **1988**, 88, 899.
- [120] (a) M. J. Frisch, J. A. Pople et al., *Gaussian 98 (Rev. A11)*: Gaussian, Inc., Pittsburgh, PA, **2001**;
(b) M. J. Frisch, J. A. Pople et al., *Gaussian 03 (Rev. C.0)*: Gaussian Inc., Wallingford CT, **2004**;
(c) R. Ahlrichs et al. *TURBOMOLE (Ver. 5.7)*: Universität Karlsruhe, **2004**.
- [121] G. Schaftenaar, J. H. Noordik, *MOLDEN*: a pre- and post-processing program for molecular and electronic structures. *J. Comput.-Aided Mol. Des.* **2000**, 123.

- [122] a) G. E. Herberich, H. Ohst, *Adv. Organomet.Chem.*, **1986**, *25*, 199.
b) G. E. Herberich, H. J. Becker, K. Carsten, C. Engelke, W. Koch, *Chem. Ber.*, **1976**, *109*, 2382.
- [123] a) A. J. Ashe III, F. J. Drone, C. M. Kausch, J. Kroker, S. M. Al-Taween, *Pure & Appl. Chem.* **1990**, *62*, 513.
b) A. J. Ashe III, J. W. Kamp, W. Klein, R. Rousseau, *Angew. Chem.* **1993**, *105*, 1112; *Angew. Chem. Int. Ed. Engl.* **1993**, *32*, 1065, and refs. therein.
- [124] E. O. Fischer, S. Breitschaft, *Angew. Chem.* **1963**, *75*, 94; *Angew. Chem. Int. Ed. Engl.* **1963**, *2*, 44.
- [125] A. J. Ashe III, S. Al-Ahmad, J. W. Kamp, V. G. Young, Jr., *Angew. Chem.* **1997**, *109*, 2104; *Angew. Chem. Int. Ed. Engl.* **1997**, *36*, 2014.
- [126] X. Fang, D. Woodmansee, X. Bu, G. C. Bazan, *Angew. Chem.* **2003**, *115*, 4648; *Angew. Chem. Int.*, **2003**, *42*, 4510.
- [127] A. Ginsberg, *Dissertation*, University of Heidelberg, **2000**.
- [128] H. Seyffer, *Dissertation*, University of Heidelberg, **1986**.
- [129] H. Schulz, H. Seyffer, B. Deobald, H. Pritzkow, W. Siebert, *Z. Naturforsch.*, **1994**, *49b*, 465.
- [130] K. Geilich, W. Siebert, *Z. Naturforsch.*, **1986**, *41b*, 671.
- [131] W. Siebert, personal communication, **2003**.
- [132] G. Brodt, *Dissertation*, University of Heidelberg, **1988**.
- [133] S. Huck, *Dissertation*, University of Heidelberg, **1997**.
- [134] P. J. Fagan, W. S. Mahoney, J. C. Calabrese, I. D. Williams, *Organometallics*, **1990**, *9*, 1843.
- [135] R. E. Dinnebier, M. Schneider, S. van Smaalen, F. Olbrich, U. Behrens, *Acta Crystallogr. Section B.*, **1999**, *55*, 35.
- [136] DFT calculations in progress, I. Hyla-Kryspin, University of Münster.
- [137] a) M. J. S. Dewar, M. K. Holloway, *J. Am. Chem. Soc.* **1984**, *106*, 6619;
b) H. Hogeveen, E. M. G. A. van Kruchten, *J. Org. Chem.*, **1981**, *46*, 1350, and refs. therein.

- [138] J. A. Morrison, *Chem. Rev.* **1991**, *91*, 35-48 (p. 41).
- [139] M. Baudler, K. Rockstein, *Z. Anorg. Allg. Chem.*, **2002**, *628*, 1741.
- [140] H. Nöth, H. Pommerening, *Angew. Chem.* **1980**, *92*, 481; *Angew. Chem. Int. Ed. Engl.* **1980**, *19*, 482.
- [141] M. L. McKee, *Inorg. Chem.*, **1999**, *38*, 321.
- [142] M. Baudler, K. Rockstein, W. Oehlert, *Chem. Ber.* **1991**, *124*, 1149.
- [143] C.-J. Maier, H. Pritzkow, W. Siebert, *Angew. Chem.*, **1999**, *111*, 1772; *Angew. Chem. Int. Ed. Engl.* *38*, 1666.
- [144] M. Atoji, W. N. Lipscomb, *J. Chem. Phys.* **1953**, *21*, 172; *Acta Crystallogr.* **1953**, *6*, 547.
- [145] T. Mennekes, P. Paetzold, R. Boese, D. Bläser, *Angew. Chem.* **1991**, *103*, 199; *Angew. Chem. Int. Ed. Engl.* **1991**, *30*, 173.
- [146] a) A. Maier, M. Hofmann, H. Pritzkow and W. Siebert, *Angew. Chem.*, **2002**, *114*, 1600; *Angew. Chem. Int. Ed.*, **2002**, *41*, 1529;
b) C. Präsang, M. Hofmann, G. Geiseler, W. Massa, A. Berndt, *Angew. Chem.*, **2002**, *114*, 1597; *Angew. Chem. Int. Ed.*, **2002**, *41*, 1526.
- [147] a) W. Mesbah, *Dissertation*, University of Marburg, **2003**;
b) W. Mesbah, C. Präsang, M. Hofmann, G. Geiseler, W. Massa, A. Berndt, *Angew. Chem.*, **2003**, *115*, 1758; *Angew. Chem. Int. Ed.*, **2003**, *42*, 1717.
- [148] O.C. Musgrave, *J. Chem. Soc.*, **1956**, 4305
- [149] a) D. Loderer, H. Nöth, H. Pommerening, W. Rattay, H. Schick, *Chem. Ber.* **1994**, *127*, 1605;
b) H. A. Ali, I. Goldberg, M. Srebnik, *Eur. J. Inorg. Chem.*, **2002**, 73.
- [150] H. Nöth, H. Schick, W. Meister, *J. Organomet. Chem.*, **1964**, *1*, 401.
- [151] A. Moezzi, M. M. Olmstead, P. P. Power, *J. Chem. Soc., Dalton Trans.*, **1999**, 2429.
- [152] H. A. Ali, I. Goldberg, M. Srebnik, *Acta Crystallogr. Section C.*, **2001**, *57*, 770.
- [153] O. P. Shitov, S. L. Loffe, V. A. Tartakowskii, S. S. Novikov, *Russ. Chem. Rev.*, **1970**, *39*, 905.
- [154] M. Balakrishnarajan, R. Hoffmann, *J. Am. Chem. Soc.* **2004**, *126*, 13119.
- [155] a) H. Nöth, R. Schwerthöffer, *Chem. Ber.*, **1981**, *114*, 3056;

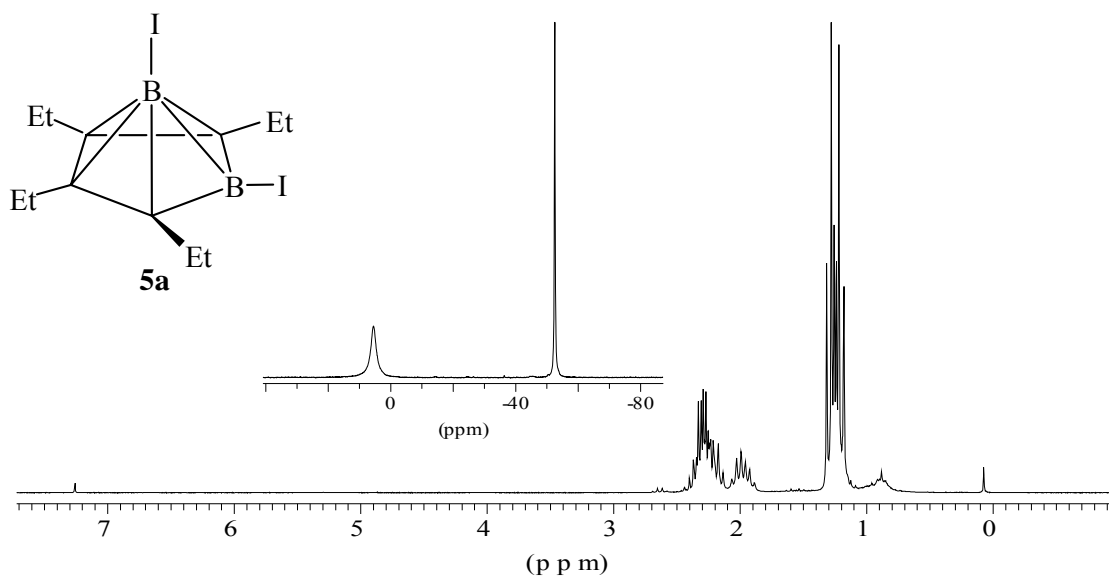
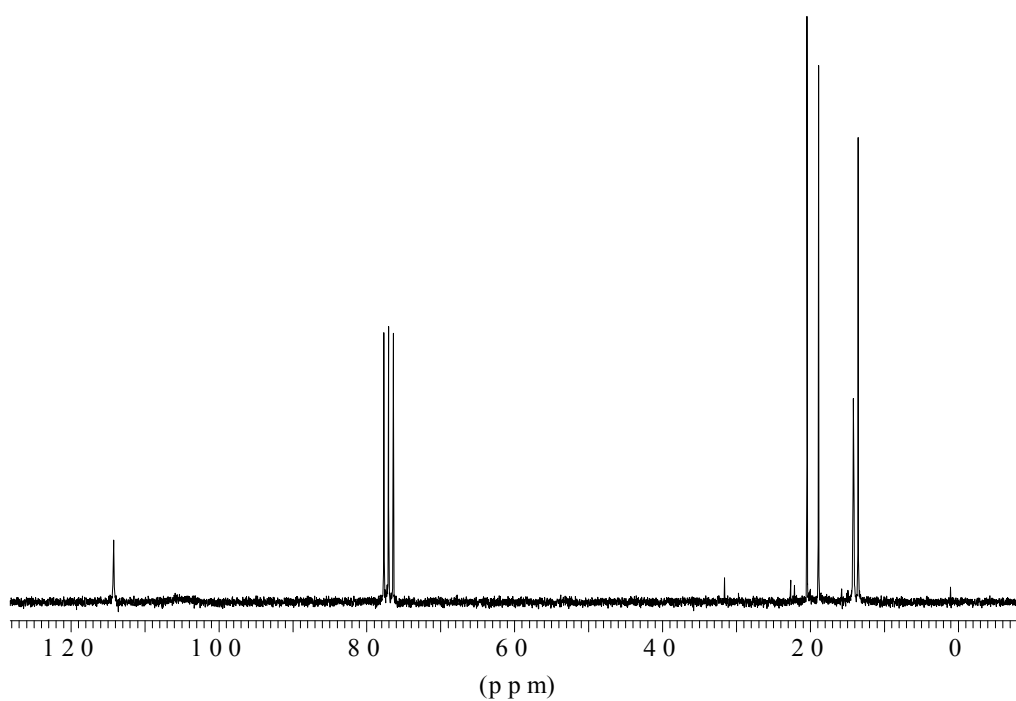
- b) H. Nöth, R. Staudigl, *Z. Anorg. Allg. Chem.*, **1981**, 481, 41.
- [156] a) J. Goubeau, H. Keller, *Z. Anorg. Allg. Chem.*, **1951**, 267, 1;
b) W. Haubold, R. Schaeffer, *Chem. Ber.*, **1971**, 104, 513.

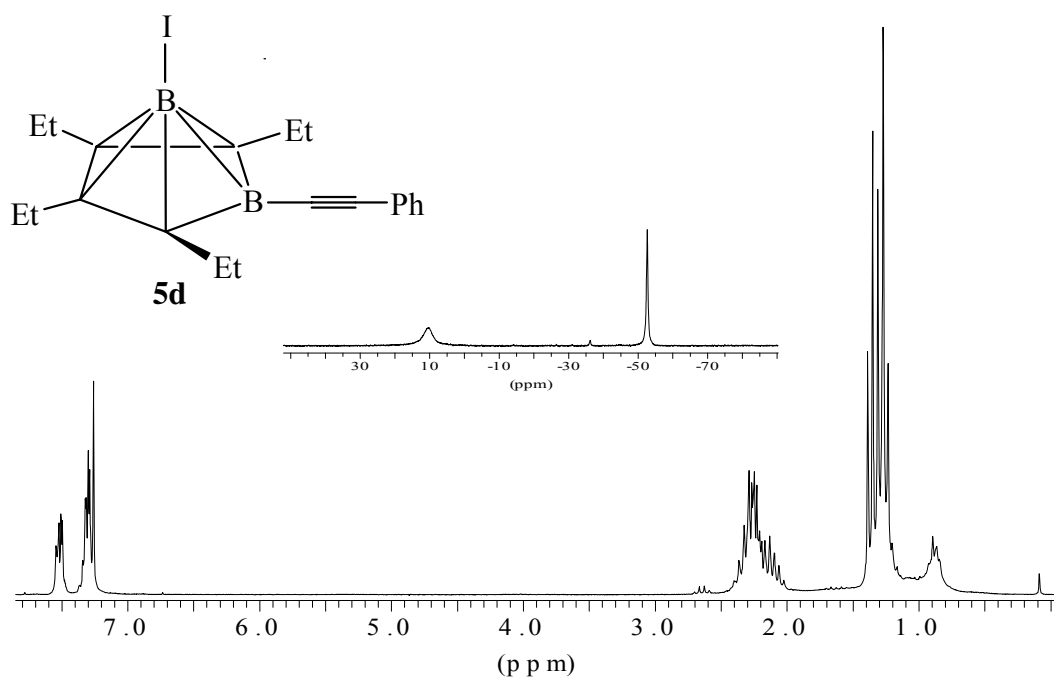
6. Appendices

6.1 Abbreviations and Symbols

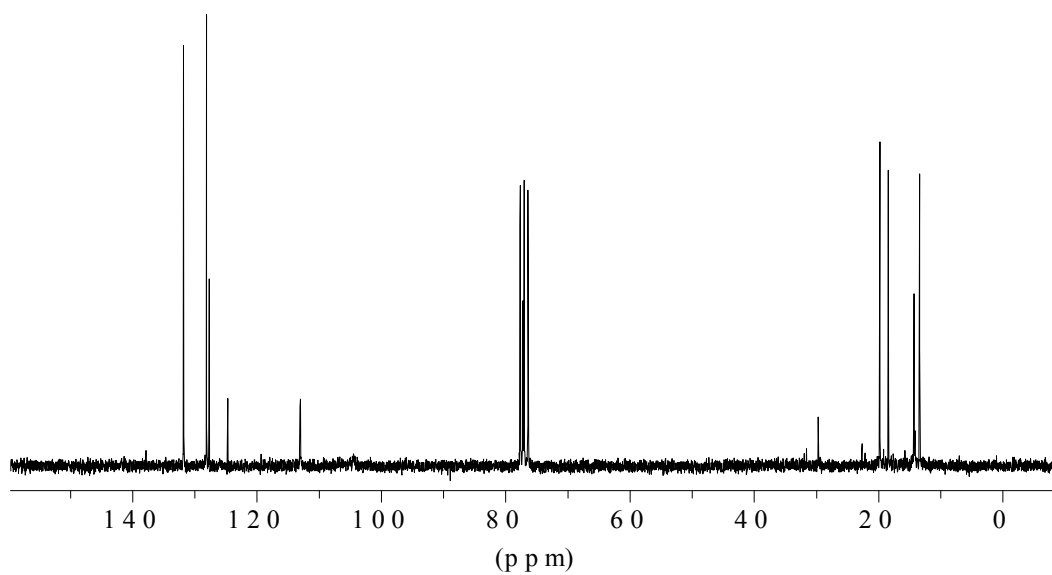
2c-2e	two-center, two-electron	MHz, Hz	megahertz, Hertz
3c-2e	three-center, two-electron	ml	milliliter
δ	chemical shift	m/z	mass/charge ratio
Ar	aryl group	mmol	millimole
b.p.	boiling point	mmu	10^{-3} molecular mass unit
br.	broad	m.p.	melting point
calcd.	calculated	MS	mass spectrum
Cat	catechol-yl	NMR	Nuclear magnetic resonance (s = singlet, d = doublet, t = triplet, q = quartet, J = coupling constant)
Cp	cyclopentadienyl		
Cp*	pentamethylcyclopentadienyl		
Don	donor	n.o	not observed
EI	Electron Impact	Ph	phenyl,
ESI	Electrospray Ionization	ppm	parts per million
FAB	Fast Atom Bombardment	Pr ⁱ	<i>iso</i> -propyl
h	hour	Py	pyridine
HOMO	Highest Occupied MO	r.t.	room temperature
HR-MS	High Resolution MS	SE	Skeletal electron
IR	infrared	THF, thf	tetrahydrofuran
K	Kelvin	TMS	tetramethylsilane
LUMO	Lowest Unoccupied MO	VE	valence electron
M	molecular ion peak, mole	<i>t</i> Bu, <i>n</i> Bu	<i>tert</i> -butyl, normal butyl
MO	Molecular Orbital	w	weak

6.2 Selected NMR and MS spectra

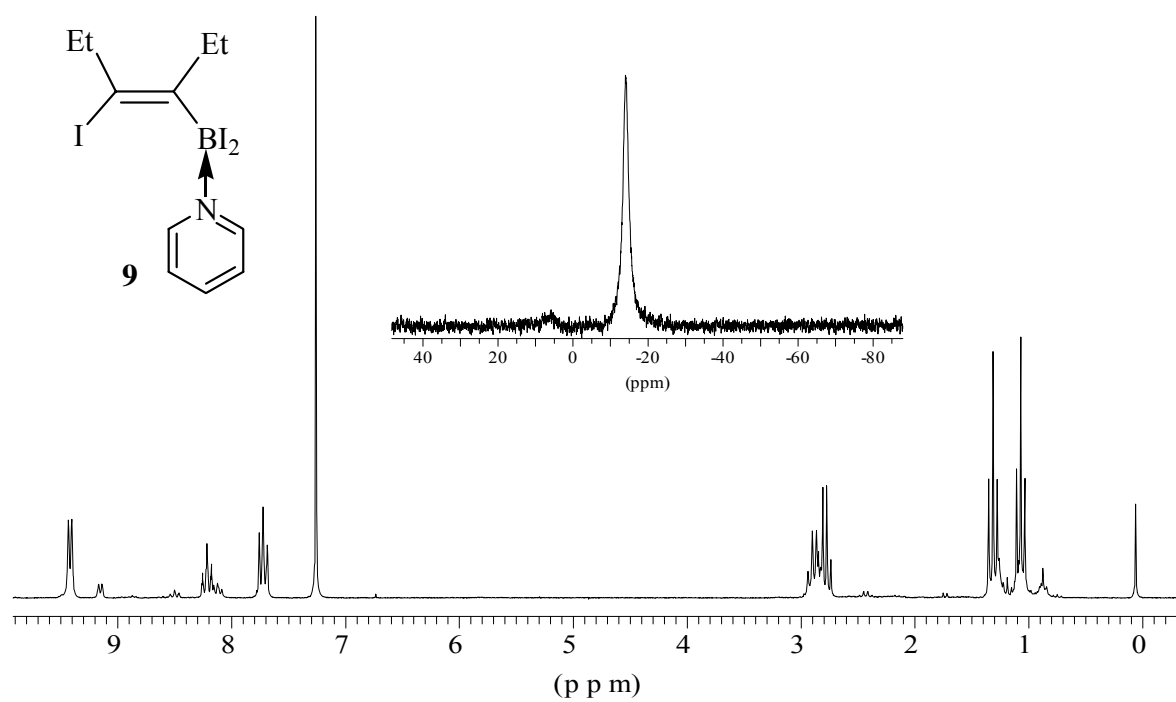
 ^1H -NMR and ^{11}B -NMR spectra of **5a** in CDCl_3  ^{13}C -NMR spectrum of **5a** in CDCl_3



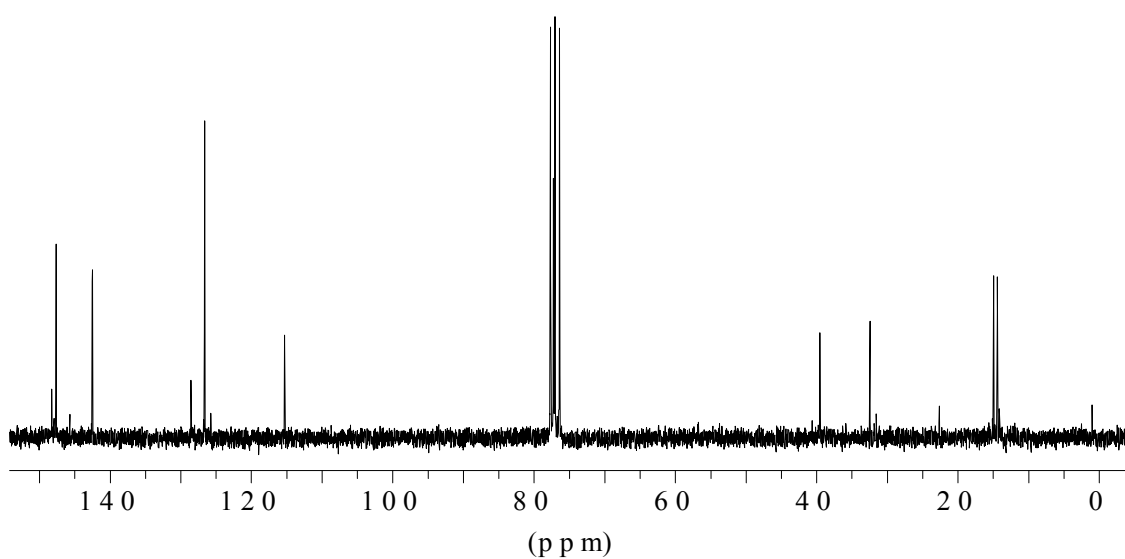
$^1\text{H-NMR}$ and $^{11}\text{B-NMR}$ spectra of **5d** in CDCl_3



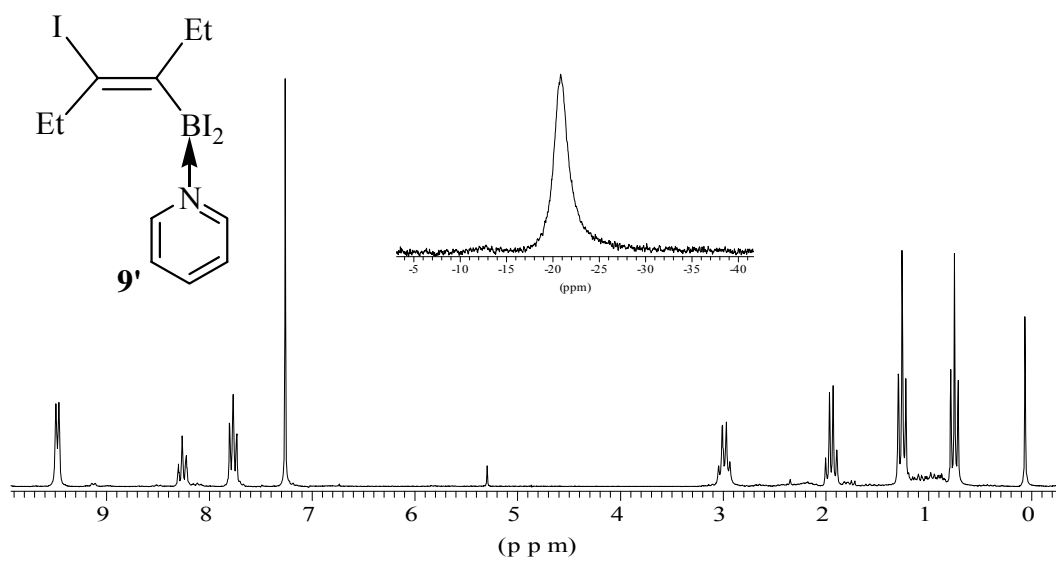
$^{13}\text{C-NMR}$ spectrum of **5d** in CDCl_3



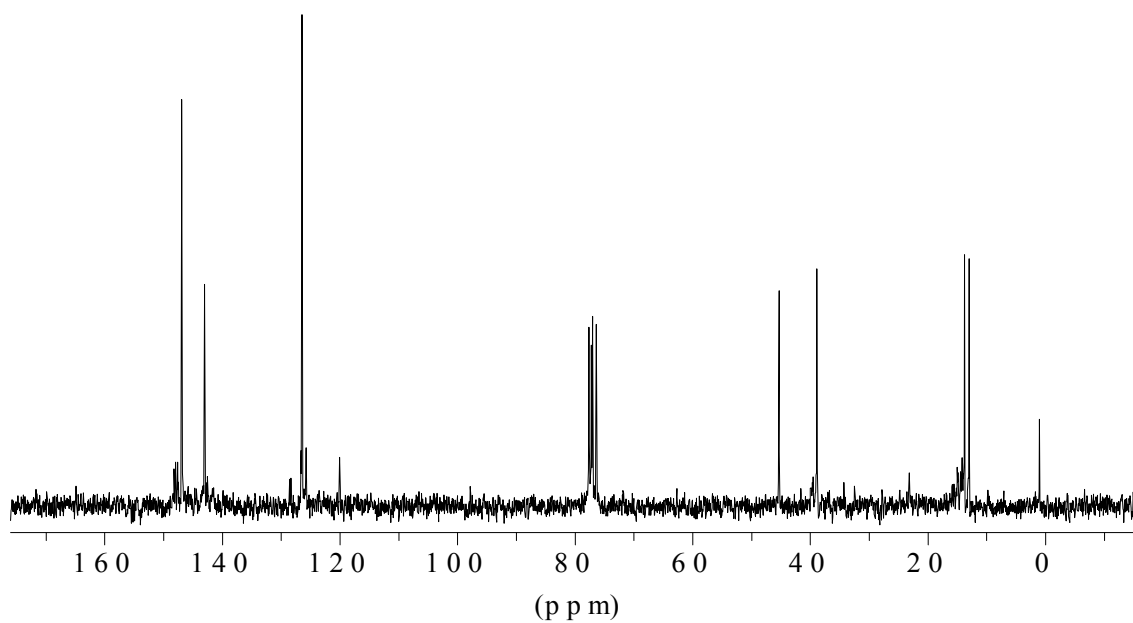
$^1\text{H-NMR}$ and $^{11}\text{B-NMR}$ spectra of **9** in CDCl_3



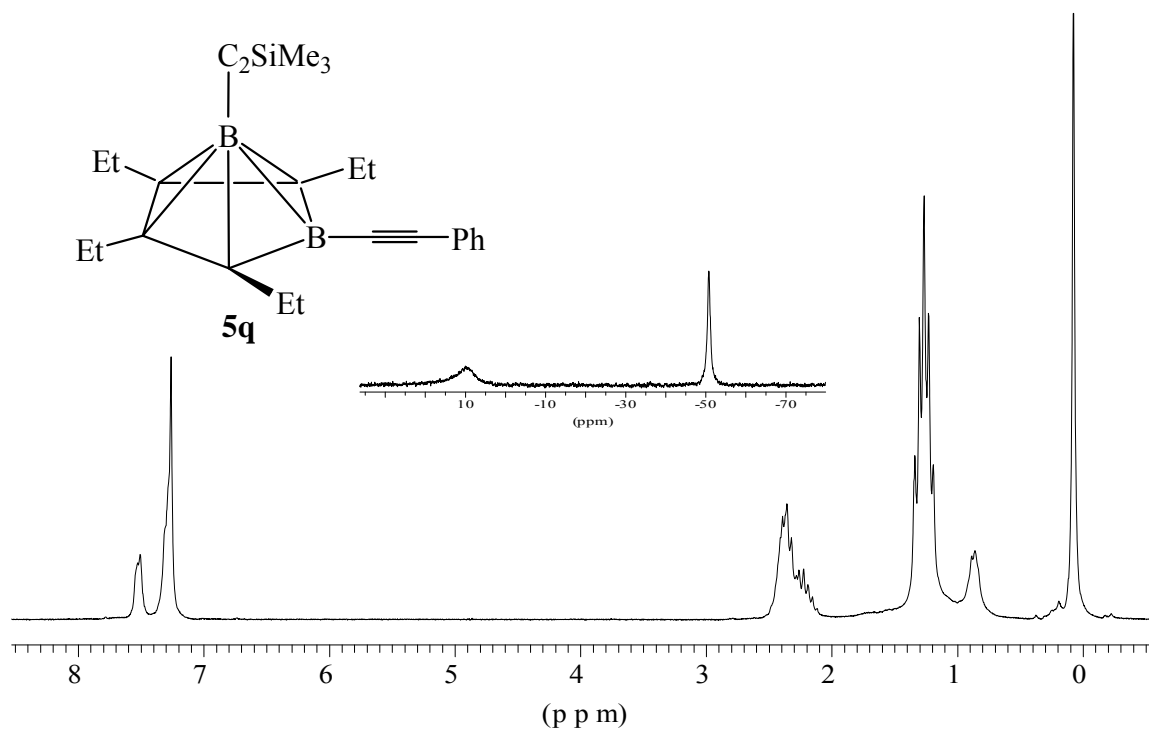
$^{13}\text{C-NMR}$ spectrum of **9** in CDCl_3



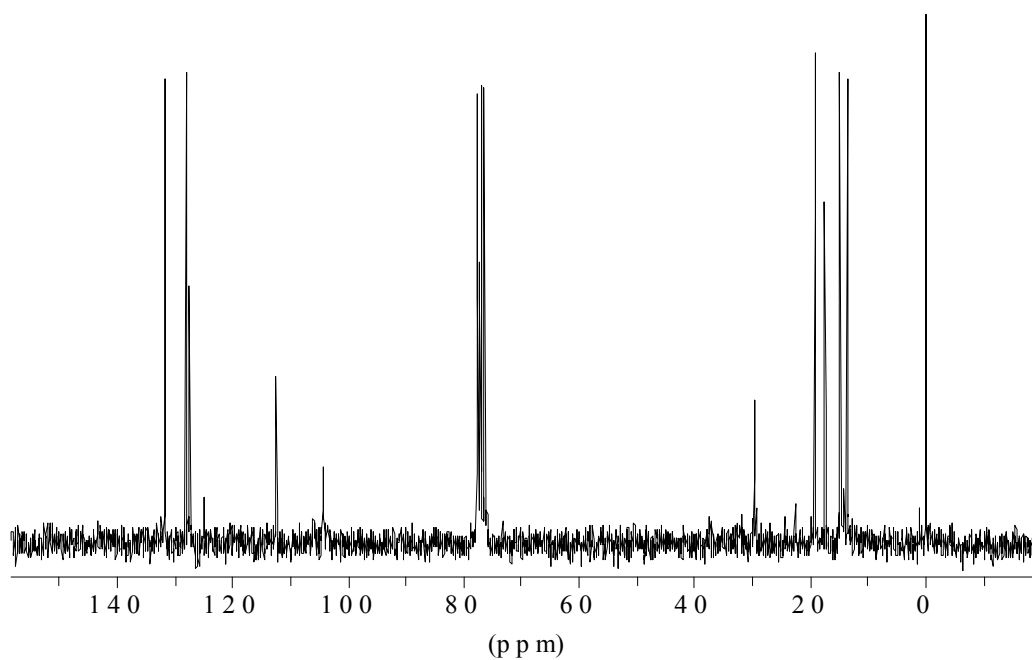
$^1\text{H-NMR}$ and $^{11}\text{B-NMR}$ spectra of **9'** in CDCl_3



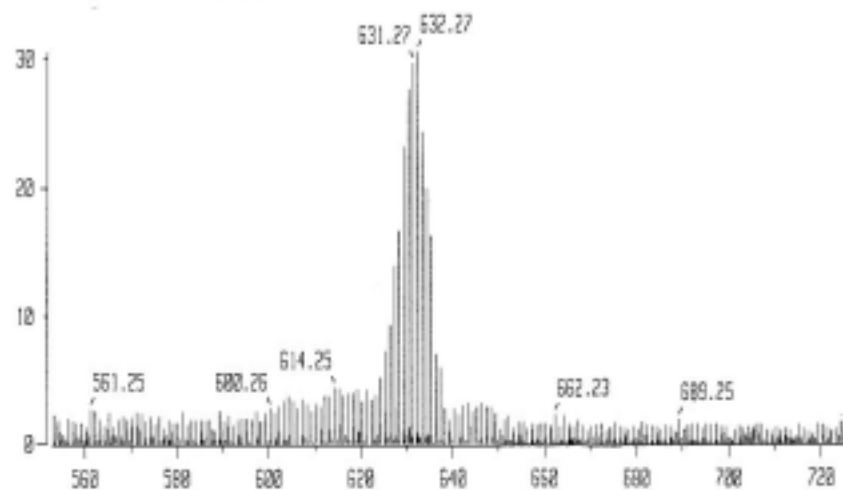
$^{13}\text{C-NMR}$ spectrum of **9'** in CDCl_3



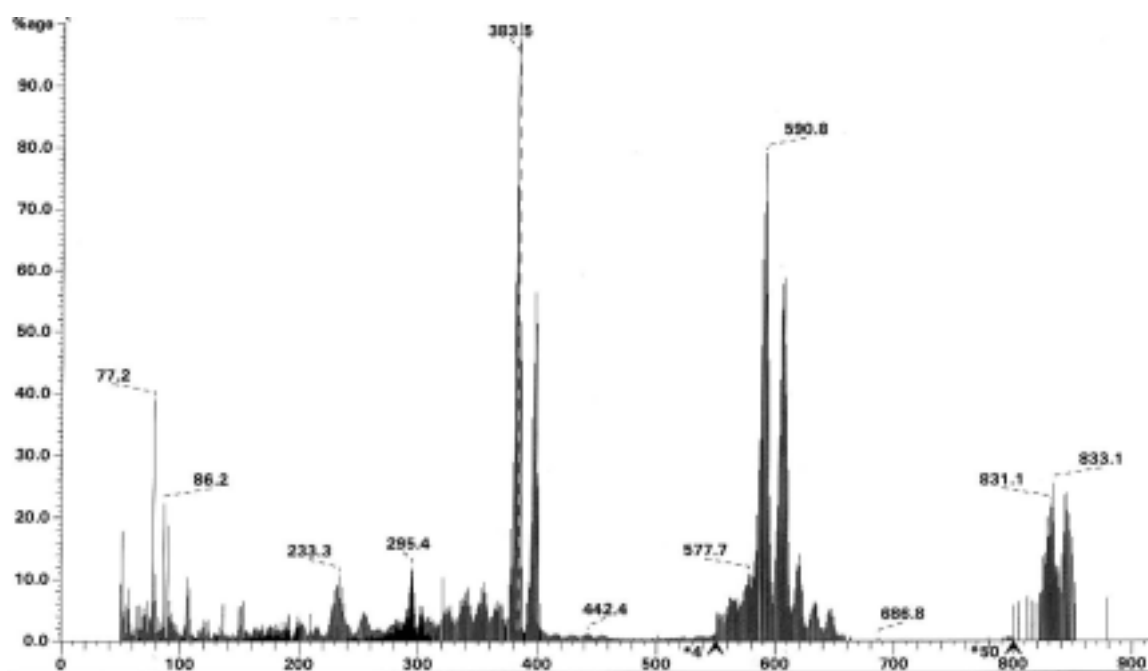
1H -NMR and ^{11}B -NMR spectra of **5q** in $CDCl_3$



^{13}C -NMR spectrum of **5q** in $CDCl_3$

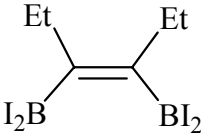
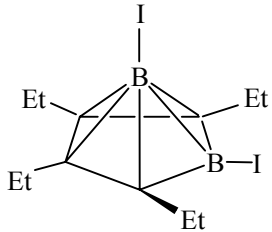


EI-MS spectrum of **46**



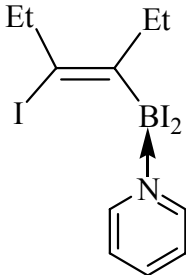
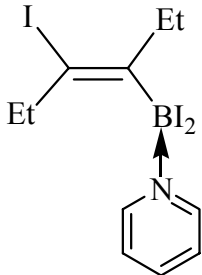
EI-MS spectrum of **58**

6.3 Crystal data and refinement details

Identification code	2	5a
		
Empirical formula	C ₆ H ₁₀ B ₂ I ₄	C ₁₂ H ₂₀ B ₂ I ₂
Formula weight	611.36	439.70
Temperature	103(2) K	103(2) K
Crystal system	monoclinic	orthorhombic
Space group	P2(1)/n	Pna2(1)
Unit cell dimensions	a = 11.9871(7) Å, α = 90° b = 7.7401(4) Å, β = 102.841 (1)° c = 14.8450(9) Å, γ = 90°	a = 12.1078(7) Å, α = 90° b = 14.3226(8) Å, β = 90° c = 9.2587(5) Å, γ = 90°
Volume	1342.89(13) Å ³	1605.60(16) Å ³
Z	4	4
Density (calculated)	3.024 g/cm ³	1.819 g/cm ³
Absorption coefficient	9.236 mm ⁻¹	3.892 mm ⁻¹
F(000)	1072	832
Crystal size	0.37 x 0.25 x 0.16 mm	0.45 x 0.15 x 0.08 mm
Θ range for data collection	1.98 to 32.03°	2.20 to 31.99°
Index ranges	-17/17, 0/11, 0/21	0/17, 0/21, -13/13
Reflections collected	412363	14404
Independent reflections	4559 [R(int) = 0.0279]	5198 [R(int) = 0.0274]
Completeness to Θ _{max}	97.4 %	98.7 %
Absorption correction	Semi-empirical from equivalents	Semi-empirical from equivalents
Max. and min. transmission	1.0000 and 0.5117	1.0000 and 0.6861
Refinement method	Full-matrix least-squares on F ²	Full-matrix least-squares on F ²
Data / restraints / parameters	4559 / 0 / 145	5198 / 1 / 226
Goodness-of-fit on F ²	1.106	1.050
Final R indices [I > 2 σ (I)]	R1 = 0.0289, wR2 = 0.0713	R1 = 0.0219, wR2 = 0.0517
R indices (all data)	R1 = 0.0343, wR2 = 0.0734	R1 = 0.0238, wR2 = 0.0526
Absolute structure parameter	---	0.50(2)
Largest diff. peak and hole	2.265/-2.149 e.Å ⁻³	1.240/-0.518 e.Å ⁻³

Identification code	5d	5g
Empirical formula	C ₂₀ H ₂₅ B ₂ I	C ₂₁ H ₂₇ B ₂ I
Formula weight	413.92	427.95
Temperature	293(2) K	298(2) K
Crystal system	triclinic	triclinic
Space group	P-1	P-1
Unit cell dimensions	a = 7.3783(6) Å, α = 86.083(1)° b = 10.4260(8) Å, β = 86.301(1)° c = 12.5718(9) Å, γ = 85.441(2)°	a = 7.8362(4) Å, α = 80.286(1)° b = 8.3469(4) Å, β = 85.038(1)° c = 18.2876(10) Å, γ = 64.989(1)°
Volume	960.09(13) Å ³	1068.29(9) Å ³
Z	2	2
Density (calculated)	1.432 g/cm ³	1.330 g/cm ³
Absorption coefficient	1.664 mm ⁻¹	1.498 mm ⁻¹
F(000)	416	432
Crystal size	0.35 x 0.09 x 0.04 mm	0.45 x 0.32 x 0.27 mm
Θ range for data collection	1.63 to 32.00°	2.26 to 26.37°
Index ranges	-10/10, -15/15, 0/18	-9/9, -10/10, 0/22
Reflections collected	16837	13336
Independent reflections	6504 [R(int) = 0.0387]	4370 [R(int) = 0.0210]
Completeness to Θ _{max}	97.8 %	100.0 %
Absorption correction	Semi-empirical from equivalents	Semi-empirical from equivalents
Max. and min. transmission	1.0000 and 0.7853	1.0000 and 0.7304
Refinement method	Full-matrix least-squares on F ²	Full-matrix least-squares on F ²
Data / restraints / parameters	6504 / 0 / 308	4370 / 0 / 319
Goodness-of-fit on F ²	1.071	1.070
Final R indices [I > 2 σ (I)]	R1 = 0.0304, wR2 = 0.0722	R1 = 0.0404, wR2 = 0.0988
R indices (all data)	R1 = 0.0402, wR2 = 0.0770	R1 = 0.0570, wR2 = 0.1106
Largest diff. peak and hole	1.322 and -1.248 e.Å ⁻³	0.985 and -0.622 e.Å ⁻³

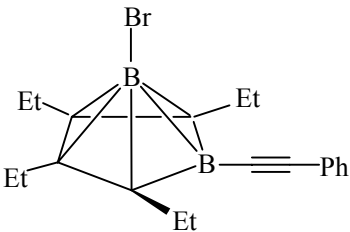
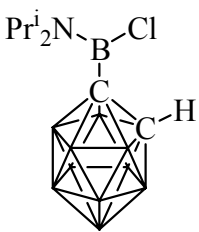
Identification code	5i	5q
Empirical formula	C ₁₉ H ₂₅ B ₂ FeIO ₂	C ₂₅ H ₃₄ B ₂ Si
Formula weight	489.76	384.23
Temperature	103(2) K	103(2) K
Crystal system	monoclinic	monoclinic
Space group	P2(1)/c	P2(1)
Unit cell dimensions	a = 9.5495(5) Å, α = 90° b = 24.2877(11) Å, β = 99.480(1)° c = 8.9340(4) Å, γ = 90°	a = 7.3346(4) Å, α = 90° b = 8.9453(4) Å, β = 91.254(1)° c = 19.1092(10) Å, γ = 90°
Volume	2043.81(17) Å ³	1253.46(11) Å ³
Z	4	2
Density (calculated)	1.592 g/cm ³	1.018 g/cm ³
Absorption coefficient	2.257 mm ⁻¹	0.101 mm ⁻¹
F(000)	976	416
Crystal size	0.32 x 0.25 x 0.20 mm	0.15 x 0.24 x 0.36 mm
Θ range for data collection	1.68 to 32.01°	2.13 to 32.01°
Index ranges	-14/14, 0/36, 0/13	-10/10, -10/13, 0/28
Reflections collected	27347	11997
Independent reflections	7027 [R(int) = 0.0239]	6728 [R(int) = 0.0247]
Completeness to Θ _{max}	99.2 %	98.2 %
Absorption correction	Semi-empirical from equivalents	Semi-empirical from equivalents
Max. and min. transmission	1.0000 and 0.8363	1.0000 and 0.8981
Refinement method	Full-matrix least-squares on F ²	Full-matrix least-squares on F ²
Data / restraints / parameters	7027 / 0 / 326	6728 / 1 / 389
Goodness-of-fit on F ²	1.215	1.066
Final R indices [I > 2 σ (I)]	R1 = 0.0290, wR2 = 0.0661	R1 = 0.0385, wR2 = 0.0977
R indices (all data)	R1 = 0.0315, wR2 = 0.0670	R1 = 0.0429, wR2 = 0.1018
Absolute structure parameter	---	0.02(8)
Largest diff. peak and hole	1.292 and -0.713 e.Å ⁻³	0.393 and -0.180 e.Å ⁻³

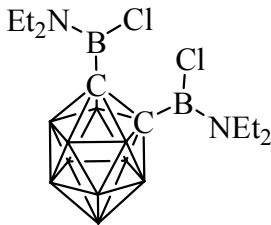
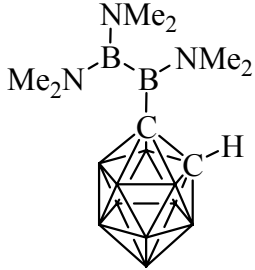
Identification code	9	9'
		
Empirical formula	C ₁₁ H ₁₅ BI ₃ N	C ₁₁ H ₁₅ BI ₃ N
Formula weight	552.75	552.75
Temperature	103(2) K	103(2) K
Crystal system	monoclinic	orthorhombic
Space group	P2(1)/n	Pbca
Unit cell dimensions	a = 11.0923(9) Å, α = 90° b = 12.0214(10) Å, β = 92.848(2)° c = 11.8779(10) Å, γ = 90°	a = 8.6602(4) Å, α = 90° b = 14.2028(7) Å, β = 90° c = 24.8358(13) Å, γ = 90°
Volume	1581.9(2) Å ³	3054.8(3) Å ³
Z	4	8
Density (calculated)	2.321 g/cm ³	2.404 g/cm ³
Absorption coefficient	5.905 mm ⁻¹	6.116 mm ⁻¹
F(000)	1008	2016
Crystal size	0.45 x 0.36 x 0.25 mm	0.25 x 0.15 x 0.12 mm
Θ range for data collection	2.41 to 32.02°	1.64 to 32.02°
Index ranges	-16/16, 0/17, 0/17	0/12, 0/21, 0/36
Reflections collected	14891	29275
Independent reflections	5345 [R(int) = 0.0270]	5281 [R(int) = 0.0374]
Completeness to Θ _{max}	97.0 %	99.5 %
Absorption correction	Semi-empirical from equivalents	Semi-empirical from equivalents
Max. and min. transmission	1.0000 and 0.6801	1.0000 and 0.6982
Refinement method	Full-matrix least-squares on F ²	Full-matrix least-squares on F ²
Data / restraints / parameters	5345 / 0 / 205	5281 / 0 / 205
Goodness-of-fit on F ²	1.117	1.095
Final R indices [I > 2 σ (I)]	R1 = 0.0273, wR2 = 0.0686	R1 = 0.0245, wR2 = 0.0571
R indices (all data)	R1 = 0.0321, wR2 = 0.0714	R1 = 0.0299, wR2 = 0.0592
Largest diff. peak and hole	1.476 and -2.388 e.Å ⁻³	1.695 and -0.694 e.Å ⁻³

Appendices

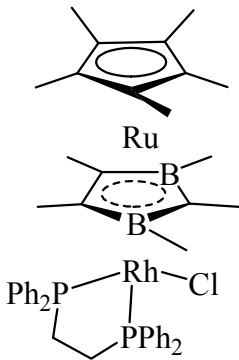
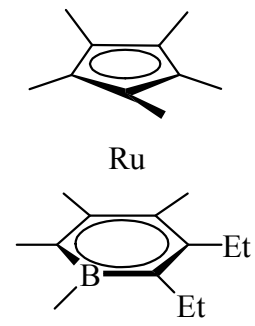
Identification code	13	14
Empirical formula	$C_{26}H_{25}B_2Co_2IO_6$	$C_{14}H_{31}B_{12}I, 2(C_2H_{12}B_{10})$
Formula weight	699.84	744.44
Temperature	103(2) K	103(2) K
Crystal system	monoclinic	monoclinic
Space group	$P2(1)/c$	$P2/c$
Unit cell dimensions	$a = 16.7233(9) \text{ \AA}, \alpha = 90^\circ$ $b = 12.4541(7) \text{ \AA}, \beta = 93.599(1)^\circ$ $c = 13.5390(8) \text{ \AA}, \gamma = 90^\circ$	$a = 26.1136(12) \text{ \AA}, \alpha = 90^\circ$ $b = 6.8725(3) \text{ \AA}, \beta = 115.469(1)^\circ$ $c = 24.6178(12) \text{ \AA}, \gamma = 90^\circ$
Volume	$2814.3(3) \text{ \AA}^3$	$3988.7(3) \text{ \AA}^3$
Z	4	4
Density (calculated)	1.652 g/cm^3	1.240 g/cm^3
Absorption coefficient	2.313 mm^{-1}	0.821 mm^{-1}
F(000)	1384	1504
Crystal size	0.33 x 0.10 x 0.06 mm	0.55 x 0.30 x 0.23 mm
Θ range for data collection	2.04 to 32.03°	1.66 to 32.04°
Index ranges	-24/24, 0/18, 0/20	-38/35, 0/10, 0/36
Reflections collected	37985	53142
Independent reflections	9662 [R(int) = 0.0429]	13706 [R(int) = 0.0342]
Completeness to Θ_{\max}	98.6 %	98.6 %
Absorption correction	Semi-empirical from equivalents	Semi-empirical from equivalents
Max. and min. transmission	1.0000 and 0.7160	1.0000 and 0.8120
Refinement method	Full-matrix least-squares on F^2	Full-matrix least-squares on F^2
Data / restraints / parameters	9662 / 0 / 434	13706 / 0 / 680
Goodness-of-fit on F^2	1.050	1.114
Final R indices [$I > 2 \sigma(I)$]	R1 = 0.0318, wR2 = 0.0693	R1 = 0.0348, wR2 = 0.0787
R indices (all data)	R1 = 0.0505, wR2 = 0.0780	R1 = 0.0432, wR2 = 0.0819
Largest diff. peak and hole	1.002 / -0.522 e. \AA^{-3}	1.197 / -1.009 e. \AA^{-3}

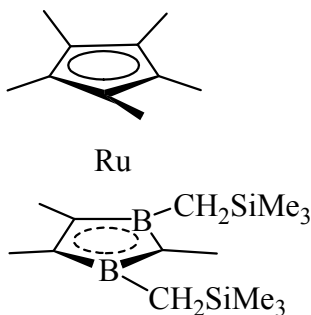
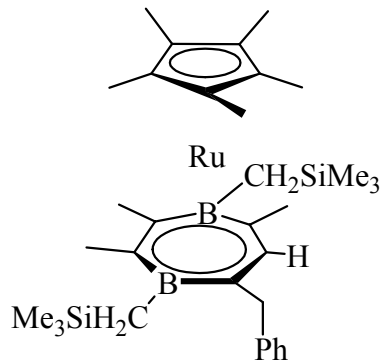
Appendices

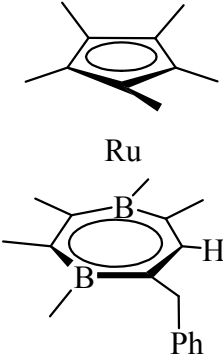
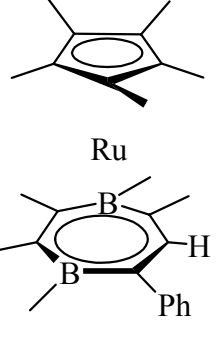
Identification code	5s	25
		
Empirical formula	C ₂₀ H ₂₅ B ₂ Br	C ₈ H ₂₅ B ₁₁ ClN
Formula weight	366.93	289.65
Temperature	103(2) K	103(2) K
Crystal system	monoclinic	monoclinic
Space group	P2(1)/c	C2/c
Unit cell dimensions	a = 7.6106(4) Å, α = 90° b = 16.0975(9) Å, β = 101.127(1)° c = 16.1470(9) Å, γ = 90°	a = 22.2667(14) Å, α = 90° b = 8.8997(6) Å, β = 105.697 (1)° c = 17.6838(11) Å, γ = 90°
Volume	1941.0(2) Å ³	3373.7(4) Å ³
Z	4	8
Density (calculated)	1.256 g/cm ³	1.141 g/cm ³
Absorption coefficient	2.114 mm ⁻¹	0.208 mm ⁻¹
F(000)	760	1216
Crystal size	0.37 x 0.24 x 0.03 mm	0.45 x 0.32 x 0.23 mm
Θ range for data collection	1.80 to 30.51°	1.90 to 31.99°
Index ranges	-10/10, 0/22, 0/23	-33/31, 0/13, 0/<=25
Reflections collected	24618	22510
Independent reflections	5932 [R(int) = 0.0427]	5762 [R(int) = 0.0401]
Completeness to Θ _{max}	100.0 %	98.3 %
Absorption correction	Semi-empirical from equivalents	Semi-empirical from equivalents
Max. and min. transmission	1.0000 and 0.7445	1.0000 and 0.8524
Refinement method	Full-matrix least-squares on F ²	Full-matrix least-squares on F ²
Data / restraints / parameters	5932 / 0 / 308	5762 / 0 / 290
Goodness-of-fit on F ²	1.080	1.056
Final R indices [I > 2 σ (I)]	R1 = 0.0487, wR2 = 0.1347	R1 = 0.0366, wR2 = 0.0877
R indices (all data)	R1 = 0.0727, wR2 = 0.1497	R1 = 0.0585, wR2 = 0.1005
Largest diff. peak and hole	0.689/-0.760 e.Å ⁻³	0.511/ -0.241 e.Å ⁻³

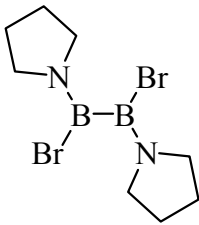
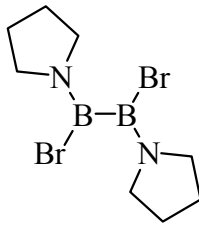
Identification code	26b	28a
		
Empirical formula	C ₁₀ H ₃₀ B ₁₂ Cl ₂ N ₂	C ₈ H ₂₉ B ₁₂ N ₃
Formula weight	378.98	297.06
Temperature	103(2) K	103(2) K
Crystal system	monoclinic	monoclinic
Space group	P2(1)/n	P2(1)/n
Unit cell dimensions	a = 10.5592(5) Å, α = 90° b = 16.9089(8) Å, β = 107.792(1)° c = 12.3339(6) Å, γ = 90°	a = 9.9411(5) Å, α = 90° b = 14.3279(7) Å, β = 94.746(1)° c = 12.9342(7) Å, γ = 90°
Volume	2096.82(17) Å ³	1835.97(16) Å ³
Z	4	4
Density (calculated)	1.201 g/cm ³	1.075 g/cm ³
Absorption coefficient	0.307 mm ⁻¹	0.054 mm ⁻¹
F(000)	792	632
Crystal size	0.27 x 0.19 x 0.12 mm	0.17 x 0.33 x 0.45 mm
Θ range for data collection	2.11 to 32.02°	2.13 to 32.02°
Index ranges	-15/14, 0/25, 0/18	-14/14, 0/21, 0/18
Reflections collected	28369	17457
Independent reflections	7219 [R(int) = 0.0329]	6272 [R(int) = 0.0314]
Completeness to Θ _{max}	99.0 %	98.1 %
Absorption correction	Semi-empirical from equivalents	Semi-empirical from equivalents
Max. and min. transmission	1.0000 and 0.8888	1.0000 and 0.9185
Refinement method	Full-matrix least-squares on F ²	Full-matrix least-squares on F ²
Data / restraints / parameters	7219 / 0 / 355	6272 / 0 / 324
Goodness-of-fit on F ²	1.071	1.063
Final R indices [I > 2 σ (I)]	R1 = 0.0336, wR2 = 0.0858	R1 = 0.0472, wR2 = 0.1189
R indices (all data)	R1 = 0.0447, wR2 = 0.0950	R1 = 0.0686, wR2 = 0.1370
Largest diff. peak and hole	0.553/-0.237 e.Å ⁻³	0.461/-0.188 e.Å ⁻³

Identification code	34	77
Empirical formula	C _{23.50} H ₄₆ B ₁₂ N ₂	C ₆ H ₁₈ B ₃ N ₃ O ₃
Formula weight	486.34	212.66
Temperature	100(2) K	100(2) K
Crystal system	monoclinic	monoclinic
Space group	C2/c	Cc
Z	8	4
Unit cell dimensions	a = 18.516(5) Å, α = 90.0° b = 11.947(4) Å, β = 100.790(7) ° c = 26.910(8) Å, γ = 90.0°	a = 10.012(9) Å, α = 90° b = 17.366(13) Å, β = 119.19(1)° c = 7.855(6) Å, γ = 90°
Volume	5848(3) Å ³	1192.3(16) Å ³
Density (calculated)	1.11 g/cm ³	1.18 g/cm ³
Absorption coefficient	0.06 mm ⁻¹	0.09 mm ⁻¹
Crystal size	0.18 x 0.09 x 0.07 mm	0.32 x 0.26 x 0.10 mm
Θ range for data collection	2.0 to 18.0°	2.3 to 28.3°
Index ranges	-16/16, -10/10, -23/23	-13/13, -23/23, -10/10
Reflections collected	10732	5951
Independent reflections	2006 (R(int) = 0.0912)	2875 (R(int) = 0.0255)
Observed reflections	1428 (I > 2 σ (I))	2671 (I > 2 σ (I))
Absorption correction	Multi.scan	Semi-empirical from equivalents
Max. and min. transmission	1.00 and 0.99	0.99 and 0.97
Refinement method	Full-matrix least-squares on F ²	Full-matrix least-squares on F ²
Data/restraints/parameters	2006 / 0 / 397	2875 / 2 / 208
Goodness-of-fit on F ²	1.03	1.10
Final R indices (I > 2 σ (I))	R1 = 0.060, wR2 = 0.146	R1 = 0.047, wR2 = 0.103
Largest diff. peak and hole	0.26/-0.21 eÅ ⁻³	0.34/-0.21 eÅ ⁻³

Identification code	51	39f
		
Empirical formula	C _{45.75} H ₅₆ B ₂ Cl _{1.50} P ₂ RhRu	C ₂₃ H ₃₇ BRu
Formula weight	946.62	425.41
Temperature	296(2) K	200(2) K
Crystal system	monoclinic	triclinic
Space group	P2 ₁ /n	P-1
Z	4	2
Unit cell dimensions	a = 12.3480(7) Å, α = 90° b = 26.9014(15) Å, β = 103.453(1)° c = 13.9044(8) Å, γ = 90.0°	a = 7.6752(9) Å, α = 92.905(2) ° b = 8.928(1) Å, β = 93.060(2)° c = 16.051(2) Å, γ = 104.370(2)°
Volume	4492.0(4) Å ³	1061.6(2) Å ³
Density (calculated)	1.40 g/cm ³	1.33 g/cm ³
Absorption coefficient	0.89 mm ⁻¹	0.74 mm ⁻¹
Crystal size	0.18 x 0.16 x 0.16 mm	0.28 x 0.11 x 0.05 mm
Θ range for data collection	2.1 to 28.3°	2.4 to 26.4°
Index ranges	-16/16, -35/35, -18/18	-9/8, -11/11, -20/20
Reflections collected	46479	6546
Independent reflections	11134 (R(int) = 0.0340)	4077 (R(int) = 0.0193)
Observed reflections	8833 (I > 2 σ (I))	3810 (I > 2 σ (I))
Absorption correction	Semi-empirical from equivalents	Semi-empirical from equivalents
Max. and min. transmission	0.87 and 0.86	0.96 and 0.82
Refinement method	Full-matrix least-squares on F ²	Full-matrix least-squares on F ²
Data/restraints/parameters	11134 / 11 / 570	4077 / 0 / 237
Goodness-of-fit on F ²	1.06	1.09
Final R indices (I > 2 σ (I))	R1 = 0.042, wR2 = 0.104	R1 = 0.031, wR2 = 0.075
Largest diff. peak and hole	1.21/-0.54 e.Å ⁻³	0.48/-0.31 e.Å ⁻³

Identification code	35b	38b
		
Empirical formula	C ₂₄ H ₄₆ B ₂ RuSi ₂	C ₃₃ H ₅₄ B ₂ RuSi ₂
Formula weight	513.48	629.63
Temperature	103(2) K	120(2) K
Crystal system	monoclinic	monoclinic,
Space group	P2(1)/c	P2(1)/n
Unit cell dimensions	a = 18.7559(8) Å, α = 90° b = 8.9859(4) Å, β = 114.131(1)° c = 18.0098(8) Å, γ = 90°	a = 11.2417(7) Å, α = 90° b = 19.6225(13) Å, β = 102.466(3)° c = 15.6347(10) Å, γ = 90°
Volume	2770.1(2) Å ³	3367.6(4) Å ³
Z	4	4
Density (calculated)	1.231 g/cm ³	1.242 g/cm ³
Absorption coefficient	0.661 mm ⁻¹	0.557 mm ⁻¹
F(000)	1088	1336
Crystal size	0.32 x 0.07 x 0.06 mm	0.34 x 0.19 x 0.06 mm
Θ range for data collection	2.27 to 32.03°	1.69 to 28.44°
Index ranges	-27/25, 0/13, 0/26	-15/15, -26/26, -20/20
Reflections collected	37947	53110
Independent reflections	9541 [R(int) = 0.0538]	8451 [R(int) = 0.0820]
Max. and min. transmission	1.0000 and 0.9025	0.9674 and 0.8333
Refinement method	Full-matrix least-squares on F ²	Full-matrix least-squares on F ²
Data / restraints / parameters	9541 / 0 / 446	8451 / 0 / 357
Goodness-of-fit on F ²	1.100	1.050
Final R indices [I > 2 σ (I)]	R1 = 0.0336, wR2 = 0.0664	R1 = 0.0477, wR2 = 0.0879
R indices (all data)	R1 = 0.0666, wR2 = 0.0816	R1 = 0.0734, wR2 = 0.0956
Largest diff. peak and hole	1.092/-0.653 e.Å ⁻³	0.813/-0.704 e.Å ⁻³

Identification code	38a	38c
		
Empirical formula	C ₂₇ H ₃₈ B ₂ Ru	C ₂₆ H ₃₆ B ₂ Ru
Formula weight	485.26	471.24
Temperature	120(2) K	120(2) K
Crystal system	triclinic	monoclinic
Space group	P-1	P2(1)/n
Unit cell dimensions	a = 7.5443(6), α = 87.062(4)° b = 8.8867(7) Å, β = 88.683(4)° c = 18.6554(15) Å, γ = 69.228(4)°	a = 10.1454(18) Å, α = 90° b = 14.508(3) Å, β = 102.198(3)° c = 16.007(3) Å, γ = 90°
Volume	1167.88(16) Å ³	2302.9(7) Å ³
Z	2	4
Density (calculated)	1.380 g/cm ³	1.359 g/cm ³
Absorption coefficient	0.683 mm ⁻¹	0.690 mm ⁻¹
F(000)	508	984
Crystal size	0.34 x 0.22 x 0.13 mm	0.44 x 0.24 x 0.18 mm
Θ range for data collection	1.09 to 28.33°	1.91 to 28.33°
Index ranges	-10/10, -24/24, -11/11	-13/13, -16/19, -21/21
Reflections collected	18121	22869
Independent reflections	5778 [R(int) = 0.0391]	5744 [R(int) = 0.0388]
Completeness to Θ _{max}	99.2 %	99.7 %
Max. and min. transmission	0.9165 and 0.8010	0.8858 and 0.7510
Refinement method	Full-matrix least-squares on F ²	Full-matrix least-squares on F ²
Data / restraints / parameters	5778 / 0 / 281	5744 / 0 / 272
Goodness-of-fit on F ²	1.083	1.043
Final R indices [I > 2 σ (I)]	R1 = 0.0401, wR2 = 0.0894	R1 = 0.0311, wR2 = 0.0761
R indices (all data)	R1 = 0.0490, wR2 = 0.0926	R1 = 0.0389, wR2 = 0.0805
Largest diff. peak and hole	1.231/-0.906 e. Å ⁻³	0.862/-0.327 e. Å ⁻³

Identification code	72b'	72b''
		
Empirical formula	C ₈ H ₁₆ B ₂ Br ₂ N ₂	C ₈ H ₁₆ B ₂ Br ₂ N ₂
Formula weight	321.67	321.67
Temperature	103(2) K	293(2) K
Crystal system	orthorhombic	triclinic
Space group	P2(1)2(1)2	P-1
Unit cell dimensions	a = 11.2890(6) Å, α = 90° b = 11.6672(6) Å, β = 90° c = 4.6012(3) Å, γ = 90°	a = 6.8944(5) Å, α = 99.210(2)° b = 8.0273(6) Å, β = 102.527(2)° c = 11.7240(9) Å, γ = 91.176(2)°
Volume	606.03(6) Å ³	624.21(8) Å ³
Z	2	2
Density (calculated)	1.763 g/cm ³	1.711 g/cm ³
Absorption coefficient	6.651 mm ⁻¹	6.458 mm ⁻¹
F(000)	316	316
Crystal size	0.45 x 0.12 x 0.10 mm	0.12 x 0.14 x 0.60 mm
Θ range for data collection	2.51 to 32.03°	1.81 to 32.00°
Index ranges	-16/16, 0/17, 0/6	-10/9, -11/11, 0/17
Reflections collected	9541	10729
Independent reflections	2085 [R(int) = 0.0353]	4211 [R(int) = 0.0265]
Completeness to Θ _{max}	99.7 %	97.1 %
Absorption correction	Semi-empirical from equivalents	Semi-empirical from equivalents
Max. and min. transmission	1.0000 and 0.3274	1.0000 and 0.4087
Refinement method	Full-matrix least-squares on F ²	Full-matrix least-squares on F ²
Data / restraints / parameters	2085 / 0 / 97	4211 / 0 / 200
Goodness-of-fit on F ²	1.060	1.037
Final R indices [I > 2 σ (I)]	R1 = 0.0194, wR2 = 0.0461	R1 = 0.0268, wR2 = 0.0603
R indices (all data)	R1 = 0.0219, wR2 = 0.0469	R1 = 0.0426, wR2 = 0.0654
Absolute structure parameter	0.341(10)	---
Largest diff. peak and hole	1.138/-0.308 e.Å ⁻³	0.749/-0.543 e.Å ⁻³

Identification code	74	75
Empirical formula	C ₁₀ H ₂₁ B ₂ Br ₃ N ₂ O	C ₈ H ₁₈ BBr ₂ N ₂ , Br ⁻ , CHCl ₃
Formula weight	446.64	512.15
Temperature	103(2) K	103(2) K
Crystal system	monoclinic	monoclinic
Space group	P2(1)/c	P2(1)
Unit cell dimensions	a = 10.9113(10) Å, α = 90° b = 10.3105(10) Å, β = 91.344(2)° c = 13.4627(12) Å, γ = 90°	a = 6.4698(3) Å, α = 90° b = 12.6903(6) Å, β = 92.057(1)° c = 11.0314(5) Å, γ = 90°
Volume	1514.2(2) Å ³	905.14(7) Å ³
Z	4	2
Density (calculated)	1.959 g/cm ³	1.879 g/cm ³
Absorption coefficient	7.982 mm ⁻¹	7.114 mm ⁻¹
F(000)	872	496
Crystal size	0.52 x 0.27 x 0.13 mm	0.50 x 0.18 x 0.17 mm
Θ range for data collection	1.87 to 32.00°	2.45 to 32.01°
Index ranges	-16/16, 0/15, 0/20	-9/9, -18/17, 0/16
Reflections collected	5134	10401
Independent reflections	5134 [R(int) = 0.0000]	5593 [R(int) = 0.0252]
Completeness to Θ _{max}	97.6 %	97.5 %
Absorption correction	Semi-empirical from equivalents	Semi-empirical from equivalents
Max. and min. transmission	0.4235 and 0.1035	1.0000 and 0.4367
Refinement method	Full-matrix least-squares on F ²	Full-matrix least-squares on F ²
Data / restraints / parameters	5134 / 0 / 247	5593 / 56 / 231
Goodness-of-fit on F ²	1.055	0.963
Final R indices [I > 2 σ (I)]	R1 = 0.0320, wR2 = 0.0712	R1 = 0.0256, wR2 = 0.0520
R indices (all data)	R1 = 0.0486, wR2 = 0.0779	R1 = 0.0309, wR2 = 0.0531
Absolute structure parameter	---	-0.005(7)
Largest diff. peak and hole	1.701/-0.815 e.Å ⁻³	0.678/-0.623 e.Å ⁻³

Acknowledgement

Nothing would have been possible for this thesis without Prof. Siebert's accepting me as a Ph. D. student in his group. Apart from his guidance of my research, I am also grateful to him for his help throughout my stay in Heidelberg.

I thank Mrs. D. Gutruf, B. Termin for the NMR tests. Thanks also go to Dr. J. Gross (OCI), Mr. N. Nieth (OCI), Mrs. A. Seith (OCI), Mr. T. Jannack, and Dr. A. Mokhir, for the MS measurements. Special thanks are due to Dr. H. Pritzkow, Dr. C.-H. Hu (RWTH Aachen), Dr. T. Oeser (OCI), Prof. H. Wadepohl, and Dr. F. Rominger (OCI) for crystal structure analyses and very helpful discussions. I am also grateful to Prof. U. Englert (RWTH, Aachen) for arranging the X-ray analyses in Aachen. Dr. I. Hyla-Kryspin (Münster) has been, and is doing the calculations on model structures **35**, **36** and **38**.

Thanks to the present and former group members in the Siebert group for help and the nice working atmosphere: Dr. B. Bach, Dr. V. Barba, Dr. M. Bayer, Dr. A. Eckert, Dr. D. Görz, A. Goswami (*the other in the same boat*), Dr. T. Köhler, L. Lörsch, Dr. A. Maier, V. Scherban, R. Schütze, Dr. A. Weiss and Prof. C.G. Yan. I am thankful to L. Lörsch for his preparative assistance (on compounds **72b** and **74**).

I like to thank Prof. L. H. Gade, Prof. H. Wadepohl and PD Dr. M. Enders for helpful discussions and suggestions, and also their group members for timely help and cooperations.

Appreciation is extended to Mrs. M. Apperman, Mrs. R. Hutter, Mrs. P. Sander for their help; to Prof. B. Wrackmeyer (Univ. Bayreuth) for sending a copy of a Ph. D thesis (Dr. A. Glöckler), to Prof. M. Wagner (Univ. Frankfurt) for sending part of his Ph. D. thesis, to Prof. A. Berndt (Univ. Marburg) for sending part of a Ph. D. thesis (Dr. W. Mesbah); to all the employees in the Dekanat (Faculty of Chemistry and Geosciences) and the Chemistry Department (administration, chemical store, glass blower, electric shop, gas station, etc.).

I am very much indebted to my parents, my wife Jinling, and relatives and friends who have given me great care, timely help and warm encouragement.

Last but not least, financial support from the University of Heidelberg and the Deutsche Forschungsgemeinschaft (DFG) is greatly acknowledged.

Hiermit erkläre ich an Eides Statt, dass ich die vorliegende Arbeit selbständig und ohne unerlaubte Hilfsmittel durchgeführt habe.

Yong Nie